PHRC Research Series Report No. 109

The Pennsylvania Housing Research Center

Performance of Structural Insulated Panels with Different Fasteners and Splines Under Monotonic and Cyclic Loading

219 Sackett Building
University Park, PA 16802
Telephone: (814) 865-2341
Facsimile: (814) 863-7304
E-mail: phrc@psu.edu
URL: www.engr.psu.edu/phrc

May 2011

Disclaimer:

The Pennsylvania Housing Research Center (PHRC) exists to be of service to the housing community, especially in Pennsylvania. The PHRC conducts technical projects—research, development, demonstration, and technology transfer—under the sponsorship and with the support of numerous agencies, associations, companies and individuals. Neither the PHRC, nor any of its sponsors, makes any warranty, expressed or implied, as to the accuracy or validity of the information contained in this report. Similarly, neither the PHRC, nor its sponsors, assumes any liability for the use of the information and procedures provided in this report. Opinions, when expressed, are those of the authors and do not necessarily reflect the views of either the PHRC or anyone of its sponsors. It would be appreciated, however, if any errors, of fact or interpretation or otherwise, could be promptly brought to our attention. If additional information is required, please contact:

Mike Turns
Associate Director
PHRC

Andrew Scanlon
Director of Research
PHRC

PHRC Research Series Report No. 109

The Pennsylvania Housing Research Center

Performance of Structural Insulated Panels with Different Fasteners and Splines Under Monotonic and Cyclic Loading

by

Stefanie Terentiuk
Ali M. Memari

219 Sackett Building
University Park, PA 16802
Telephone: (814) 865-2341
Facsimile: (814) 863-7304
E-mail: phrc@psu.ed
URL: www.engr.psu.edu/phrc

May 2011

PERFORMANCE OF STRUCTURAL INSULATED PANELS WITH DIFFERENT FASTENERS AND SPLINES UNDER MONOTONIC AND CYCLIC LOADING

by

Stefanie Terentiuk

Former Graduate Student, Department of Architectural Engineering
The Pennsylvania State University, 104 Engineering Unit A, University Park, PA 16802

and

Ali M. Memari

Professor, Department of Architectural Engineering
The Pennsylvania State University, 104 Engineering Unit A, University Park, PA 16802

May 2011

ABSTRACT

The ease of construction and high thermal capacity of Structural Insulated Panel (SIP) wall systems has helped significant increase in their use for residential and light commercial buildings over the past few years. Unlike wood-frame wall systems, there has been very limited number of shear loading tests performed on SIPs. Due to the highly competitive nature of the SIP market many SIP manufacturers perform their own testing and choose to keep the analysis and findings proprietary. This lack of published research in part results in some reluctance and resistance by contractors, engineers, and homeowners to use the product more extensively. For the same reason, the International Residential Code (ICC, 2006) limited the use of SIPs in seismic regions to sites within Seismic Design Category (SDC) A, B, or C.

This report, presents the results of a preliminary study involving a total of twenty-one 8 ft x 8 ft shear walls tested under monotonic and cyclic loading. Four 4.5 in. thick SIP panels and one traditional wood-frame wall were tested under monotonic loading according to ASTM E 564-06, and thirteen 4.5 in. thick SIP panels and three wood-frame walls were tested under the CUREE loading protocol according to ASTM E 2126-08. Parameters such as fastener type, spline design, hold-down anchor location, and sheathing bearing were adjusted throughout the testing in order to determine their effects on the SIP's performance. Performance parameters such as peak load and displacement, energy dissipation, allowable drift load capacity and seismic compatibility were determined as in a pilot study for all of the specimens and used to compare the SIP walls to the wood-frame walls and to determine the most efficient SIP design. Besides

providing some racking performance data, the report is intended to illustrate one of the approaches to determine seismic response parameters for SIP systems. Further testing as noted in the report is required before the results can be used for design purposes.

ACKNOWLEDGEMENT

This research presented in this report was made possible through partial support of Structural Insulated Panel Association (SIPA). The SIP panels for testing were donated by Timberline Panel Company. These contributions are gratefully acknowledged. In development of the research program and throughout the study the researchers benefitted from suggestions and comments by several individuals including Bill Wachtler, Jim DeStefano, Scott Maxwell, Jim Whalen, Borjen Yeh, Todd Bergstrom, Eric Tompos, Joe Hagerman, and Joe Pasma. For the experimental study the help of the following students is acknowledged: Dan Clark, Dan Navarrete, Joe Ridgeway, and Hiroki Ota. In particular, the invaluable help of BERL Laboratory Supervisor, Paul Kremer, in all aspects of the experimental work including test setup design, data acquisition system design, and data analysis is acknowledged. Finally, special thanks go to Professor Bo Kasal as the former Hankin Chair of Residential Construction (Penn State, Civil and Environmental Engineering Department, Pennsylvania Housing Research center) for his guidance throughout the project. The views and opinions expressed in this report are those of the authors and do not necessarily represent SIPA's or PHRC's position.

DISCLAIMER

The material presented in this report is for general public information on the subject. The material in this report including the test data and analytical results shall not be relied upon under any circumstances for any specific application or actual projects involving the SIP systems without consultation by a licensed design professional experienced in the field of light-frame design. Anyone using the material in this report assumes all liability resulting from such use, and the authors, Penn State University, PHRC, or SIPA are not in any way liable for such use.

TABLE OF CONTENTS

LIST OF FIGURES

LIST OF TABLES

Chapter 1

Introduction

1.1 Background

Structural Insulated Panel (SIP) wall systems have been used in residential and light commercial buildings for the past sixty years. Some of the earliest forms of the sandwich panel were developed at the end of World War II in response to a scarcity of building materials and to the development of new core and facing materials (Palms and Sherwood, 1979). These panels had a paper honeycomb core and their facings were usually made out of plywood or veneer (Palms and Sherwood, 1979). The sandwich panels used today mimic those of the past in which both are structural systems composed of a core material bonded to high strength facing materials. Some sandwich panels are made out of two reinforced slabs of precast concrete with a foam barrier, while others have aluminum sheets and a honeycomb interior. The most commonly used structural insulated panels in residential construction in the United States consist of a rigid foam insulation core of expanded polystyrene (EPS) and in some cases extruded polystyrene (XPS), polyisocyanurate, or polyurethane sandwiched between two sheets of either plywood or oriented strand board (OSB). Most manufacturers pressure-laminate the three pieces together to create SIPs, while some may use a foam-in-place method that requires injection of liquid foam (polyurethane or polyiscyanurate) between OSB skins. Under loading, every component of the SIP is stressed. The OSB or plywood skins act as

slender columns and must resist compression and tension while the core stabilizes the skins and resists buckling. According to Morley (2006), a SIP with a thicker core has the ability to resist more buckling than a panel with a thin core. Figure 1.1 shows an example of a home with walls made out of SIPs during the construction phase.

Figure 1.1: SIP home under construction (Insulspan, 2008)

Although SIPs have been present for decades, their demand has grown significantly in recent years (Mullens and Arif, 2006). This increase in popularity is the result of many different factors, some of which include the high thermal capacity of the panels and ease of construction. With the ever increasing energy costs, SIPs are very attractive with their ability to reduce heat loss by 40%-60% (Insulspan, 2008). More specifically, according to Insulspan (2008) a 4 in. thick SIP wall has an R-value of 13.83 compared to a traditional 2x4 stud wall with fiberglass insulation, which only has an

overall R-value of 9.68 or a 2x6 stud wall with fiberglass insulation and an R-value of 11. The erection time for a SIP house is significantly less than that of a traditional timber framed residence. The study performed by Mullens and Arif (2006) shows that using SIPs reduces the framing labor for walls and roofs by about two-thirds, which has a direct effect on the construction time. SIPs are easy to put together because they arrive on site pre-cut to the engineer's specifications. The individual panels are then joined together in the field with a spline and connection hardware. SIP manufacturers and contractors use various spline designs and different types of connection hardware which affects the construction procedure and panel strength.

Although extensive research has been performed on timber shear walls under high wind and seismic loading, there have been very limited number of similar tests performed on SIPs. Also, a majority of the research which has been performed is privately owned by individual SIP manufacturers. This lack of substantial information in part results in reluctance or resistance by contractors, engineers, and homeowners to more extensively use the product in various regions. Furthermore, for the same reason of lack of sufficient test data and better understanding of the seismic load resistance of SIP systems, the International Residential Code (ICC, 2006) has limited the use of SIPs to sites with Seismic Design Category (SDC) A, B, or C, which effectively limits its use in states like California that have SDC categories of D_1, D_2, E, or F (ASCE, 2005).

1.2 Objectives

The purpose of this preliminary research was to investigate the performance of SIP wall systems under a cyclic racking loading protocol. Parameters such as spline design, connection hardware, hold-down methods, and bearing of the sheathing on the bottom and top sill plates were studied throughout the testing in order to determine the effect they exhibit on panel strength. A traditional wood-frame wall was also tested under the same loading protocol so that the results obtained can be compared to those of the SIP walls. The comparison then allows one to determine if a SIP wall system will react similarly to a wood-frame wall under high wind and seismic loads. Another objective of this research was to illustrate one approach for determination of seismic response coefficients for SIP systems. A comprehensive testing program is necessary to develop seismic response parameters for practical design applications.

1.3 Research Approach

In order to accomplish the research objectives, a full-scale testing program was developed. A number of SIP wall systems with varying parameters were tested. The two most common spline designs used in the field were tested while the connection hardware was kept constant. Then, the three most commonly used connection hardware were tested while the spline design was held constant. A conventional wood-frame wall made out of the same OSB panels used on the SIP walls was also tested. Each specimen type was initially tested under monotonic loading so that the ultimate deflection could be obtained. Identical wall specimens were then tested under cyclic loading. The

experimental testing helped illustrate implementation of one approach to determine seismic characteristics of the wall system such as strength, stiffness, energy dissipation, and developing seismic response parameters. The data obtained from the experimental testing was then used to determine the effects varying parameters have on a SIP system so the most efficient design could be determined. Seismic characteristics of the SIPs were compared to those of the conventional wood-frame.

1.4 Report Organization

The material presented in this report is organized as follows:

Chapter 2 – The result of a literature review performed on structural insulated panel systems and shear walls under monotonic and cyclic loading is presented.

Chapter 3 – A description of the research program such as loading protocol and test matrix is discussed in addition to explanation of the test facility, specimen construction, and the instrumentation used to test the walls.

Chapter 4 – A description of the failure modes of the SIP shear walls and the traditional wood-frame walls under monotonic and cyclic loading is presented. Load vs. Displacement graphs, Envelope Curves, and photographs are also presented.

Chapter 5 – The characteristic values for the specimens tested, determined by following ASTM E 2126-08 and ICC-ES 130 are presented.

Chapter 6 – Parametric analysis of SIP and wood-frame shear wall designs based on characteristic values, their load capacity at allowable drifts, energy dissipated during cyclic loading, and fatigue loading are presented. A comparison of SIP shear walls to wood-frame walls according to ICC-ES AC04 Appendix A (2005) is also presented.

Chapter 7 – Summary of work performed, conclusions obtained and recommendations for future follow-up research is presented.

Chapter 2

Literature Review

2.1 Introduction

Due to the highly competitive nature of structural insulated panel manufacturers and contractors, the majority of the research performed in the past contains proprietary information. As a result, published experimental research studies on SIP wall systems is scarce compared to other innovative wall systems for residential construction such as steel stud panels and insulated concrete form (ICF) systems. SIP shear walls perform the same purpose as wood-frame shear walls but there is minimal information available that compares the two systems. The following sections summarize available research reports and articles pertaining to structural insulated panels and their performance as shear walls.

2.2 Construction Process

The first step in designing with structural insulated panels is to develop a detailed set of shop drawings through computer-aided drafting which show openings, corner connections, edges, and wiring chases (Pugh, 2006). From these shop drawings, the panels can be manufactured in a controlled plant environment to the exact specifications and delivered to the job site with pre-cut windows, doors, spline joints, and wiring chases. The controlled manufacturing environment aids in preventing warping and bending of the panels, which results in easier installation and better quality workmanship

(Pugh, 2006). Once the panels are on site, they are raised in full wall sections on the appropriate base and connected with the manufacturer suggested spline and fastener schedule. The use and placement of sealant and adhesive vary from contractor to contractor because currently the industry lacks specifications that would control the type or use of such products.

Mullens and Arif (2006) studied the effects SIPs have on the residential construction process by observing a case study of two Habitat for Humanity homes. One home was made out of SIPs, while the second was constructed with conventional wood-frame walls. Factors such as labor productivity, worker safety, waste material, necessary skill levels, and equipment requirements were compared. Mullens and Arif (2006) found that using SIPs saved two-thirds of the site framing labor for the walls and roof, and the Habitat for Humanity volunteers surveyed felt that SIPs reduced their effort by 50% in comparison to using conventional wood-frame walls. The study concluded that in order to make SIPs more attractive, the manufacturers should support homebuilders by increasing communication throughout the design-to-manufacturing phase, utilize panel waste, perform construction tasks in the factory such as inserting splines and framing out the windows and doors and reducing the costs of the panels.

2.3 Manufacturers

In May 2007, Section R614 was added as a supplement to the International Residential Code (ICC, 2007). Section R614 is a code-recognized prescriptive method to be used in SIP construction. The supplement is considered an important step for the SIP

industry because it means that contractors can demonstrate equivalence with the IRC by following the parameters of Section R614. They will no longer need the seal of a registered engineer to qualify for a building permit. The only problem is that Section R614 is limited to SIP designs that include surface splines and 8d nails. If the SIP design does not fall within the restrictions of Section R614 then SIP manufacturers must hire third party certified labs to perform tests on their panels. Most often the International Code Council – Evaluation Service, Inc. (ICC-ES) is then hired to take the testing results and arrange them into a form that is consistent with the intent of the code. The ICC-ES Report must then be accepted by the local code official (Maxwell, 2007).

Due to this practice (Maxwell, 2007), most SIP manufacturers have ICC-ES Reports readily available. The ICC-ES Legacy Report for Insulspan (ICC-ES, 2004) reports that the allowable racking load for panels with stapled 3 in. wide and 5/8 in. thick AD plywood surface splines is 208 plf, while it is 385 plf for nailed 2x Spruce Pine Fir wood splines. In Insulspan's Technical Bulletin No. 111 (INSULSPAN, 2007), the racking shear strength of SIPs with varying spline designs and nail spacing was determined. Insulspan followed ASTM E72 (2005) as modified by ICC-ES AC04 (2005) to test their panels. They reported the resulting allowable racking shear loads for 6.5 in. thick panels as follows:

-For 5.5 in. x 3 in. OSB insulated spline with 8d nails at 6 in. o.c., $P_{allowable}$ = 349 plf

-For Double 2x6 DF spline with 8d nails at 6 in. o.c. ., $P_{allowable}$ = 502 plf

-For Single 2x6 DF spline with 8d nails at 4 in. o.c. ., $P_{allowable}$ = 803 plf

-For Single 2x6 DF spline with 8d nails at 2 in. o.c. ., $P_{allowable}$ = 881 plf

These results demonstrate the effects spline design and connection spacing have on the racking shear strength of a SIP wall system.

In the ES Report PFC-6054 for Precision Panel Building Panels (ICBO Evaluation Service, Inc., 2002) , the allowable shear wall racking loads are 170 plf for 4.5 in. thick panels and 155 plf for 6.5 in. to 12.5 in. thick panels. Such results are for panels connected with 3 in. wide 7/16 in. OSB surface splines and fastened with 8d box or common nails at a maximum of 6 in. o.c.

The panels tested in the ICC-ES Legacy Report for Intermountain Building Panels L.L.C. (ICC-ES, 2003) are different from those previously presented because unlike the wood, OSB, or SIP splines most commonly used, Intermountain Building Panels uses metal studs to connect their panels. The panels are also fastened at the joints with 1.25 in. long, No. 6, Type S steel drill screws. As a result, the allowable in-plane racking shear load for a 6.5 in. thick panel with fasteners spaced at 3 in. o.c. is 415 plf. When the fasteners are spaced at 6 in. o.c. the allowable racking shear load is 360 plf.

The Load Design Charts provided by R-Control SIP manufacturers (R-Control Building Systems, 2008) do not specify the loading protocol which was followed, or the type of spline design or connection schedule used for the walls. The load design chart for a wall under shear loading does state that both a 4.5 in. thick and 6.5 in. thick panel can resist a shear load of 335 plf though.

According to the R-Control Tech Bulletin (R-Control Building Systems, 2008), 8 ft x 8 ft SIP walls and wood-frame walls were tested under the Structural Engineering Association of Southern California (SEAOSC) loading protocol (SEAOSC, 1997). This was the only SIP manufacturer that readily provided publicly available data of their wall

systems under cyclic loading. Both 4½ in. thick and 6½ in. SIP walls were tested. They both had 4x splines, top plates, bottom plates, and end posts. Hold-downs were used on the vertical boundaries, and in order to comply with IBC specifications, Do-All-Ply Sealant was only applied to the 4x wood members and the EPS core. The wood-frame wall had 2x framing members spaced at 24 in. o.c. and 4x top plates, bottom plates, and end posts. Both sides of the wall were sheathed with 7/16 in. OSB. 8d cooler nails spaced at 2 in. o.c. were used for the SIP and wood-frame walls. R-Control (R-Control Building Systems, 2008) followed the ICC-ES AC04 (2005) to compare the SIP and wood-frame wall and found that the SIPs were equivalent to the wood-frame shear wall under racking loading. The allowable racking shear load of the 4½ in. and 6½ in. thick SIPs was found to be 715 plf based on an 1/8 in. deflection.

Architectural Testing, Inc. followed ICC-ES AC04 (2005) to test Agriboard Industries' 8 ft x 8 ft compressed agricultural fiber sandwich panels (Architectural Testing, 2005). Two panel designs were tested, a 4 3/8 in. thick wall and a 7 7/8 in. wall. Both panels were sheathed with 7/16 in. OSB and had cores consisting of compressed wheat straw. 3½ in. laminated timbers were glued and stapled around the edges of the panels. The SEAOSC loading protocol (SEAOSC, 1996) was used to test the panels. ATI found that the average maximum force of the 4 3/8 in. wall was 14.1 kips, while that for the 7 7/8 in. wall was 23.7 kips. In both cases, the failure mode occurred in the shoe connector that was used to anchor down the walls. Unlike any other testing previously stated in this literature review, ATI calculated the seismic response modification coefficient. ATI reported calculated R=3.6 for the 4 3/8 in. wall and R=4.1 for the 7 7/8 in. wall. These values are simple approximations and cannot be used for design. In fact,

one of the major issues in obtaining code acceptance for SIPs in Seismic Design Categories D-F is that the seismic response coefficient, R has yet to be determined for SIP wall systems.

These are just a few examples of the many different SIP and sandwich panel manufacturers across the country. As can be seen, each manufacturer follows its own methods on issues such as framing, spline design and fastener schedule. These design differences have a direct effect on the strength of the panels. A commonality among the majority of SIP manufacturers presented is their lack of publicly available information concerning their panel's performance under cyclic loading. The monotonic shear strength can be used to determine a material's reaction to wind loading but it is not very indicative of the material's performance under seismic loading. R-Control and Agriboard Industries have tested their panels under cyclic loading but their reports lack a parametric analysis of the design methods such as spline design, connection hardware, or hold-down methods.

Based on the information reviewed in this section, the allowable loads (lb/ft) reported by various manufacturers are summarized in Table 2.1. Normally such allowable loads are determined by dividing the ultimate load by a safety factor of 3.0. In the table shown, the presumed ultimate load (lb/ft) is also estimated and listed. In addition, the ultimate load for an 8 ft long wall is calculated and listed. It can be seen that for all walls the predicted ultimate load capacity is less than 20,000 lb, with the exception of the Insulspan's specimen with a single 2x6 spline and 8d nails at 2 in. o.c. that shows an ultimate load capacity of 21,144 lb for an 8 ft long wall.

Table 2.1: Capacity of SIP shear walls

Manufacturer	Description of SIP	Allowable Load (lb/ft)	Ultimate Load (lb/ft)	Ultimate Load for 8 ft Long Wall (lb)
Insulspan	5.5 in.x3 in. OSB spline, 8d nails at 6 in. o.c., 6 in. thick SIP	349	1047	8376
	(2)2x6 spline, 8d nails at 6 in. o.c., 6 in. thick SIP	502	1506	12048
	(1)2x6 spline, 8d nails at 4 in. o.c., 6 in. thick SIP	803	2409	19272
	(1)2x6 spline, 8d nails at 2 in. o.c., 6 in. thick SIP	881	2643	21144
Precision Panel Building Panels	3 in.x7/16 in. surface spline, 8d nails at 6 in. o.c., 4.5 in. thick SIP	170	510	4080
	3 in.x7/16 in. surface spline, 8d nails at 6 in. o.c., 6.5 in.-12.5 in. thick SIP	155	465	3720
Intermountain Building Panels	1.25 in. long steel drill screws at 3 in. o.c., 6.5 in. thick SIP	415	1245	9960
	1.25 in. long steel drill screws at 6 in. o.c., 6.5 in. thick SIP	360	1080	8640
R-Control Building Panels	4.5 in.-6.5 in. thick SIP (spline and hardware not specified)	335	1005	8040

2.4 Performance

SIPs have become a popular building panel system not only for their thermal capacity and ease in construction, but also because of their structural strength. Every part of a SIP wall is stressed under loading. The outer skins resist compression and tension in such a way that they act like slender columns, while the inner core provides a continuous

bracing to the sheathing to resist forces trying to deflect or buckle the wall (Morley, 2007). The outer facing and inner core of the SIP work together to create a product which is much stronger than the OSB or polystyrene alone. As a result, the strength of the wall is completely dependent upon the bond between the two materials. According to NAHB (1995), SIPs perform very well under wind and seismic loading because they have structural sheathing on both sides as opposed to conventional wood-frame walls, which commonly only have structural sheathing on one side.

Palms and Sherwood (1979) investigated the long-term performance of different types of sandwich panels under various weathering conditions over a 31 year period. The research facility was designed so that the various sandwich panels could be removed, tested and reinstalled or replaced periodically. The original unit built in 1947 consisted of panels with plywood or veneer sheathing and paper honeycomb cores. Over the years the panels were replaced with new types of sandwich panels, for instance, panels with cement asbestos board facings and hardboard facings. In 1968 a pair of extruded polystyrene (XPS) panels with ¼ in. Douglas-fir plywood was used in the unit. All of the panels were tested for stiffness in accordance with ASTM E72-74a(1) (ASTM, 1974) before they were installed in the unit. The panels were then tested to failure when they were replaced. Palms and Sherwood (1979) found that the plywood-faced panels with corrugated paper cores performed the best. They actually became stiffer with age. The strength decreased over time in panels faced with paperboard, aluminum, and hardboard. The strength remained unchanged in a majority of the panels, however. Failure was usually caused by shearing in the core no matter what type of core material was tested. Palms and Sherwood (1979) noted that the polystyrene and polyurethane panels installed

in 1968 performed well both structurally and in terms of thermal capacity. The polystyrene and polyurethane panels demonstrated greater deflection than the panels with paper cores. This might be due to a "greater moisture content differential between inside and outside facings".

2.5 Design/Analysis

The APA's report, "Design and Fabrication of Plywood Sandwich Panels" (APA, 1990) presents recommended methods to follow when designing and fabricating plywood sandwich panels. Traditional engineering formulas were used to develop the methods and were then verified through experimental tests performed by the APA. The report provides equations to determine column buckling load, skin buckling, deflection, bending stress, combined stress, and shear stress. The structural design of other important details such as connections, joints, and finishes were not specified in the APA report.

There are a limited number of resources available that present design methods for SIPs but there are many available for conventional wood-frame walls. For instance, Tuomi and McCutcheon (1978) developed a mathematical method for determining the racking strength of wood-frame walls and then verified their method with laboratory tests. Their method is based upon the belief that the racking strength of a wall is closely related to the lateral strength of the connections used. Tuomi and McCutcheon made the following assumptions when developing their equations: 1) there is a linear load/distortion relationship for a nail during cyclic loading; 2) during loading the sheathing remains in its original shape while the frame distorts into a parallelogram

shape; 3) the nails are "evenly and symmetrically spaced"; and 4) the deflections of the wall are minimal. The theoretical equations developed take into account the geometry of the sheathing, the number of horizontal and vertical nails used, and the lateral resistance of the nails. Both small-scale and large-scale setups were tested under static loading per ASTM E72-74a (ASTM, 1974) to verify the theoretical equations. Tuomi and McCutcheon (1978) found that the theoretical equations correctly predicted the racking strength of the wall and that small-scale tests provided consistent results with the large-scale tests. Unlike previous racking strength equations of their time, Tuomi and McCutcheon's equations account for panel geometry and nailing patterns.

Folz and Filiatrault (2001) used previous static loading analysis techniques, such as Tuomi and McCutcheon's research, to develop their own model. Folz and Filiatrault (2001) developed a numerical model which could be used to determine the response of conventional wood shear walls under cyclic loading, which is more indicative of a structure's response under seismic loading. Assumptions that were made during the model formulation process include the following: the basic structural components of a wood shear wall are framing members, sheathing panels, sheathing-to-framing connectors, and hold-down anchorage devices. In addition, the framing members are rigid and modeled with pin-ended connections, each panel experiences four degrees of freedom, and a dowel-type connector in a shear wall is nonlinear under monotonic loading and "exhibits pinched hysteretic behavior with strength and stiffness degradation under general cyclic loading". Folz and Filiatrault (2001) decided to create a "specific hysteretic model based on a minimum number of path-following rules" in order to mimic how a connector would react under cyclic loading. The numerical model was then

incorporated into the computer program CASHEW, which allowed them to predict the load-displacement response and energy dissipation of the shear wall under quasistatic cyclic loading. CASHEW was then used to calibrate a nonlinear single degree of freedom model. This SDOF model was used to determine the seismic response of a shear wall under ground motions caused by an earthquake. The model was verified with shake table tests.

2.6 Experimental Research

The first notable published study on the performance on SIPs under in-plane shear loading is by Jamison (1997) who performed monotonic and cyclic tests on several 8 ft x 8 ft SIP specimens. In this study, ASTM E564 was followed for monotonic tests, while the Sequential Phased Displacement (SPD) procedure developed by Porter (1987) was used for cyclic racking tests. The latter test procedure was later adopted with slight modifications by Structural Engineers Association of Southern California (SEAOSC) in 1996 and is known as "Standard Test Method of Cyclic (Reversed) Test for Shear Resistance of Framed Walls for Buildings" or simply the "SEAOSC Method".

In Jamison's study, twelve monotonic and eleven cyclic tests were carried out on four different configurations, with the reference configuration consisting of one 2 in. x 4 in. top and bottom plates, 1 in. x 4 in. end studs, and one 2 in. x 4 in. middle stud used to connect the two 4 ft x 8 ft panels to make 8 ft x 8 ft wall specimens. The three main variations to this basic configuration included one configuration with double bottom plates, one configuration with tie-down devices on the outside of end studs, and one

configuration with ½ in. x 5 in. spline and 2x4 end studs. In these specimens, construction adhesive and drywall screws were used to attach the panels to framing members and top and bottom plates. ASTM E564 was followed for the test setup.

Some of the conclusions of the study are as follows: 1) the variation of vertical connecting elements between panels and on panel ends do not significantly affect the performance; 2) the bottom plate connection is the critical connection; 3) the addition of tie-down anchors will shift the failure point away from the bottom plate and increase the capacity as well as stiffness and energy dissipation capacity; and 4) with respect to capacity, the difference between monotonic test results and the initial cycles of cyclic test is minimal. The study further compared the SIP wall capacities with available wood-frame wall capacities and concluded that SIP walls without tie-down anchors had much lower peak load resistance, but those with tie-down anchors had comparable load resistance. The study acknowledged that it was the first cyclic testing investigation on SIPs and further research was necessary. Noted recommendations for future research included the effect of other fastener types and spacing, vertical gravity load along with tie-down anchors and parameters important for seismic design including stiffness, ductility, damping, and energy dissipation.

The APA has recently been conducting a number of experimental studies for the Structural Insulated Panel Association (SIPA). In the APA Report T2006P-33 (2006) expanded polystyrene (EPS) Premier Building Systems SIPs were tested under four different loading protocols: racking shear, axial loading, transverse loading and lintel test. For the Prescriptive Method study, APA used the test setup recommended in ASTM E72-05 (2005) as required by ICC-ES AC04 (2005) document. Shear design capacities were

developed for four different specimen configurations consisting of 4 ½ in. x 8 ft x 8 ft, 6 ½ in. x 8 ft x 8 ft, 4 ½ in. x 8 ft x 10 ft, and 6 ½ in. x 8 ft x 10 ft wall dimensions. In all of the tests, 3 in. wide OSB surface spline and common 8d nails at 6 in. o.c. were used. The panels were bolted to the test facility at bottom and top plates and the load was applied through the top load beam. The shear test results reported include ultimate load, allowable design load (ultimate/3.0), and load at 1/8 in. deflection. The majority of the failure modes occurred in the nailed connections along the splines. The report is a useful resource for builders and engineers but it does not further research design aspects such as connection type, spacing and spline design in order to determine their effect on wall performance. APA Report T2006P-33 also fails to address the use of SIPs in seismic design categories D, E, and F.

Kermani and Hairstans (2006) tested SIPs under racking loads and combined bending and axial compression in order to determine the effects size and location of openings have on the performance of SIPs. They then compared the results to expected design values found with BS 5268 and Eurocode 5 (BSI, 2004). BS EN 594:1996 and BS 5268: Section 6.1: 1996 were followed in order to perform the racking load tests. The polystyrene specimens tested were 4.6 in. x 8 ft x 8 ft with a wood stud as the spline and 1.38 in. long, 0.104 in. diameter screws spaced at 9.8 in. o.c. as the connection hardware. The bottom of the wall was screwed into the base while the top of the wall experienced a constant vertical load of 0 kN, 12.5 kN, or 25 kN. Polystyrene specimens without any cut-outs were tested and compared to specimens with cut-outs of various size and location. The failure mode of walls with and without any openings occurred in the connection hardware. In this case, screws were used like Jamison's research but unlike

the APA Report. It would be an important resource to have research comparing connection hardware types on identical test specimens and under a constant test setup. Kermani and Hairstans (2006) concluded that not only is the racking strength of SIPs directly related to the size of the openings but SIPs with openings are more efficient than identical stud walls. They also found the performance of SIPs with and without openings to be adequately consistent with the Eurocode 5 design values.

Similar to the previously stated tests, Carradine, et al. (2004) found in their research that during monotonic testing of SIPs connected as diaphragms to wood-frame the failure mode occurred in the screws used to attach the two elements. The objective of their research was to demonstrate the increased lateral strength of a wood-frame with SIP diaphragms and to determine the effect connection spacing and edge boards have on the system's cyclic characteristics. Roof panel assemblies of both 8 ft x 24 ft and 20 ft x 24 ft with OSB surface splines and 8d ring shank nails at 8 in. o.c. to connect the SIPs and 11.78 in. x 0.19 in. screws at 12 in. o.c. to attach the SIPs to the wood-frame were tested under both monotonic and cyclic loading. Information such as diaphragm strength and stiffness data were obtained through the monotonic testing. The CUREE loading protocol (Carradine et al., 2004) was used to determine ductility, strength and stiffness degradation and energy dissipation. Carradine et al. (2004) concluded that increasing the size or decreasing the spacing of the screws used to connect the SIPs to the wood-frame would increase the shear capacity of the system. The cyclic testing allowed them to verify the IBC 2000 (ICC, 2000) design procedures and suggest that designers use a Response Modification Coefficient, R, of 1.5 when calculating seismic forces. The study noted that a complete diaphragm-frame interaction design cannot be executed without

additional testing performed on SIP and wood-frame end walls to determine their stiffness and strength.

Manbeck and Taylor (1991) used testing facilities at Pennsylvania State University to determine the structural properties of Murus structural insulated panels in accordance with suggestions made by the Building Officials and Code Administrators International, Inc (BOCA). The testing included the SIP performance under lab aging, flatwise tension, edgewise compression, flatwise compression, flexural properties, and racking capacity. Murus panels are different than those used in the previously stated research reports in regards to the fact that they have a urethane foam core and a cam lock system which acts as the spline. Three different wall specimen designs were tested, a full size 4.5 in. x 8 ft x 10 ft wall specimen, the same size wall as the first but with a 2.7 ft x 4.5 ft window cut-out, and a wall with a 2.4 ft x 7 ft door cut-out. All specimens were attached to a timber load beam and base beam with screws at 8 in. o.c. The base beam was then attached to the foundation with ½ in. bolts at 24 in. o.c. Following the loading protocol described in ASTM 564-76, Manbeck and Taylor found that the full panel specimen performed better than both the door and window specimens. The failure mode of all three specimens occurred in the screws that attached the SIPs to the base beam. This failure mode is consistent with previously stated research. The data obtained from the racking tests was then compared to Toumi and McCutcheon's (1978) method of analysis. The study concluded that the analysis and experimental values were very closely related.

2.7 Summary

There are a significant number of articles describing the advantages of SIP wall systems but it is evident that there is a limited amount of available experimental testing performed on SIPs under cyclic loading. As a result, cyclic testing performed on wood-frame shear walls were used to help guide this research in terms of test setup, the importance of certain parameters, and the expected mode of failure of the wall system.

Chapter 3

Research Program and Test Setup

3.1 Objectives

The primary objective of this study was to gain a better understanding of how structural insulated panels perform under large lateral loads caused by seismic events and wind. Parameters such as joint design, connection hardware, sheathing bearing and hold-down methods were tested in order to determine their effect on the SIP wall system. The preliminary data and results obtained are intended to develop better understanding of the seismic behavior of SIP wall systems with different fasteners and splines and also help development of more comprehensive follow-up studies. The panels tested were provided by Timberline Panel Company, LLC, a SIP manufacturer prevalent in the current SIP market. Hold-downs were used but sealants were not used. The hold-down anchors help to resist overturning and achieve a failure mode under ultimate loading. Previous studies have found that sealants and adhesives have an effect on the performance of SIP and wood-frame shear walls (Filiatrault and Foschi, 1991), but manufacturers not only use their own types of sealants and adhesives but they also use different techniques to apply them. In order to make sure the results of this research are useful to the industry, the sealants and adhesives were left out. The results will be conservative regardless of the type of manufacturing method used.

The shear resistance of the SIP wall system was compared to that of a conventional wood-frame under static monotonic and cyclic loading. ASTM E 564-06 (2006) was followed to place the wall systems under static load. The procedure for full-scale in-plane racking followed the CUREE loading protocol (Carradine et al., 2004) as prescribed by ICC-ES AC130 (2007). ASTM E 2126-08, ICC-ES AC130 and ICC-ES AC04 Appendix A (2005) were used to evaluate the SIP wall systems. The results also provide a basis for comparison of the effects the parameters have on SIP wall systems.

In order to accomplish these objectives, a number of tasks were performed:

- Review the available literature
- Determine the design and construction of the specimens that mimic the methods used in the field
- Develop a test setup that demonstrates conventional boundary elements
- Develop plan for instrumentation and data acquisition system to use for testing
- Test SIP configurations under monotonic loading and collect data
- Test wood-frame shear walls under monotonic loading and collect data
- Test SIP configurations under reversed cyclic loading and collect data
- Test wood-frame shear walls under reversed cyclic loading and collect data
- Compare performance of various SIP configurations
- Compare performance of SIP wall systems and wood-frame shear walls based on ICC-ES AC04 Appendix A (2005)
- Develop conclusions and recommendations
- Write research report

3.2 Experimental Procedure

3.2.1 Monotonic Tests

In order to determine the response of a SIP wall under cyclic racking, the wall must first be tested under static monotonic loading. From the static monotonic loading a load-displacement relationship can be determined as well as the shear stiffness and strength of the panel (ASTM E564-06, 2006). Standardized monotonic loading procedures for wood-frames are presented in ASTM E 72-05 (2005) and ASTM E 564-06 (2006). The major difference between the two test procedures lies in the required test setup. ASTM E 72-05 calls for a large timber load beam, tie-rods used to prevent vertical deflection of the wall at the load application point, and a stop at the bottom corner of the wall to prevent the wall from sliding. In ASTM E 564-06 the load is applied directly to the top plate of the wall and hold-downs and anchors consistent with those used in the field are used to prevent uplift and sliding of the wall. ASTM E 564-06 was followed in this testing program to determine the load-displacement relationship of the wall systems as noted in ICC-ES AC130 Acceptance Criteria for Prefabricated Wood Shear Panels.

3.2.2 Cyclic Tests

Testing shear walls under static monotonic loading is useful in determining the shear stiffness and strength of the panel under wind loading, but there has been some concern within the engineering field that the quasi-static testing is not consistent with the load imposed on a shear wall during a seismic event. The extensive damage caused by

the Northridge Earthquake in 1994 caused the engineering field to assume that static-monotonic testing provides unconservative results in relation to seismic loading (Gatto and Uang, 2003). As a result, a number of cyclic loading protocols such as the CUREE-Caltech standard (Carradine et al., 2004), the Standard Method of Cyclic (Reversed) Test for Shear Resistance of Framed Walls for Buildings by the Structural Engineers Association of Southern California (SEAOSC, 1996), the Sequential Phased Displacement (SPD), Forintek Canada Corporation (FCC), and the ISO 16670 Protocol have been developed. Gatto and Uang (2003) researched the effects different loading protocols have on the performance of the shear walls. They tested 8 ft x 8 ft wood-frame shear walls under monotonic, CUREE, ISO, SPD, and CUREE Near Fault loading protocols. Gatto and Uang concluded that wood-frame shear walls tested under the standard CUREE loading protocol had failure modes which were the most consistent with those developed during seismic behavior. They recommended that the CUREE protocol be established as the standard for wood-frame testing.

Based on previous testing and research, the loading protocol developed as part of the CUREE-Caltech Wood-frame project was used in this study. The standard CUREE loading protocol is also consistent with Appendix A of the ICC-ES AC130 Acceptance Criteria for Prefabricated Wood Shear Panels and research performed by Filiatrault and Folz (2002), Wilcoski et al (2002), Lebeda et al (2005), and McMullin and Merrick (2007). The loading protocol is based on the hysteretic response of wood-frame structures. The protocol was developed specifically for wood-frame shear wall testing and has the ability to model ordinary ground motions typically experienced during earthquakes in California. The loading history consists of three major cycles. The first

cycles are the initiation cycles which are applied at the very beginning and used to determine the force-deformation response at small amplitudes, the second cycles are the primary cycles, which are larger than the initiation cycles, and the trailing cycles which are 75% of the amplitude of the primary cycles are the final cycles. All of the testing is controlled by deformation (Krawinkler et al. 2001). Figure 3.1 shows a graph of the CUREE loading protocol and Table 3.1 describes the sequence of cycles. In Table 3.1 Δ=0.6 Δ_m, where Δ_m is the monotonic deformation capacity found when the load capacity drops below 80% of the maximum load. The 0.6 factor takes into account the cumulative damage incurred during cyclic testing, which will cause earlier deterioration of strength of the wall panel in comparison to monotonic testing (Krawinkler et al, 2001).

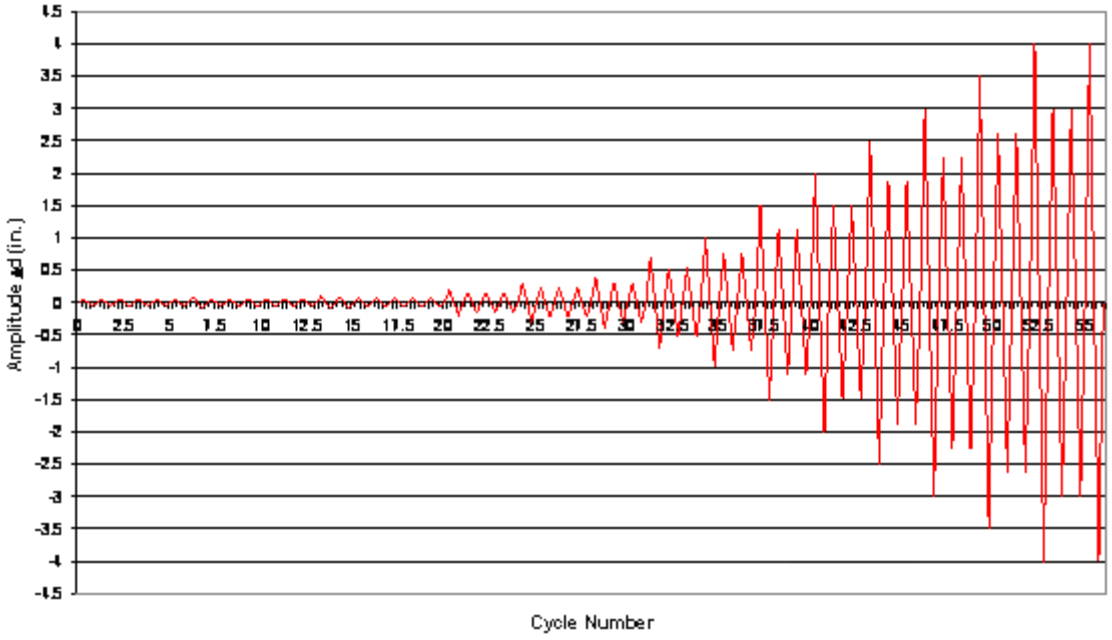

Figure 3.1: CUREE loading protocol showing cycle number vs. target displacement

Table 3.1: CUREE Basic Loading History For Prefabricated Shear Panels

Cycle Number	**%Δ**
1 to 6	5.0
7	7.5
8 to13	5.6
14	10
15 to 20	7.5
21	20
22 to 24	15
25	30
26 to 28	23
29	40
30 to 31	30
32	70
33 to 34	53
35	100
36 to 37	75
38	150
39 to 40	1□3

3.3 Test Setup

The Dynamic Racking Facility in the Architectural Engineering Lab at The Pennsylvania State University was used to test the wall systems. The test facility can

apply a maximum load of 20,000 lb and can displace a total of 6 in. In Jamison's (1997) testing program the 8 ft x 8 ft x 4.5 in. SIP shear walls attached with 6 in. o.c. drywall screws and secured with Simpson tie-downs failed at a load of 7,050 lb and 0.68 in. under monotonic loading and 6,450 lb and 0.60 in. under cyclic loading. In Kermani and Hairstans' (2006) report the 8 ft x 8 ft x 4.6 in. SIP shear walls attached with 9.84 in. o.c. screws failed at 2,878 lb under monotonic loading. The mean ultimate failure load of the SIP walls tested in the APA Report T2006P-33 (2006) was 7,848 lb. The specimens were 8 ft x 8 ft x 4.5 in. and connected with 8d common nails spaced at 6 in. o.c. Finally, as shown in Table 2.1, the ultimate load capacity determined based on reported allowable load for almost all types of SIP configurations had values smaller than 20,000 lb. Due to this previous research it was assumed that the Dynamic Racking Facility in the Architectural Engineering Lab had the adequate capacity to fully test and fail the SIP specimens chosen for the study.

Figures 3.2, 3.3, and 3.4 show photographs of the test facility with the wall in place and Figures 3.5 through 3.12 are AutoCAD drawings which show more hardware detail. 5/8 in. diameter cap screws spaced at 1 ft from each end of the wall and then 2 ft o.c. were used to attach the sill plate to the L8x6x1/2 and the top plate to the MC8x20. USP PHD6 hold-downs were attached to the double end posts of the wall with eighteen WS3 wood screws and into the sill plate and base support (L8x6x1/2) with 7/8 in. diameter bolts. The base support consisted of a L8x6x1/2 attached with 1 in. diameter cap screws to the bottom sliding steel tube of the test facility. The MC8x20 was sized according to ASTM E 2126-07a (2007) so that it did not apply any substantial vertical load. Additional vertical load increases the lateral stiffness and energy dissipation

capacity of a wall leading to unconservative results (Johnston et al., 2006). The load was applied from the sliding steel tube of the test facility to the MC8x20 through a threaded rod into a sliding connection. The sliding connection was cut into a L6x6x3/4 attached to the end of the MC8x20. The angle was thick enough to resist bending and the sliding connection allowed the wall to deflect vertically in both directions a maximum of 1 in. As can be seen in Figures 3.7 and 3.9, L5x3x1/4 angles were attached to the underside of the upper sliding tube on the facility and hooked into the MC8x20 in order to prevent out-of-plane deflection of the wall.

During the design process of this test setup, much consideration was given to ASTM standards, ICC-ES Acceptance Criteria, previous research performed on structural insulated panels and wood-frame shear walls, and suggestions made by engineers, contractors, and lab technicians in the engineering field.

Toothman (2003) tested 4 ft x 8 ft wood-frame walls with various sheathing materials under both monotonic and cyclic loading. He followed ASTM E 564-95 (1995) for the monotonic loading and the SPD cyclic loading protocol described in ASTM E 2126-01 (2001). Toothman found that both the sheathing material and hold-downs had a significant effect on the strength of the wall. Ultimately the failure mode in the OSB sheathed walls occurred in the bottom plate when the nails pulled out of the framing or through the sheathing. At that point the end stud then separated from the top plate which caused the wall to fail.

Johnston et al. (2006) and Lebeda et al. (2005) both researched the effects hold-down anchors have on 8 ft x 8 ft wood shear walls under the CUREE loading protocol. Johnston et al. (2006) found that hold-down anchors nearly doubled the strength of a

wood-frame wall under cyclic loading. The hold-down anchors had minimal effect on the stiffness and energy dissipation capacity of the wall when a vertical load of at least 850 lb/ft was applied. Walls with the hold-down anchors experienced failure due to crushing of the sheathing corners and pull-out of the sheathing nails along the sill plate and spline, while walls without hold-down anchors failed when the wall detached from the bottom sill plate and the remaining wall shifted as a single unit. Lebeda et al. (2005) determined that the misplacement of hold-down anchors caused a reduction in the shear wall energy absorption and affected the failure mode.

Figure 3.2: Photograph of test facility with wall in place

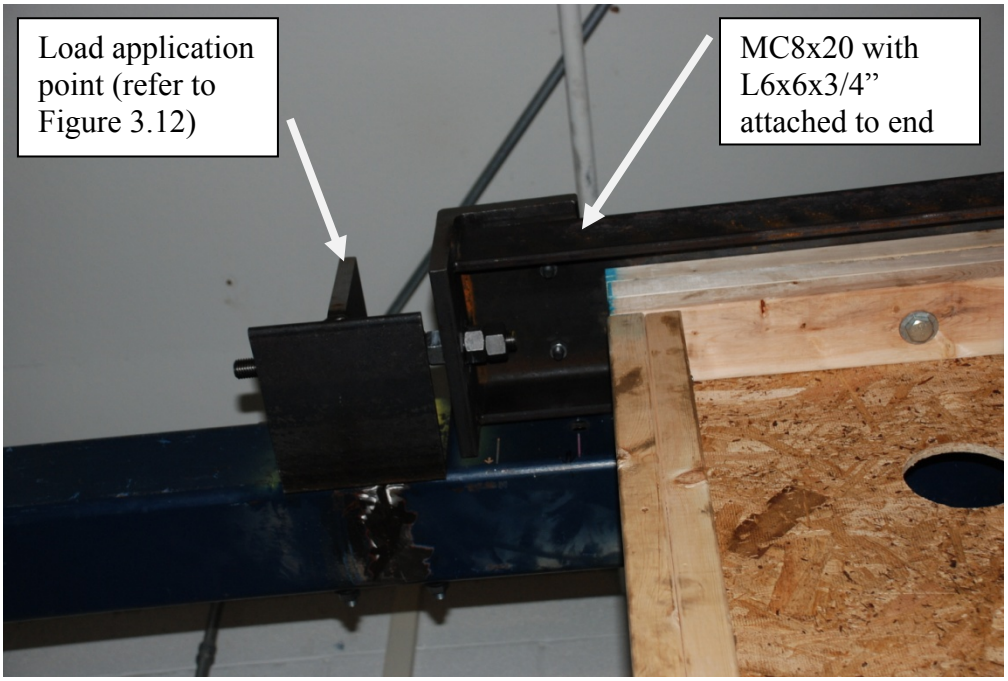

Figure 3.3: Load application point located at top left of wall

Figure 3.4: UPS PHD 6 hold-down anchor

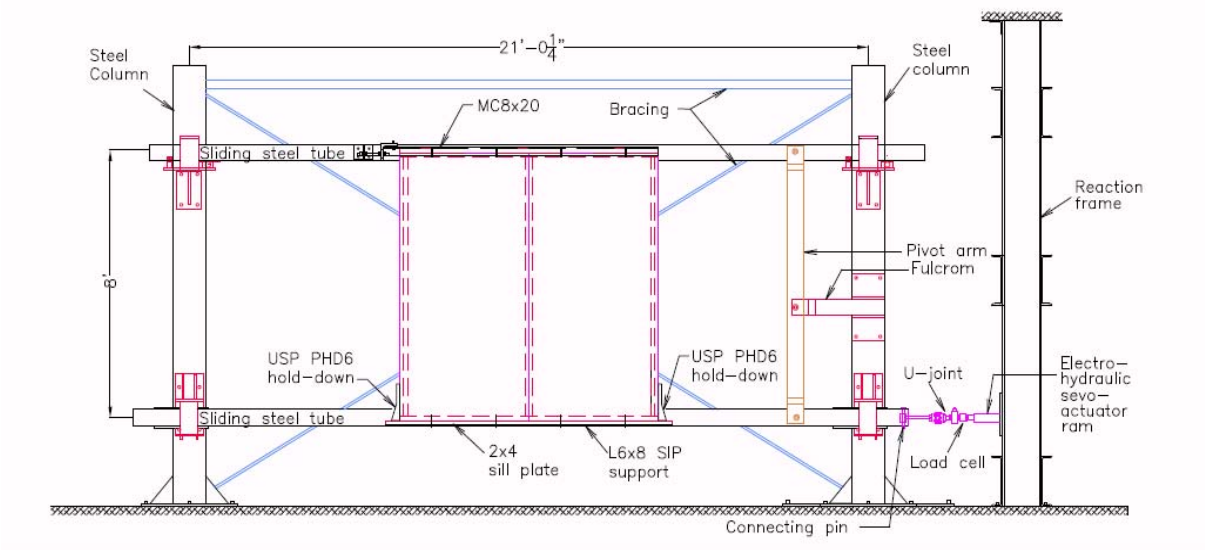

Figure 3.5: Cyclic racking test facility

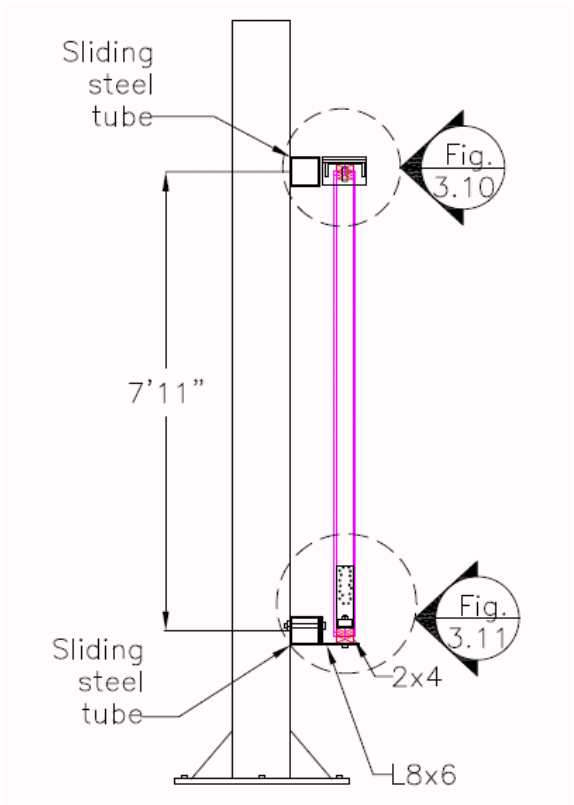

Figure 3.6: Vertical section through cyclic racking test facility

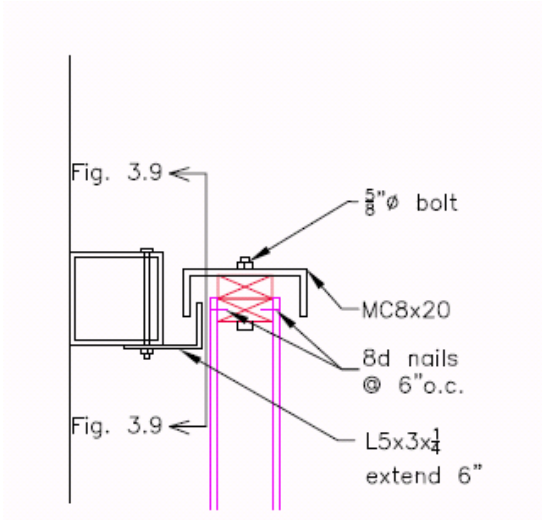

Figure 3.7: Top of wall connection showing out-of-plane brace

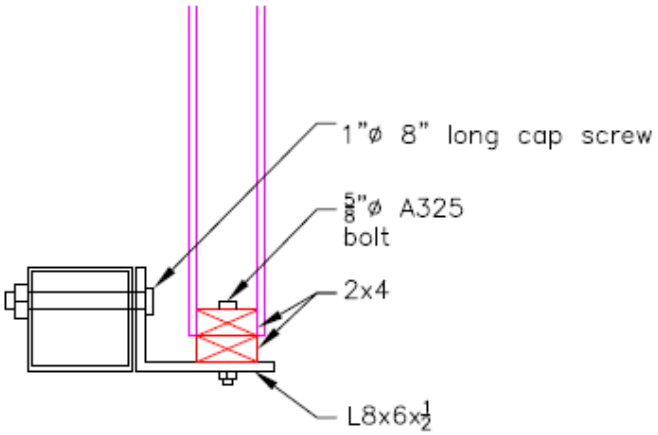

Figure 3.8: Bottom of wall connection

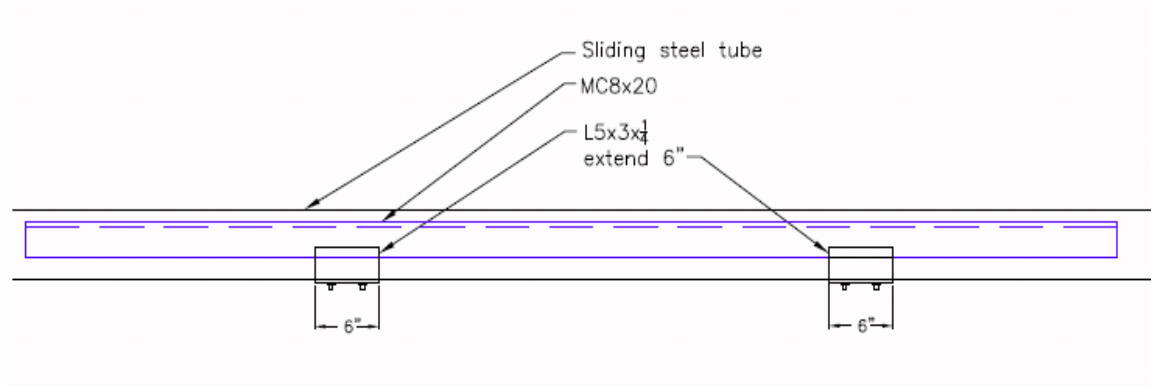

Figure 3.9: Out-of-plane bracing attached along sliding steel tube of racking facility

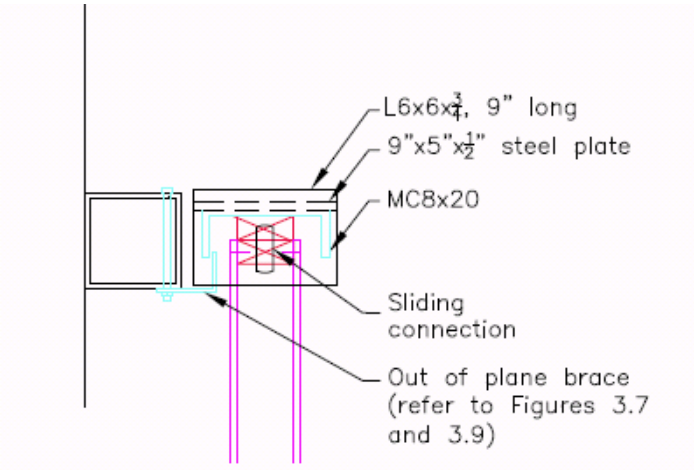

Figure 3.10: Top of wall detail showing load application connection

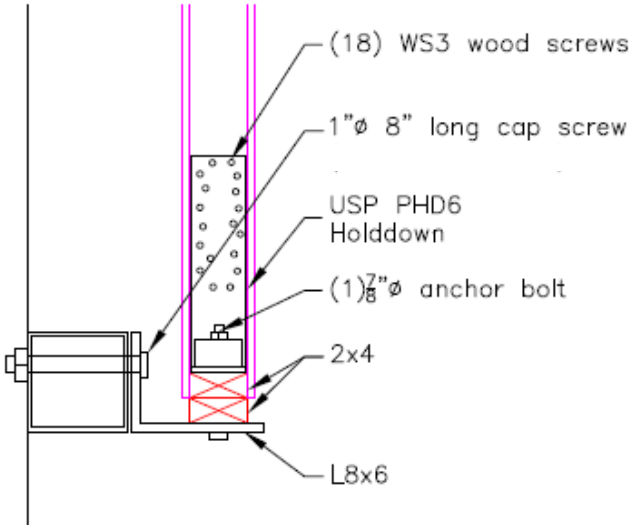

Figure 3.11: Bottom of wall detail with hold-down anchor

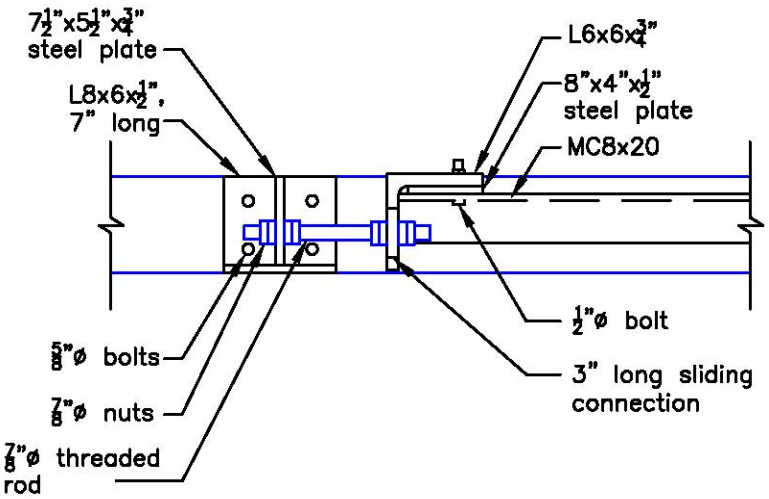

Figure 3.12: Load application detail along top sliding steel tube of racking facility

3.4 Specimens

Four of the most common joint configurations currently used in the field are identified in Figure 3.13, 3.14, 3.15, and 3.16. Testing involved the two most common types, that is, the OSB surface spline (Figure 3.13-Joint A) and the double 2x4 spline (Figure 3.14-Joint B). A conventional 8 ft x 8 ft wood-frame wall was also tested and used as a comparison for the SIP walls. In addition to testing the joint configurations, three different types of connection hardware such as nails, staples, and screws were tested. To mimic current practices, the fasteners include 8d common nails at 6 in. o.c., 1.25 in. screws at 6 in. o.c., and 1.5 in. 16 gage staples at 6 in. o.c. Table 3.2 describes the details of the configurations tested. In order to minimize the number of different configurations because of resource limitations, the OSB spline configuration with three types of fasteners were considered, but only nail fasteners were used for the double 2x4 spline. To determine the effect of cutting into a SIP to place an internal hold-down, which is the common practice in the field, one of the walls was tested with an internal hold-down. Also, a wall in which the sheathing bears on the sill plate and top plate was also tested. As a result, in Table 3.2, there are six different SIP configurations and one conventional timber stud wall configuration. A total of twenty-one walls were tested.

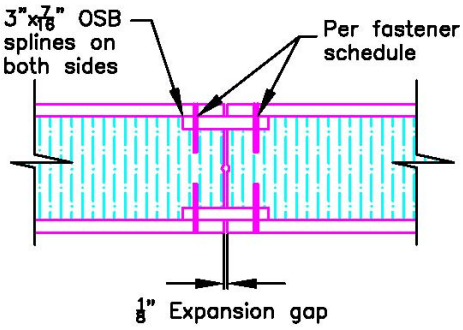

Figure 3.13: Joint A – Surface spline made out of 3 in. x 7/16 in. OSB

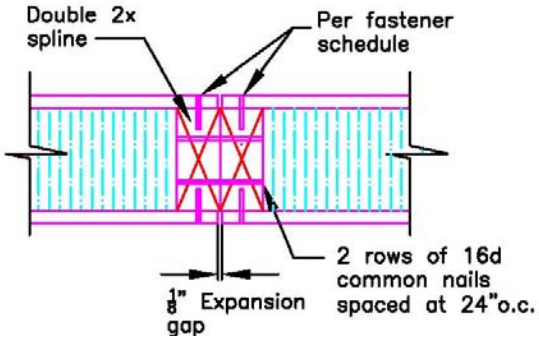

Figure 3.14: Joint B – Double 2x spline

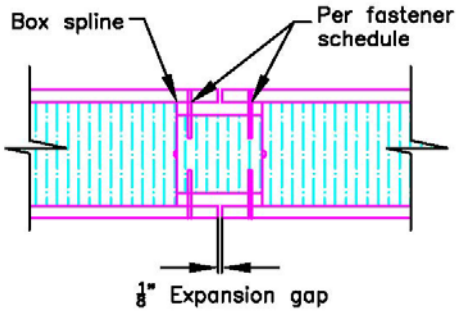

Figure 3.15: Joint C – Box spline made out of smaller SIP

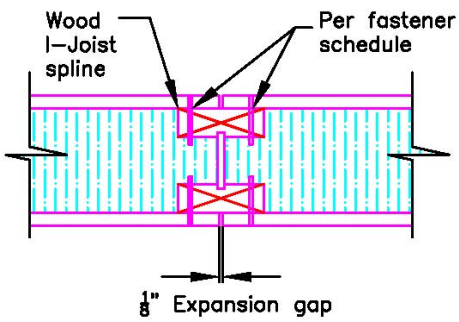

Figure 3.16: Joint D – Wood I-joist spline

Table 3.2: Test Matrix of Specimens Tested

Panel Type	Panel to Panel Connection	Bottom Plate	Top Plate	End Posts	Fastener Hardware	Fastener Spacing	Bearing	External Hold-down
A1 Includes: A1-1M A1-1C A1-2C	7/16"x3" OSB surface spline	(1) 2x4	(1) 2x4	(2) 2x4	8d common nail	6" o.c.	No	Yes
A1 Bearing- 3C	7/16"x3" OSB surface spline	(1) 2x4, (1) 2x6 sill plate	(1) 2x4, (1) 2x6 top plate	(2) 2x4	8d common nail	6" o.c.	Yes	Yes
A1 Internal- 4C	7/16"x3" OSB surface spline	(1) 2x4	(1) 2x4	(2) 2x4	8d common nail	6" o.c.	No	No (internal hold-down)
A3 Includes: A3-1M A3-1C A3-2C A3-2C(2)	7/16"x3" OSB surface spline	(1) 2x4	(1) 2x4	(2) 2x4	1.5" 16ga. staple	6" o.c.	No	Yes
A4 Includes: A4-1M A4-1C A4-2C A4-3C	7/16"x3" OSB surface spline	(1) 2x4	(1) 2x4	(2) 2x4	1.25" screw	6" o.c.	No	Yes
B Includes: B-1M B-1C B-2C B-3C	Double 2x4 spline	(1) 2x4	(1) 2x4	(2) 2x4	8d common nail	6" o.c.	No	Yes
C (Wood-frame) Includes: C-1M C-1C C-2C C-3C	-	(1) 2x4	(2) 2x4	(1) 2x4	8d common nail	6" o.c. ext, 12" o.c. int	No	Yes

The base test setup included two 4 ft x 8 ft panels joined with a OSB spline and fasteners at 6 in. o.c. All of the wood used was Spruce Pine Fir of Grade 2 or better bought at a local lumber yard. The top and bottom plates were 2x4 and an additional 2x4 was attached to the top and bottom plates in order to connect the wall to the test facility. This additional 2x4 prevented bearing between the sheathing and test setup. Common

practice in the field is to have the sheathing bear directly on the sill plate, but testing the walls with non-bearing sheathing will actually provide conservative results. The double end posts and the top and bottom plates were connected with 16d common nails spaced per the 2006 International Building Code (ICC, 2006). For the base test setup, USP PHD6 Hold-downs were attached to the outside of the SIP and conventional wood-frame wall.

In Specimen A1 Bearing, the only variation from the base setup involved the top and bottom plates. In place of the 2x4's used to attach the bottom plate to the angle and the top plate to the wide flange beam, 2x6's were used. This allowed determination of the effect non-bearing sheathing has on the SIP's performance. In Specimen A1 Internal, the fastener spacing was still 6 in. o.c., but 15.5 in. x 13.5 in. sections were cut out of the SIP wall to place the two USP PHD6 Hold-downs on the inside of the panel. The OSB sheathing along the end posts and the base plate were not cut so the sheathing was still attached along the bottom corners of the panel with the typical nailing pattern.

The SIPs were 4.5 in. thick with a 3.5 in. thick core of expanded polystyrene (EPS) and 7/16 in. OSB facings. Two 4 ft x 8 ft panels were connected along the 8 ft vertical side to create one large 8 ft x 8 ft panel, as shown in Figure 3.2.

The traditional wood-frame wall was sheathed on both sides with 7/16 in. OSB oriented vertically. The OSB was donated by Timberline Panel Company, LLC and taken from the same batch that was used to make the SIPs tested in this research. 2x4 Spruce Pine Fir of Grade 2 or better were used as studs and placed at 16 in. o.c. The specimens had a double 2x4 top plate, single 2x4 base plate and double 2x4 end posts to mimic common field practices. The sheathing was attached to the studs with 8d common

nails spaced at 6 in. o.c. for the exterior of the panel and 12 in. o.c. at the interior of the panel. The nailing patterns described in the 2006 International Building Code (ICC, 2006) were followed to connect the framing members with 16d common nails (just like the SIP specimens). Similar to the SIP specimens, a 2x4 was placed above the top plate and below the base plate of the wood-frame specimen to prevent the sheathing from bearing against the test facility. The USP PHD 6 hold-down anchors were placed on the exterior of the wood wall to mimic the test setup of the SIP specimens.

3.5 Instrumentation

Two LVDTs, eight string potentiometers, and two rotation sensors were used to measure the deflection in the wall system and the test setup. There were also two linear potentiometers on the racking facility used to measure the displacement of the top and bottom sliding steel tubes. The racking facility also had a sensor used to measure the displacement of the actuator and a load cell placed at the end of the actuator to measure the load applied to the test setup. Figure 3.17 shows the sensor placement. The channel descriptions are as followed:

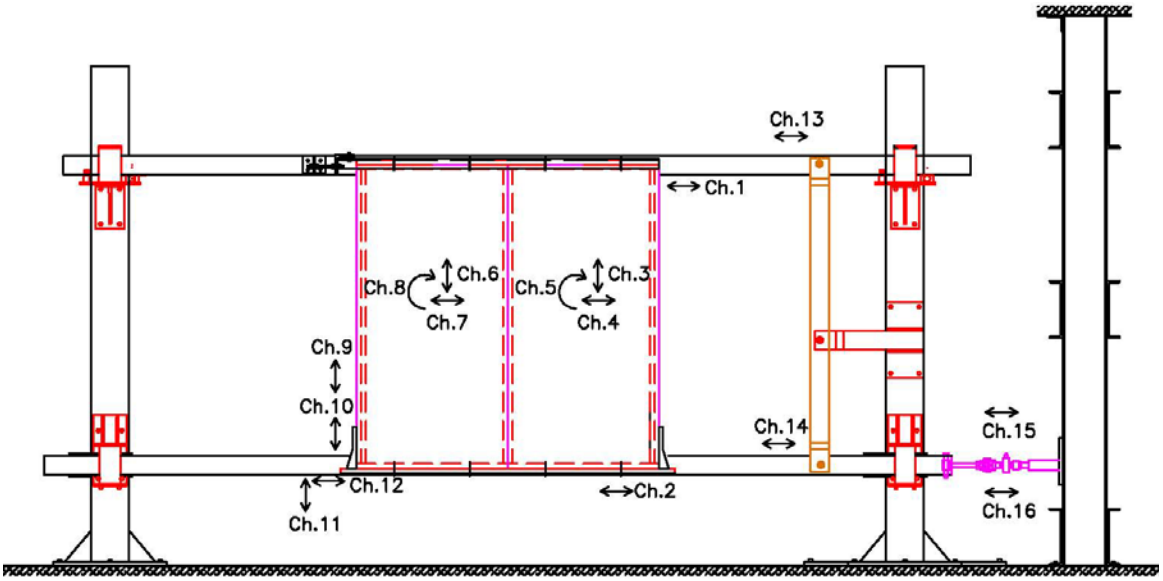

Figure 3.17: Elevation view of sensor locations

Ch. 1: LVDT – Horizontal deflection of the top plate relative to top sliding steel tube. Refer to Figure 3.18.

Ch. 2: LVDT – Horizontal deflection of the base plate relative to bottom sliding steel tube. Refer to Figure 3.19.

Ch. 3: String Potentiometer – Vertical deflection of the sheathing on Panel 1.

Ch. 4: String Potentiometer – Horizontal deflection of the sheathing on Panel 1.

Ch. 5: Rotation Sensor – Rotation of sheathing on Panel 1.

Ch. 6: String Potentiometer – Vertical deflection of the sheathing on Panel 2.

Ch. 7: String Potentiometer – Horizontal deflection of the sheathing on Panel 2.

Ch. 8: Rotation Sensor – Rotation of sheathing on Panel 2.

Ch. 9: String Potentiometer – Vertical deflection of double end posts relative to USP PHD6 hold-down. Refer to Figure 3.20.

Ch. 10: String Potentiometer – Vertical deflection of USP PHD6 hold-down relative to sill plate. Refer to Figure 3.20.

Ch. 11: String Potentiometer – Vertical deflection of sill plate relative to bottom sliding steel tube. Refer to Figure 3.21.

Ch. 12: String Potentiometer – Horizontal deflection of sill plate relative to bottom sliding steel tube. Refer to Figure 3.21.

Ch. 13: Linear Potentiometer – Horizontal deflection of top sliding steel tube. Refer to Figure 18.

Ch. 14: Linear Potentiometer – Horizontal deflection of bottom sliding steel tube.

Ch. 15: Sensor – Horizontal deflection of hydraulic actuator measured internally.

Ch. 16: Load Cell

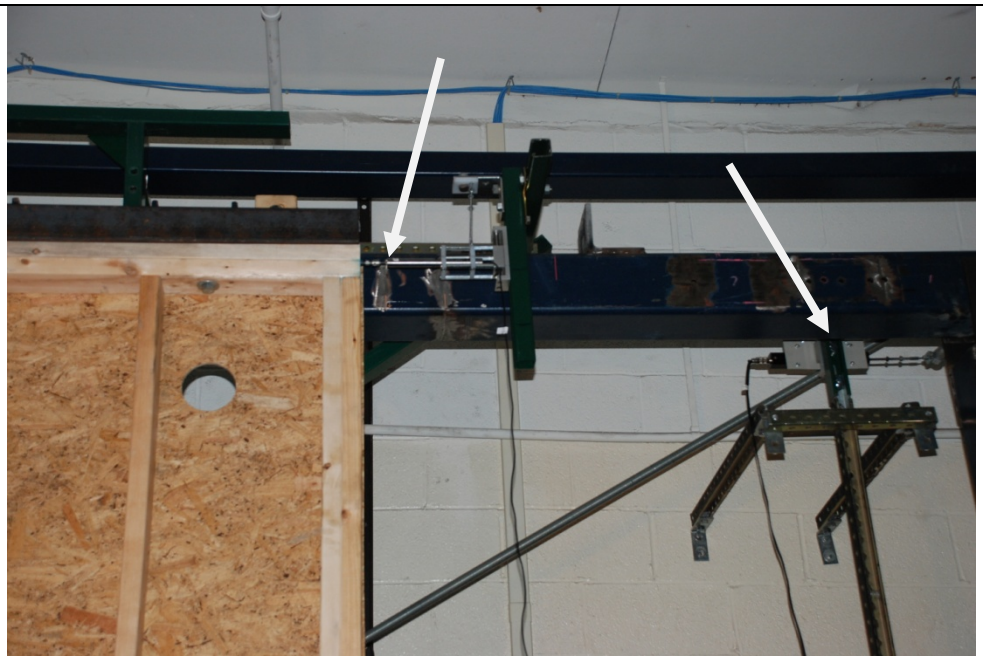

Figure 3.18: LVDT used to measure deflection of top plate (left arrow) and linear potentiometer used to measure deflection of top sliding steel tube (right arrow)

Figure 3.19: Z shaped metal piece attached to base plate and LVDT in order to measure deflection

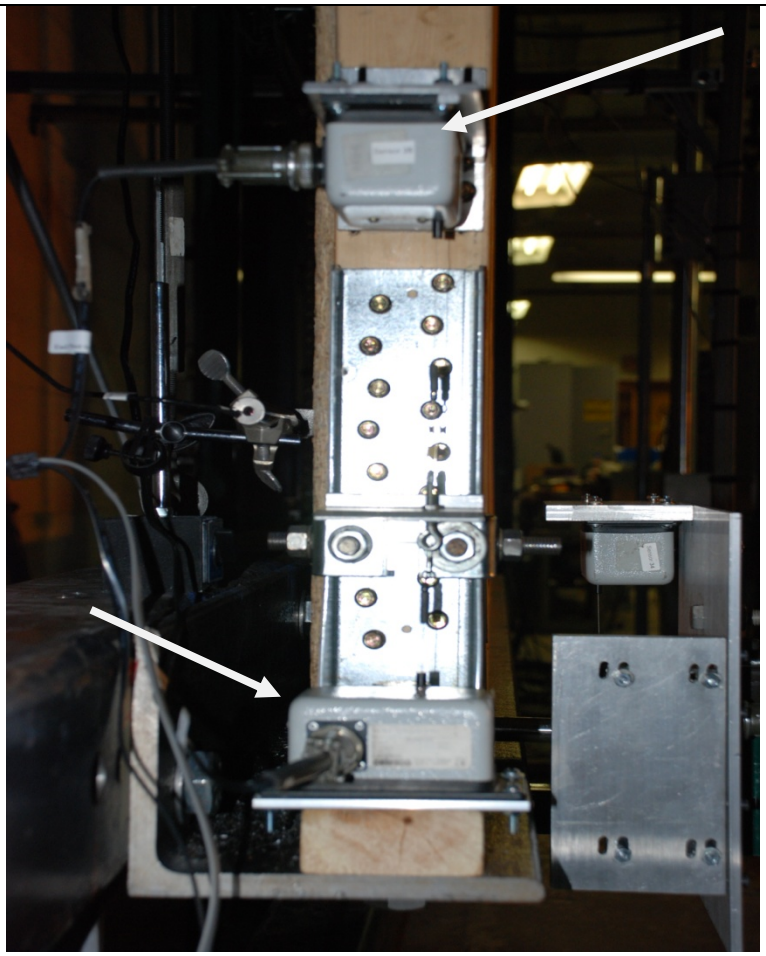

Figure 3.20: String potentiometer used to measure horizontal deflection of end post relative to hold-down and string potentiometer used to measure horizontal deflection of hold-down relative to sill plate

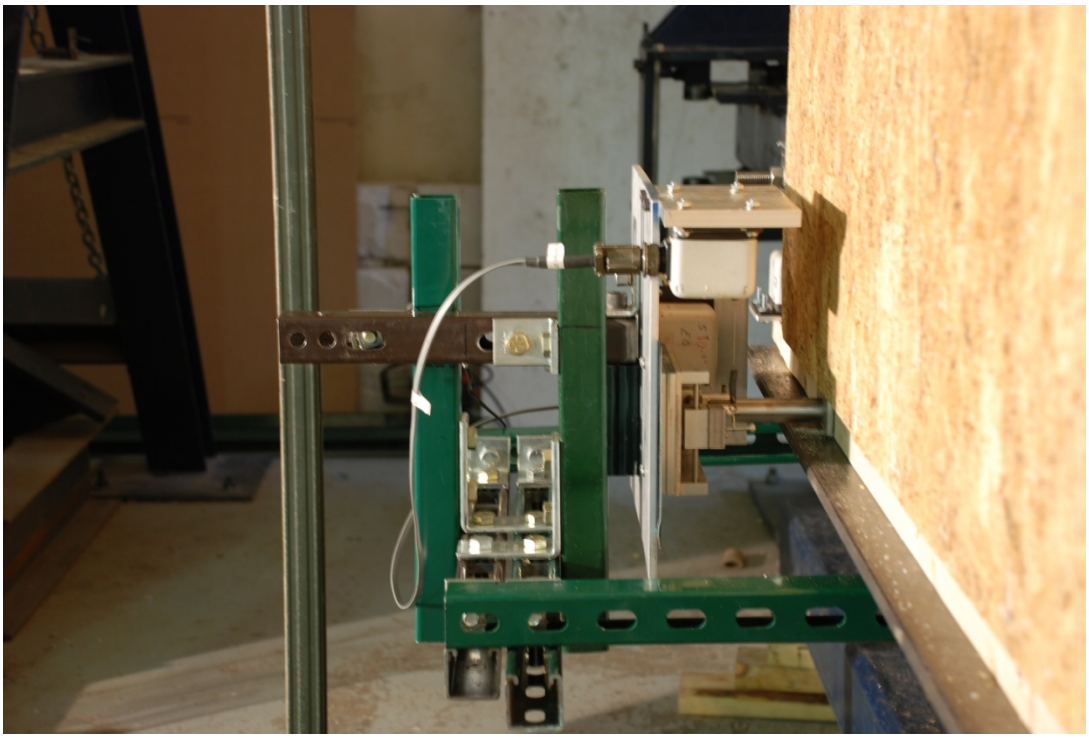

Figure 3.21: String potentiometers secured to mount and attached to X-Y slide used in measuring horizontal and vertical deflection of sill plate.

Chapter 4

Discussion of Test Results and Observations

4.1 Introduction

The following sections include the monotonic and cyclic performance of the SIP and wood-frame specimens tested. The information is presented in the order of weakest to strongest walls.

4.2 Specimens A3

Specimens A3 had 7/16 in. x 3 in. x 8 ft OSB splines that were connected to the SIP facing with 16 gage, 7/16 in. crown, 1.5 in. long staples at 6 in. o.c. The framing lumber was also attached to the SIP facing with the same staples at 6 in. o.c. The USP PHD6 hold-downs were placed at the exterior of the 8 ft x 8 ft wall.

4.2.1 Specimen A3-1M

Specimen A3-1M was tested under monotonic loading according to ASTM E564-06. The failure occurred in the staples as they pulled out of the base plate and top plate. There was also some tear-out damage to the sheathing along the spline. Figure 4.1 shows the Load vs. Displacement graph.

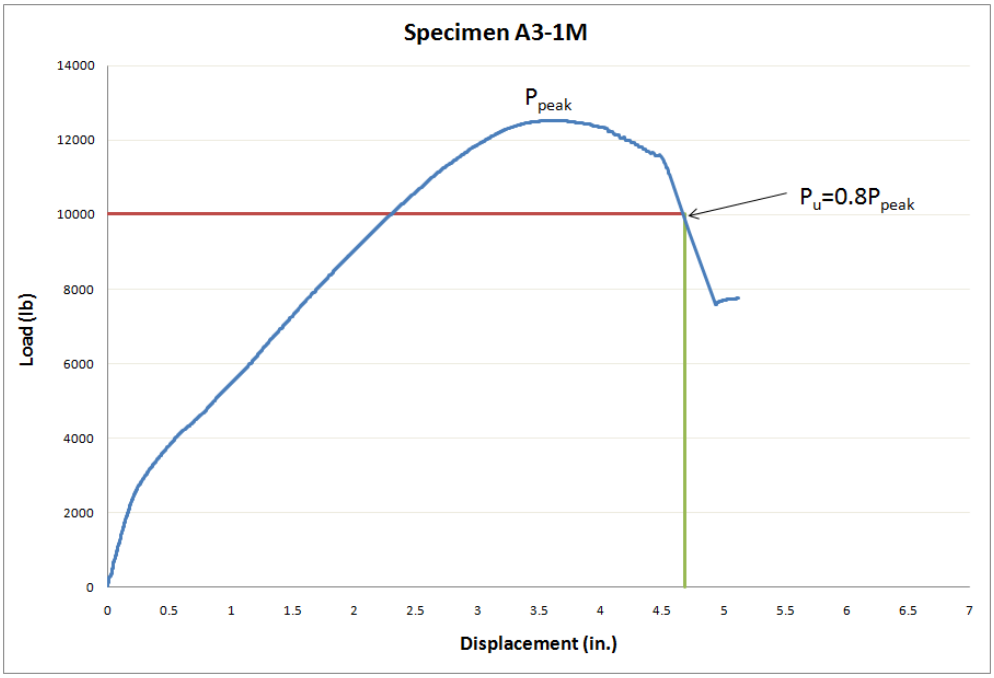

Figure 4.1: Load vs. Displacement diagram resulting from monotonic load testing of Specimen A3-1M

4.2.2 Specimen A3-1C

Specimen A3-1C was tested under cyclic loading with a target displacement of 3.08 in. for the CUREE protocol. The failure of the wall system first occurred when the staples along the spline sheared. This caused the load to be transferred to the top and base plate, which caused shearing and pull-out of about half of the staples along the top and base plate. Figure 4.2 shows the Load vs. Displacement graph and Figure 4.3 shows the envelope curve developed from the Load vs. Displacement graph. Figures 4.4, 4.5, and 4.6 are photographs of the specimen before and after the cyclic test.

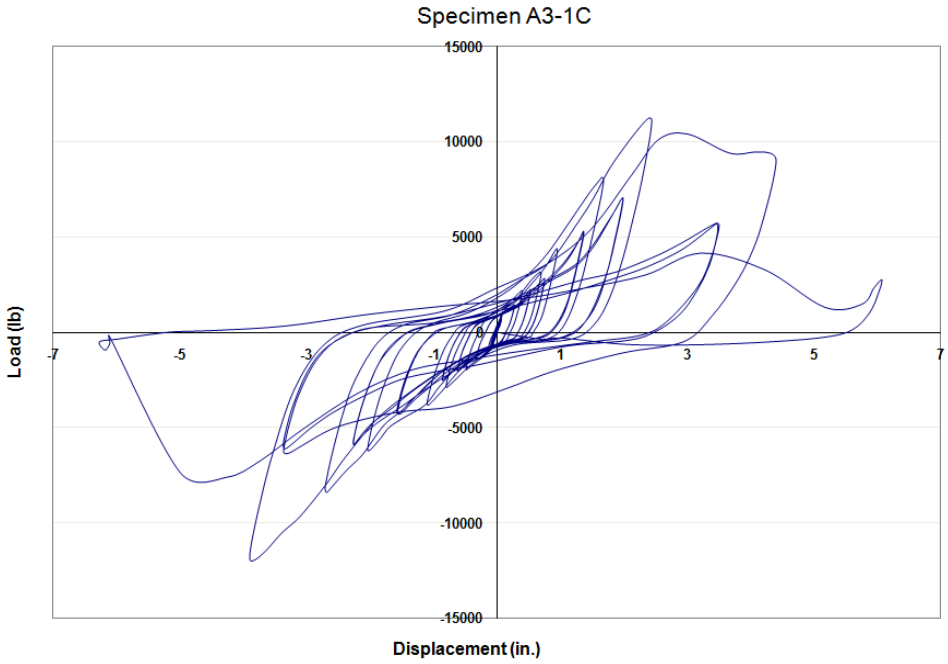

Figure 4.2:Load vs. Displacement diagram resulting from cyclic load testing of Specimen A3-1C

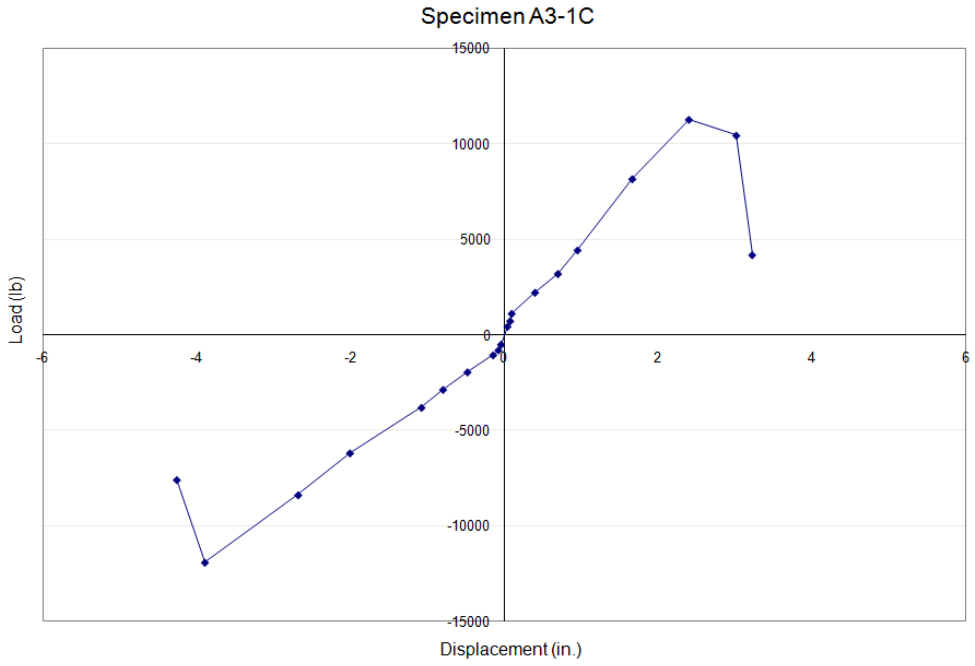

Figure 4.3: Envelope curve from Load vs. Displacement diagram of Specimen A3-1C

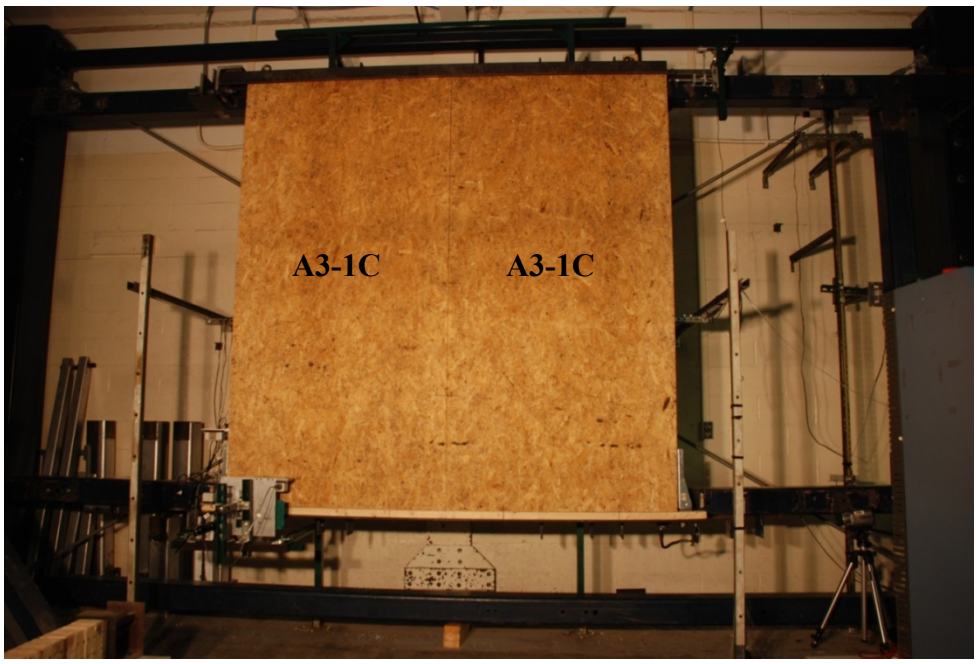

Figure 4.4: Specimen A3-1C prior to cyclic loading

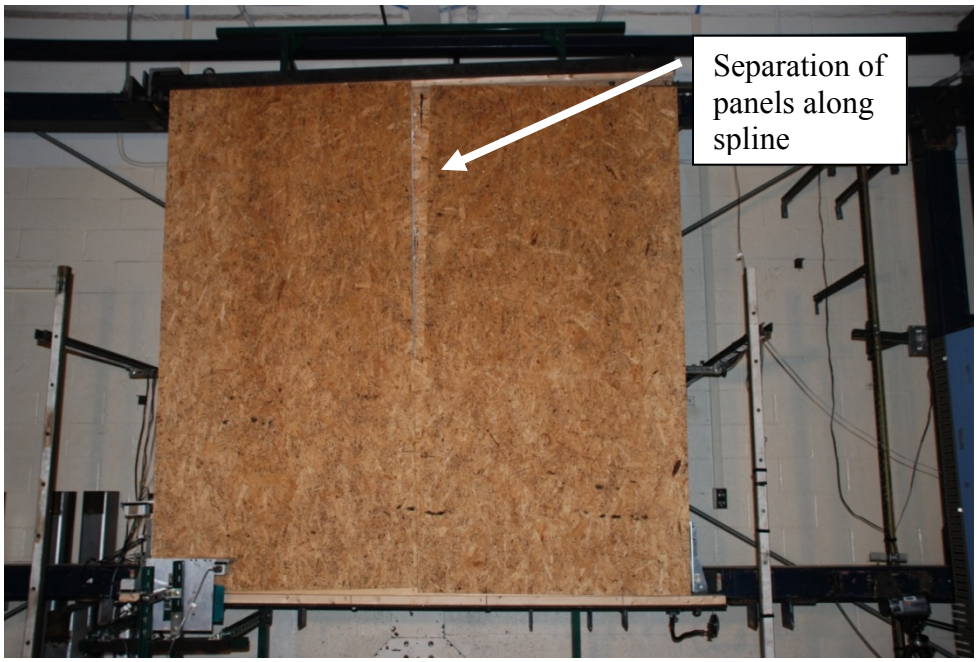

Figure 4.5: Specimen A3-1C after wall failed under cyclic loading

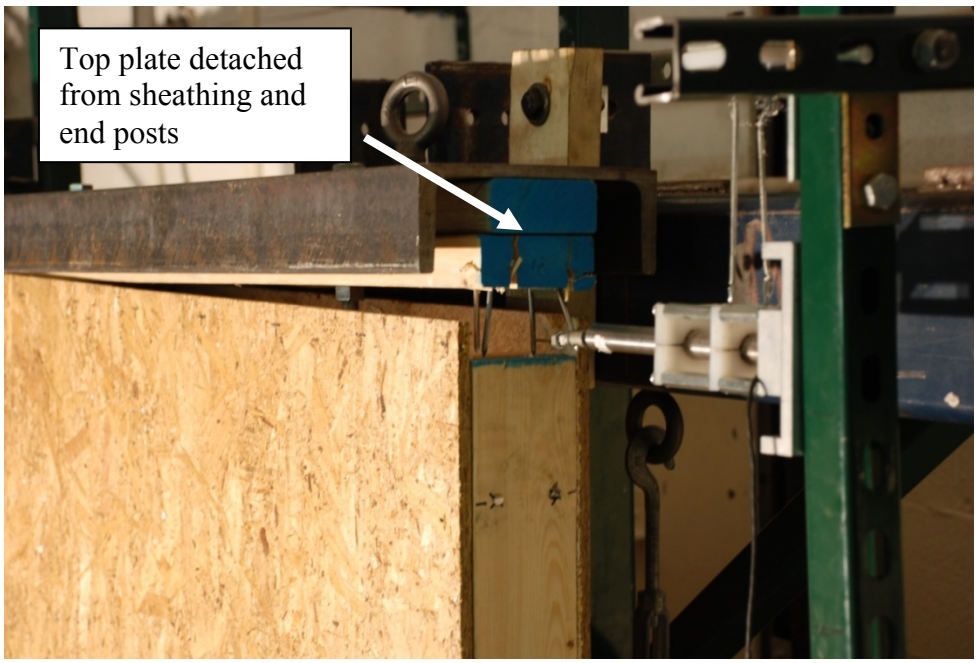

Figure 4.6: Shearing of staples along top plate allowed top plate to pull away from end posts in Specimen A3-1C

4.2.3 Specimens A3-2C and A3-2C (2)

Specimen A3-2C was a replicate of Specimen A3-1C and was tested and analyzed in the same manner in order to validate the results of Specimen A3-1C. After Specimen A3-2C failed under cyclic loading, the wall was re-stapled and the repaired wall was titled Specimen A3-2C(2). The original staples from Specimen A3-2C were not removed; instead new staples about ¾ in. from the edge of the sheathing and 1 in. away from the original staples were added for Specimen A3-2C(2).

The initial failure of Specimen A3-2C occurred along the spline when the staples sheared. As a result, the staples sheared along the top plate and pulled out along the base

plate. Figures 4.7 through 4.11 show the Load vs. Displacement graph, envelope curve and photographs of the specimen before and after the testing.

When Specimen A3-2C failed, the test was stopped before there was a complete failure of the framing members. The MC8x20 channel, which was placed on top of the wall to apply the load evenly across the top plate (Figure 4.6), made it impossible to reattach the top plate to the end posts if they had completely pulled out. Retesting the wall without the top plate properly attached to the end posts would have significantly affected the results. In order to preserve the framing of the wall for retesting the repaired specimen, the test was stopped after the hardware failed, but before the framing failed; as a result, the wall did not experience an 80% drop in load. The failure point of the envelope curve was estimated based on the failure behavior of Specimen A3-1C.

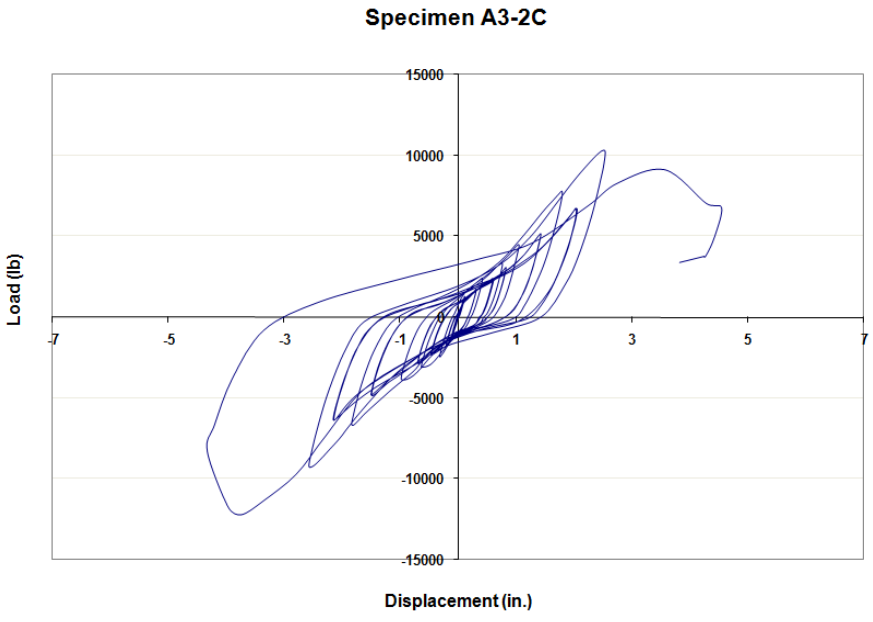

Figure 4.7: Load vs. Displacement diagram resulting from cyclic load testing of Specimen A3-2C

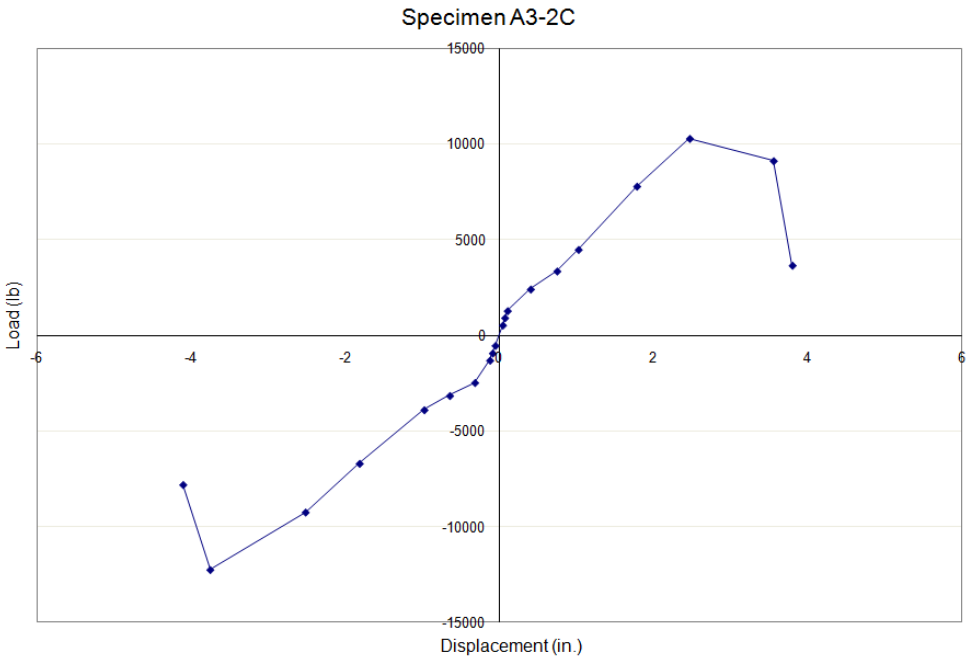

Figure 4.8: Envelope curve from Load vs. Displacement diagram of Specimen A3-2C

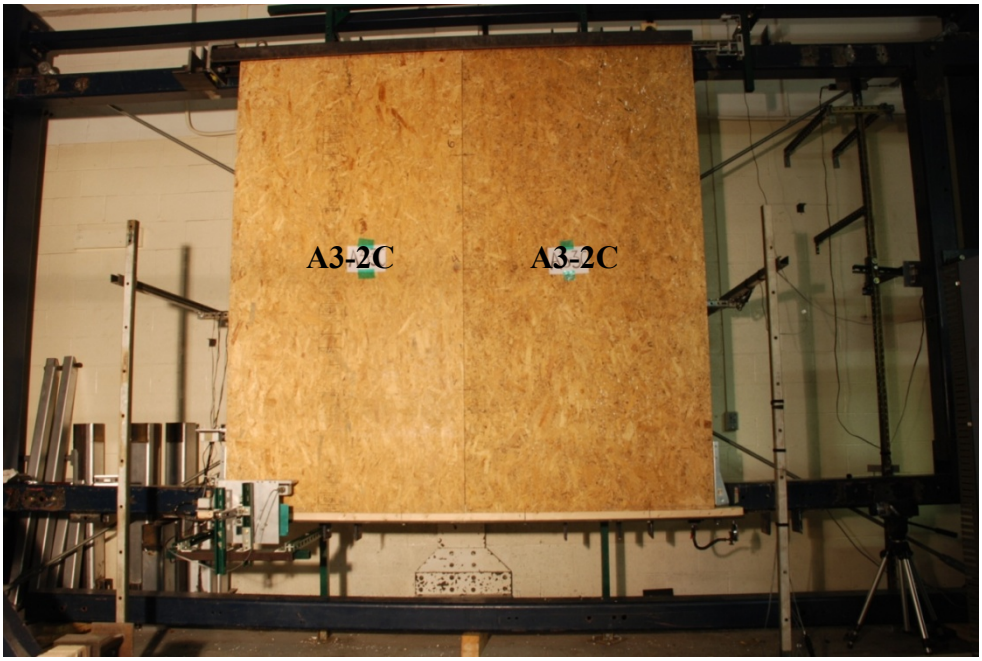

Figure 4.9: Specimen A3-2C on test facility prior to cyclic loading

Figure 4.10: Displacement of panels along base plate and vertical sliding of SIP panels after cyclic loading of Specimen A3-2C

Figure 4.11: Displacement of panels along top plate after cyclic loading of Specimen A3-2C

At the completion of the initial test, the wall was brought back to its original starting location and the wall was re-stapled at about 1 in. from the original staple location. Due to the test setup, re-stapling was not done at the following locations: along the entire base plate of the back side of the wall (Refer to Figure 3.8, notice how the leg of L8x6x1/2 is in the way), the first three staples along the base plate on the front (Refer to Figure 3.21, sill plate deflection sensors are in the way), and the top corners of the back side of the wall. At this point, the wall was re-tested under cyclic loading to determine whether or not the wall would retain its original strength. This repaired specimen is titled Specimen A3-2C(2). Just like Specimen A3-2C, the failure first occurred when the staples along the spline sheared and pulled out. The staples along the top plate sheared as the staples along the base plate pulled out. Refer to Figures 4.12 through 4.16.

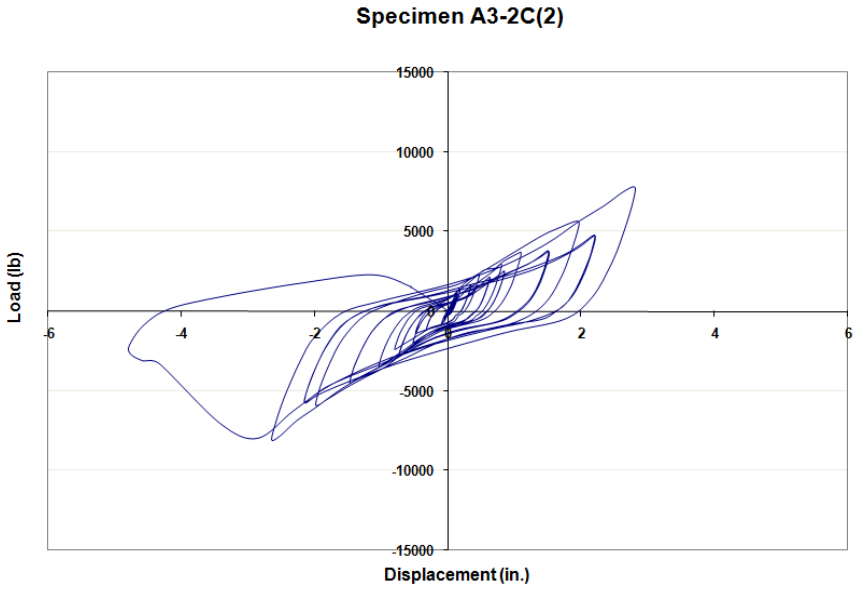

Figure 4.12: Load vs. Displacement diagram resulting from cyclic load testing of Specimen A3-2C(2)

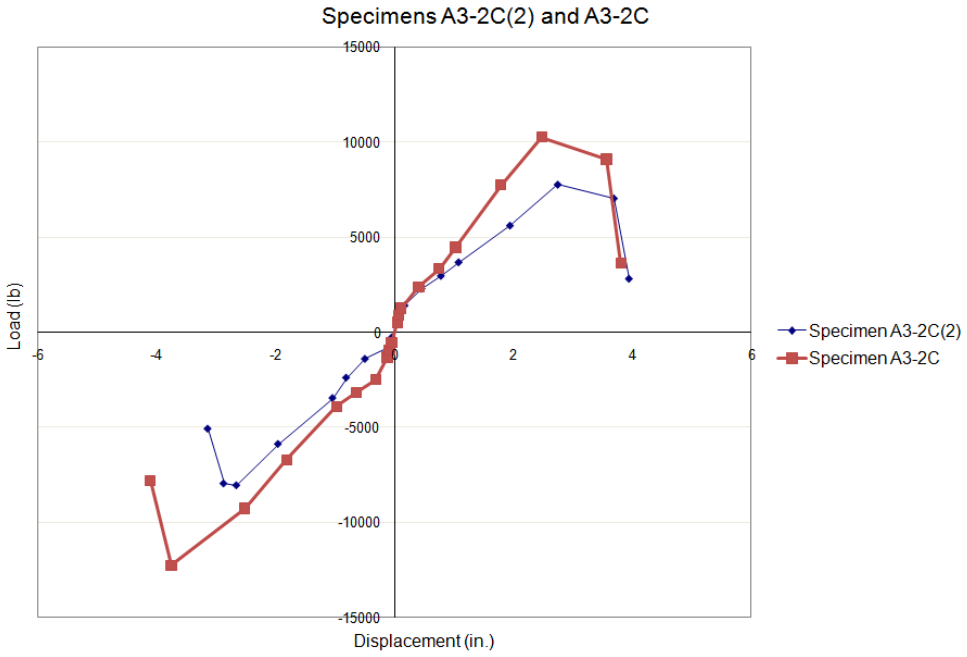

Figure 4.13: Envelope curve from Load vs. Displacement diagram of Specimen A3-2C(2) in comparison with Specimen A3-2C

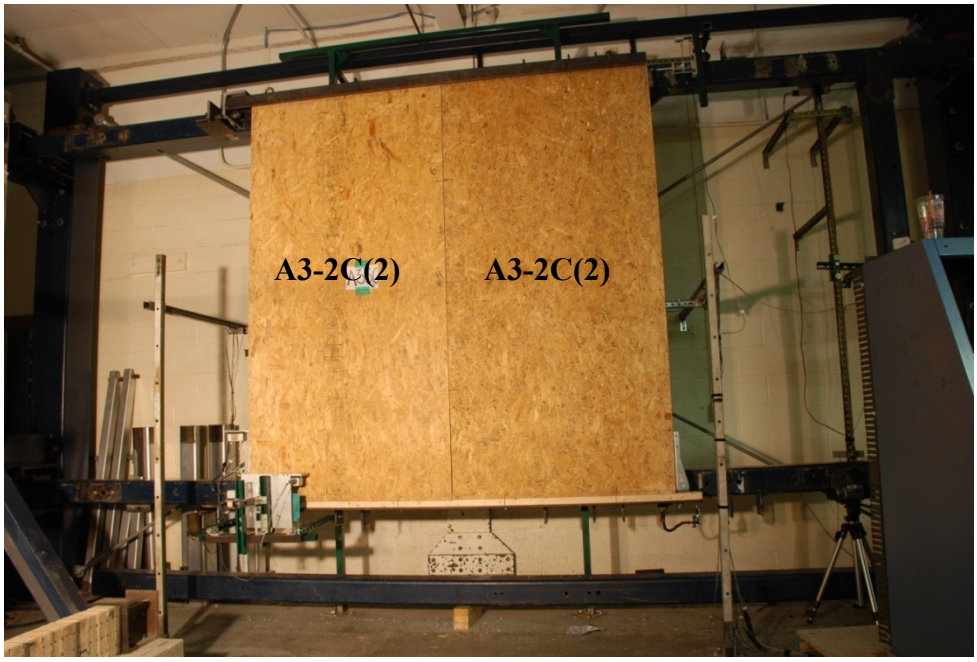

Figure 4.14: Specimen A3-2C(2) before cyclic loading

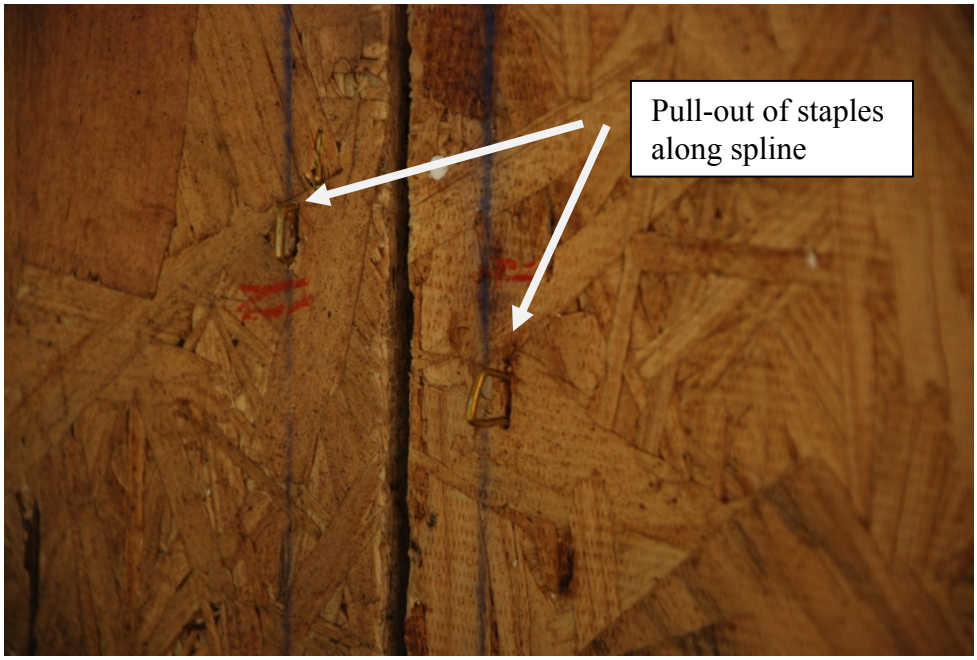

Figure 4.15: Pull-out and shearing of staples along spline after Specimen A3-2C(2) failure

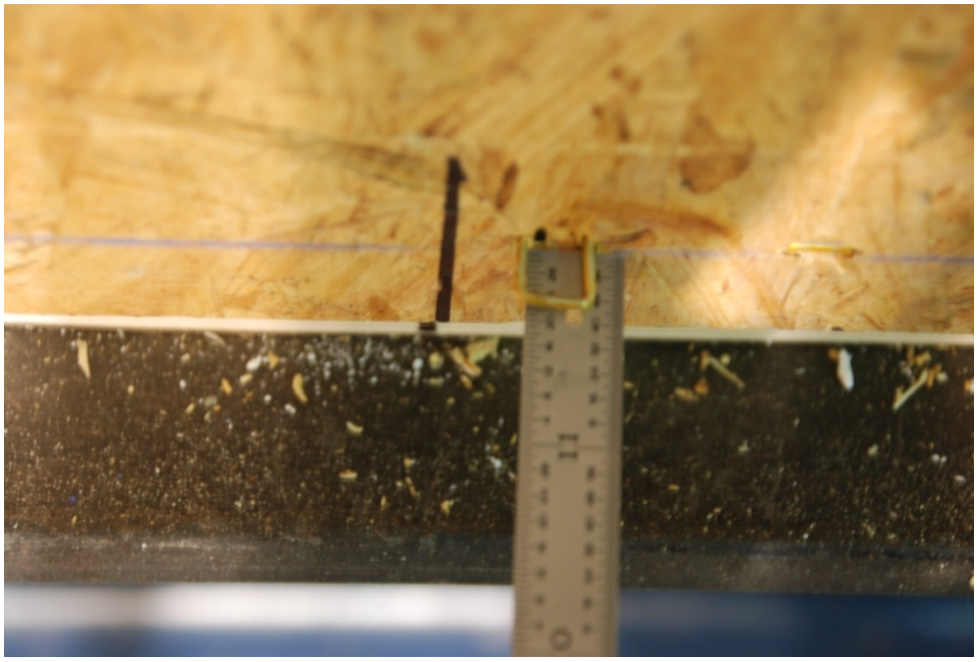

Figure 4.16: Shearing and pull-out of staples along base plate of Specimen A3-2C(2) after failure

4.2.4 Summary of Specimens A3 Tests

The initial failure of Specimens A3 occurred along the spline when the staples pulled out and sheared. At that point, the load was transferred to the sheathing connection along the top plate and base plate. The staples tended to shear along the top plate and pull out along the base plate. The failure in the fastener hardware allowed the two SIP panels to rotate independently of each other no longer performing as a single rigid diaphragm. Specimens A3, more specifically Specimens A3-1C and A3-2C, were able to withstand an average peak load of 11413 lb and an average peak displacement of 3.13 in.

Specimen A3 was able to withstand a larger force and displacement under monotonic loading than cyclic loading. Specimen A3-1M reached a peak force of 12522 lb, which is 9% greater than the average of Specimens A3-1C and A3-2C placed under cyclic loading. The maximum displacement of Specimen A3-1M was 3.64 in. which is 14% greater than the average displacement of Specimens A3-1C and A3-2C.

4.3 Specimens A4

Specimens A4 had 7/16 in. x 3 in. x 8 ft OSB splines which were connected to the SIP facing with 1.25 in. long, flat head, steel screws spaced at 6 in. o.c. The framing lumber was also attached to the SIP facing with the same screws at 6 in. o.c. The USP PHD6 hold-downs were placed at the exterior of the 8 ft x 8 ft wall.

4.3.1 Specimen A4-1M

Specimen A4-1M was tested under monotonic loading according to ASTM E 564-06. The failure was caused by the screws shearing along the spline and then along the top and base plates. There was a secondary failure in the 2x4 top plate; two of the 16d common nails used to connect the top plate to the end posts pulled out of the end posts, while the other two nails caused splitting in the top plate. Figure 4.17 shows the Load vs. Displacement graph and Figures 4.18 through 4.20 show photographs of the specimen after the monotonic loading.

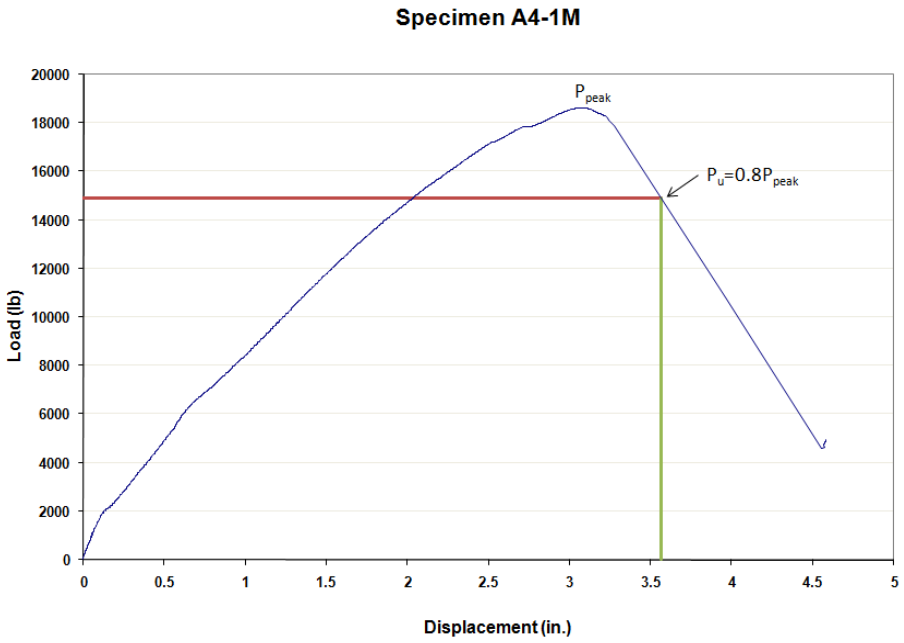

Figure 4.17: Load vs. Displacement diagram resulting from monotonic load testing of Specimen A4-1M

Figure 4.18: Deflection of SIP panels after the monotonic loading of Specimen A4-1M

Figure 4.19: Shearing of a screw along the top plate and separation of the panel from the OSB spline of Specimen A4-1M

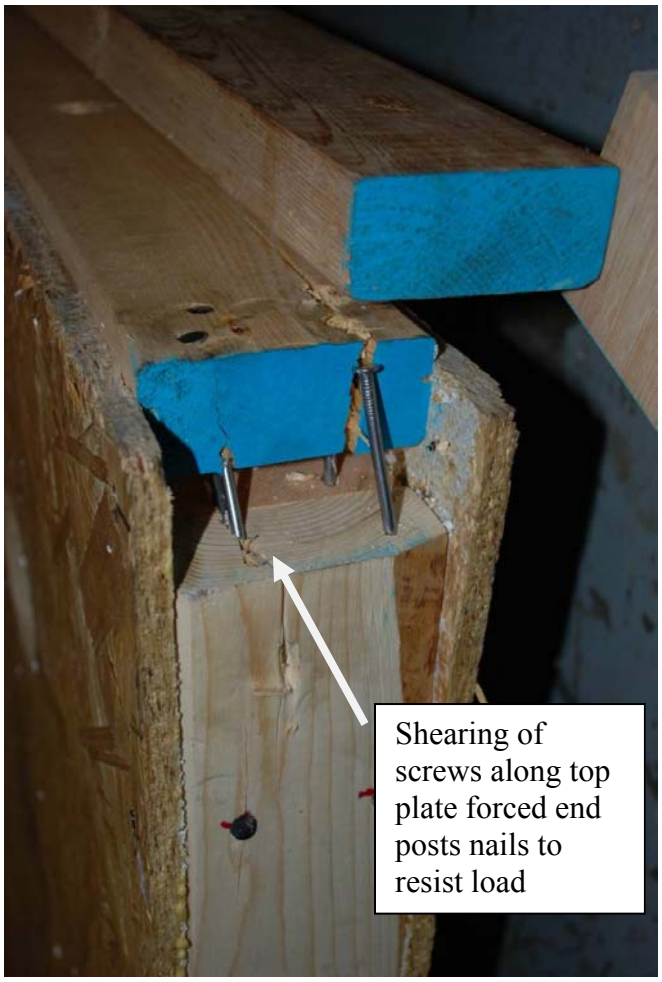

Figure 4.20: Top plate failure (Specimen A4-1M) occurred at the end where (4) 16d common nails were used to attach top plate to end posts (Picture taken after wall was removed from facility)

4.3.2 Specimen A4-1C

Specimen A4-1C was tested under cyclic loading with a target displacement of 2.75 in. for the CUREE protocol. The failure of the wall system first occurred when the screws along the spline sheared. This caused the load to be transferred to the top and base plate, which caused the top plate to pull away from the sheathing and the end posts

resulting in sheared screws along the top and base plate as well. Figures 4.21 and 4.22 show the Load vs. Displacement graph and envelope curve. Figures 4.23, 4.24, and 4.25 are photographs of the specimen before and after cyclic loading.

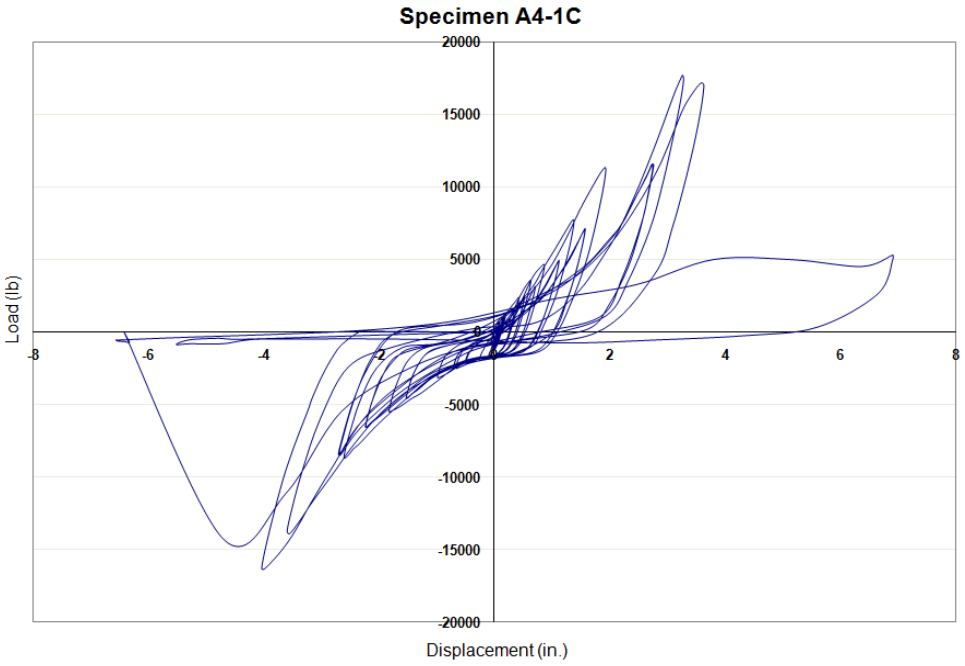

Figure 4.21: Load vs. Displacement diagram resulting from cyclic load testing of Specimen A4-1C

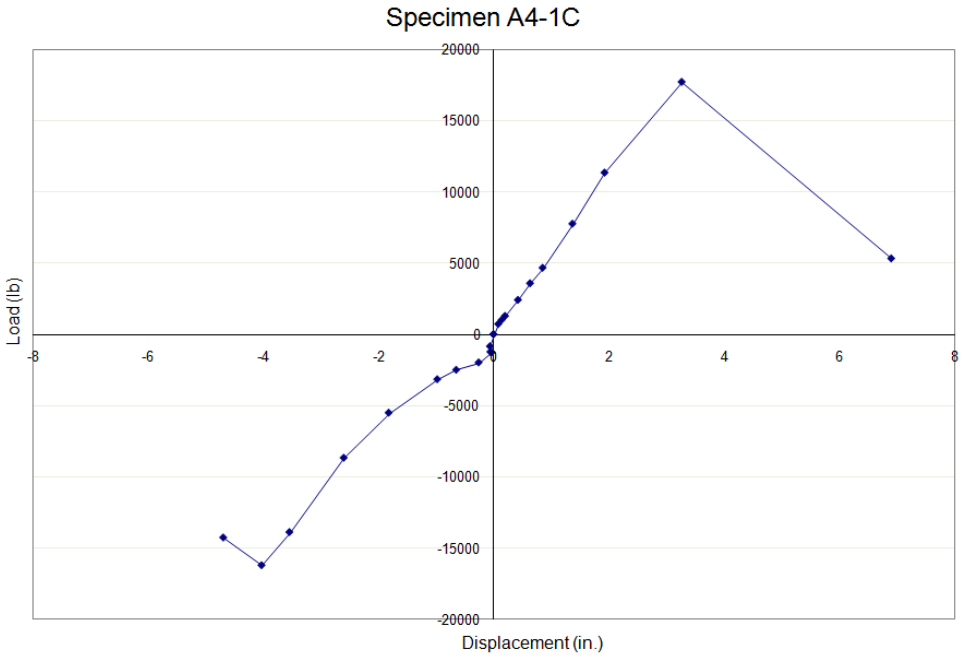

Figure 4.22: Envelope curve from Load vs. Displacement diagram of Specimen A4-1C

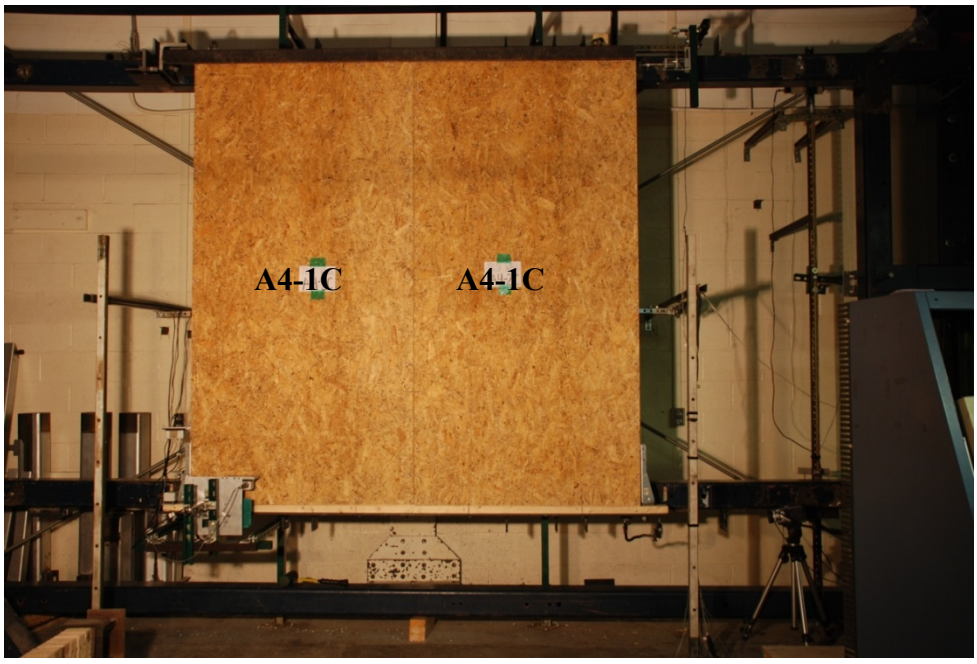

Figure 4.23: Specimen A4-1C before cyclic loading

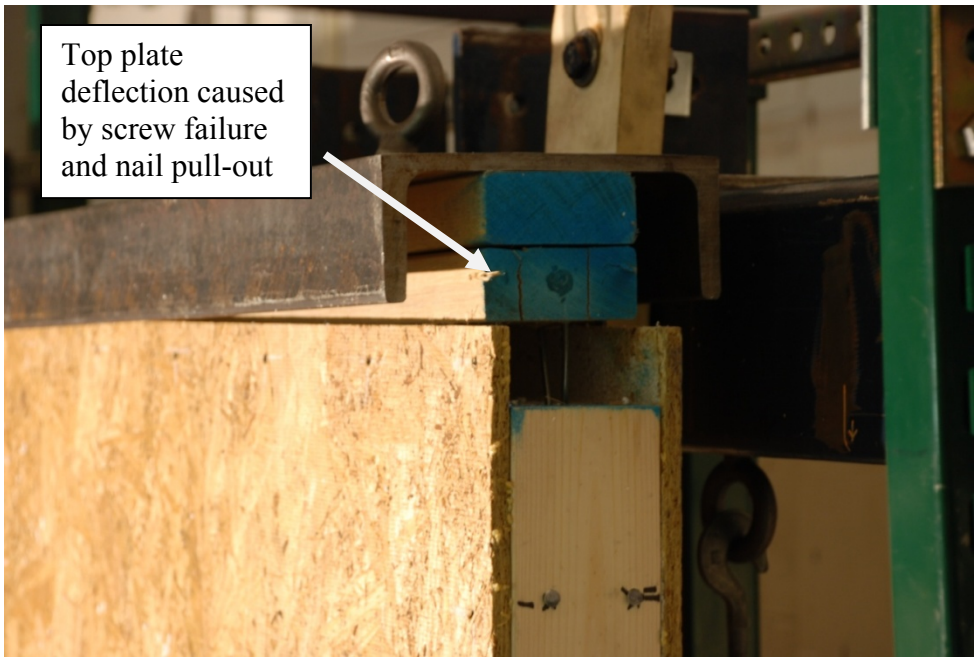

Figure 4.24: Failure of screws along top plate allowed 2x4 to deflect upwards and pull away from end posts on Specimen A4-1C

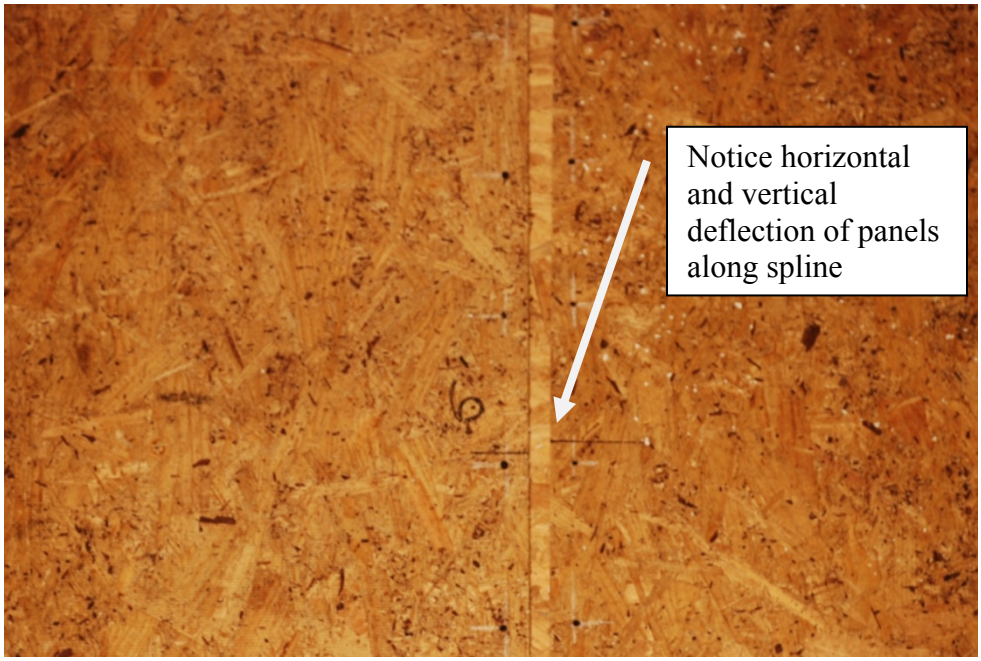

Figure 4.25: Deflection of SIP panels six feet high on Specimen A4-1C after cyclic loading

4.3.3 Specimen A4-2C

Specimen A4-2C was a replicate of Specimen A4-1C and was tested and analyzed in the same manner in order to validate the results of Specimen A4-1C. Specimen A4-2C initially failed when the screws located along the spline sheared. The top plate then pulled away from the right panel causing the screws attaching the sheathing to the top plate to shear. The nails used to attach the top plate to the end posts pulled out of the end posts. There was also damage to the base plate. Figures 4.26 and 4.27 show the Load vs. Displacement relationship and envelope curve of Specimen A4-2C. Figures 4.28 through 4.31 are photographs of the specimen before and after cyclic loading.

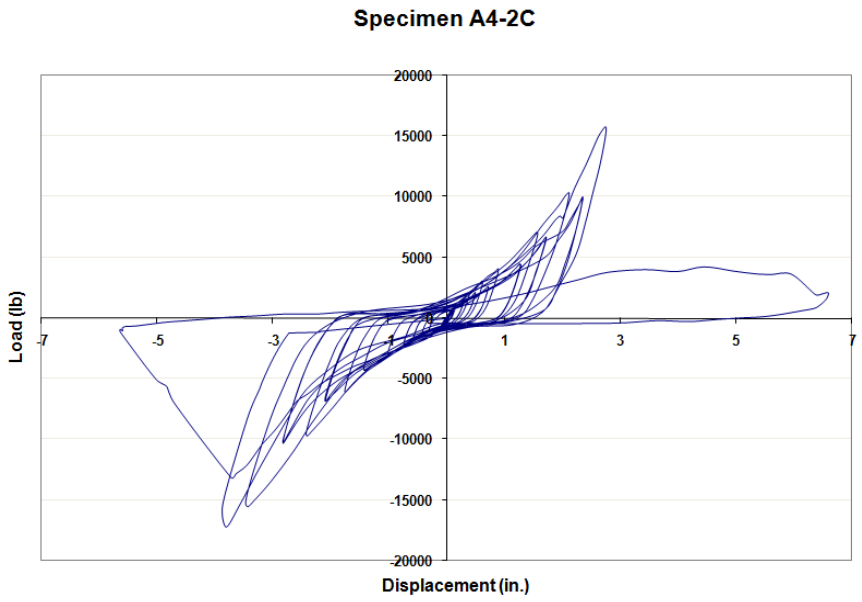

Figure 4.26: Load vs. Displacement diagram resulting from cyclic load testing of Specimen A4-2C

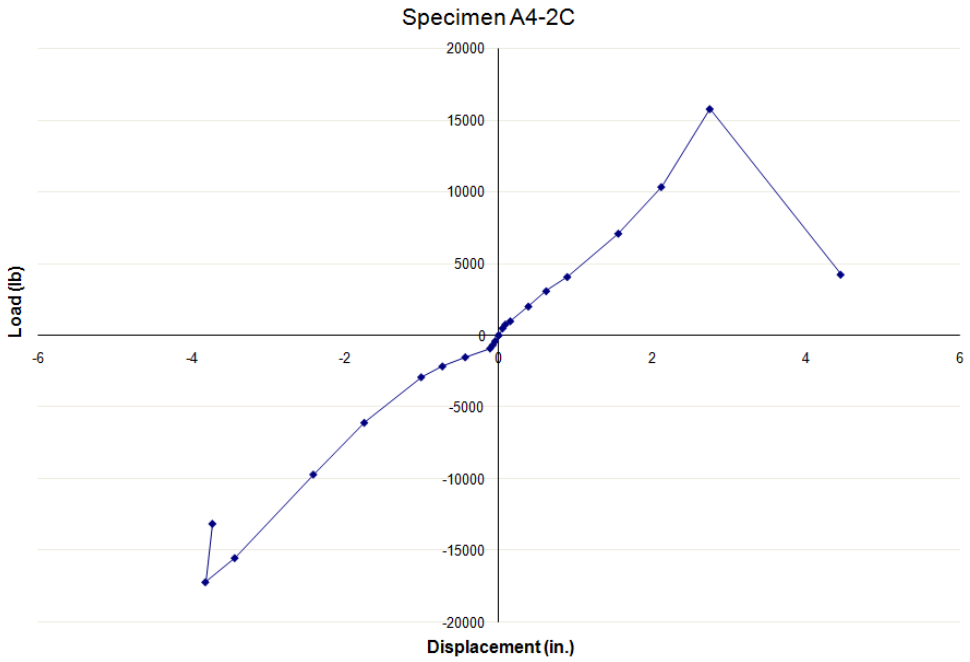

Figure 4.27: Envelope curve from Load vs. Displacement diagram of Specimen A4-2C

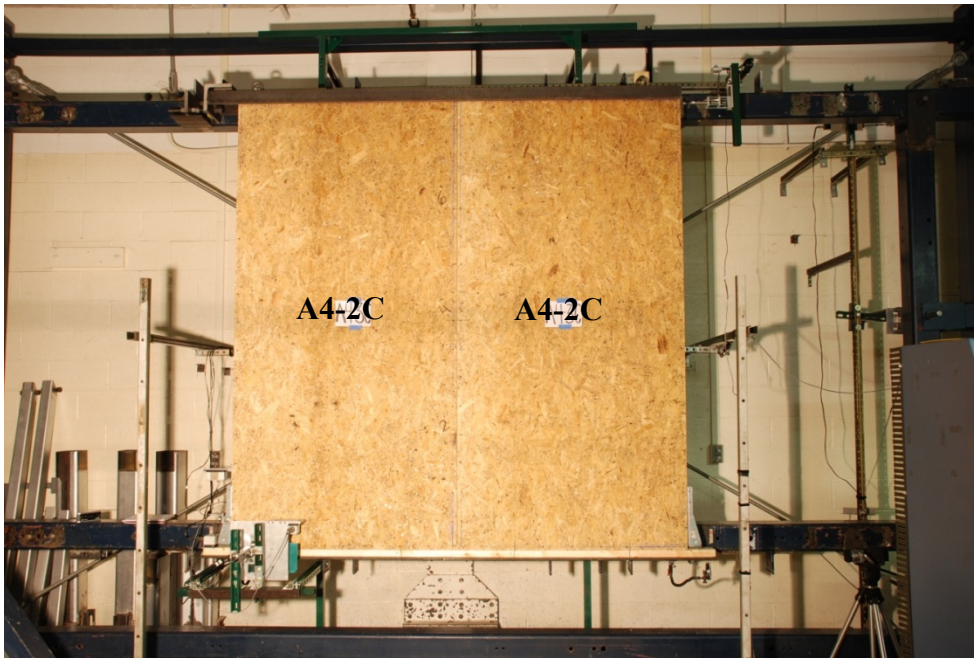

Figure 4.28: Specimen A4-2C before cyclic loading

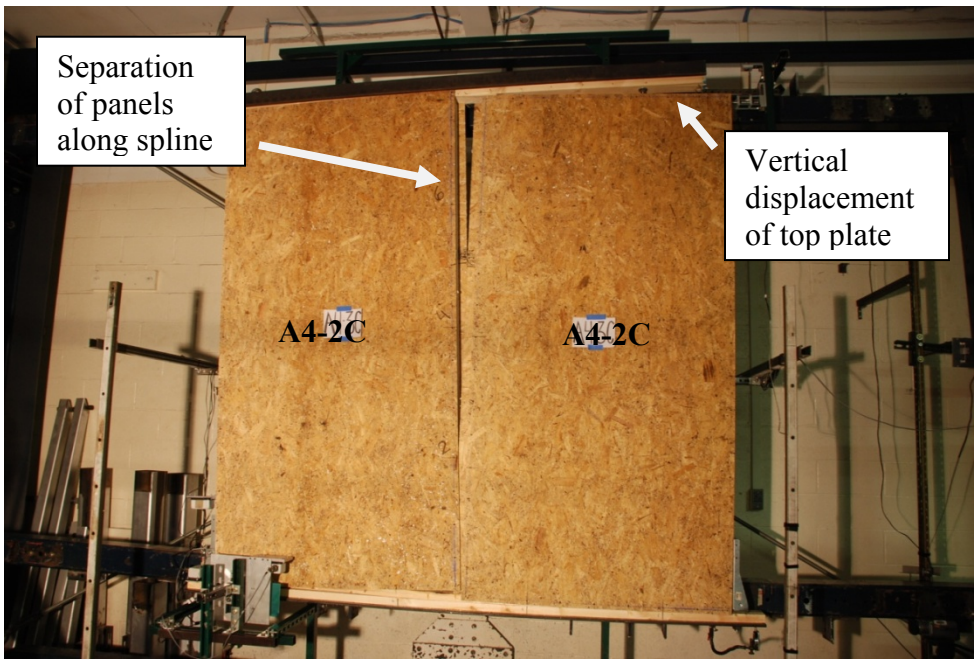

Figure 4.29: Failure of Specimen A4-2C after cyclic loading

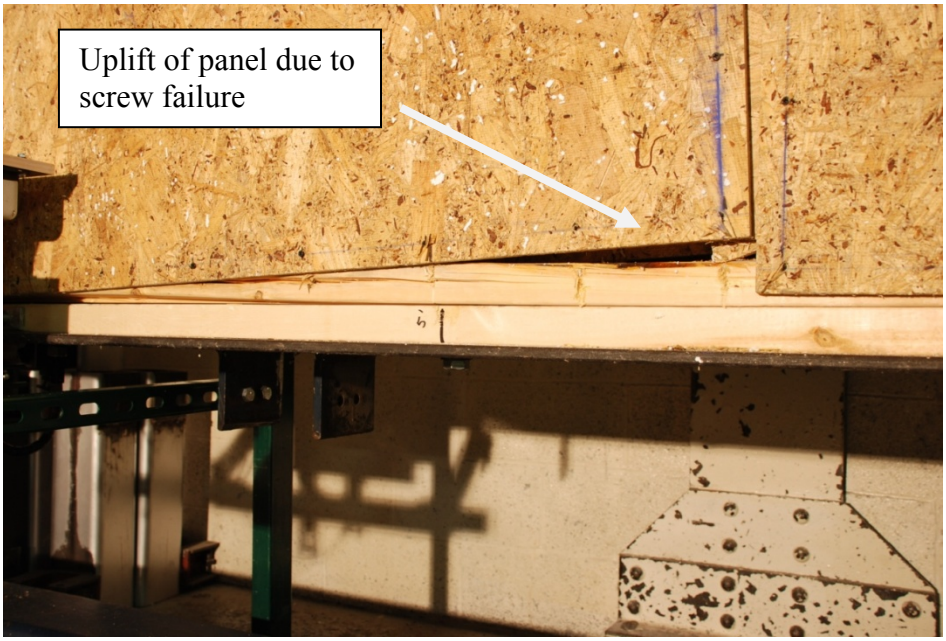

Figure 4.30: Base plate damage caused by displacement of SIP panels and failure of screws on Specimen A4-2C

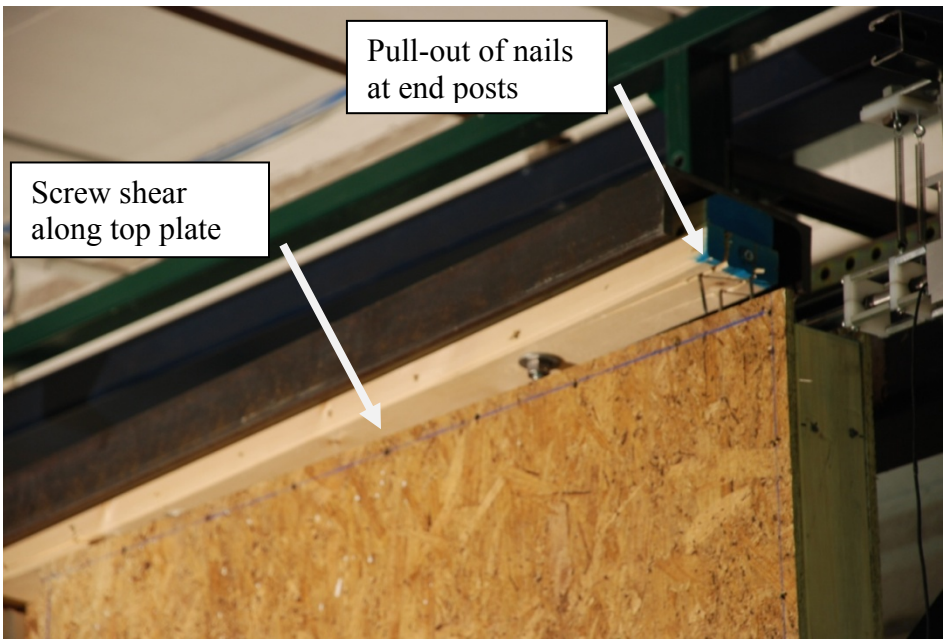

Figure 4.31: Top plate uplift which occurred after screws along top plate sheared and nails pulled out of end posts on Specimen A4-2C

4.3.4 Specimen A4-3C

Specimen A4-3C was a replicate of Specimens A4-1C and A4-2C and was tested and analyzed in the same manner in order to validate the results of the previously tested walls with screw fasteners. The failure of Specimen A4-3C first occurred when the screws along the spline sheared. All of the screws along the top plate sheared, which allowed the top plate to horizontally deflect 1.12 in. A majority of the screws along the base plate also sheared. Figures 4.32 and 4.33 show the Load vs. Displacement graph and the envelope curve. Due to the intense failure of the wall, in order to make sure the sensors were not damaged the test was stopped before an 80% drop in load was reached

on the negative side of the hysteresis loops. As a result, the failure point was estimated based on previous tests.

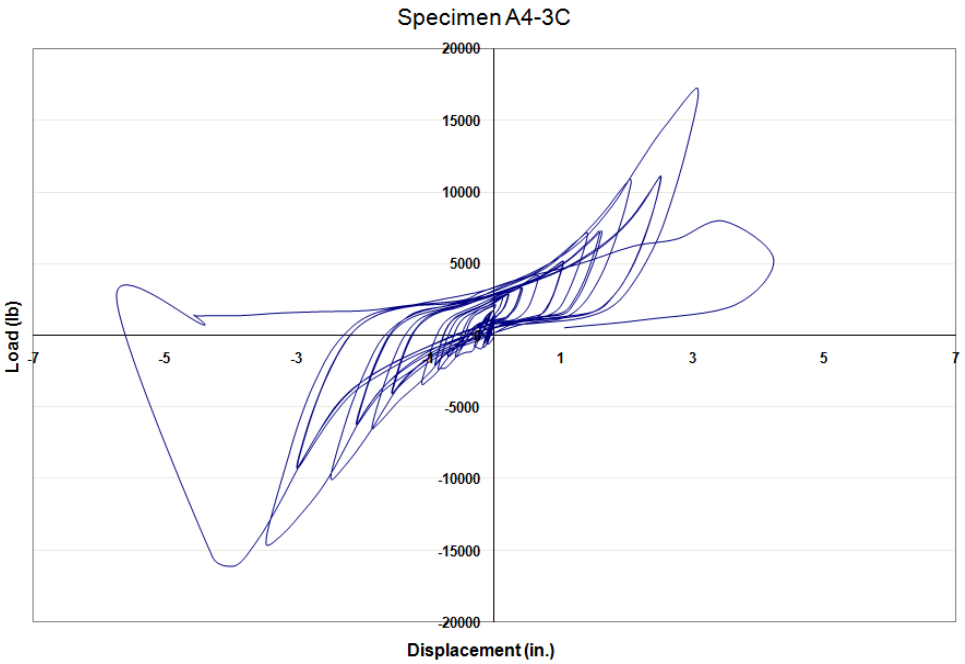

Figure 4.32: Load vs. Displacement diagram resulting from cyclic load testing of Specimen A4-3C

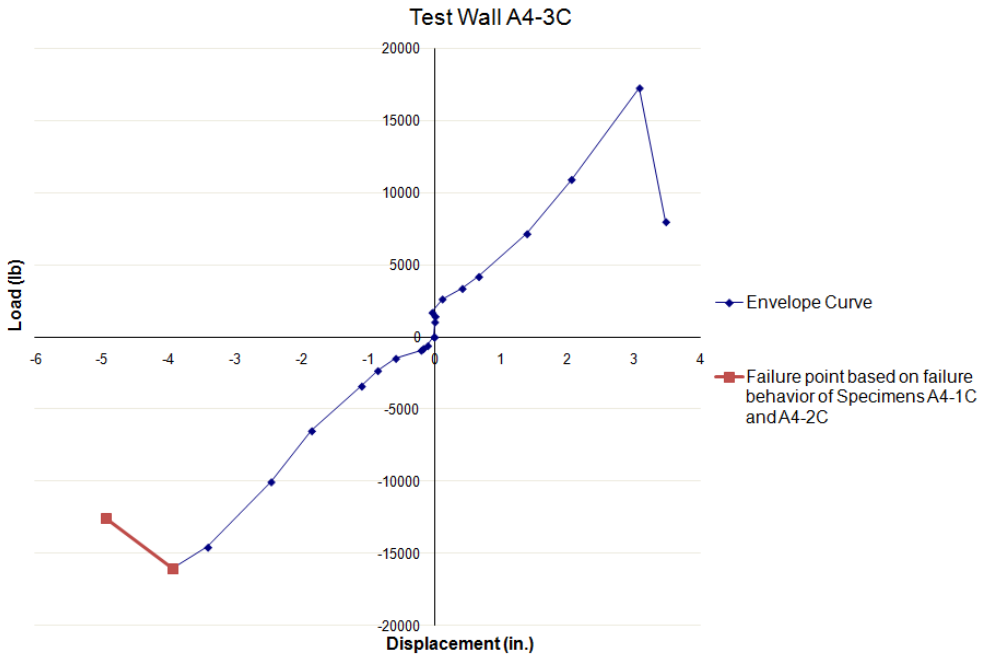

Figure 4.33: Envelope curve from Load vs. Displacement diagram of Specimen A4-3C

4.3.5 Summary of Specimens A4 Tests

The load-displacement graphs of Specimens A4 demonstrate the brittle and sudden failure of the connection hardware used in the wall design. The initial failure occurred when the screws located along the spline sheared. The load was then transferred to the top and base plates. The top plate and base plate would then pull away from the SIP panels causing the screws in the sheathing to shear. The nails used to connect the top plate to the end posts pulled out and also caused the top plate to split.

The peak load and displacement of the specimen under monotonic loading was 18613 lb and 3.10 in. The average values obtained for the same specimen under cyclic loading were 16689 lb and 3.48 in., about 10% less.

4.4 Specimens A1

Specimens A1 had 7/16 in. x 3 in. x 8 ft OSB splines which were connected to the SIP facing with 8d common nails at 6 in. o.c. The framing lumber was also attached to the SIP facing with 8d common nails at 6 in. o.c. The A1 specimens turned out to be stronger than anticipated, based on previous published research results discussed in Section 3.3 (APA, 2006; Kermani and Hairstans, 2006). The 20,000 lb testing facility maximum was reached before the wall experienced an 80% drop in peak load capacity. As a result, trend lines and failure points estimated by analyzing Specimens A3 and A4 were used to estimate the failure point of the A1 specimens corresponding to an 80% drop in load capacity. It should be noted that such failure information is of interest for use in the methodology to develop seismic response parameters. In this study, although for some specimens such data points could not be obtained due to the limitation of the test facility, post-peak points corresponding to 20% drop in peak load capacity were estimated for calculation purposes as will be discussed in later chapters.

4.4.1 Specimen A1-1M

Specimen A1-1M was tested under monotonic loading based on ASTM E 564-06. The specimen was pushed up to about 18000 lb at a drift of 4.5 in. This drift corresponds to a drift ratio of 4.7%, which is approximately twice the allowable drift ratio per IBC 2006. According to ASCE 7-05, adopted by IBC 2006, the maximum allowable drift ratio is 2.5%. Signs of failures at the completion of the test included deformation and pull-out of the nails along the spline. Also, there was sheathing damage along the inner corner of the panel at the top plate, and the sheathing at the inner corner of the panels along the base plate began to tear out. Figure 4.34 shows the Load vs. Displacement graph, and Figures 4.35 through 4.38 show photographs of Specimen A1-1M before and after the monotonic loading.

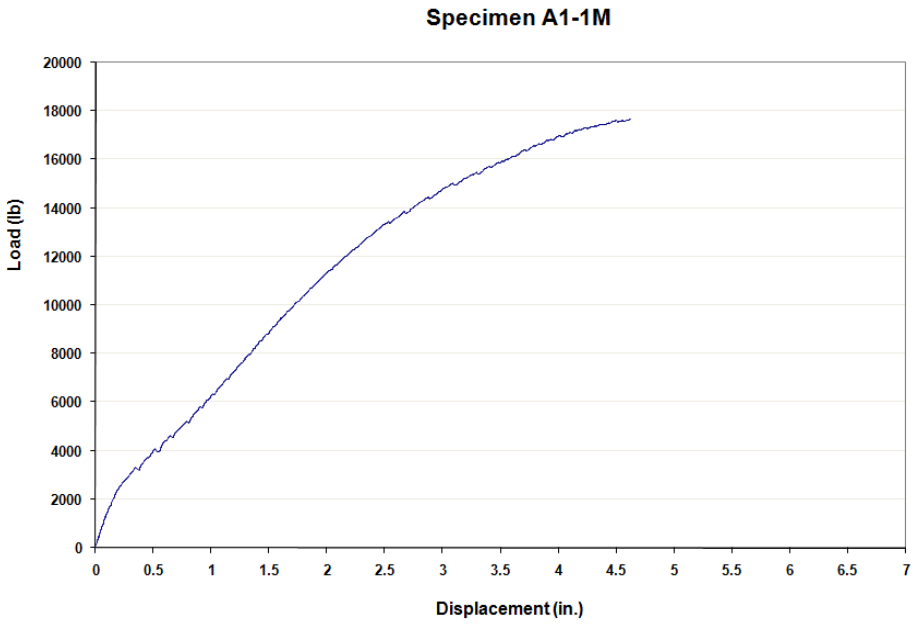

Figure 4.34: Load vs. Displacement diagram resulting from monotonic load testing of Specimen A1-1M

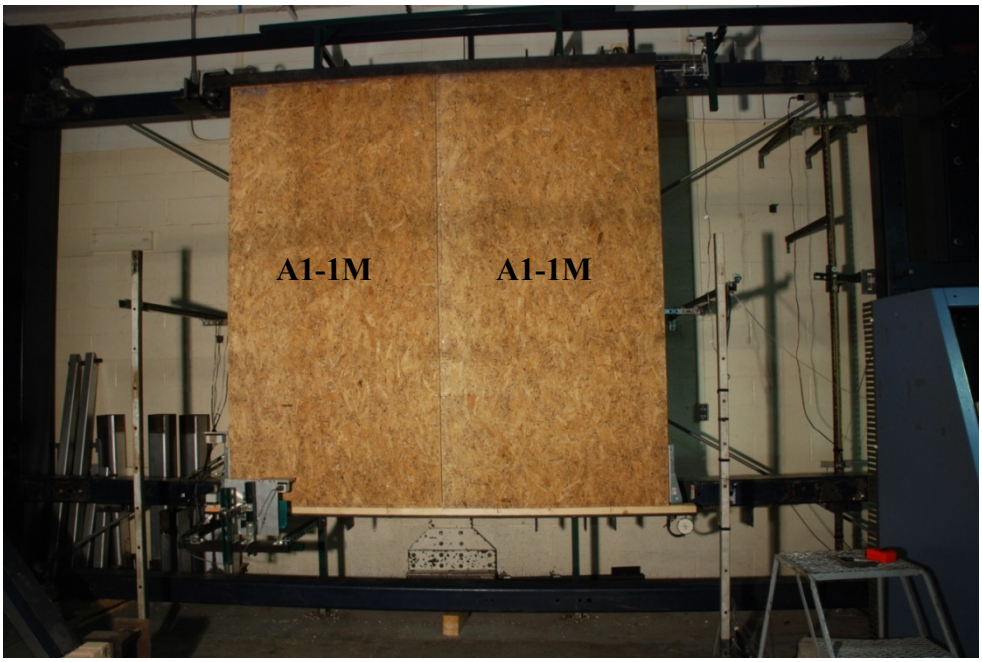

Figure 4.35: Specimen A1-1M before monotonic loading

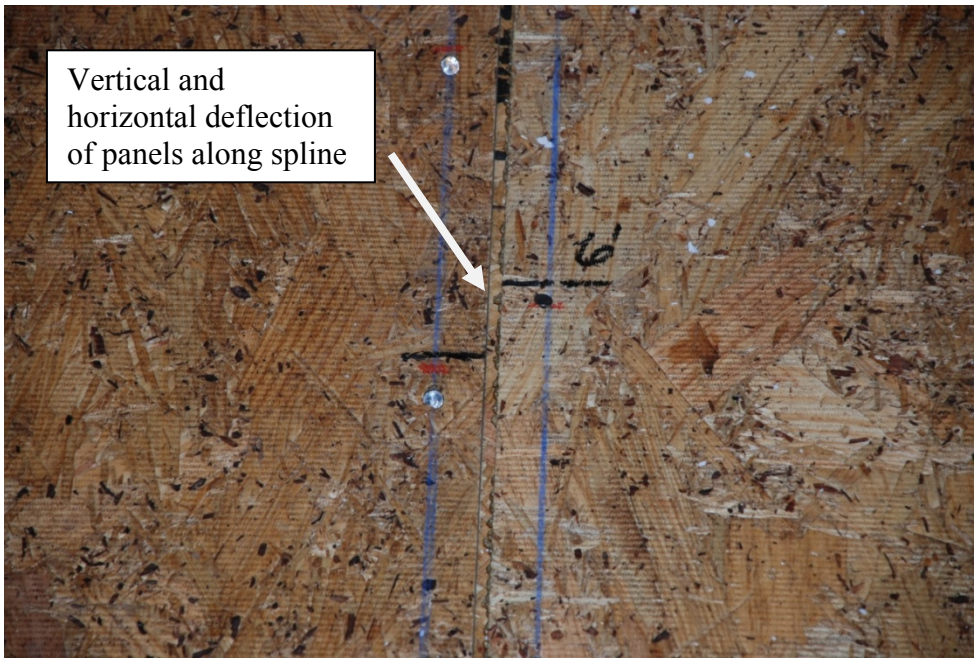

Figure 4.36: Vertical sliding of the panels with respect to each other shown at the 6 ft high mark after monotonic loading of Specimen A1-1M

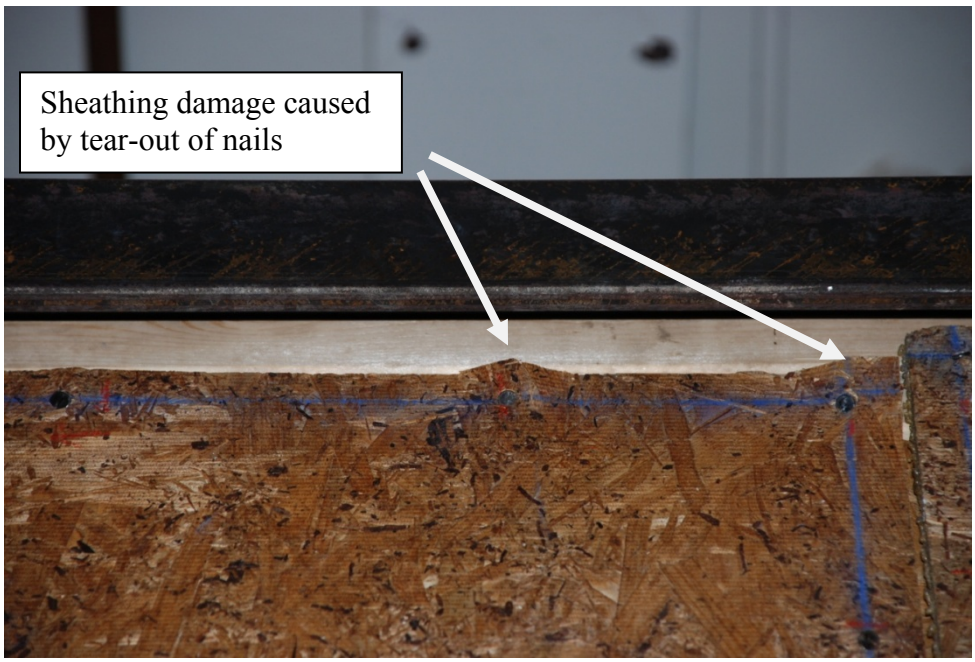

Figure 4.37: Sheathing damage along top plate of Specimen A1-1M

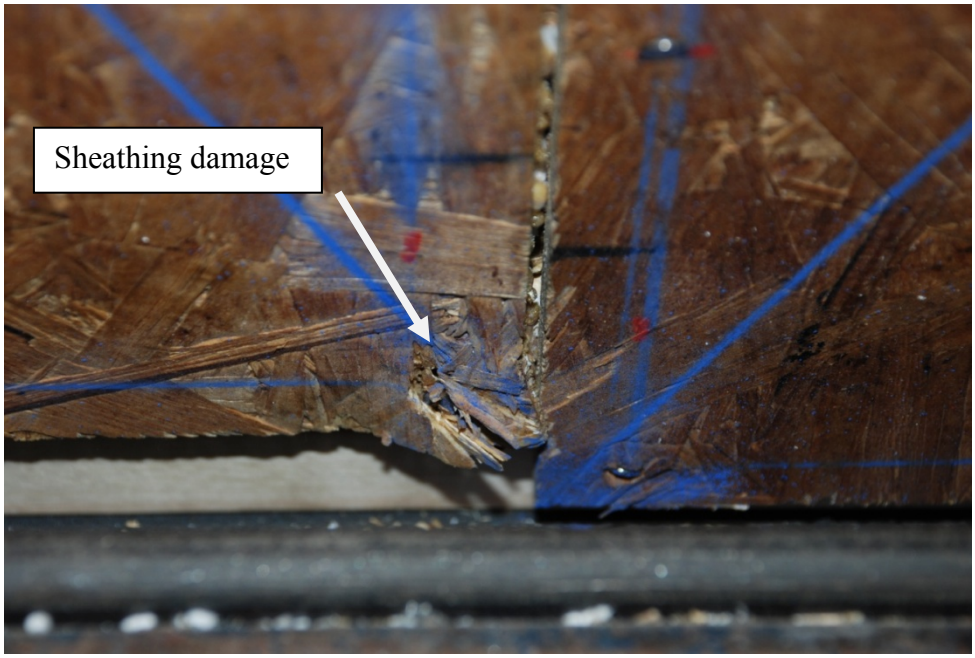

Figure 4.38: Sheathing damage at inner corner of panels along base plate of Specimen A1-1M

4.4.2 Specimen A1-1C

Specimen A1-1C was tested under cyclic loading and with a target displacement of 6 in. for the CUREE protocol. The specimen was pushed up to about 18000 lb at a drift of about 5 in. (5.2% drift ratio), and underwent the first thirty-seven cycles of the CUREE loading protocol. The wall showed signs of failure before the test was stopped. The failure in the wall first occurred when the nails pulled out along the spline and then completely along the top plate and partially along the bottom plate. Specimen A1-1C was stronger than anticipated and showed strengths higher than an 80% drop in maximum load when the displacement capacity of the test facility was reached at which point the test was stopped. A series of trend lines were then used to estimate the failure point (where load resistance drops to 80% of the peak load) of the wall. The trend lines used were developed by fitting third and fourth power polynomial curves to the data points already obtained from the testing. The curves made it possible to extend the test data points and predict the failure point for use in the methodology to determine seismic response parameters. An average of the third and fourth polynomial curves was also plotted. The average failure behavior of Specimens A3 and A4 was also plotted on the envelope curve graph. This was determined by finding the percentage that the displacement increased, beyond Δ_{peak}, when Specimens A3 and A4 experienced an 80% drop in peak load. The average of the percentages increase in displacement was calculated and that average percentage was applied to the Δ_{peak} of Specimen A1-1C to determine Δ_U. All of these trend lines and estimated failure points were then analyzed according to ASTM E 2126-08 (2008) and ICC-ES AC130 (2007) and used to determine

the minimum and maximum values of load, displacement, strength, stiffness, and shear modulus needed to describe the specimen's performance. Figure 4.39 shows the Load vs. Displacement graph and Figure 4.40 shows the envelope curve and the trend lines used to analyze the failure point. Figures 4.41 through 4.44 are photographs of Specimen A1-1C before and after the loading.

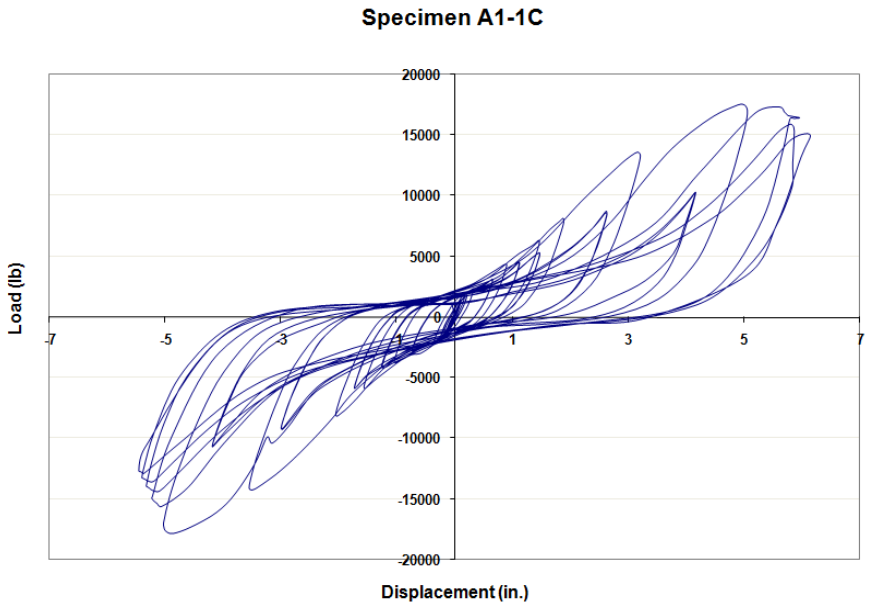

Figure 4.39: Load vs. Displacement diagram resulting from cyclic load testing of Specimen A1-1C

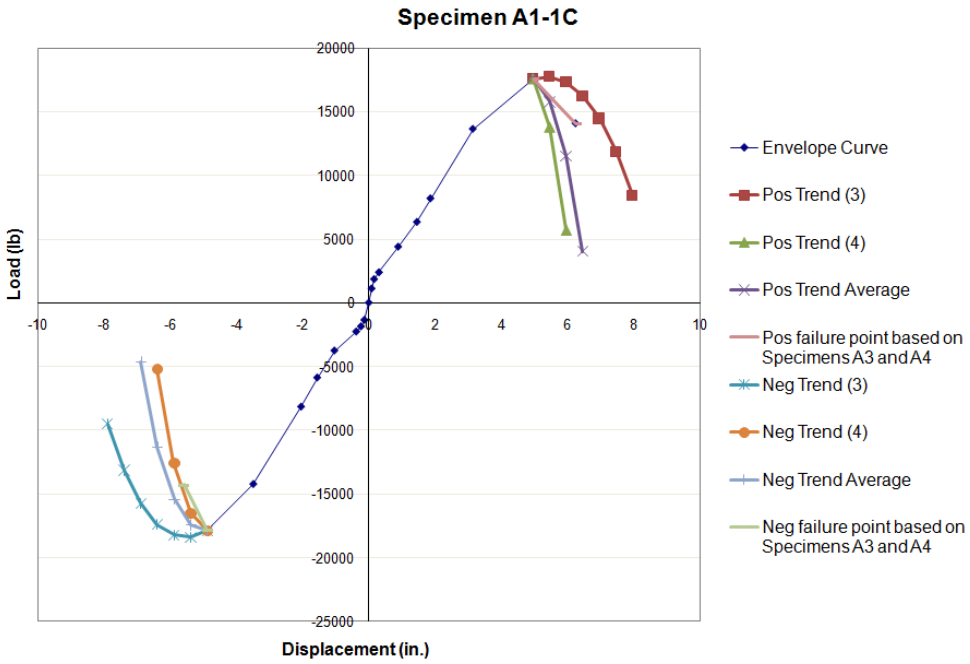

Figure 4.40: Envelope curve and trend lines from Load vs. Displacement diagram of Specimen A1-1C

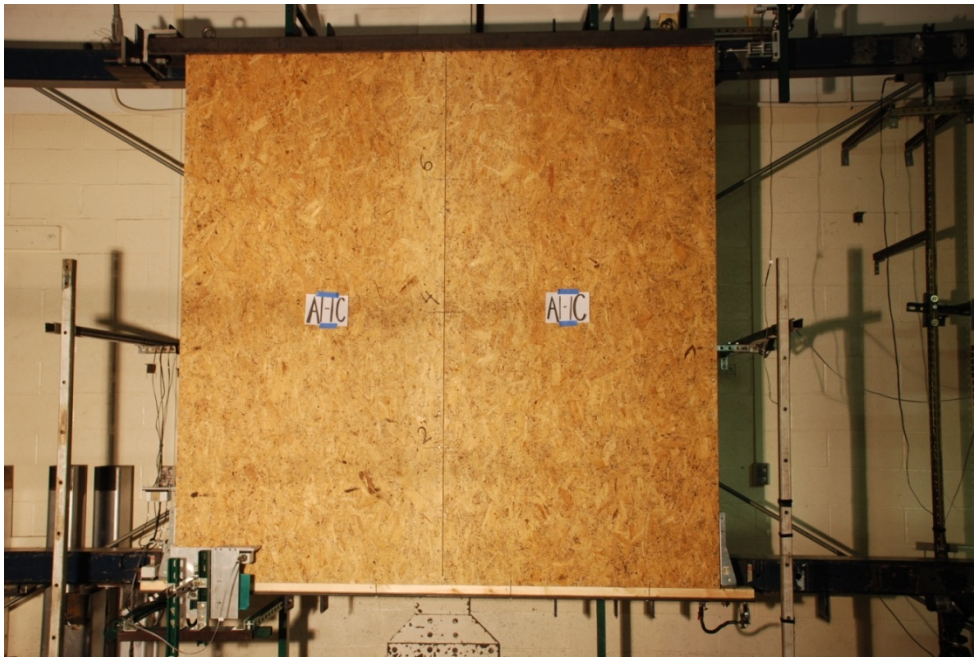

Figure 4.41: Specimen A1-1C before cyclic loading

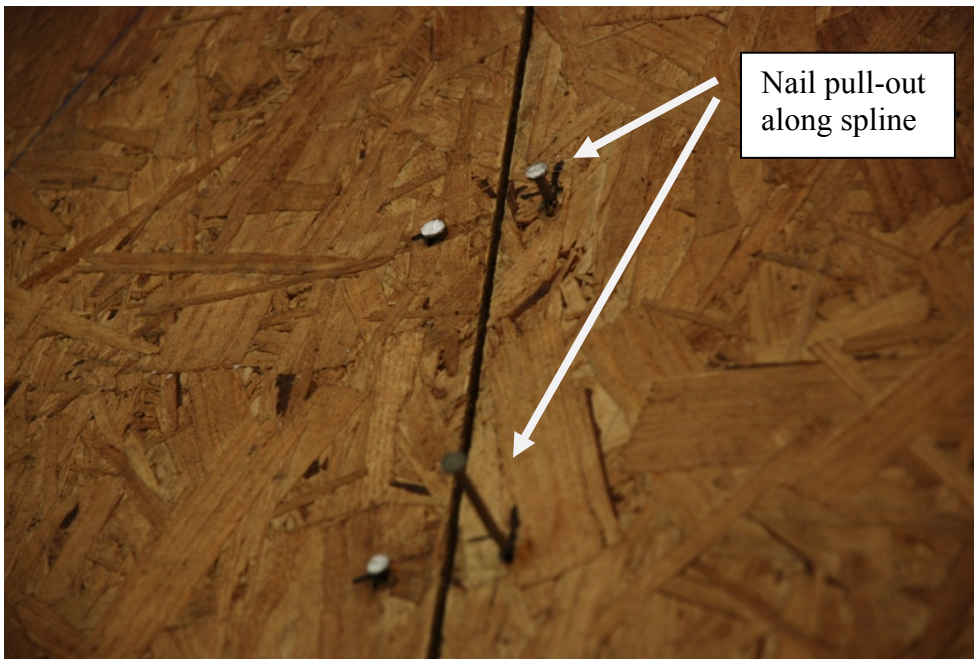

Figure 4.42: Pull-out of nails along spline after cyclic loading of Specimen A1-1C

Figure 4.43: Pull-out of nail along spline after cyclic loading of Specimen A1-1C

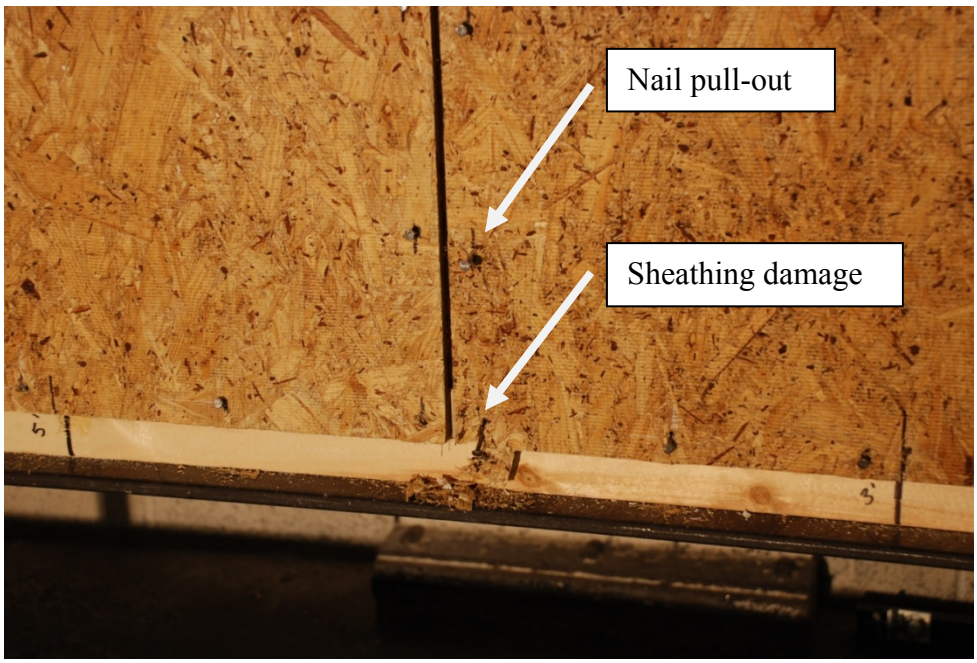

Figure 4.44: Damage to inner corner of sheathing along base plate of Specimen A1-1C

4.4.2.1 Specimen A1-1C Fatigue Tests

In this report, the word "fatigue" refers to loading the specimen under the first thirty-seven cycles of the CUREE cyclic loading protocol after it has already been loaded once before. The specimen is not repaired in anyway between each fatigue loading. After the initial signs of failure for Specimen A1-1C were recorded, without any repair the wall was run through the first thirty-seven cycles of the CUREE cyclic loading protocol a second time to determine the behavior of the wall. The process was repeated two additional times for a total of three fatigue tests. Figure 4.45 shows the envelope curves of the three fatigue tests in comparison to the original test. There was an obvious reduction in strength of the wall as it experienced the fatigue cycles. The ductile nails

used to connect the panels together allowed the specimen to yield but not rupture throughout the loading.

At the completion of Specimen A1-1C Fatigue 1, all of the nails along the spline had pulled out, a majority of the nails along the top plate and base plate pulled out, and there was additional sheathing damage to the inside corners of the sheathing. About half of the nails along the top plate and base plate had also sheared in addition to pulling out. At the end of all three fatigues, the nails along the spline completely pulled out to the point where some fell to the floor. The sheathing on Panel 1 (SIP panel on the right) tore away from the base plate. Figures 4.46, 4.47, 4.48, 4.49, and 4.50 show photographs of Specimen A1-1C after Fatigue 1, Fatigue 2, and Fatigue 3 tests.

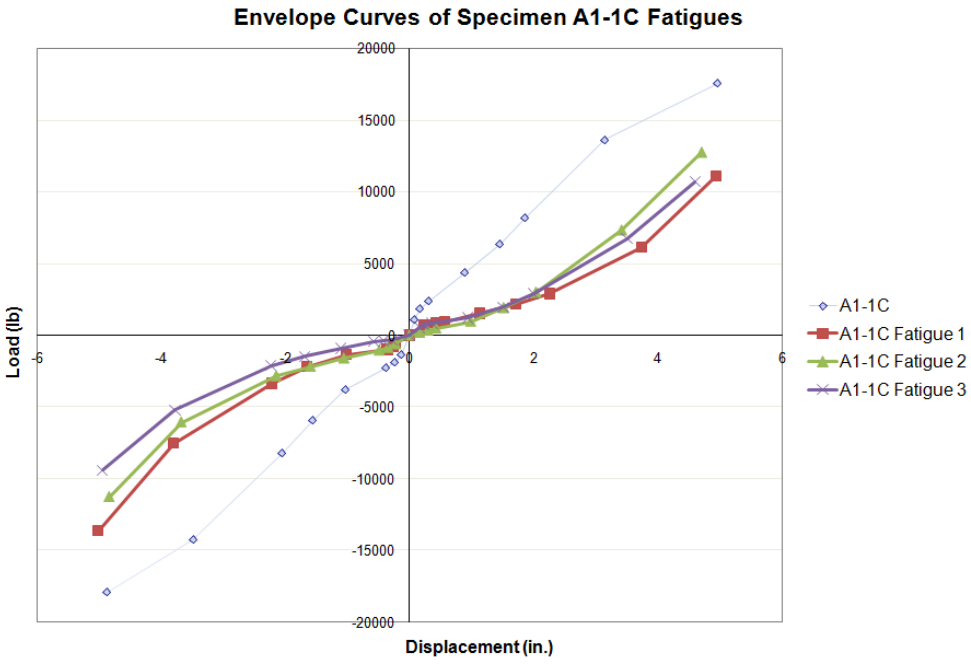

Figure 4.45: Envelope curves of Specimen A1-1C Fatigues based on appropriate Load vs. Displacement diagrams

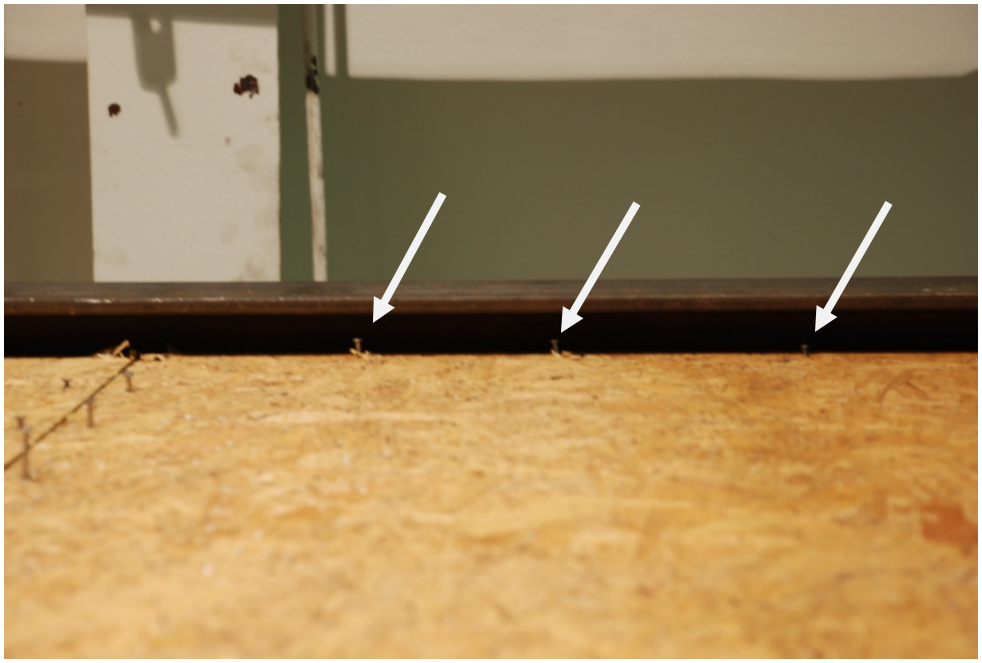

Figure 4.46: Nail pull-out along top plate (refer to arrows) and spline of Specimen A1-1C after Fatigue 1

Figure 4.47: Nail pull-out along spline of Specimen A1-1C after Fatigue 1

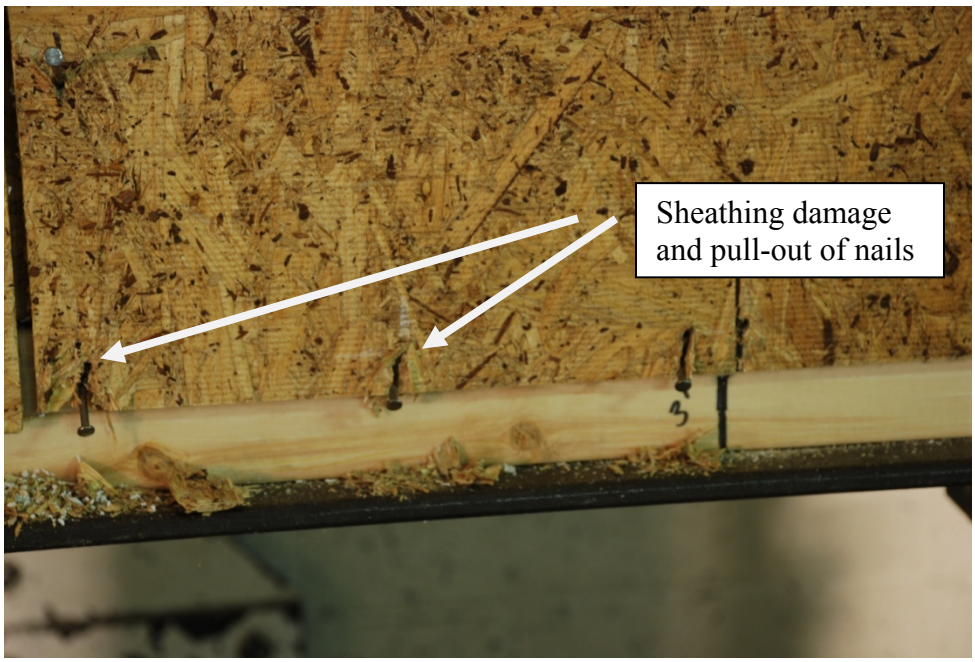

Figure 4.48: Sheathing damage along base plate of Panel 1 of Specimen A1-1C after Fatigue 3

Figure 4.49: Nail pull-out along spline of Specimen A1-1C after Fatigue 3

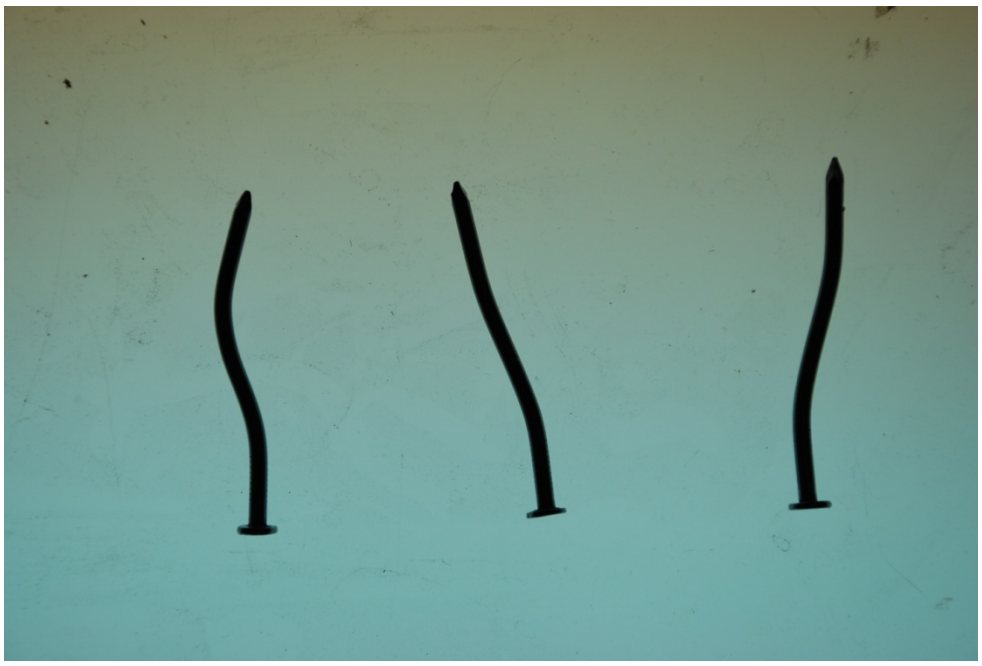

Figure 4.50: Bent nails taken from spline of Specimen A1-1C at the completion of Fatigue 3

4.4.3 Specimen A1-2C

Specimen A1-2C is a replicate of Specimen A1-1C and was tested and analyzed in the same manner in order to validate the results of Specimen A1-1C. Similar to Specimen A1-1C, the initial failure of Specimen A1-2C occurred when the nails along the spline pulled out. Some of the nails along the top plate and base plate then began to pull-out. There was also sheathing damage along the inner corners of the panels along the top plate.

Specimen A1-2C experienced the first thirty-seven cycles of the CUREE loading protocol and was taken to a load of about 18300 lb and a displacement of about 5.17 in.

(5.4% drift ratio). The test was stopped at the drift capacity of the facility before Specimen A1-2C experienced an 80% drop in peak load capacity and before the thirty-eighth cycle of the CUREE loading protocol, which would have most likely caused a complete failure in the specimen. The failure point was determined in the same manner as Specimen A1-1C, using polynomial trend lines and failure points estimated from the failures of Specimens A3 and A4. Figure 4.51 shows the Load vs. Displacement graph and Figure 4.52 shows the envelope curve based off of the hysteresis loops. Figures 4.53, 4.54, and 4.55 are photographs of Specimen A1-2C before and after cyclic loading.

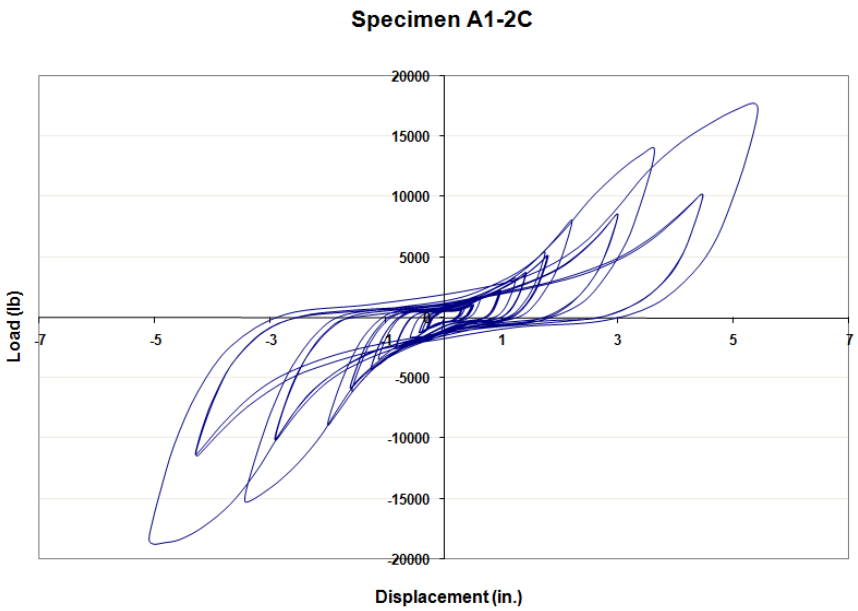

Figure 4.51: Load vs. Displacement diagram resulting from cyclic load testing of Specimen A1-2C

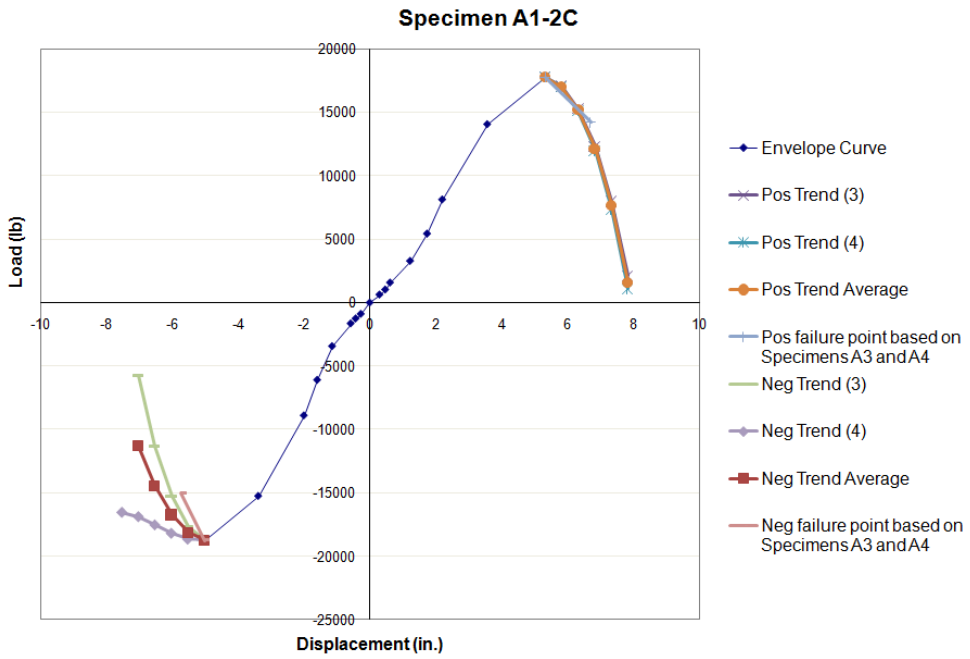

Figure 4.52: Envelope curve and trend lines from Load vs. Displacement diagram of Specimen A1-2C

Figure 4.53: Specimen A1-2C prior to cyclic loading

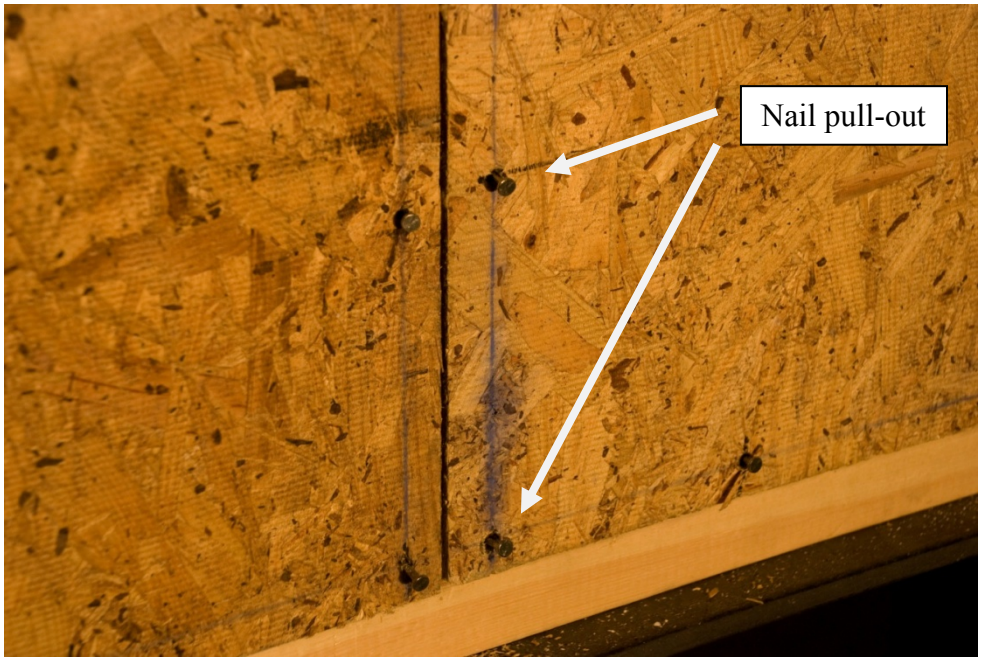

Figure 4.54: Pull-out of nails along spline and base plate caused by cyclic loading of Specimen A1-2C

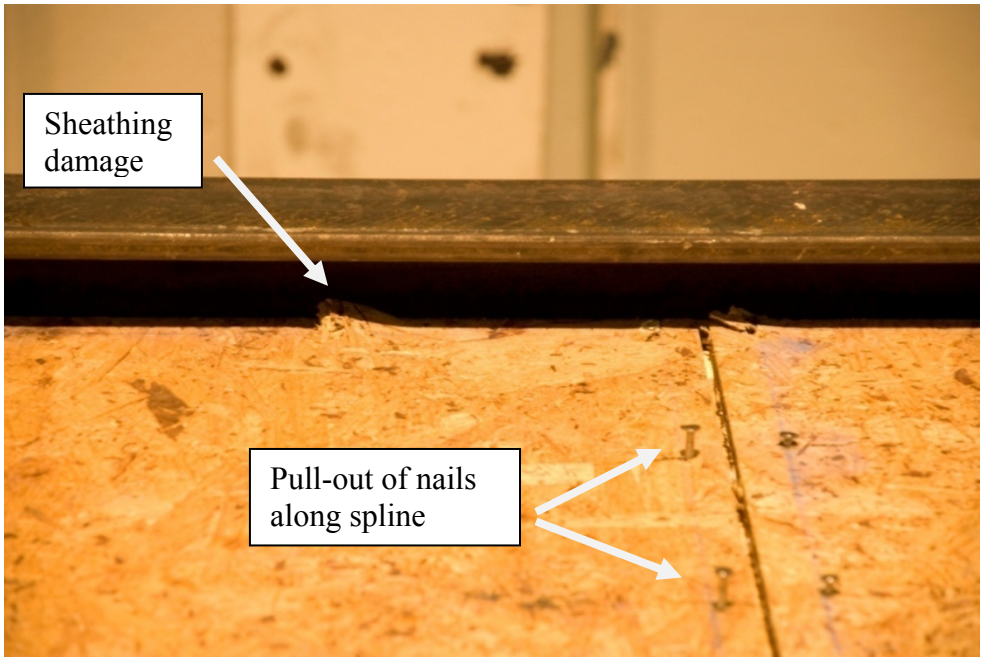

Figure 4.55: Pull-out of nails along spline and sheathing damage along top plate after cyclic loading of Specimen A1-2C

4.4.3.1 Specimen A1-2C Fatigue Tests

As can be seen in Section 4.4.3, Specimen A1-2C was loaded under the first thirty-seven cycles of the CUREE cyclic loading protocol but due to the strength and ductility of the specimen, it did not completely fail. In order to observe the behavior of Specimen A1-2C under fatigue loading, the wall was then loaded through the same thirty-seven cycles of the loading protocol three additional times. Figure 4.56 shows the envelope curves obtained from the hysteresis loops of Specimen A1-2C after Fatigue 1, Fatigue 2, and Fatigue 3 tests in comparison to the original envelope curve of Specimen A1-2C.

Similar to the fatigues of Specimen A1-1C, at the completion of Fatigues 1, 2 and 3 of Specimen A1-2C all of the nails along the spline pulled out in the range of ½ in. to 2 in. Half of the nails along the base plate and top plate pulled out and the two nails located on the inner corner of the sheathing along the base plate sheared in addition to pulling out. There was also sheathing damage along the inner corners of the panels along the top plate. Figures 4.57, 4.58, and 4.59 show photographs of Specimen A1-2C after Fatigue 1, Fatigue 2, and Fatigue 3 tests.

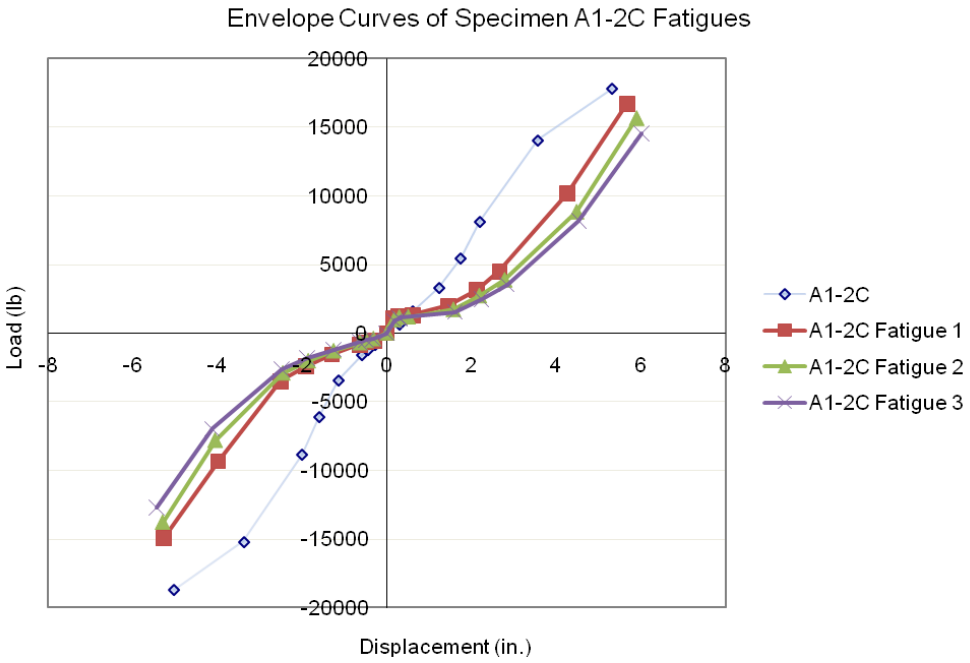

Figure 4.56: Envelope curves of Specimen A1-2C Fatigues based on appropriate Load vs. Displacement diagrams

Figure 4.57: Nail pull-out along spline of Specimen A1-2C after Fatigue 1

Figure 4.58: Nail pull-out along spline of Specimen A1-2C after Fatigue 3

Figure 4.59: Nail pull-out along base plate of Specimen A1-2C after Fatigue 3

4.4.4 Summary of Specimens A1 Fatigue Tests

When Specimens A1-1C and A1-2C were placed under fatigue loading they experienced a loss in strength which is evident from their envelope curves. The ductile nature of the nails allowed the walls to yield a great deal without rupturing. With each fatigue loading the nails along the splines of the specimens continued to withdraw until some of the 2.5 in. long nails completely fell out by the third fatigue. The nails along the top and base plates also pulled out and some sheared. There was also sheathing damage along the top and base plates caused by tear-out of the nails. By the third fatigue, Panel 2 had completely detached from the base plate when all of the nails tore through the sheathing.

The nail pull-out caused a softening of the specimen which affected the specimen's load-displacement relationship. As can be seen in Figures 4.45 and 4.56, the initial slopes of fatigue specimen tests are lower than the original test. However, the stiffness gradually increases and approaches or exceeds the original curve's stiffness near the maximum load. It can further be noted that after an initial drop in the maximum load reached at the facility's displacement limit there is minimal difference between the fatigue test loads. This indicates that the system will have relatively small strength degradation under cyclic fatigue loading after an initial drop and before peak load capacity is reached.

4.4.5 Specimen A1 Bearing-3C

Specimen A1Bearing-3C was different compared to Specimens A1-1C and A1-2C in that the sheathing of the SIP was bearing directly on the loading elements. In Specimens A1-1C and A1-2C, a 2x4 was attached to the top plate and the base plate so that the MC8x20 and the L8x6 load beams did not rest directly on the sheathing. For Specimen A1Bearing-3C, a 2x6 was attached to the top plate and base plate, which replicated actual field conditions and created bearing along the sheathing. The LVDT attached to the top plate of Specimen A1Bearing-3C malfunctioned during the cyclic loading. As a result, the horizontal displacement of the wall was based strictly on the upper sliding steel tube, lower sliding steel tube, and the base plate. By reviewing other tests it can be determined that the wall could have deflected an additional ¾ in. at the maximum displacement.

At the completion of the cyclic loading, there was more extensive damage to the sheathing on Specimen A1Bearing-3C than Specimens A1-1C and A1-2C. There was sheathing failure at the inner corners of the panels along the top plate. Some of the nails along the top plate and the base plate and all of the nails along the spline pulled out.

Specimen A1Bearing-3C was loaded under thirty-seven cycles of the CUREE loading protocol and at that point reached a load of about 19700 lb and a displacement of 4.20 in. (4.4% drift ratio). The testing was stopped after the thirty-seventh cycle when the maximum 20,000 lb load of the facility was reached. The failure point of Specimen A1Bearing-3C was estimated in the same manner as Specimens A1-1C and A1-2C. Figure 4.60 shows the Load vs. Displacement graph and Figure 4.61 shows the envelope curve with the trend lines used to estimate the specimen failure. Figures 4.62, 4.63, and 4.64 are photographs of Specimen A1Bearing-3C.

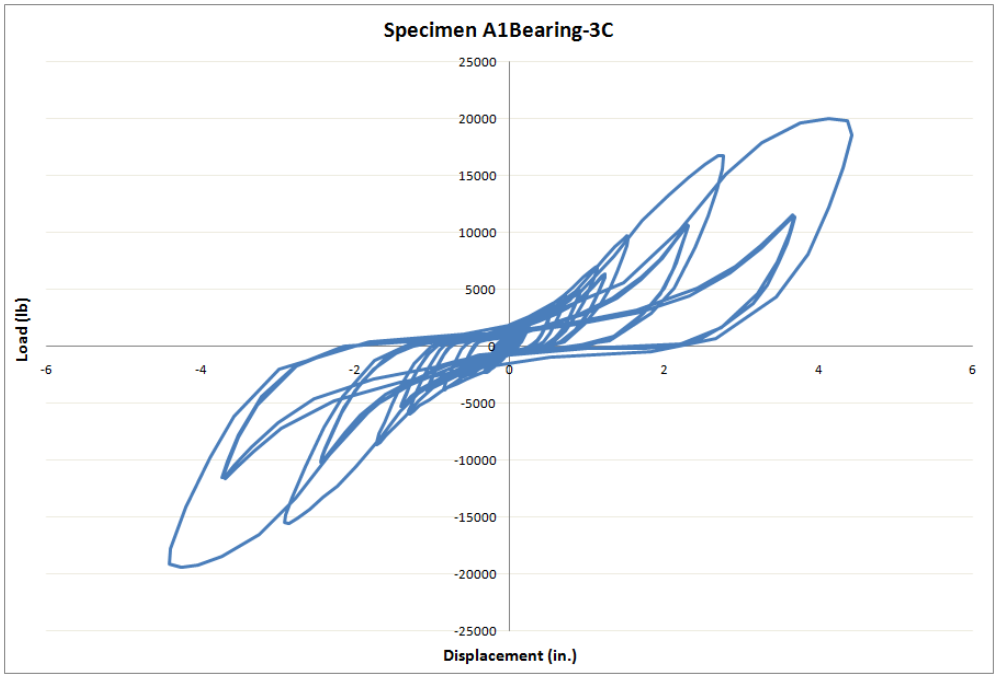

Figure 4.60: Load vs. Displacement diagram resulting from cyclic load testing of Specimen A1Bearing-3C

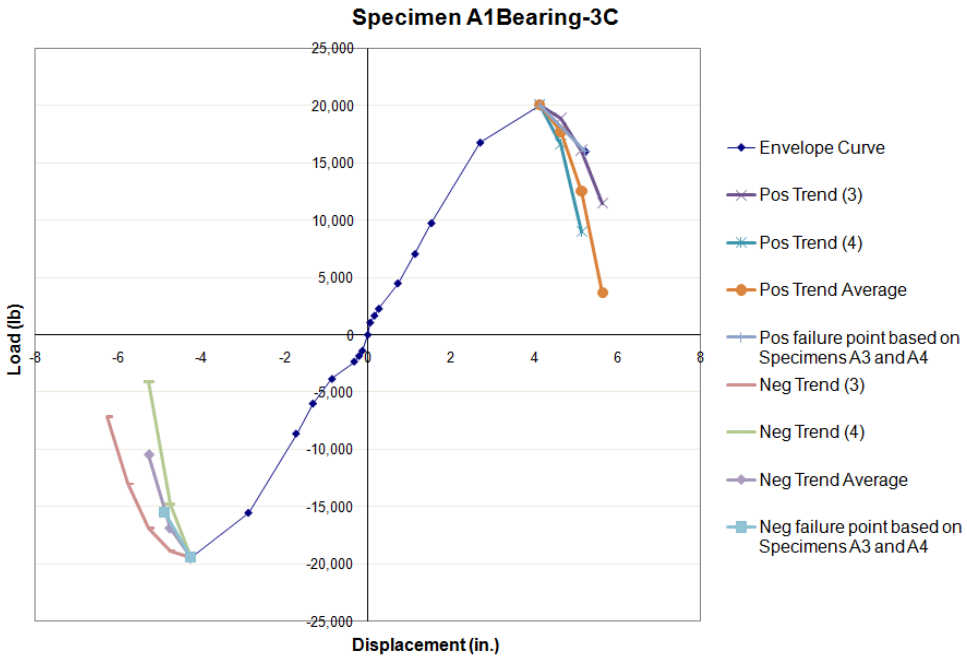

Figure 4.61: Envelope curve and trend lines from Load vs. Displacement diagram of Specimen A1Bearing-3C

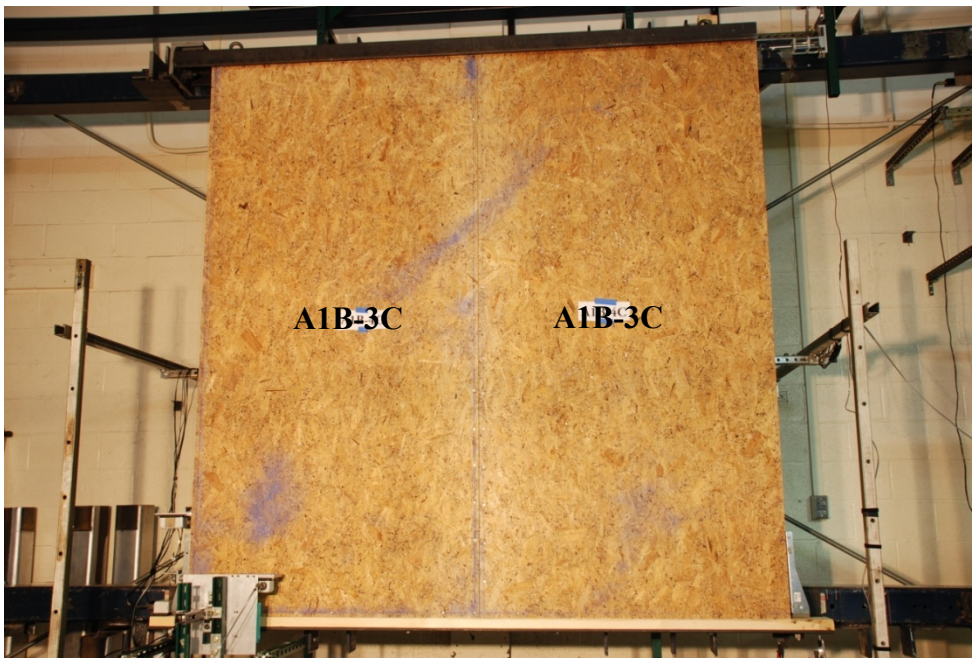

Figure 4.62: Specimen A1Bearing-3C prior to cyclic loading

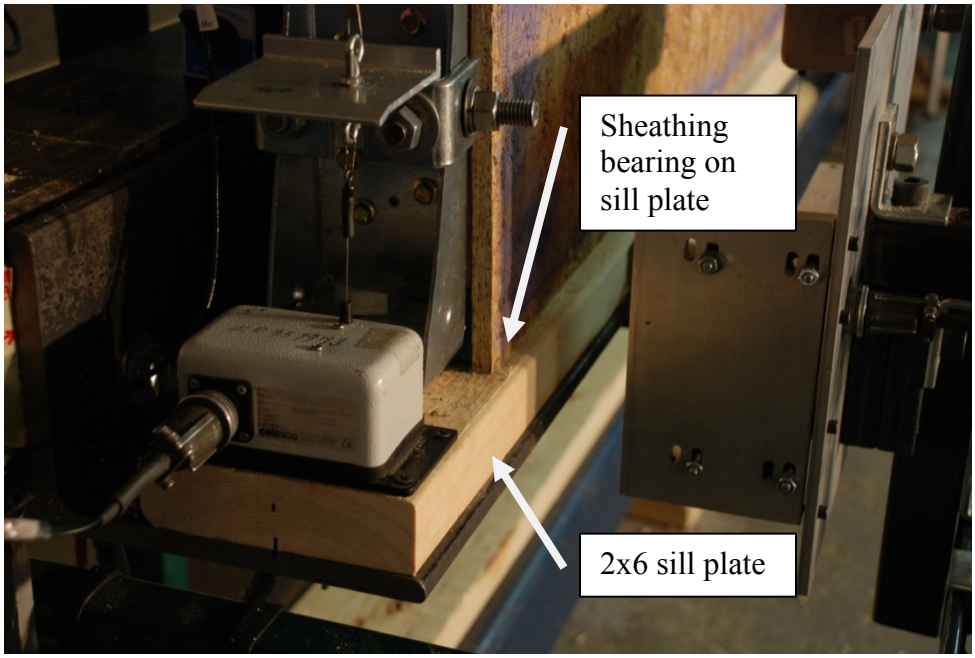

Figure 4.63: 2x6 Sill plate used to create bearing on sheathing of Specimen A1Bearing-3C

Figure 4.64: Pull-out of nails along spline and damage to sheathing along top plate after cyclic loading of Specimen A1Bearing-3C

4.4.5.1 Specimen A1Bearing-3C Fatigue 1

An additional loading of the first thirty-seven cycles of the CUREE cyclic loading protocol was applied to Specimen A1Bearing-3C to determine the specimen's performance under fatigue loading. Unlike Specimens A1-1C and A1-2C, Specimen A1Bearing-3C failed after the first set of fatigue loading. Figure 4.65 shows the Load vs. Displacement graph of Specimen A1Bearing-3C Fatigue 1. As can be seen in Figure 4.65, there was a significant drop in load and increase in displacement right after the specimen reached a load of about 12,600 lb and a displacement of about 4 in. Due to the amount of damage caused to the specimen, for safety concerns the test was stopped

before the trailing cycles could be run. Figure 4.66 shows the envelope curve of Specimen A1Bearing-3C in comparison to the envelope curve of the specimen after Fatigue 1.

After Fatigue 1 of Specimen A1Bearing-3C all of the nails along the spline proceeded to withdraw even further than the initial loading. There was also nail pull-out along the top plate and base plate as well as sheathing damage along the inner corners of the panels along the top plate. The extreme failure occurred along the top plate which split at both ends at the nail line used to attach the top plate to the end posts. In relation to the sheathing, the top plate moved vertically about 1 in. and horizontally about 1.5 in. Figures 4.67, 4.68, 4.69, 4.70, and 4.71 are photographs of Specimen A1Bearing-3C after Fatigue 1.

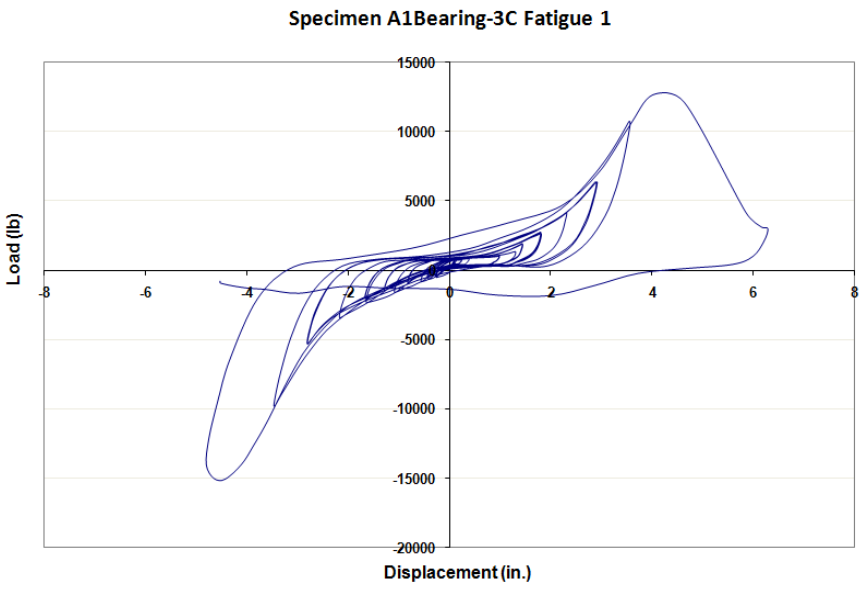

Figure 4.65: Load vs. Displacement diagram resulting from cyclic load testing of Specimen A1Bearing-3C Fatigue 1

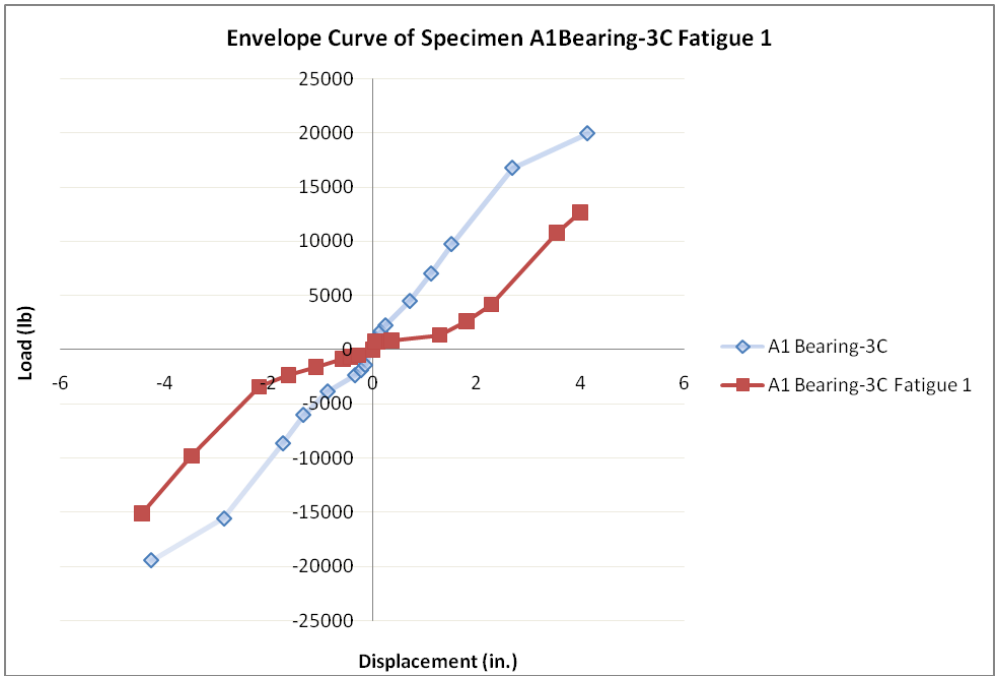

Figure 4.66: Envelope curves of Specimen A1Bearing-3C and Fatigue 1

Figure 4.67: Specimen A1Bearing-3C before Fatigue 1

Figure 4.68: Nail pull-out along top plate (see arrows) after Fatigue 1 of Specimen A1Bearing-3C

Figure 4.69: Nail pull-out along spline of Specimen A1Bearing-3C after Fatigue 1

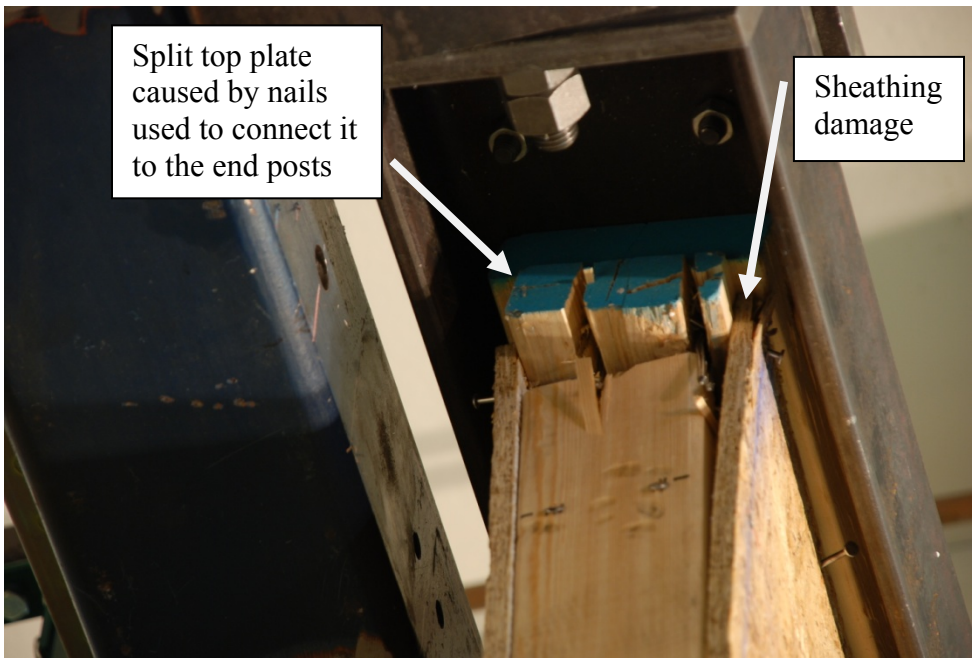

Figure 4.70: Damage to top plate and sheathing of Specimen A1Bearing-3C after Fatigue 1

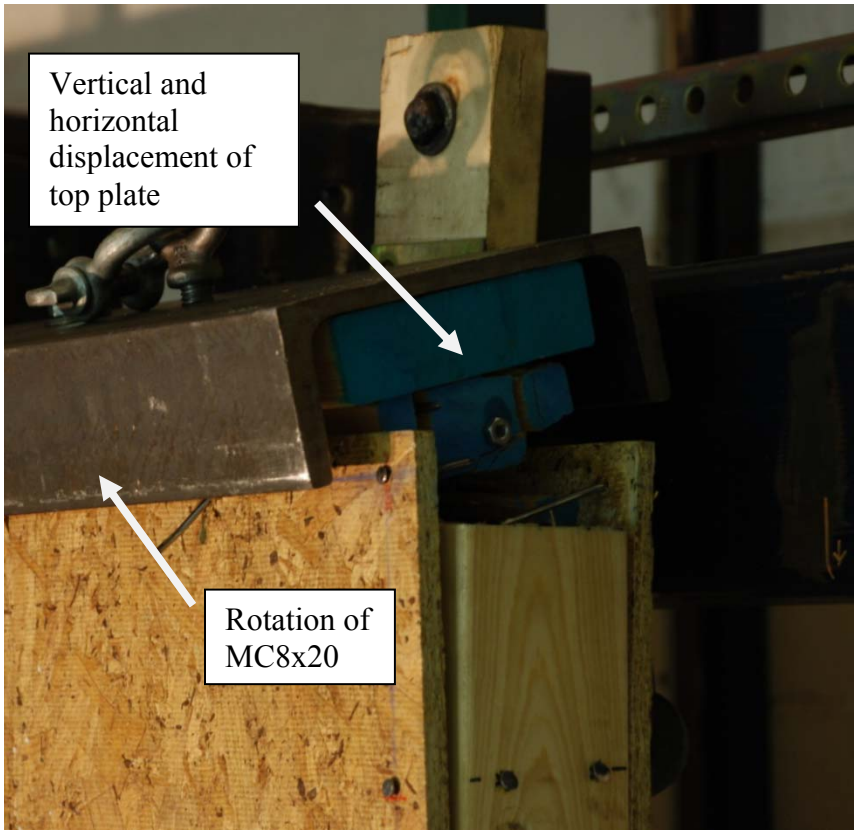

Figure 4.71: Tear-out of top plate from end posts and sheathing after Fatigue 1 of Specimen A1Bearing-3C. Displacement of MC8x20 channel which is used to apply load to specimen.

4.4.6 Specimen A1 Internal-4C

Specimen A1Internal-4C was exactly the same as Specimens A1-1C and A1-2C except the USP PHD 6 hold-down was placed on the interior of the double studded end posts. In order to attach the hold-downs to the interior of the end posts, a 15.5 in. x 13.5 in. section was cut out of the back side of the SIP panels. The OSB sheathing along the end posts and the base plate were not cut so the sheathing was still attached along the bottom corners of the panel with the typical nailing pattern.

The initial failure of Specimen A1Internal-4C occurred along the spline when the nails pulled out. There was also sheathing damage along the inner corner of the panels on the front side of the wall and along the 1.5 in. wide sheathing along the base plate beneath the cut-out for the internal hold-down on Panel 2 (panel on the left when looking at the front of the wall). A foot-long split in the base plate also occurred in Panel 2.

Specimen A1Internal-4C experienced a maximum load of about 16600 pounds and a maximum displacement of about 5.11 in. (5.3% drift ratio) after thirty-seven cycles of the CUREE loading protocol. As previously stated, the wall system showed signs of failure. Due to the displacement limitation of the test facility the testing was stopped after the thirty-seventh cycle. The failure point of the specimen was determined in the same manner as Specimens A1-1C, A1-2C, and A1Bearing-3C. Figure 4.72 shows the Load vs. Displacement graph and Figure 4.73 shows the envelope curve with the trend lines used to estimate the specimen failure. Figures 4.74, 4.75, 4.76, and 4.77 are photographs of Specimen A1Internal-4C.

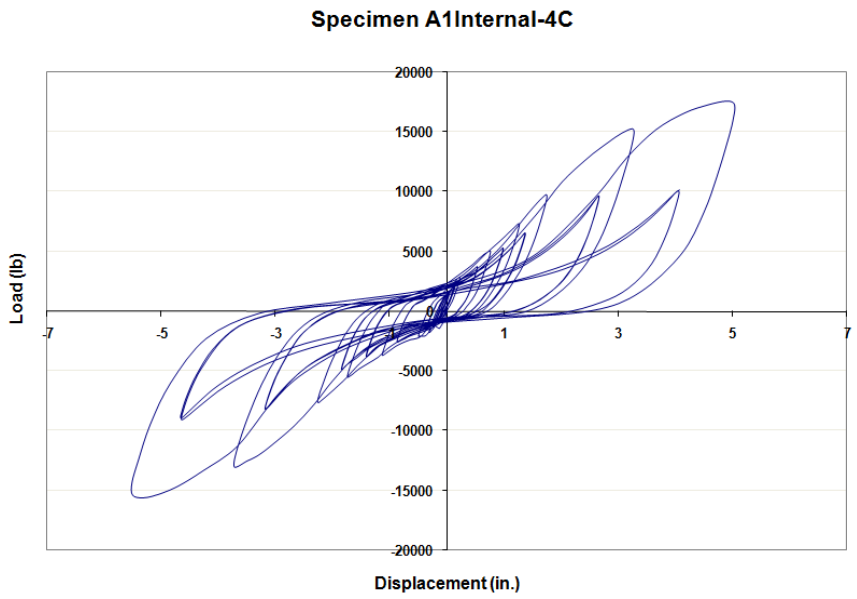

Figure 4.72: Load vs. Displacement diagram resulting from cyclic load testing of Specimen A1Internal-4C

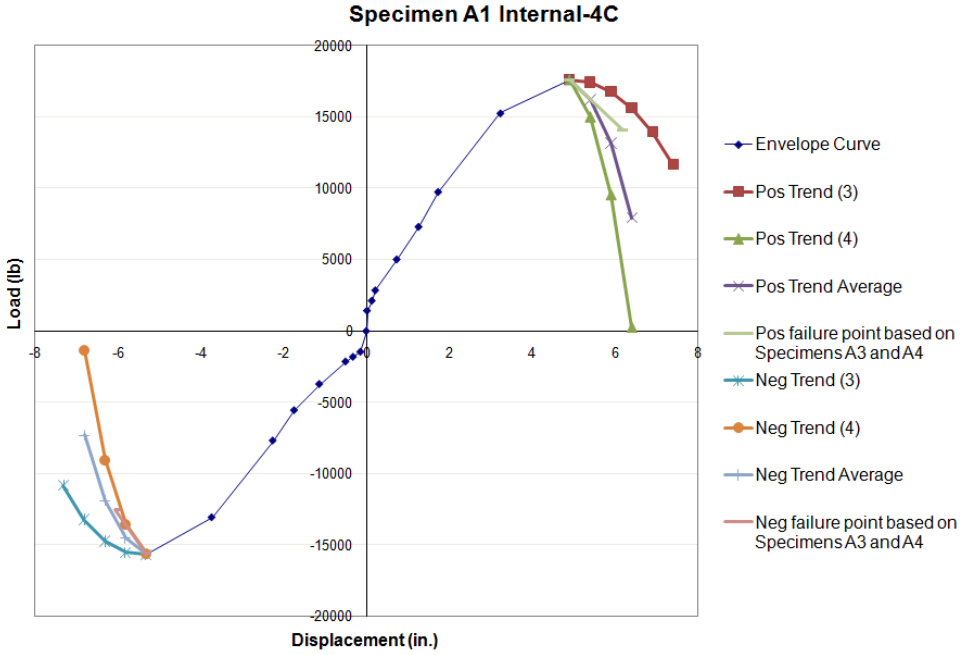

Figure 4.73: Envelope curve and trend lines from Load vs. Displacement diagram of Specimen A1Internal-4C

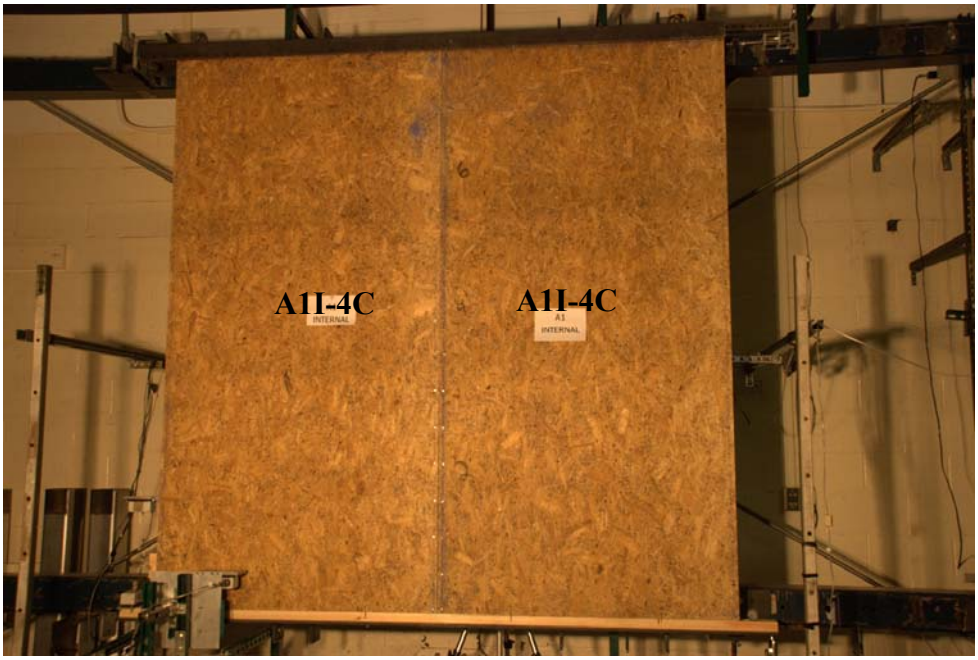

Figure 4.74: Specimen A1Internal-4C prior to cyclic loading

Figure 4.75: Internal USP PHD6 hold-down fit into 13.5 in.x15.5 in. cut-out in SIP panel of Specimen A1Internal-4C

Figure 4.76: Sheathing damage at inner corner of panels along base plate after cyclic loading of Specimen A1Internal-4C

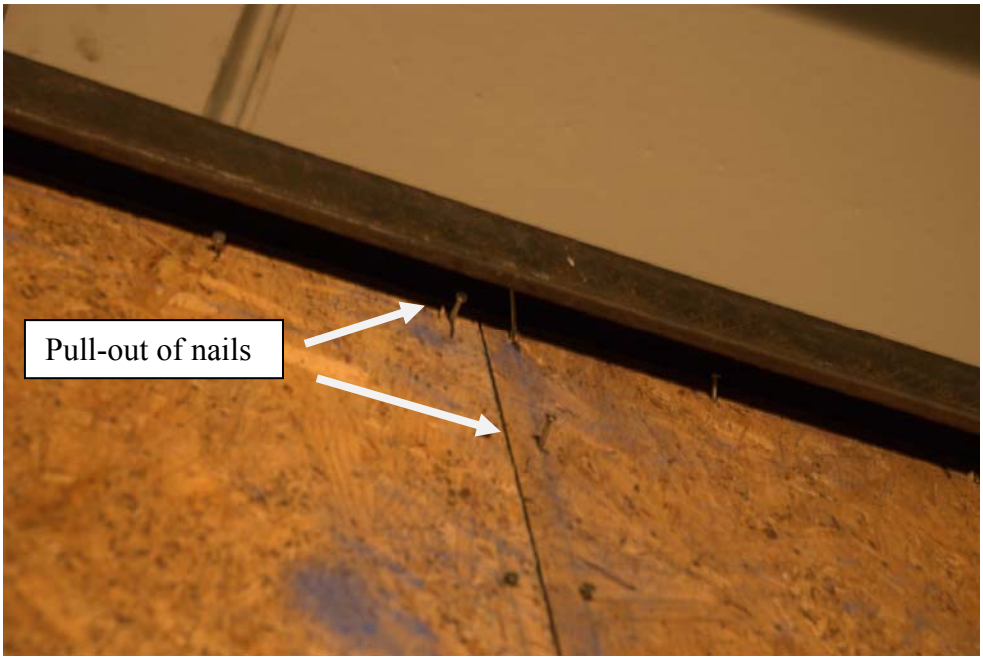

Figure 4.77: Pull-out of nails along spline and top plate after cyclic loading of Specimen A1Internal-4C

4.4.6.1 Specimen A1Internal-4C Fatigue Tests

As discussed in Section 4.4.6, Specimen A1Internal-4C was loaded under the first thirty-seven cycles of the CUREE cyclic loading protocol but it did not completely fail before the capacity of the facility was reached. In order to observe the behavior of Specimen A1Internal-4C under fatigue loading, the wall was then loaded through the same thirty-seven cycles of the loading protocol three additional times. Figure 4.78 shows the Envelope Curves obtained from the hysteresis loops of Specimen A1Internal-4C after Fatigue 1, Fatigue 2, and Fatigue 3 in comparison to the original envelope curve of Specimen A1Internal-4C. The envelope curves show that the specimen did not reach complete failure at maximum displacement capacity of the facility but there is an obvious decrease in strength with each additional fatigue loading.

At the completion of the first fatigue test of Specimen A1Internal-4C, there was additional sheathing damage along the base plate. After Fatigues 2 and 3 the nails along the spline pulled out between 0.75 in. to 1.75 in. away from the sheathing. There was also additional sheathing damage from the inner corners to the center of the panels along the base plate. Figures 4.79, 4.80, 4.81, 4.82, and 4.83 are photographs of Specimen A1Internal-4C after Fatigue 1, Fatigue 2, and Fatigue 3 tests.

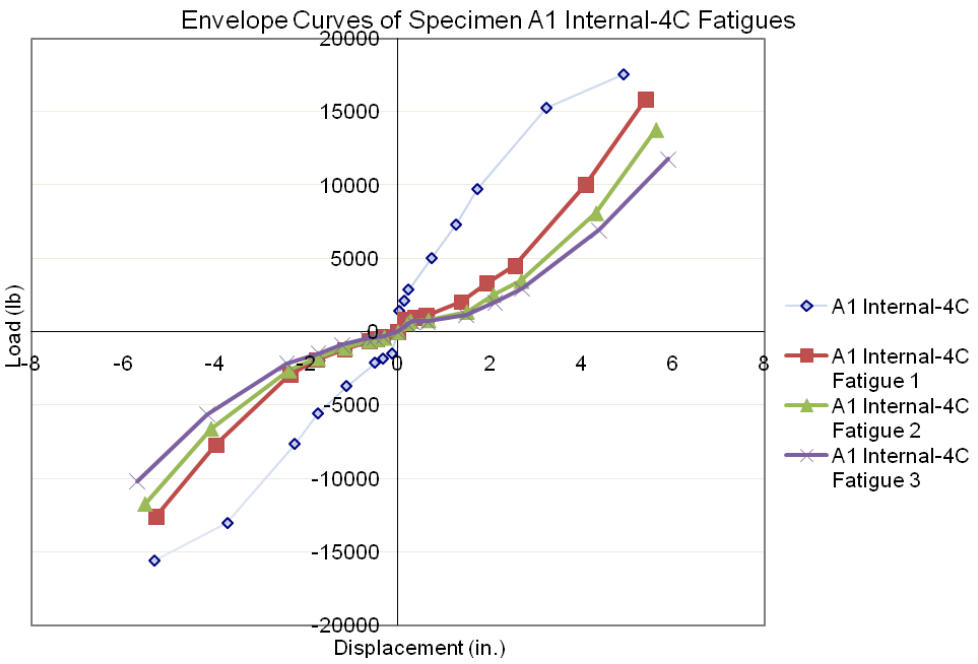

Figure 4.78: Envelope curves of Specimen A1Internal-4C Fatigues based on appropriate Load vs. Displacement diagrams

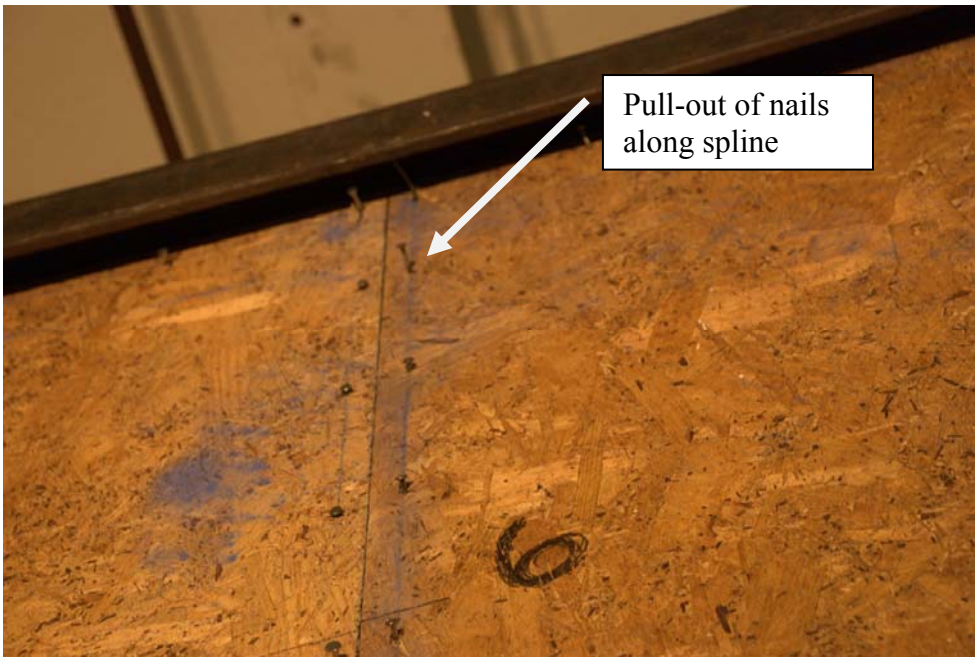

Figure 4.79: Nail pull-out along spline of Specimen A1Internal-4C after Fatigue 1

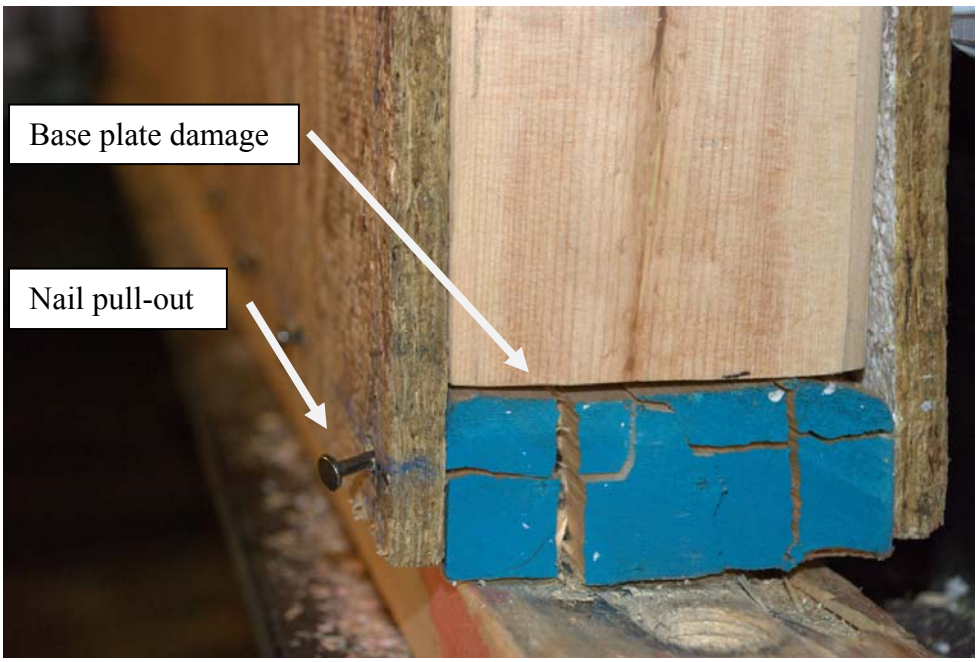

Figure 4.80: Nail pull-out along base plate and splitting of base plate of Specimen A1Internal-4C after Fatigue 2

Figure 4.81: Nail pull-out along spline of Specimen A1Internal-4C after Fatigue 3

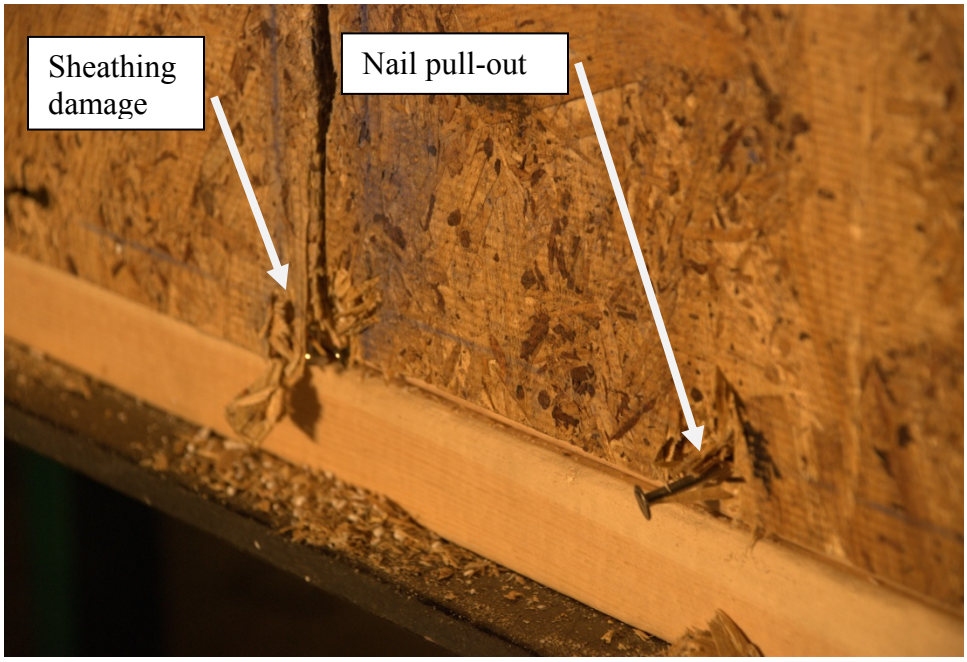

Figure 4.82: Nail pull-out and sheathing damage along base plate of Specimen A1Internal-4C after Fatigue 3

Figure 4.83: Nail pull-out along spline and top plate of Specimen A1Internal-4C after Fatigue 3

4.4.7 Summary of Specimens A1 Tests

Specimens A1 with OSB splines and 8d common nails at 6 in. o.c. showed peak strengths in excess of the facility's 20,000 lb capacity at a large drift, and also showed many nail pull-outs, especially under fatigue loading. Specimens A1-1C and A1-2C were able to resist a maximum load ranging between 17998 lb and 18174 lb at a displacement ranging from 5.05 in. to 5.30 in. (5.3% to 5.5% drift ratio). Under monotonic loading the maximum force resisted ranged from 17565 lb to 17631 lb at displacements ranging from 4.50 in. to 5.00 in. (4.7% to 5.2% drift ratio). The load range under monotonic loading was about 3% less than the peak load range under cyclic loading. The displacement under monotonic loading was about 9% less than the displacement under cyclic loading. During the cyclic loading of Specimen A1, the initial failure occurred when the nails pulled out along the spline. The load was then transferred to the top and base plates, which caused the nails to pull-out along the top and bottom of the panels. There was also sheathing damage along the inner corners of the panels.

Specimen A1Bearing-3C experienced more extensive damage to the sheathing along the top and base plates in comparison to Specimens A1-1C and A1-2C. This was because the sheathing was bearing on lumber, which is consistent with field design. Similar to Specimens A1-1C and A1-2C, nails along the spline pulled out as well as nails along the top and base plates. The maximum load resisted by A1Bearing-3C was about 8% greater than A1-1C and A1-2C and the displacement was about 17% less.

Specimen A1Internal-4C acted very similarly to A1-1C and A1-2C. The maximum load resisted and the subsequent displacement were within 8% of A1-1C and

A1-2C. The initial failure occurred when the nails pulled out along the spline. There was sheathing damage at the inner corners of the panels and along the 1.5 in. wide section attached to the base plate beneath the hold-down cut-out. The base plate experienced a foot-long split along the left side of the wall.

4.5 Specimens B

Specimens B had a (2) 2x4 spline, which were connected together with (2) 16d common nails spaced at 4 in. from each end of the 7 ft 9 in. spline and 24 in. o.c. The spline and the framing lumber were attached to the OSB sheathing of the SIP with 8d common nails spaced at 6 in. o.c. The USP PHD6 hold-downs were placed at the exterior of the 8 ft x 8 ft wall.

4.5.1 Specimen B-1M

Specimen B-1M was tested under monotonic loading according to ASTM E 564-06. The specimen was pushed up to about 17000 lb at a drift of about 5 in. (5.2% drift ratio) The wall did not reach complete failure but the test was stopped due to displacement limitations of the facility. Signs of failure in the wall included the withdrawal and deformation of nails located along the top plate. There was also sheathing damage at the inner top and bottom corners of the panels. Also, each 2x4 of the (2) 2x4 spline started to split apart and move with the SIP panel it was nailed.

Even though the test was stopped before there was an 80% drop in load, it is evident that the strength limit state shear force was reached. Figure 4.84 shows the Load vs. Displacement graph which levels off around 17000 lb.

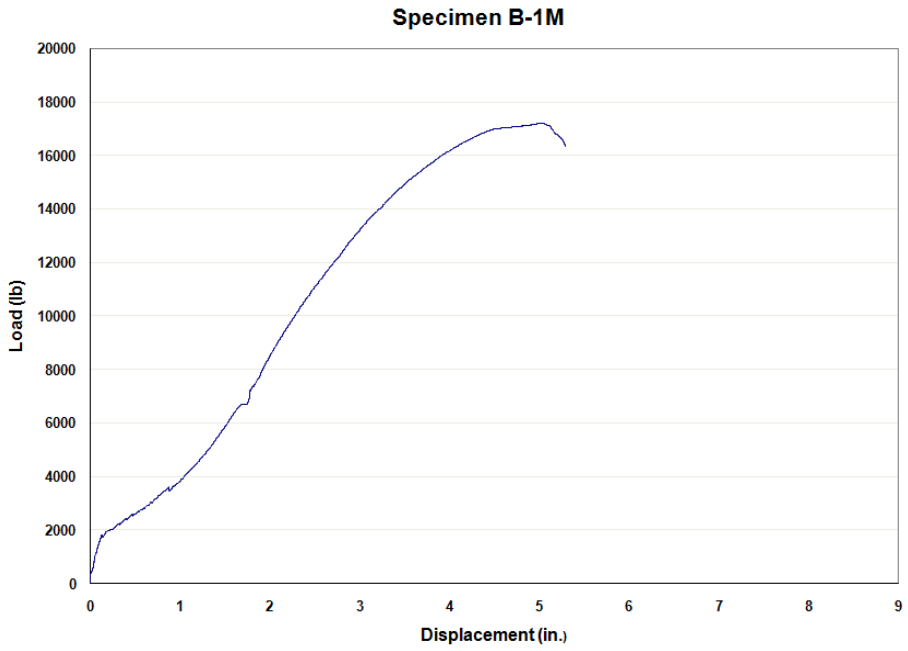

Figure 4.84: Load vs. Displacement diagram resulting from monotonic load testing of Specimen B-1M

4.5.2 Specimen B-1C

Specimen B-1C was tested under cyclic loading using a target displacement of 6 in. for the CUREE protocol. The specimen was loaded to thirty-seven cycles of the CUREE loading protocol forcing the wall to a maximum load of about 17411 lb and a drift of about 5.15 in. (5.4% drift ratio). Even though the ultimate failure was not reached

after the thirty-seventh cycle of the loading protocol there were signs of failure. The (2) 2x4 spline of the specimen began to pull away from each other and move with the individual SIP panels they were nailed to. There was also tear-out sheathing failure along the top plate and pull-out of nails in the base plate. The displacement limitation of the test facility did not allow the wall to reach an 80% drop in load. As a result, similar to Specimens A1, the failure point of the wall was estimated using trend lines and failures of previous specimens.

Figure 4.85 shows the Load vs. Displacement graph and Figure 4.86 shows the envelope curve and trend lines for Specimen B-1C**.** Figures 4.87 and 4.88 are photographs of the specimen after it was placed under cyclic loading.

After the test was complete it was noticed that six nails along the base plate of the back side of Panel 1 were missing. The nails at the corners were still attached, but the intermediate nails were missing.

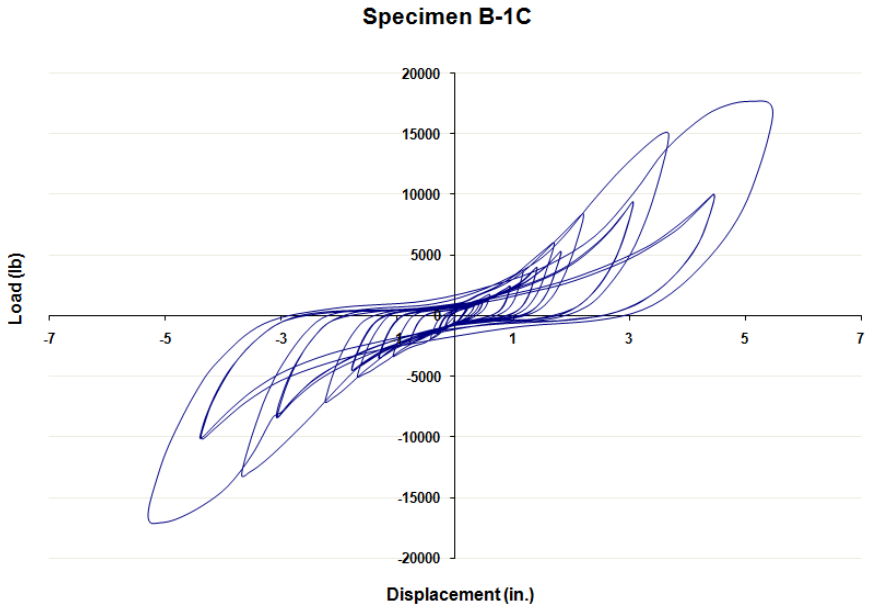

Figure 4.85: Load vs. Displacement diagram resulting from cyclic load testing of Specimen B-1C

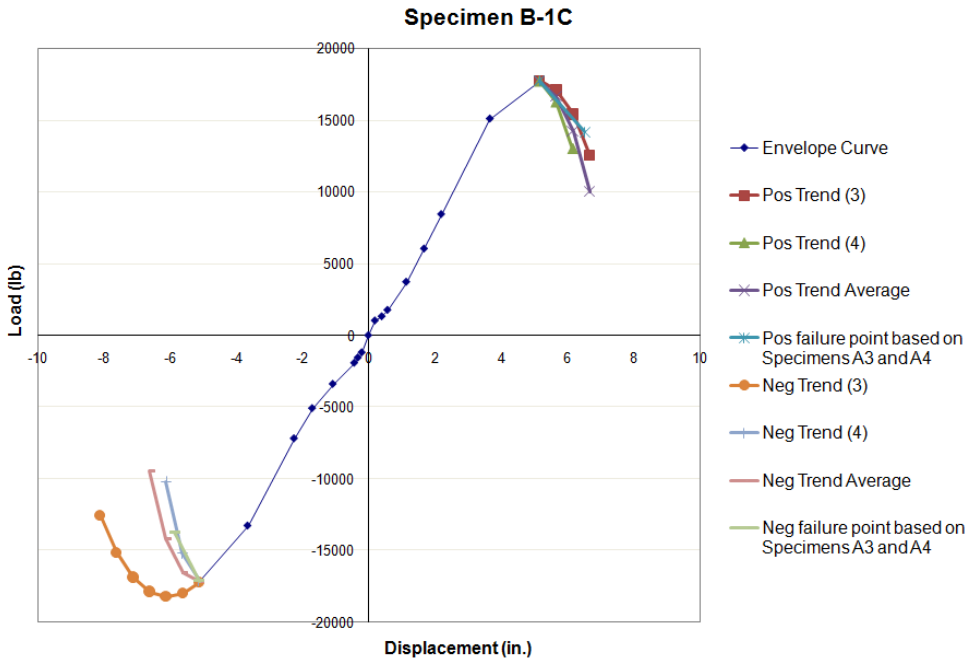

Figure 4.86: Envelope curve and trend lines from Load vs. Displacement diagram of Specimen B-1C

Figure 4.87: Horizontal separation of (2) 2x4 spline shown at the 6 ft high mark of Specimen B-1C after cyclic loading

Figure 4.88: Sheathing damage along base plate after cyclic loading of Specimen B-1C

4.5.2.1 Specimen B-1C Fatigue 1

Specimen B-1C did not completely fail after the initial loading but it did fail when the specimen was loaded a second time under the first thirty-seven cycles of the CUREE loading protocol. The Fatigue 1 of Specimen B-1C failed when the wall reached a load of about 15000 lb and a displacement of 5.60 in. (5.8% drift ratio). Figure 4.89 shows the Load vs. Displacement graph of Specimen B-1C Fatigue 1 and Figure 4.90 shows the envelope curve of Specimen B-1C Fatigue 1 in comparison to Specimen B-1C.

Specimen B-1C experienced extensive failure after Fatigue 1. The (2) 2x4 spline completely split apart. The sheathing failed along the top plate and the bottom plate. The top plate split and completely separated from Panel 1 (SIP panel on the right). There was also damage to the base plate along Panel 2. Figures 4.91, 4.92, 4.93, 4.94, and 4.95 are photographs of Specimen B-1C after the Fatigue 1 test.

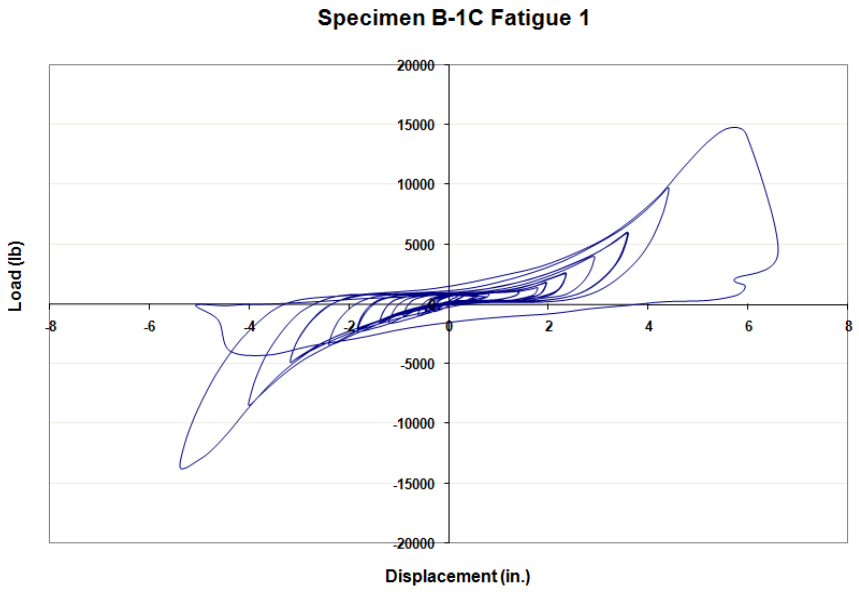

Figure 4.89: Load vs. Displacement diagram resulting from cyclic load testing of Specimen B-1C Fatigue 1

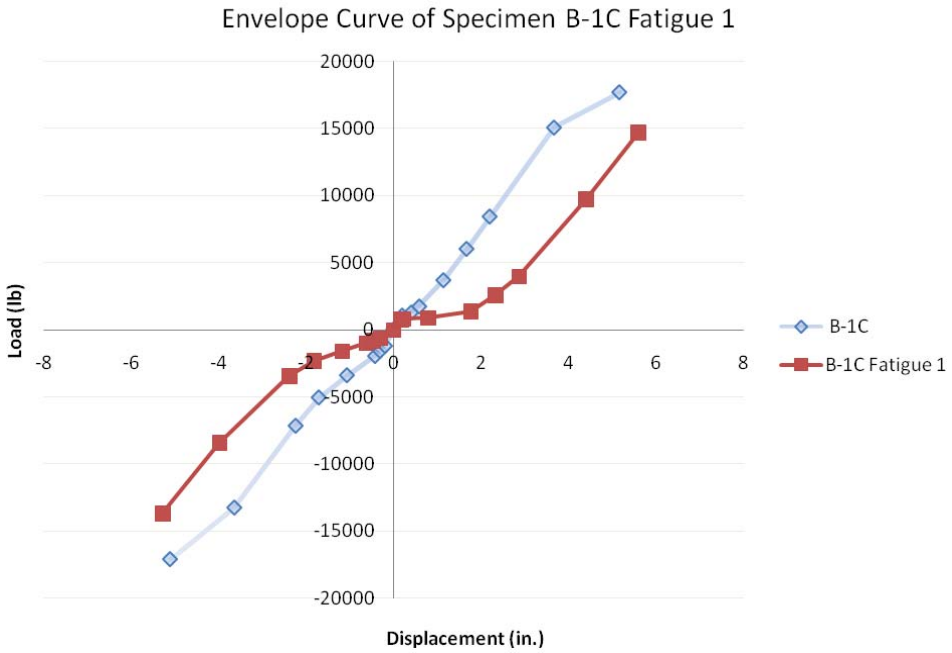

Figure 4.90: Envelope curve of Specimen B-1C Fatigue 1 based on appropriate Load vs. Displacement diagram

Figure 4.91: Displacement of panels in relation to each other after Fatigue 1 of Specimen B-1C

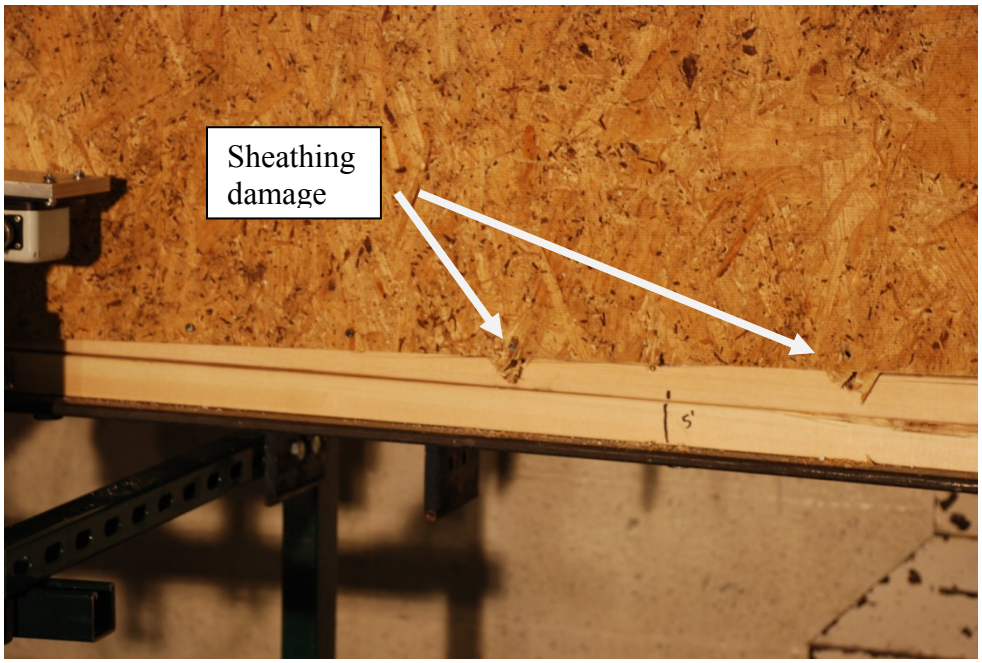

Figure 4.92: Sheathing damage along base plate of Specimen B-1C after Fatigue 1

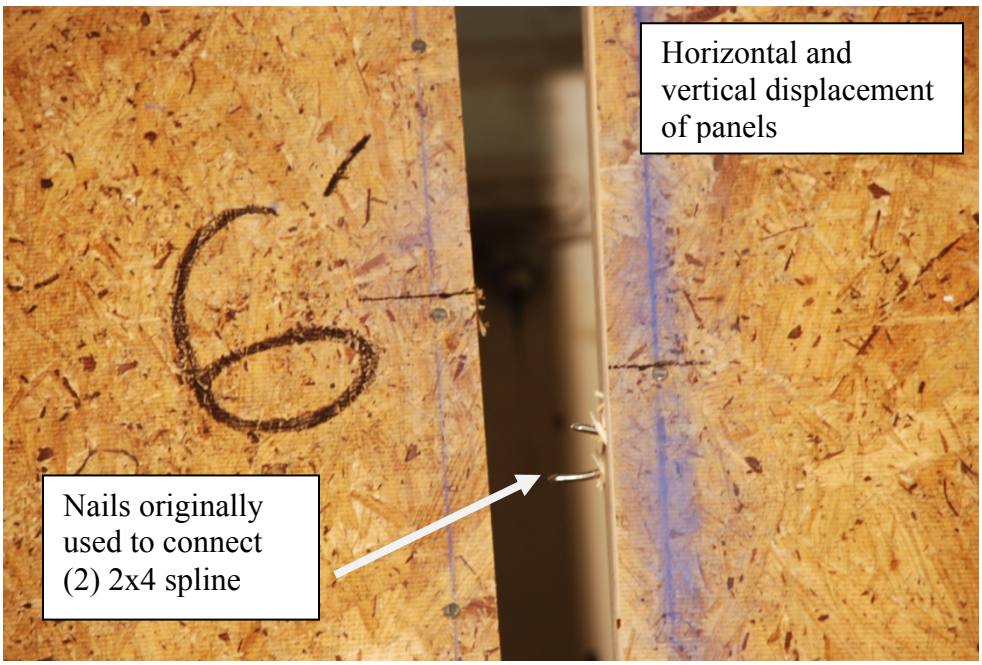

Figure 4.93: 2.5 in. horizontal and 1.3 in. vertical deflection between SIP panels at 6 ft vertical mark along Specimen B-1C after Fatigue 1. Notice bent nails originally used to connect (2) 2x4 spline.

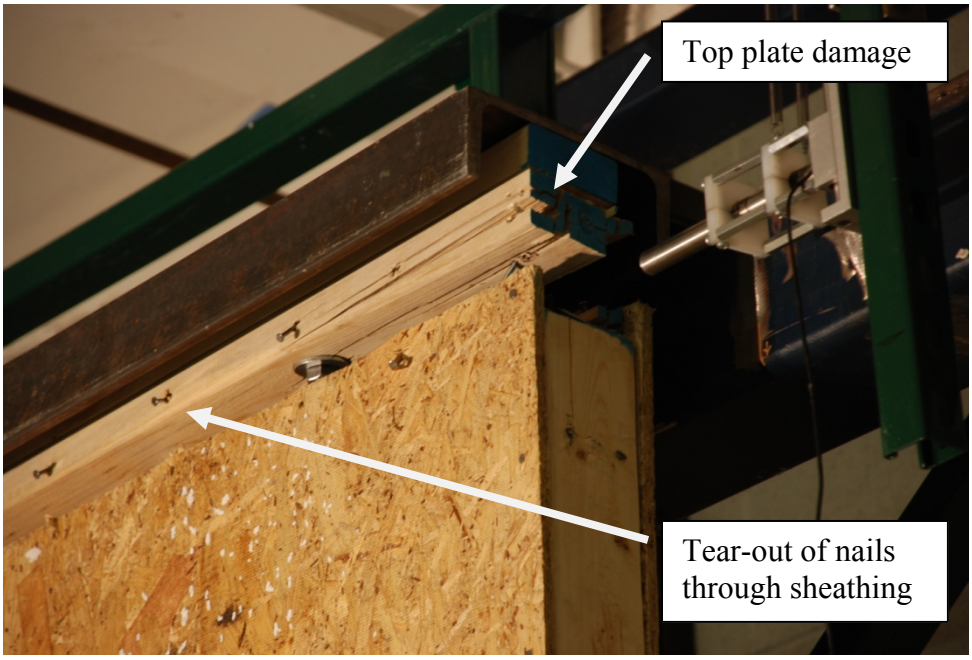

Figure 4.94: Deflection of top plate from sheathing and end posts caused by sheathing failure and splitting of top plate along nail line connecting top plate to end posts in Specimen B-1C after Fatigue 1

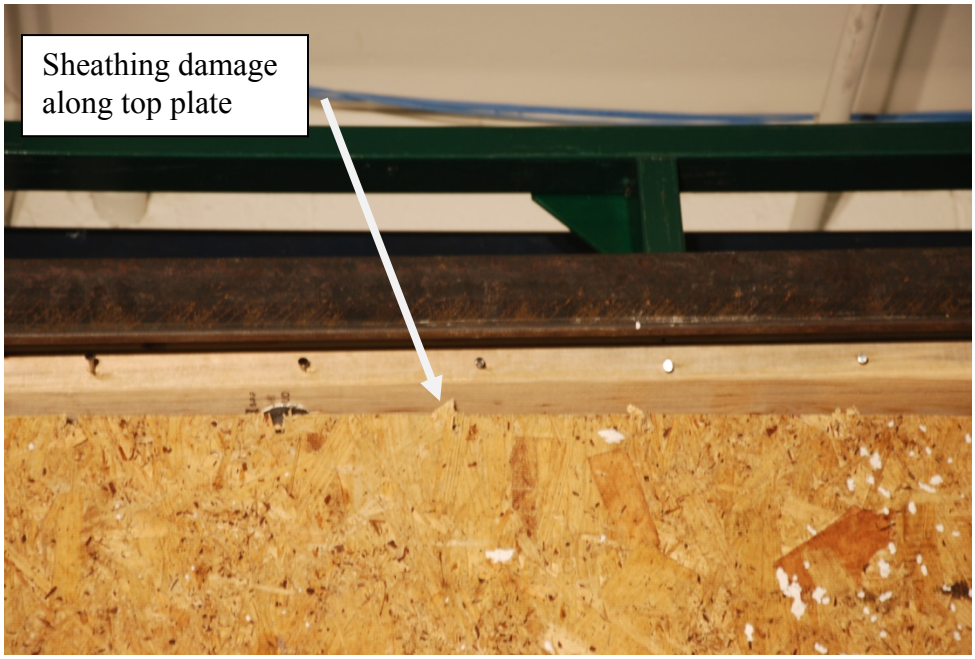

Figure 4.95: Sheathing failure along top plate of Specimen B-1C after Fatigue 1

4.5.3 Specimen B-2C

Specimen B-2C, a replicate of Specimen B-1C, was tested and analyzed in the same manner in order to validate the results of Specimen B-1C. The specimen was loaded under thirty-seven cycles of the CUREE loading protocol and taken to a maximum load of about 19700 lb at a drift of about 5 in. (5.2% drift ratio). The failure modes of Specimen B-2C were very similar to Specimen B-1C. The (2) 2x4 spline split apart ranging from a gap of 0.30 in. at 2 ft up the spline to 0.35 in. at 6 ft up the spline. There was sheathing damage in the top plate and nail pull-out along the base plate.

The cyclic loading of Specimen B-2C was stopped when the 20,000 lb load capacity of the facility was met, but before the specimen reached an 80% decrease in peak load capacity. The failure point was determined using the same method as Specimens A1 and B-1C. Figure 4.96 shows the Load vs. Displacement graph and Figure 4.97 shows the envelope curve and trend lines for Specimen B-2C. Figures 4.98 and 4.99 are photographs of the specimen before and after it was placed under cyclic loading.

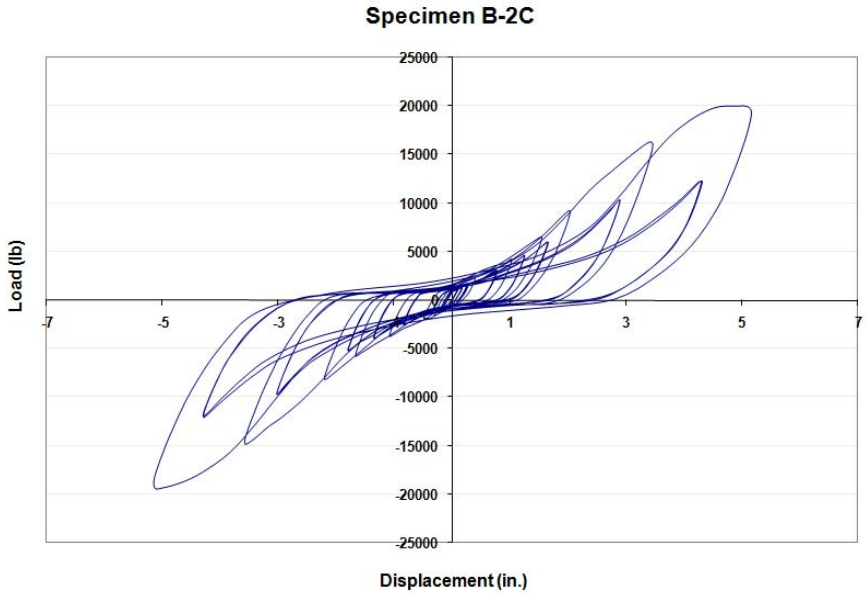

Figure 4.96: Load vs. Displacement diagram resulting from cyclic load testing of Specimen B-2C

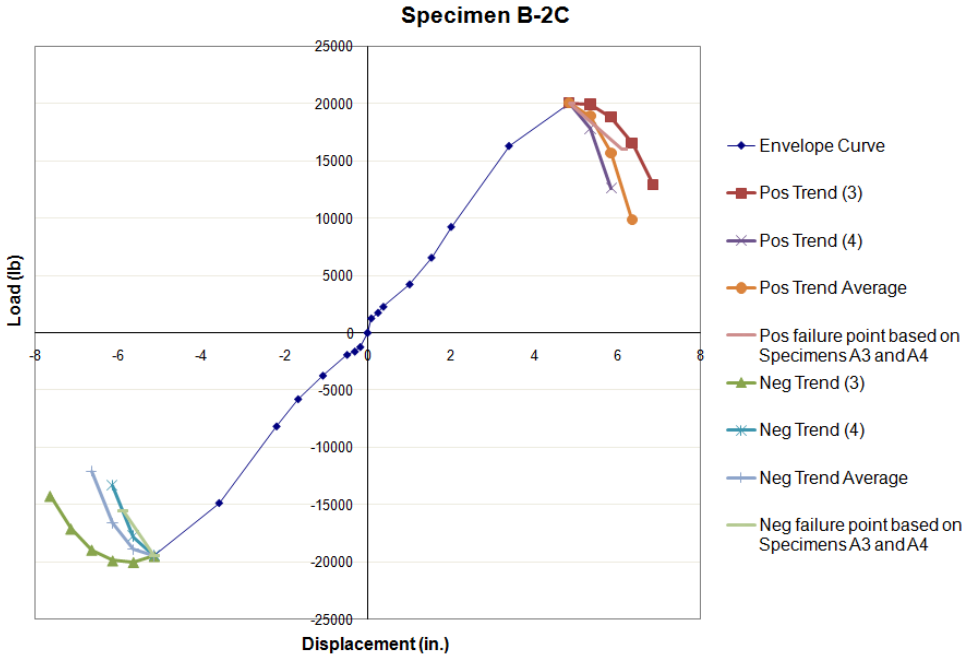

Figure 4.97: Envelope curve and trend lines from Load vs. Displacement diagram of Specimen B-2C

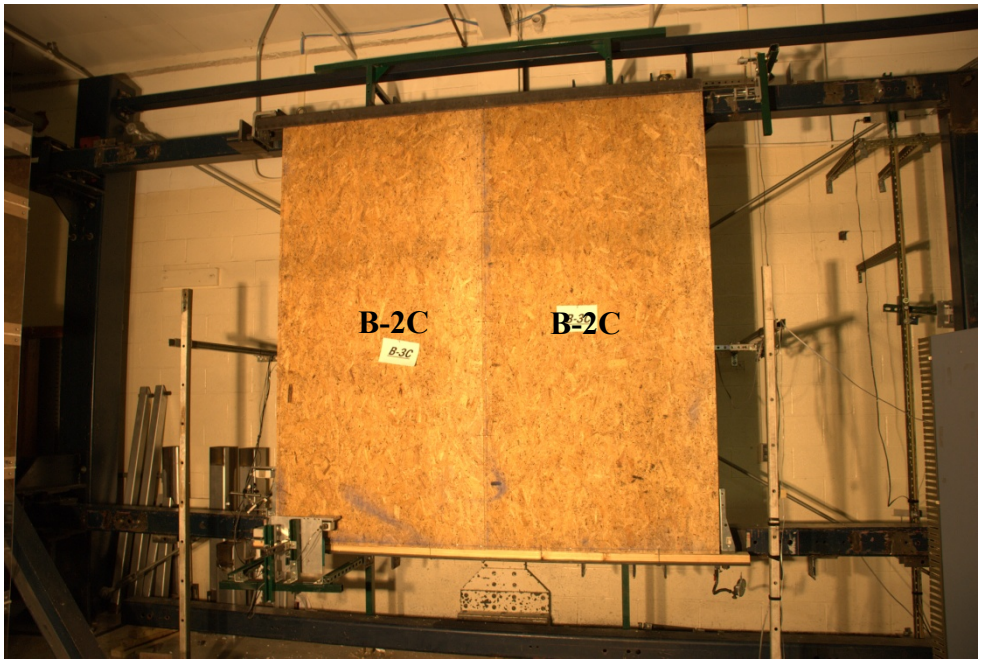

Figure 4.98: Specimen B-2C on test facility prior to cyclic loading

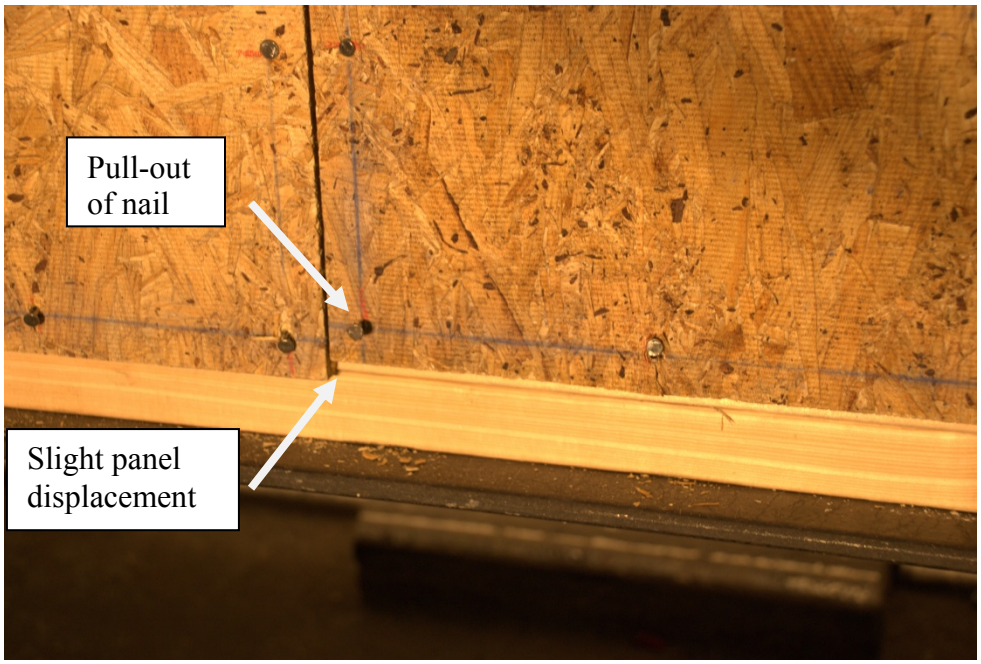

Figure 4.99: Displacement of panels and slight pull-out of nails after cyclic loading of Specimen B-2C

4.5.3.1 Specimen B-2C Fatigue Tests

Similar to Specimen B-1C, Specimen B-2C did not show complete failure under the initial first thirty-seven cycles of the CUREE loading protocol. In order to determine how Specimen B-2C would react under fatigue loading, the first thirty-seven cycles of the CUREE loading protocol were loaded onto the specimen two additional times. However, unlike Specimen B-1C, Specimen B-2C did not completely fail after the first fatigue test. Figure 4.100 shows the envelope curves of Fatigue 1 and 2 in relation to the original Specimen B-2C.

After the Specimen B-2C Fatigue 2 test, the nails along the top plate and base plate further pulled away from the sheathing. There was also sheathing damage mostly along the top plate and partially along the base plate. With each additional fatigue the two SIP panels split further apart. By the end of the Fatigue 2 test, Panel 1 and Panel 2 had split apart by about 0.33 in. vertically and about 0.20 in. horizontally. Figures 4.101 and 4.102 are photographs of Specimen B-2C after the Fatigue 2 test.

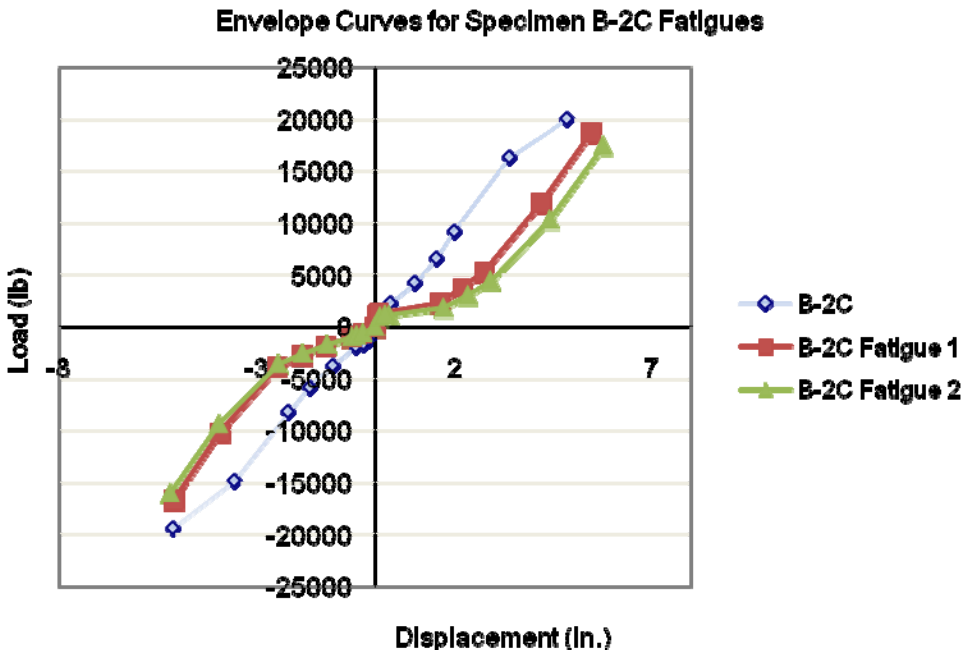

Figure 4.100: Envelope curve of Specimen B-2C Fatigue 1 and Fatigue 2 based on appropriate Load vs. Displacement diagram

Figure 4.101: Horizontal and vertical deflection of Panel 1 and Panel 2 along spline of Specimen B-2C after the Fatigue 2 test

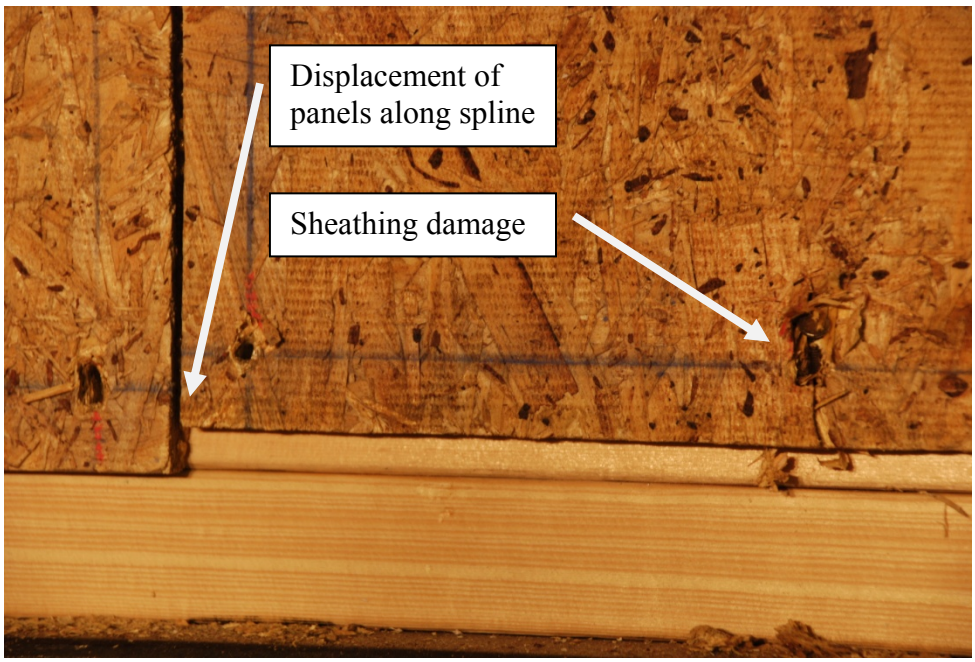

Figure 4.102: Displacement of sheathing along base plate of Specimen B-2C after the Fatigue 2 test

4.5.4 Specimen B-3C

Specimen B-3C, a replicate of Specimens B-1C and B-2C, was tested and analyzed in the same manner in order to validate the results of Specimen B-1C. Unlike Specimens B-1C and B-2C, however, the peak load capacity of Specimen B-3C was reached within thirty-seven cycles of the CUREE loading protocol, and resulted in a maximum load of about 17718 lb at a drift of about 5.40 in. (5.6% drift ratio). As can be seen in the Load vs. Displacement graph in Figure 4.103 there was a significant drop in load during the trailing cycles of the eighth primary cycle, which signifies failure in the specimen. The initial failure of Specimen B-3C occurred when the (2) 2x4 spline split

apart. The horizontal displacement between the 2x4's was 0.33 in. at the very bottom of the SIP panels and 2.52 in. at 6 ft up from the bottom. Almost all of the nails along the base plate pulled out and caused sheathing failure. A majority of the failure along the top plate was sheathing damage and a couple nails pulled out. There was also sheathing damage along the end post of the front side of Panel 2.

The 6 in. displacement limit of the testing facility prevented placing the specimen under a ninth primary cycle of the CUREE loading protocol which would have resulted in a displacement corresponding to an 80% drop in peak load. As a result, trend lines and previous specimen failures were used to determine the failure point. The same method was used for Specimens A1, B-1C, and B-2C. Figure 4.103 shows the Load vs. Displacement graph and Figure 4.104 shows the envelope curve and trend lines for Specimen B-3C. Figures 4.105 and 4.106 are photographs of the specimen before and after it was placed under cyclic loading.

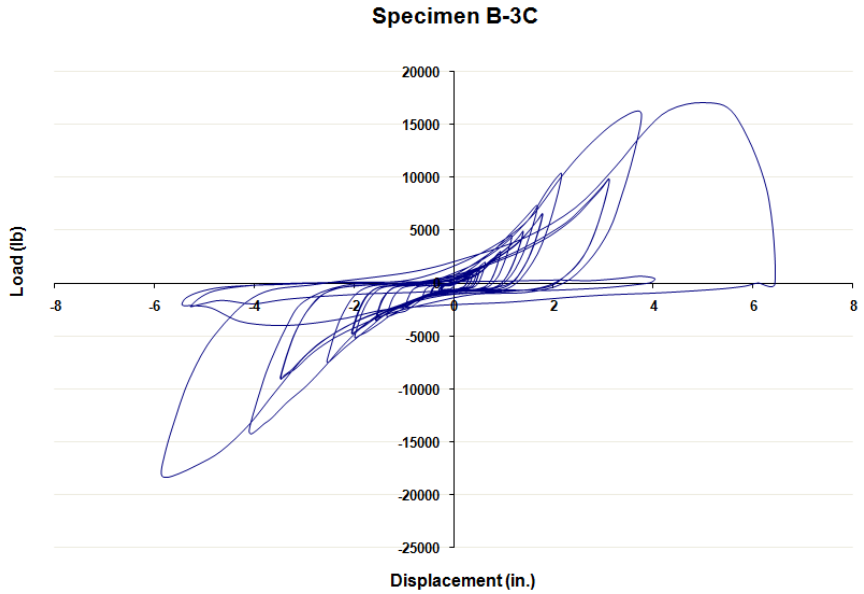

Figure 4.103: Load vs. Displacement diagram resulting from cyclic load testing of Specimen B-3C

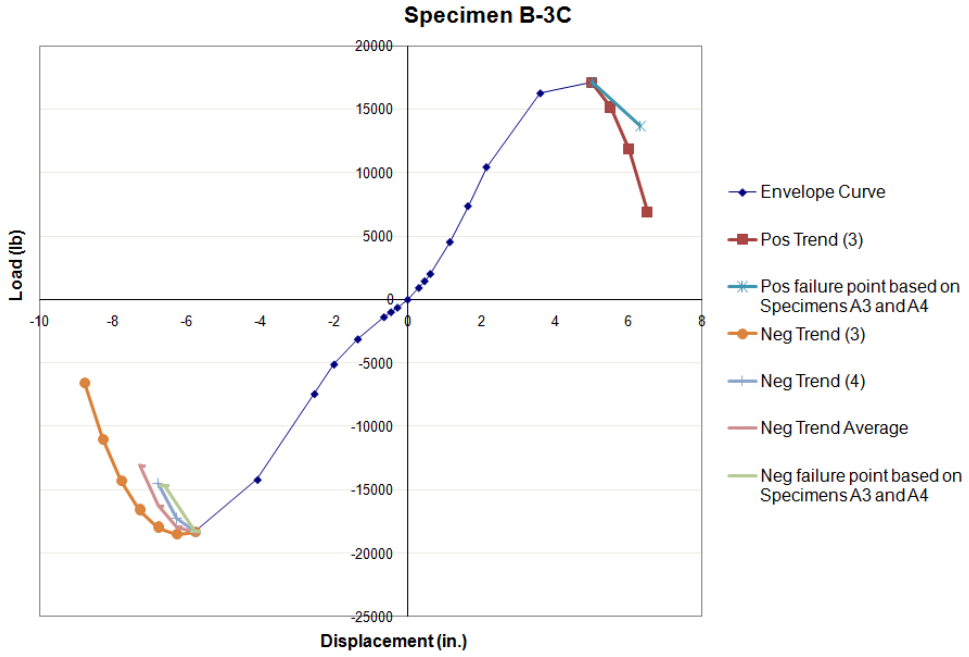

Figure 4.104: Envelope curve and trend lines from Load vs. Displacement diagram of Specimen B-3C

Figure 4.105: Specimen B-3C on test facility prior to cyclic loading

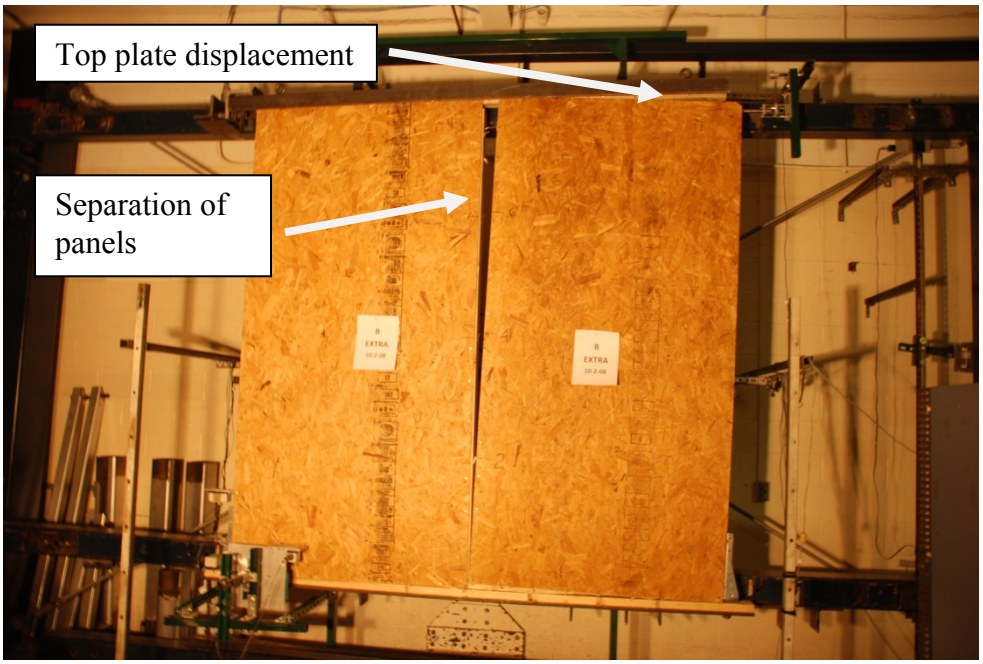

Figure 4.106: Separation of panels along spline, base plate, and top plate after failure of Specimen B-3C

4.5.5 Summary of Specimens B Tests

The major failure in Specimen B under cyclic loading occurred when the (2) 2x4 spline split apart along the nailed connection. When the spline split along the vertical axis, the panel attached to each individual piece of 2x4 moved along with it. As a result, the two panels began to rotate independently of each other. At that point, the nails tore through the sheathing along the top plate and pulled out along the base plate. Even though the three specimens tested under cyclic loading failed at different points, some during the first thirty-seven cycles of the loading protocol and some after two fatigues, all three specimens had the same failure modes. The maximum load resisted by Specimen B under cyclic loading ranged from 17564 lb to 17882 lb at displacements ranging from 5.27 in. to 5.64 in. (5.5% to 5.9% drift ratio). The values obtained under cyclic loading were within 2% of those found under monotonic loading. It should be noted that the data obtained through testing and up to the load and displacement capacity of the testing facility are significantly beyond what is expected based on the building code prescribed seismic loads and allowable displacements (e.g., 2.5%). The test specimens as mentioned were loaded to significantly beyond this ratio. Therefore, the data generated can be used to develop a better understanding of the response of the tested SIP systems at design drift levels as well as relative capacities of the SIP systems.

4.6 Specimens C

Specimens C were conventional wood-frame walls. Both sides of the wall were sheathed with 7/16 in. x 4 ft x 8 ft sheets of OSB oriented vertically with the OSB

running parallel to the studs. The studs were 2x4 SPF No. 2 or better spaced at 16 in.o.c. nailed according to the IBC. The sheathing was attached to the wall with 8d common nails spaced at 6 in.o.c. along the outer perimeter and spline and 12 in.o.c. along the studs. There was a double top plate and a single base plate.

4.6.1 Specimen C-1M

Specimen C-1M was tested under monotonic loading according to ASTM E 564-08. The specimen was pushed to about 19,000 lb at a drift just under 6 in. (6.2% drift ratio) when the test was stopped at the facility's drift capacity. Unlike all of the other specimens, the displacement of Specimen C-1M was determined by multiplying the actuator displacement by two and factoring in the displacement of the top plate and the base plate relative to the top and bottom sliding steel tubes. The displacement for all of the other specimens was determined by directly measuring the displacement of the top and bottom sliding steel tubes and factoring in the movement of the top and base plates. Damages to the top and bottom tube sensors caused the adjustment in the displacement measuring methods.

The wall experienced damage in the form of nail withdrawal along the spline and slight sheathing damage along the vertical inner edges of the OSB panels. Figure 4.107 shows the Load vs. Displacement graph while Figures 4.108 and 4.109 show photographs of the specimen before and after the monotonic loading.

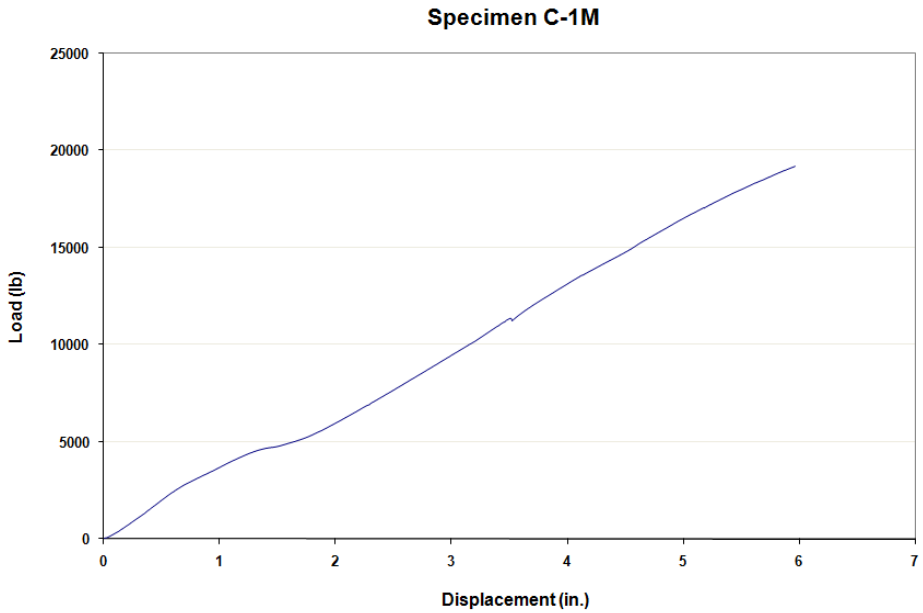

Figure 4.107: Load vs. Displacement diagram resulting from monotonic load testing of Specimen C-1M

Figure 4.108: Specimen C-1M prior to monotonic loading

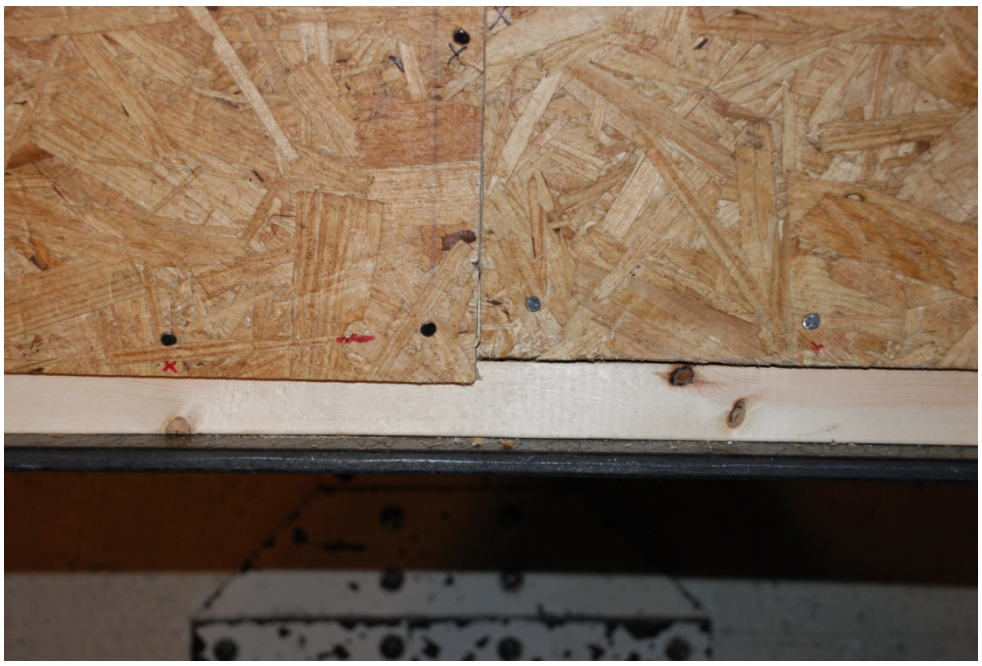

Figure 4.109: Displacement of Specimen C-1M after monotonic loading

4.6.2 Specimen C-1C

Specimen C-1C was tested under cyclic loading using a target displacement of 6 in. for the CUREE protocol. The specimen was loaded to thirty-seven cycles of the CUREE loading protocol forcing the wall to a maximum load of about 20,000 lb and a drift of about 5.00 in. (5.2% drift ratio). The test was stopped at the 20,000 lb load capacity of the facility before the specimen experienced an 80% drop in peak load capacity. Initial signs of failure occurred when the nails along the spline began to pull out and then nails along the base plate and end posts began to pull out. During the test there was also noticeable uplift in the panels.

Similar to Specimens A1 and B, trend lines and failure points from previous tests were used to estimate the failure point of the specimen. Unlike Specimens A1 and B, the hysteresis loops for Specimen C-1C did not begin to level off towards the end of the test. As a result, trend lines were drawn from the actual peak point of the thirty-seventh cycle of the test and, they were drawn from a point extended to a 15% increase in load. The maximum trend line and the minimum trend line were then analyzed to determine the maximum and minimum values. Figure 4.110 shows the Load vs. Displacement graph and Figure 4.111 shows the Envelope Curve and trend lines for Specimen C-1C. Figures 4.112, 4.113, 4.114, and Figure 4.115 are photographs of the specimen before and after it was placed under cyclic loading.

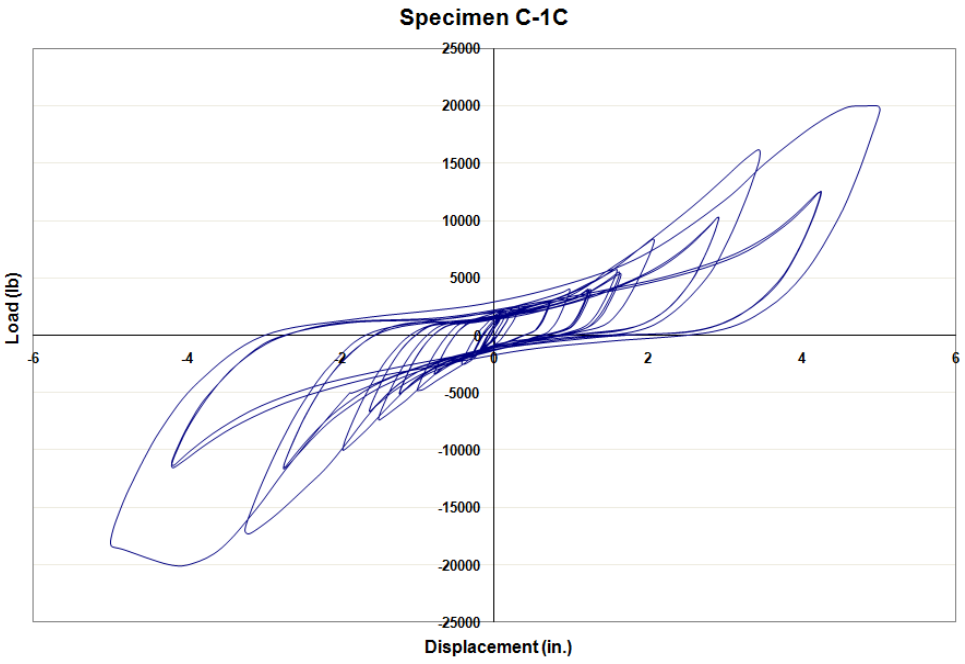

Figure 4.110: Load vs. Displacement diagram resulting from cyclic load testing of Specimen C-1C

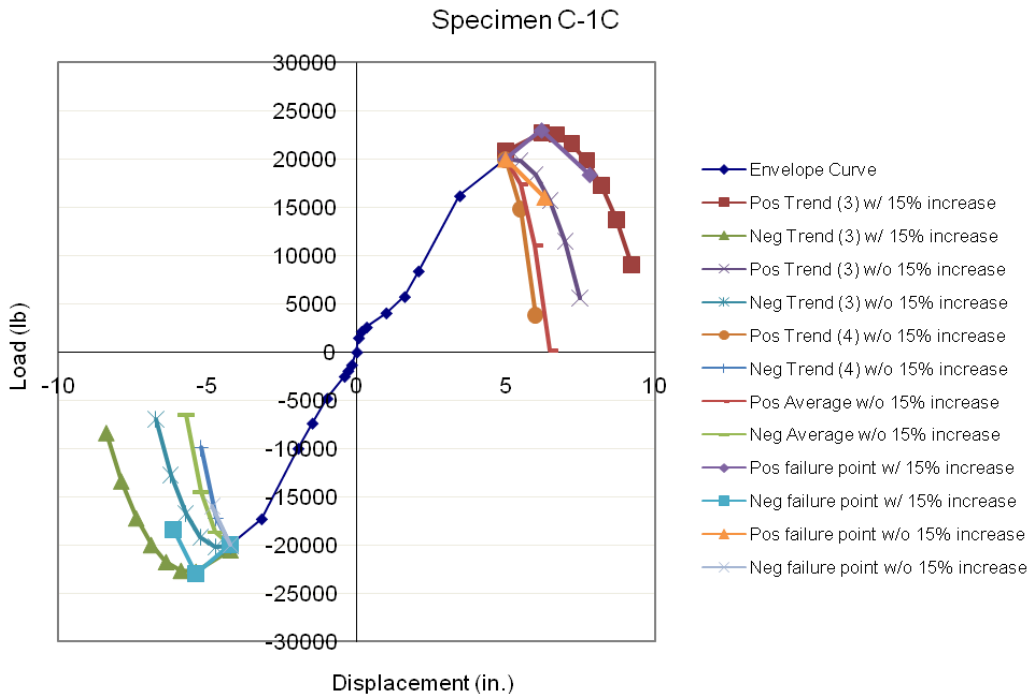

Figure 4.111: Envelope curve and trend lines from Load vs. Displacement diagram of Specimen C-1C

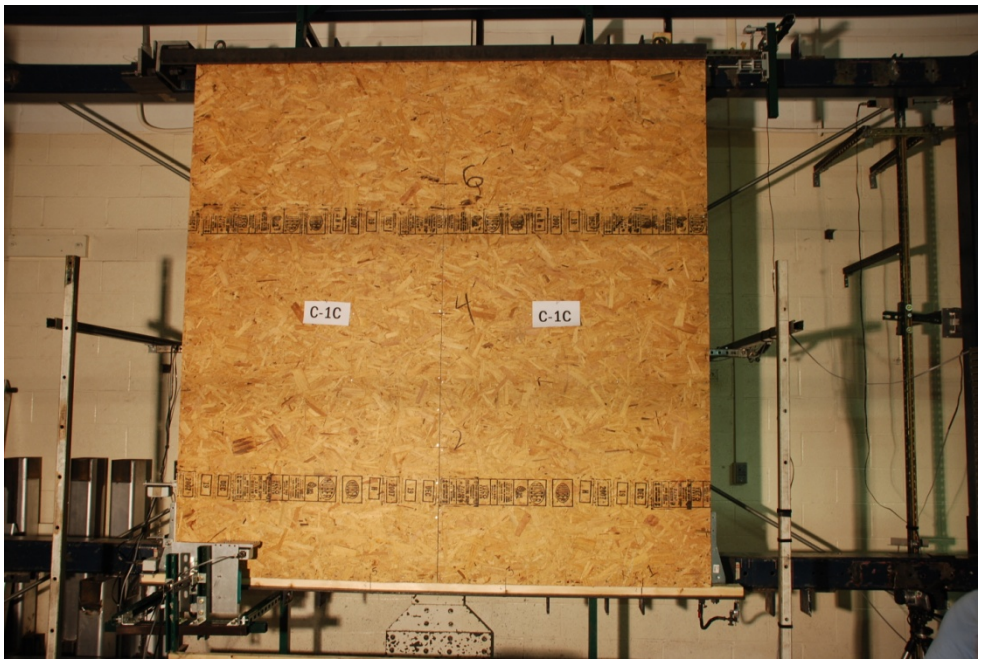

Figure 4.112: Specimen C-1C prior to cyclic loading

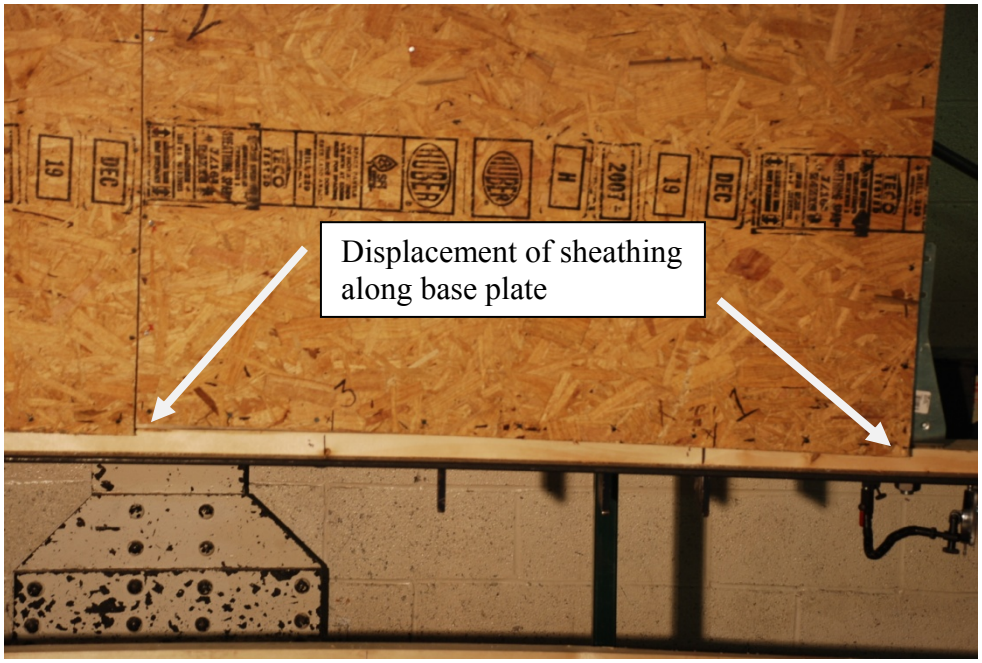

Figure 4.113: Displacement of panels after cyclic loading of Specimen C-1C

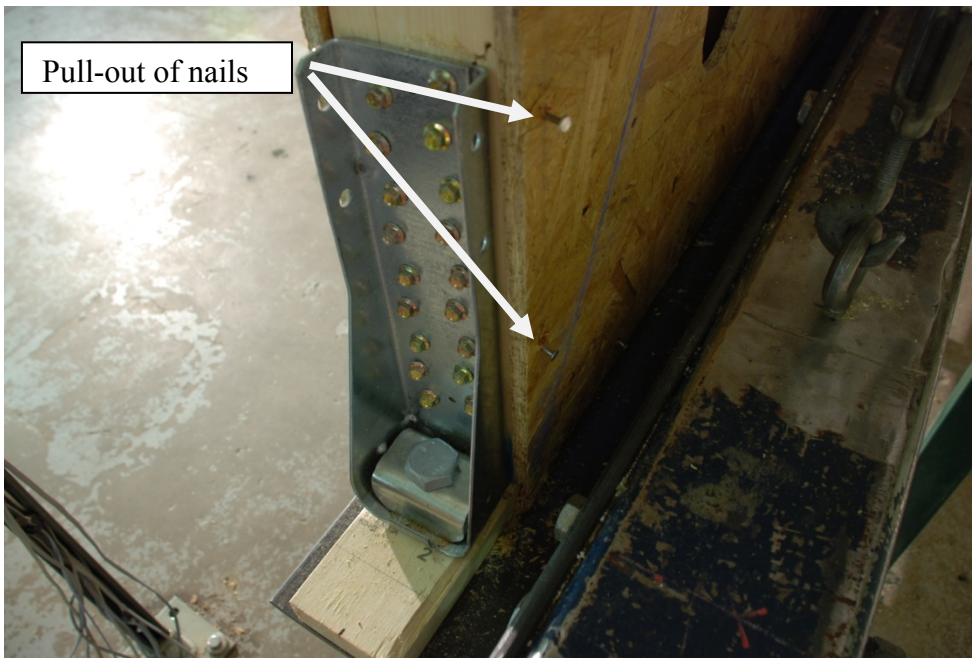

Figure 4.114: Pull-out of nails along end post after cyclic loading of Specimen C-1C

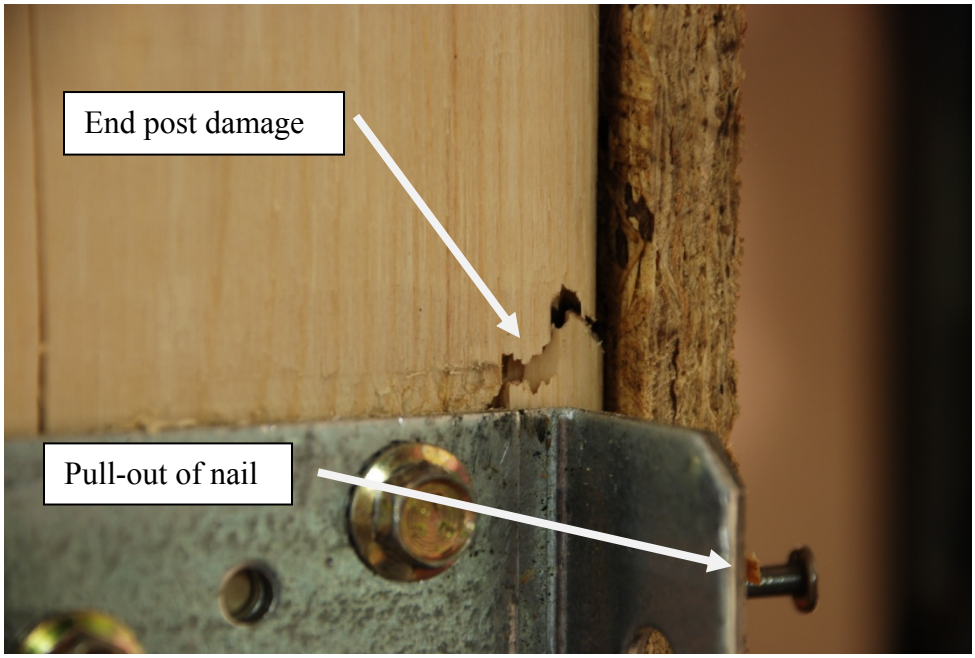

Figure 4.115: Damage to end post at USP PHD 6 hold-down after cyclic loading of Specimen C-1C

4.6.2.1 Specimen C-1C Fatigue Tests

Specimen C-1C did not completely fail under the first thirty-seven cycles of the CUREE loading protocol, so it was placed under the same loading two additional times to determine the behavior of the wall under fatigue loading. Figure 4.116 shows the envelope curve of Fatigue 1 and Fatigue 2 of Specimen C-1C. The specimen retained its strength during the fatigue loading but the slope of the envelope curve changed in comparison to the original cyclic loading.

After Fatigue 1 of Specimen C-1C the nails continued to pull out along the spline and base plate. There was damage to the sheathing down the spline. The sheathing damage caused the two SIP panels to move independently of each other without any rubbing at the spline. Fatigue 2 of Specimen C-1C caused a majority of the nails along the spline on the Panel 1 side to withdraw. There was also sheathing damage along the spline and at the inner and outer corners of Panel 1. A couple of nails along the top plate and base plate also began to pull out.

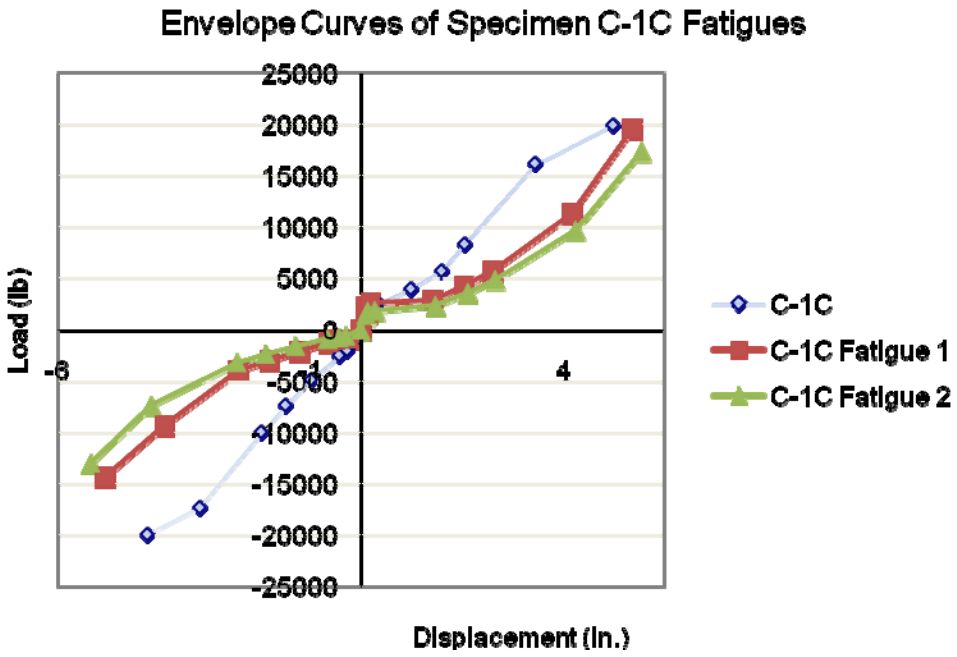

Figure 4.116: Envelope curve of Specimen C-1C Fatigue 1 and Fatigue 2 based on appropriate Load vs. Displacement diagram

4.6.3 Specimen C-2C

Specimen C-2C was a replicate of Specimen C-1C and was tested and analyzed in the same manner in order to validate the results of Specimen C-1C. Specimen C-2C was tested under cyclic loading using a target displacement of 6 in. for the CUREE protocol. The specimen was loaded to thirty-seven cycles of the CUREE loading protocol forcing the wall to a maximum load of about 20000 lb and a drift of about 4.15 in. (4.3% drift ratio). Even though the ultimate failure was not reached after the thirty-seventh cycle of the loading protocol, there were signs of failure. The nails along the spline began to pull out and there was sheathing damage at the upper inside corner along the spline. The

displacement and load limitations of the test facility did not allow the wall to reach an 80% drop in load.

Specimen C-2C was analyzed in the same manner as Specimen C-1C. Figure 4.117 shows the Load vs. Displacement graph and Figure 4.118 shows the envelope curve and trend lines for Specimen C-2C.

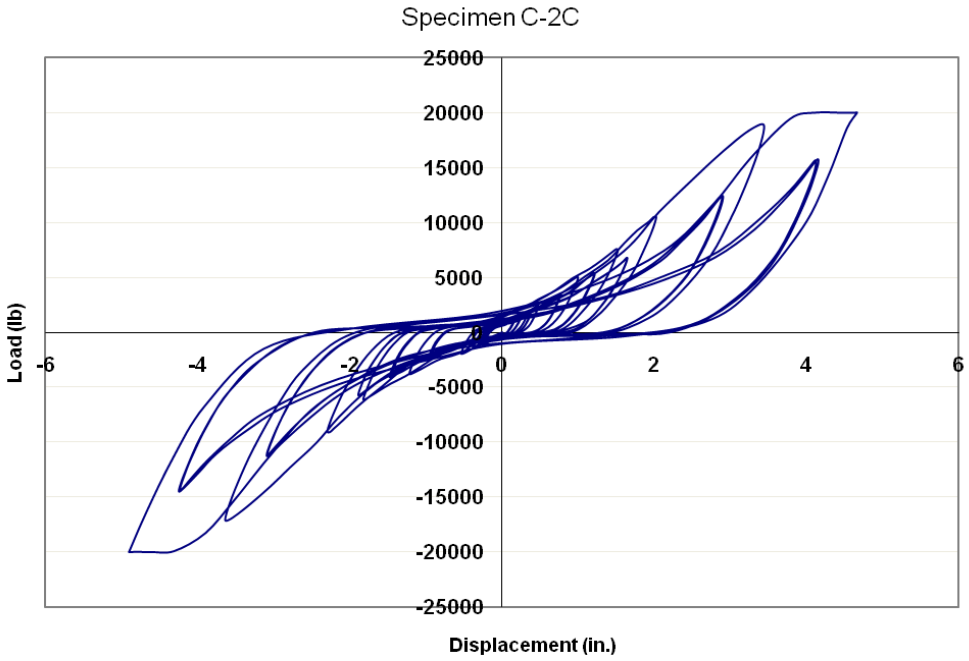

Figure 4.117: Load vs. Displacement diagram resulting from cyclic load testing of Specimen C-2C

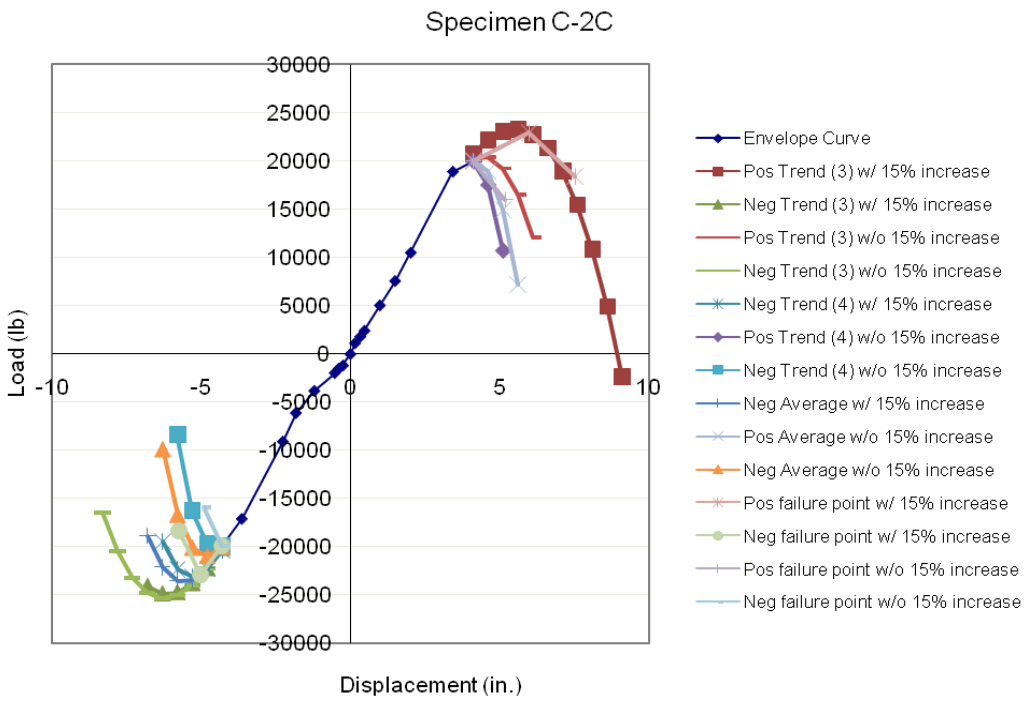

Figure 4.118: Envelope curve and trend lines from Load vs. Displacement diagram of Specimen C-2C

4.6.3.1 Specimen C-2C Fatigue Tests

Similar to Specimen C-1C, Specimen C-2C did not completely fail after reaching a load of 20000 lb and a drift of about 4.15 in. so it was loaded two additional times under the first thirty-seven cycles of the CUREE loading protocol. Figure 4.119 shows the envelope curves of Fatigue 1 and Fatigue 2 of Specimen C-2C. The specimen retained its strength during the fatigue loading but the slope of the envelope curve changed in comparison to the original cyclic loading.

After the two fatigue tests of Specimen C-2C there was pull-out of the nails along the spline and there was extensive sheathing damage on both the front and back of Panel

2 caused by the nails tearing out of the sheathing in areas where the nails were 0.75 in. or less from the edge. There were some areas where the nails punched through the sheathing. A couple of the nails along the base plate also pulled out. Figures 4.120, 4.121, and 4.122 show photographs of different types of sheathing failure which occurred after Specimen C-2C was placed under the Fatigue 2 test.

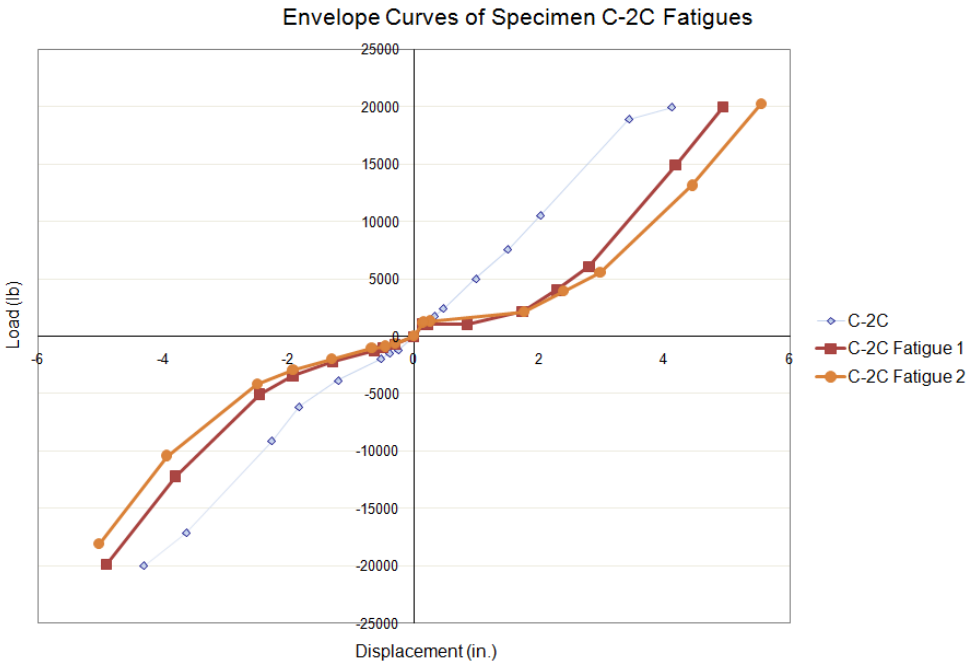

Figure 4.119: Envelope curve of Specimen C-2C Fatigue 1 and Fatigue 2 based on appropriate Load vs. Displacement diagram

Figure 4.120: Punch through of nail along spline of Specimen C-2C after Fatigue 2 test

Figure 4.121: Tear-out of nail along spline of Specimen C-2C after Fatigue 2 test

Figure 4.122: Damage to sheathing along base plate of Specimen C-2C after Fatigue 2 test

4.6.4 Specimen C-3C

Specimen C-3C, a replicate of Specimens C-1C and C-2C, was tested and analyzed in the same manner in order to validate the results of Specimen C-1C. Specimen C-3C was tested under cyclic loading using a target displacement of 6 in. for the CUREE protocol. The specimen was loaded to eight primary cycles of the CUREE loading protocol forcing the wall to a maximum load of about 20000 lb and a drift of about 4.40 in. (4.6% drift ratio). The test was stopped at the load capacity of the facility before the specimen experienced an 80% drop in peak load capacity. Initial signs of failure occurred when the nails along the spline began to withdraw.

Specimen C-3C was analyzed in the same manner as Specimens C-1C and C-2C. Figure 4.123 shows the Load vs. Displacement graph and Figure 4.124 shows the envelope curve and trend lines for Specimen C-3C.

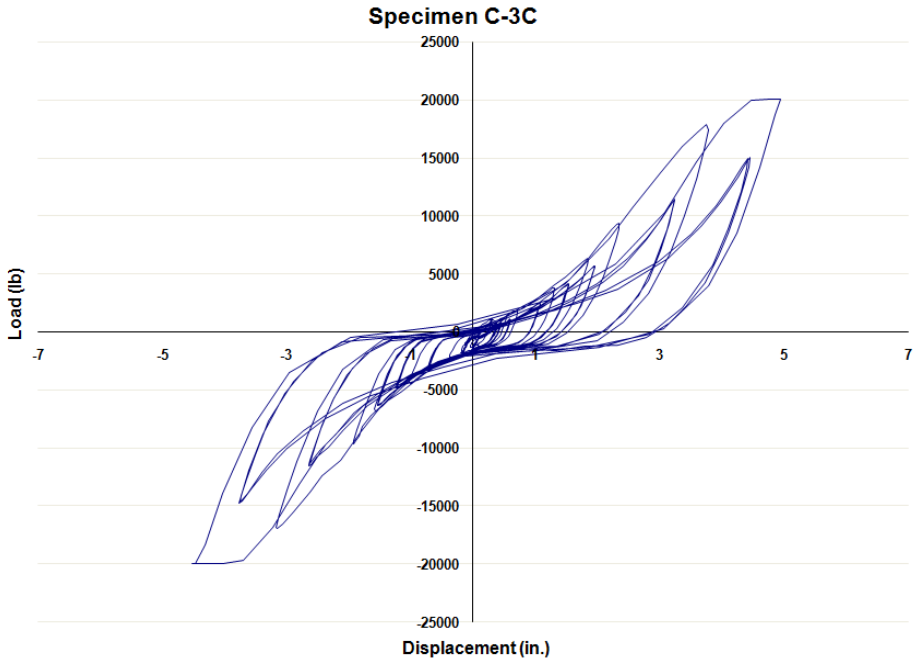

Figure 4.123: Load vs. Displacement diagram resulting from cyclic load testing of Specimen C-3C

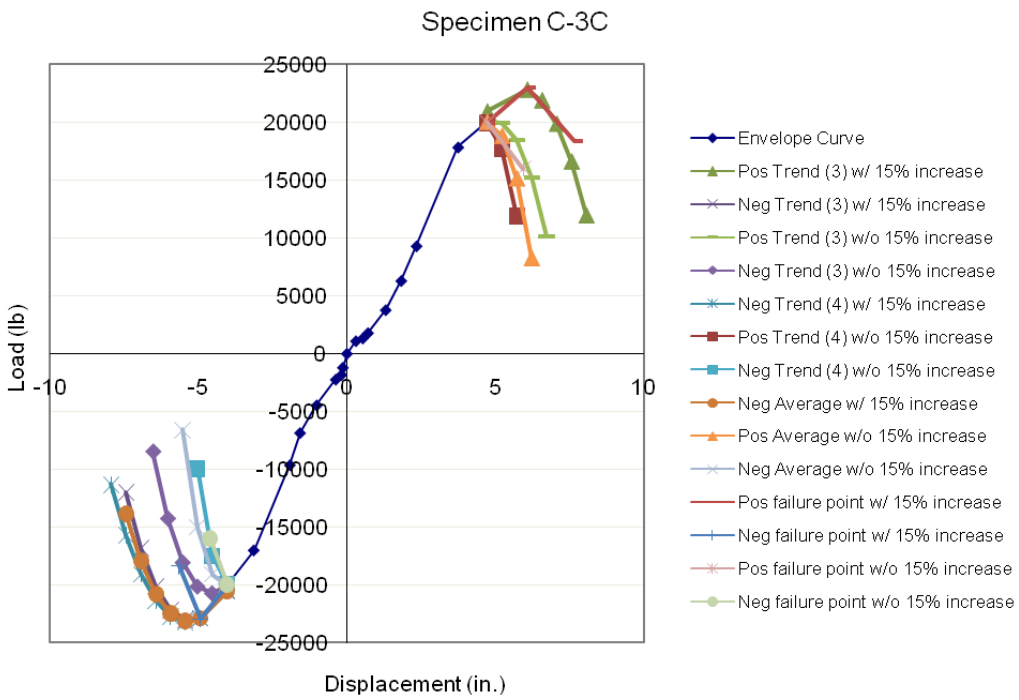

Figure 4.124: Envelope curve and trend lines from Load vs. Displacement diagram of Specimen C-3C

4.6.4.1 Specimen C-3C Fatigue Tests

Similar to Specimens C-1C and C-2C, Specimen C-3C was loaded two additional times under the first thirty-seven cycles of the CUREE loading protocol to determine the specimen's behavior under fatigue loading. Figure 4.125 shows the envelope curves of Fatigue 1 and Fatigue 2 tests. The specimen retained its strength during the fatigue loading but the slope of the envelope curve changed from the original cyclic loading test.

There was a 0.10 in. increase in the vertical displacement of the spline of Specimen C-3C after Fatigue 1 test. After Fatigue 2 test, the vertical displacement of the spline increased by about 0.05 in. putting the total displacement, including the

displacement after the first cyclic loading, at 0.34 in. The horizontal displacement of the spline after Fatigue 2 test was 0.38 in. at the 2 ft high mark on the panel and 0.12 in. at the 6 ft high mark on the panel. Similar to Specimens C-1C and C-2C there was sheathing damage along the spline of Specimen C-3C after Fatigue 2 test. A few of the nails along the spline and the top plate also pulled out. Figures 4.126, 4.127 and 4.128 show photographs of Specimen C-3C after the fatigue tests.

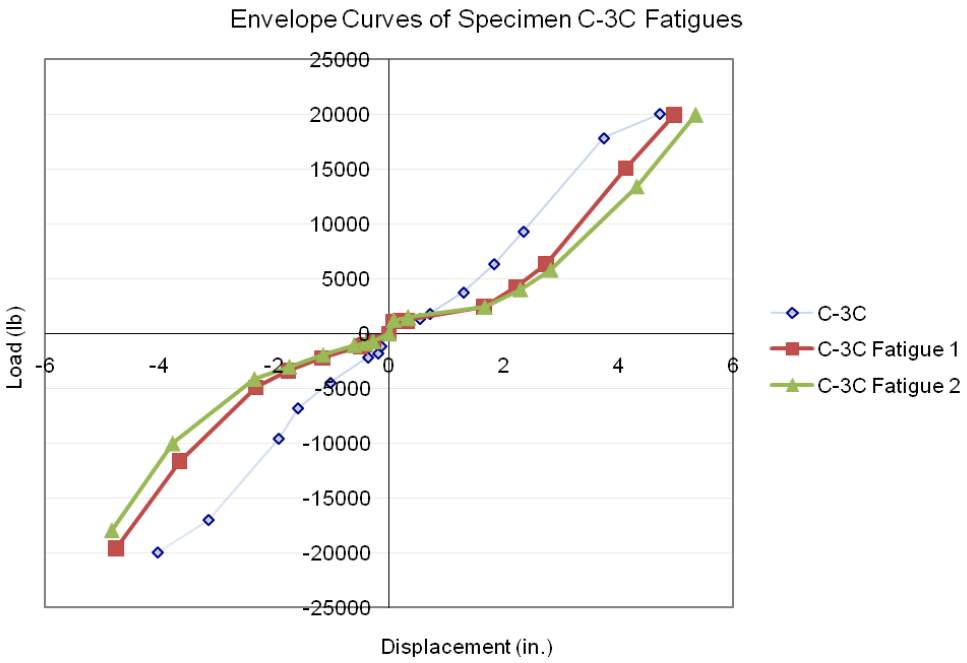

Figure 4.125: Envelope curve of Specimen C-3C Fatigue 1 and Fatigue 2 based on appropriate Load vs. Displacement diagram

Figure 4.126: Displacement of panels after Fatigue 1 test of Specimen C-3C

Figure 4.127: Further displacement of panels of Specimen C-3C after Fatigue 2 test

Figure 4.128: Pull-out of nails along top plate of Specimen C-3C after Fatigue 2 test

4.6.1 Summary of Specimens C Tests

Based on the experimental tests, Specimens C showed the largest strength capacity. The maximum force experienced under cyclic loading ranged between 19978 lb and 23400 lb at displacements of 4.40 in. to 5.89 in. (4.6% to 6.1% drift ratio). Under monotonic loading the specimen resisted a maximum load ranging between 20300 lb and 25400 lb at displacements ranging from 7.00 in. to 9.50 in. The values beyond 20,000 lb and 6.00 in. were estimated from the envelope curves that included trend lines. The monotonic loading tests produced forces about 8% greater and displacements about 16% greater than those under the cyclic loading tests.

The initial signs of failure for Specimen C occurred when the nails along the spline pulled out. There was also sheathing damage along the spline. Nails also pulled out along the base plate and end posts. Placing the specimen under two additional fatigue tests caused the nails to pull out even further along the spline, base plate and end posts. Nails began pulling out along the top plate as well. Sheathing damage along the spline caused by nail pull-out and punch-through created about 0.40 in. horizontal and vertical displacements between the panels in relation to each other. The panels began moving independently of each other. These failure modes resulted in a minimal decrease in the specimen's strength.

4.7 Summary and Conclusions

All of the SIP specimens performed much better under monotonic and cyclic loading than expected. Most specimens of A1, B, and C types were able to withstand drifts of 5.00 in. (5.2% drift ratio) and greater, which is well beyond the practical application of these systems. As noted earlier, according to ASCE 7-05, the maximum allowable drift ratio is 2.5%. Therefore, most of the specimens showed capacities at least twice this limit. This shows that the wall systems are not only very strong but they are also very flexible. The wood-frame walls also performed very well and retained their strength during the fatigue loading. It is important to realize that the wood-frame walls were sheathed on both sides which made them much stronger than if they were only sheathed on one side, which is how they are typically tested. Previous published research testing wood-frame walls with single sided sheathing obtained significantly lower peak

loads and displacement (Lebeda et al., 2005; Johnston et al., 2006). It is safe to assume that the Specimens A1 and B would have outperformed the traditional wood-frame specimen had it only been sheathed on one side.

The design specifications of each specimen varied, yet the failure modes were consistent. The fastener hardware proved to be the weakest factor of every specimen which is consistent with previous studies on shear walls (Carradine et al., 2004; Jamison, 1997; Kermani and Hairstans, 2006). In Specimen A3 the staples sheared along the spline and pulled out along the base and top plates. The major failure in Specimen A4 also occurred when the screws located along the spline sheared. In Specimen A1 the nails withdrew along the spline, top plate and base plate. There was also sheathing damage along the spline. The major failure of Specimen B occurred along the spline like Specimens A3, A4, and A1 but it was not because the nails were pulling out, instead the (2) 2x4 split apart. This is due to the inability of the 16d common nails used to join the two 2x4's to adequately resist the cyclic loading of the specimen. Specimen C experienced serviceability issues when the nails pulled out along the spline, base plate and end posts.

This chapter presented the load vs. displacement graphs and envelope curves of various 8 ft x 8ft x 4.5 in. SIP specimens and 8 ft x 8ft traditional wood-frame walls. The failure modes experienced were also explained as well as the behavior of Specimens A1, B, and C under fatigue loading. The following conclusions can be drawn:

- One common failure feature in all specimens was the failure of the fastener hardware.

- All specimens performed better than previously reported tests by showing larger than expected load and drift capacities. This can be due to the large hold-down capacity of the anchors and the high quality sheathing used on the structural insulated panels.
- Specimen A3, with the OSB surface spline and staples, was the weakest specimen with the ability to resist a maximum load of 11413 lb at a displacement of 3.13 in. (3.3% drift capacity).
- Specimen A4, with the OSB surface spline and screws, had the most sudden and brittle failure due to the brittle nature of the screws which caused them to shear instead of bend, like the nails.
- Specimen C, the wood-frame shear wall, was the strongest and most ductile specimen. It was able to resist a maximum load ranging between 19978 lb and 23400 lb at displacements of 4.40 in. to 5.89 in. (4.6% to 6.1% drift ratio).
- Sheathing bearing, which was tested in Specimen A1Bearing-3C, had an effect on the performance of the specimen. The maximum load increased by 8% and the displacement decreased by 17% in comparison to Specimens A1-1C and A1-2C. There was also more extensive damage to the sheathing along the top and base plates.
- There was minimal difference between the specimens tested with the hold-downs on the exterior of the wall than Specimen A1Internal-4C which had hold-downs placed in cut-outs on the interior of the wall.

- Decreasing the spacing between the 16d common nails used to connect the splines of Specimen B would significantly increase the capacity of the wall.

Chapter 5

Data Analysis and Calculations

5.1 Introduction

The following sections describe the analytical evaluation associated with each specimen in terms of ASTM E 2126-08 and ICC-ES AC130. The data obtained during the monotonic and cyclic loading of the wall systems was used to determine performance parameters of the various SIP wall designs. The objective of the analytical study presented in this chapter is to illustrate application of the standards referred to here in determining seismic response parameters and a preliminary comparison of various SIP systems considered. According to ASTM E 2126-08, the shear strength of the wall system was found by determining the absolute value of the load per unit length of the specimen, $\nu_{peak} = \frac{P_{peak}}{L}$. The secant shear modulus at both $0.4P_{peak}$ and P_{peak} as seen in Figure 5.1 was found by using the relation: $G' = \frac{P}{\Delta} x \frac{H}{L}$. The $\frac{H}{L}$ refers to the aspect ratio of the specimen. The cyclic ductility ratio is defined as the ratio of the ultimate displacement and the yield displacement, $D = \frac{\Delta_u}{\Delta_{yield}}$. An equivalent energy elastic-plastic (EEEP) curve was developed by circumscribing the area enclosed by the envelope curve. The enclosed area was bordered by the origin, the ultimate displacement, and the displacement axis of the envelope curve. The envelope curve consisted of the extreme

points of the load-displacement hysteresis loops. An EEEP curve can be used as a visual comparison between differing wall designs and materials. (ASTM E 2126-08, 2008)

ICC-ES AC130 was followed to determine if the specimens are deemed seismically compatible to a code-defined seismic-force resisting system. First, the ultimate displacement of the specimen divided by the displacement at the ASD design load must be greater than or equal to 11, or $\frac{\Delta_u}{\Delta_{ASD}} \geq 11$. The ASD design load is 70% of the load of the specimen found at a displacement of 0.6 in. (ICC-ES AC130). Refer to Section 5.2.2.1 in this report for an example of the steps taken to determine the ASD design load. Next, the ultimate displacement must be greater than 2.8% of the height of the specimen, as described in the equation, $\Delta_U \geq 0.028H$. Finally, the ratio of the peak load to the ASD design load must be between or equal to 2.5 to 5.0, $2.5 \leq \frac{P_{peak}}{P_{ASD}} \leq 5.0$. If all of these requirements are met the prefabricated panels can be used in a seismic force resisting system and the specimen can be assigned the following values:

Response Modification Coefficient: R = 6.5

System Overstrength Factor: $\Omega_0 = 3$

Deflection Amplification Factor: Cd = 4

ICC-ES AC130 was developed to use with prefabricated wood-frame shear panels but will be applied to structural insulated panels as well in this report.

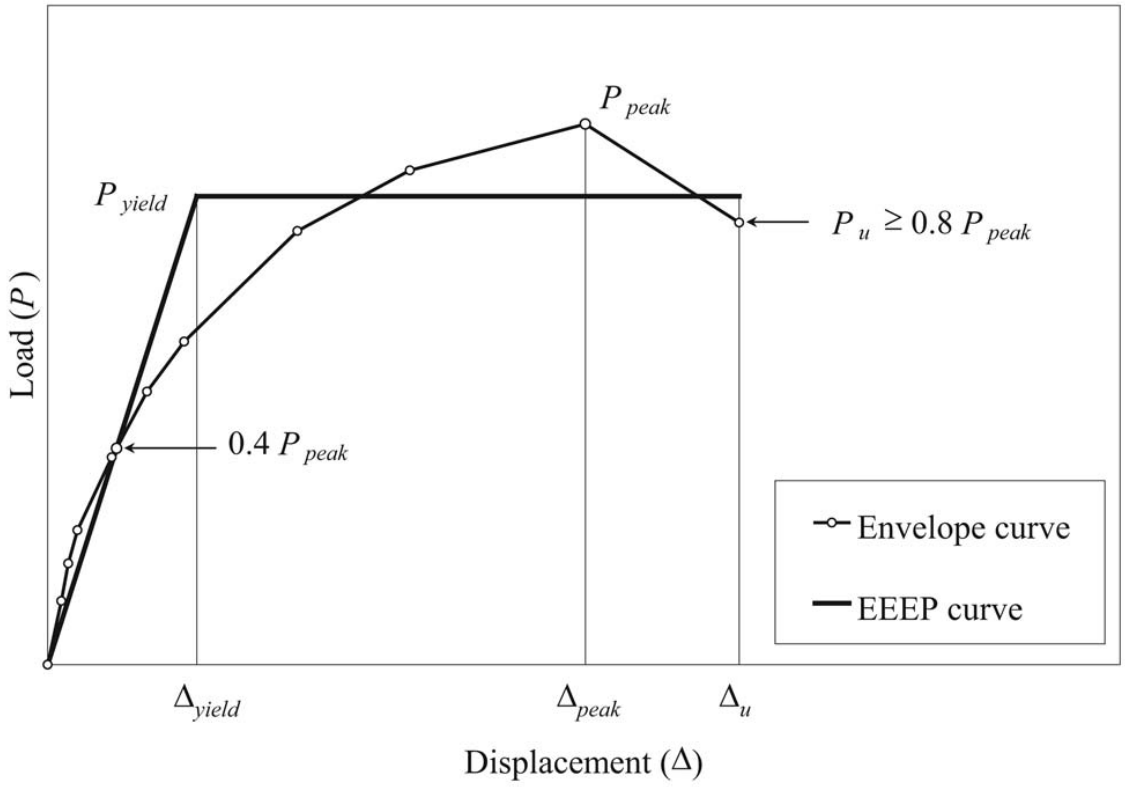

Figure 5.1: Performance parameter of specimen (ASTM E 2126-08, 2008)

5.2 Specimens A3

Specimens A3 had a 7/16 in. x 3 in. x 8 ft OSB spline which was connected to the SIP facing with 16 gage, 7/16 in. crown, 1.5 in. long staples at 6 in. o.c. The framing lumber was also attached to the SIP facing with the same staples at 6 in. o.c. The USP PHD6 hold-downs were placed at the exterior of the 8 ft x 8 ft wall.

5.2.1 Specimen A3-1M

Specimen A3-1M was tested under monotonic loading in correspondence with ASTM E 564-06. The parameters shown in Table 5.1 were obtained by analyzing the Load vs. Displacement graph of the specimen shown in Chapter 4. As can be seen below, ASTM E 2126-08 was followed to determine the values in Table 5.1.

5.2.1.1 Specimen A3-1M Calculations

ASTM E 2126-08

Relevant sections of the document are shown below for each quantity being calculated.

9.1.1 Shear Strength

Vpeak = 12522 lb/8 ft = 1565 lb/ft

9.1.2 Secant Shear Modulus

G' at Ppeak = 12522 lb/3.64 in. = 3442 lb/in.

G' at 0.4Ppeak = 5009 lb/0.87 in. = 5761 lb/in.

9.1.3 Cyclic Ductility Ratio and EEEP Curve

D = 4.67 in./1.95 in. = 2.39

G' at Ppeak < G' at 0.4Ppeak $\longrightarrow$ Generate EEEP Curve

9.1.4 Generating an EEEP Curve and determining yield limit state

Pu = 0.8*12522 lb = 10018 lb

Δu = 4.67 in. (From graph)

Ke = 5009 lb/0.87 in. = 5761 lb/in.

Area Under Backbone Curve = 41487 lb*in.

$\Delta u^2 = 4.67^2 = 21.81$ in^2 > $2A/Ke = 2(41487)/5761 = 14.40$ in^2

⟶ Pyield = (4.67 – sqrt(21.81 – 14.40)*5761 = 11234 lb

⟶ Δyield = 11234 lb/ 5761 lb/in. = 1.95 in.

Table 5.1: Specimen A3-1M Results

	Strength Limit State	Yield Limit State
Displacement (in.)	3.64	1.95
Shear Force (lb)	12522	11234
Shear Modulus (lbf/in.)	3442	5761
Ductility	2.39	
Shear Strength (lbf/ft)	1565	
Elastic Stiffness (lbf/in.)	5761	

5.2.2 Specimen A3-1C

Specimen A3-1C was tested under cyclic loading. The calculations used to develop performance parameters according to ASTM E 2126-08 and also to check seismic compatibility of the specimen with a code recognized wall system according to ICC-ES AC130 are shown below. The characteristic values of the specimen were found by analyzing the hysterisis loops in the positive quadrant of the graph and those in the negative quadrant of the graph seperately and then averaging the absolute value of them together. The summary of the results is in Table 5.2**.**

5.2.2.1 Specimen A3-1C Calculations

ASTM E 2126-08

Relevant sections of the document are shown below for each quantity being calculated.

9.1.1 Shear Strength

(+)	Vpeak	= 11240 lb/8 ft		=	1405 lb/ft
(-)		= 11914 lb/8 ft		=	1489 lb/ft

9.1.2 Secant Shear Modulus

(+)	G' at Ppeak	=	11240 lb/2.40 in.	=	4687 lb/in.
(-)		=	11914 lb/3.89 in.	=	3061 lb/in.
(average)				=	3874 lb/in.
(+)	G' at 0.4Ppeak	=	4496 lb/0.97 in.	=	4650 lb/in.
(-)		=	4765 lb/1.45 in.	=	3290 lb/in.
(average)				=	3970 lb/in.

9.1.3 Cyclic Ductility Ratio and EEEP Curve

(+)	D	=	3.06 in./2.49 in.	=	1.23
(-)		=	4.09 in./3.23 in.	=	1.27

G' at Ppeak < G' at 0.4Ppeak ⟶ Generate EEEP Curve

9.1.4 Generating an EEEP Curve and determining yield limit state

(+)	Pu	=	0.8*11240 lb	=	8992 lb
(-)		=	0.8*11914 lb	=	9531 lb
(+)	Δu	=	3.06 in. (From graph)		
(-)		=	4.09 in. (From graph)		

(+) Ke = 4496 lb/0.97 in. = 4650 lb/in.

(-) = 4765 lb/1.45 in. = 3290 lb/in.

(+) Area Under Backbone Curve = 21034 lb*in.

(-) = 26340 lb*in.

(+) $\Delta u^2 = 3.06^2 = 9.37$ in^2 > $2A/Ke = 2(21034)/4650 = 9.05$ in^2

⟶ Pyield = (3.06 – sqrt(9.37 – 9.05)*4650 = 11579 lb

⟶ Δyield = 11579 lb/ 4650 lb/in. = 2.49 in.

(-) $\Delta u^2 = 4.09^2 = 16.76$ in^2 > $2A/Ke = 2(26340)/3290 = 16.01$ in^2

⟶ Pyield = (4.09 – sqrt(16.76 – 16.01)*3290 = 10623 lb

⟶ Δyield = 10623 lb/ 3290 lb/in. = 3.23 in.

ICC-ES AC130

Relevant sections of the document are shown below for each quantity being calculated.

5.1.3.1 Allowable Stress Design

5.1.3.1.1 Drift Limit (Seismic)

a) бx = min(Δa = 2.40 in. or Δpeak = 3.15 in.)⟶ бx = 2.40 in.

b) бxe = (бx*I)/Cd = 2.40 in.*(1.0)/4 = 0.60 in.

c) P at бxe = 2586 lb (average of positive and negative P values from graph)

d) P_{ASD} = 0.7*(2586 lb) = 1810 lb

e) Δ_{ASD} = 0.36 in. (average of positive and negative delta values from graph)

5.1.3.1.2 Drift Limit (Wind)

Δ = 8 ft/180 = 0.53 in.

0.53 in. > 0.35 in. ⟶ No need to continue with calculations

5.1.3.1.3 Strength Limit (Wind and Seismic)

(+) Δ at Pu/2.5 = 8992 lb/2.5 = 3597 lb

(-) = 9531 lb/2.5 = 3812 lb

P at Strength Limit > P at Drift Limit ⟶ No need to continue with calculations

Allowable Stress Design

P_{ASD} = 1810 lb

Δ_{ASD} = 0.36 in.

5.2 Seismic Design Compatibility

5.2.2

$\Delta u/\Delta_{ASD}$ = 3.58 in./0.36 in. = 10.02 < 11 ⟶ No good!

5.2.3

Δu = 3.58 in. > 0.028*(8 ft *12) = 2.688 in. ⟶ Good!

5.2.4

P_{peak}/P_{ASD} = 11577 lb/1810 lb = 6.39 >2 ⟶ Good!

>5 ⟶ No Good!

⟶ Does not meet Seismic Specifications

Table 5.2: Specimen A3-1C Results

		Strength Limit State	Yield Limit State
Displacement (in.)	+	2.40	2.49
	-	3.89	3.23
	Average	3.15	2.86
Shear Force (lb)	+	11240	11579
	-	11914	10623
	Average	11577	11101
Shear Modulus (lbf/in.)	+	4688	4650
	-	3061	3290
	Average	3874	3970
Ductility	+	1.23	
	-	1.27	
	Average	1.25	
Shear Strength (lbf/ft)	+	1405	
	-	1489	
	Average	1447	
Elastic Stiffness (lbf/in.)	+	4650	
	-	3290	
	Average	3970	
Seismic Compatibility		No	

According to the results of the calculations presented, Specimen A3-1C does not meet the seismic specifications set forth by ICC-ES AC130 (2007) and explained in Section 5.1. As a result, alternate means must be used to determine the response modification coefficient, system overstrength factor, and the deflection amplification factor.

5.2.3 Specimen A3-2C and Specimen A3-2C(2)

Specimen A3-2C was a replicate of Specimen A3-1C and was tested and analyzed in the same manner in order to validate the results of Specimen A3-1C. After Specimen

A3-2C failed under cyclic loading the wall was re-stapled and the repaired wall was titled Specimen A3-2C(2). The calculations used to determine the parameters found in Table 5.3 and Table 5.4 can be found in Appendix A.

Table 5.3: Specimen A3-2C Results

		Strength Limit State	Yield Limit State
Displacement (in.)	+	2.47	2.25
	-	3.75	2.94
	Average	3.11	2.60
Shear Force (lb)	+	10259	9862
	-	12238	11312
	Average	11249	10587
Shear Modulus (lbf/in.)	+	4154	4377
	-	3263	3846
	Average	3708	4111
Ductility	+	1.60	
	-	1.34	
	Average	1.47	
Shear Strength (lbf/ft)	+	1282	
	-	1530	
	Average	1406	
Elastic Stiffness (lbf/in.)	+	4377	
	-	3846	
	Average	4112	
Seismic Compatibility		Yes	

According to the results of the calculations presented, unlike Specimen A3-1C, Specimen A3-2C meets the requirements stated in ICC-ES AC130 (2007) and described in Section 5.1. Accordingly, the specimen can be considered qualified within a seismic-force resisting system with the following values of seismic response parameters:

Response Modification Coefficient: $R = 6.5$

System Overstrength Factor: $\Omega_0 = 3$

Deflection Amplification Factor: Cd = 4

However, as can be seen in Appendix A, Specimen A3-2C did not meet the specifications in Section 5.2.4 of ICC-ES AC130 as described earlier. Therefore, in order to be considered compliant. the evaluation report for the panel must include "a requirement that collectors and their connections, bearing and anchorage of the panel, and the lateral load path to the panel are designed in accordance with the special load combinations of Section 12.4.3 of ASCE 7, using E_m where E_m is calculated using the test panel overstrength" (ICC-ES AC130, 2007).

Table 5.4: Specimen A3-2C(2) Results

		Strength Limit State	Yield Limit State
Displacement (in.)	+	2.75	1.86
	-	2.65	2.16
	Average	2.70	2.01
Shear Force (lb)	+	7777	6835
	-	8064	7075
	Average	7921	6955
Shear Modulus (lbf/in.)	+	2824	3669
	-	3040	3276
	Average	2932	3473
Ductility	+	2.01	
	-	1.39	
	Average	1.70	
Shear Strength (lbf/ft)	+	972	
	-	1008	
	Average	990	
Elastic Stiffness (lbf/in.)	+	3669	
	-	3276	
	Average	3473	
Seismic Compatibility		No	

There is a noticeable drop in displacement, shear force, shear modulus, shear strength, and elastic stiffness and an increase in ductility in Specimen A3-2C(2) in comparison to Specimen A3-2C. It can be assumed that Specimen A3-2C(2) would have performed as well as Specimen A3-2C if the test setup did not interfere with re-stapling along the base plate and other locations.

5.3 Specimens A4

Specimens A4 had a 7/16 in. x 3 in. x 8 ft OSB spline which was connected to the SIP facing with 1.25 in. long, flat head, steel screws spaced at 6 in. o.c. The framing lumber was also attached to the SIP facing with the same screws at 6 in. o.c. The USP PHD6 hold-downs were placed at the exterior of the 8 ft x 8 ft wall.

5.3.1 Specimen A4-1M

Specimen A4-1M was tested under monotonic loading in correspondence with ASTM E 564-06. The parameters shown in Table 5.5 were obtained by analyzing the Load vs. Displacement graph of the specimen shown in Chapter 4. Similar to Specimen A3-1M, ASTM E 2126-08 was followed to determine the characteristic values of the specimen. Refer to Section 5.2.1.1 for an example of the equations used to determine the parameters.

Table 5.5: Specimen A4-1M Results

	Strength Limit State	Yield Limit State
Displacement (in.)	3.10	2.35
Shear Force (lb)	18613	16450
Shear Modulus (lbf/in.)	6000	7002
Ductility	1.52	
Shear Strength (lbf/ft)	2327	
Elastic Stiffness (lbf/in.)	8772	

5.3.2 Specimen A4-1C

Specimen A4-1C was tested under cyclic loading with a target displacement of 2.75 in. for the CUREE protocol. The calculations used to determine the parameters found in Table 5.6 are the same as those used to determine Specimens A3-1C, A3-2C, and A3-2C(2) which are located in Appendix A.

Table 5.6: Specimen A4-1C Results

		Strength Limit State	Yield Limit State
Displacement (in.)	+	3.27	2.98
	-	4.02	3.52
	Average	3.65	3.25
Shear Force (lb)	+	17705	16322
	-	16208	13776
	Average	16956	15049
Shear Modulus (lbf/in.)	+	5421	5486
	-	4026	3912
	Average	4724	4699
Ductility	+	1.45	
	-	1.46	
	Average	1.45	
Shear Strength (lbf/ft)	+	2213	
	-	2026	
	Average	2120	
Elastic Stiffness (lbf/in.)	+	5630	
	-	3149	
	Average	4389	
Seismic Compatibility		Yes	

According to the results of the calculations presented, Specimen A4-1C meets the requirements stated in ICC-ES AC130 (2007). Accordingly, the specimen can be considered qualified within a seismic-force resisting system with the following values of seismic response parameters:

Response Modification Coefficient: $R = 6.5$

System Overstrength Factor: $\Omega_0 = 3$

Deflection Amplification Factor: $Cd = 4$

However, Specimen A4-1C did not meet the specifications in Section 5.2.4 of ICC-ES AC130. Therefore, in order to be considered compliant, the evaluation report for the panel must include "a requirement that collectors and their connections, bearing and

anchorage of the panel, and the lateral load path to the panel are designed in accordance with the special load combinations of Section 12.4.3 of ASCE 7, using E_m where E_m is calculated using the test panel overstrength" (ICC-ES 130, 2007).

5.3.3 Specimen A4-2C

Specimen A4-2C was a replicate of Specimen A4-1C and was tested and analyzed in the same manner in order to validate the results of Specimen A4-1C. The calculations used to determine the parameters found in Table 5.7 are the same as those used to determine the previously stated specimens.

Table 5.7: Specimen A4-2C Results

		Strength Limit State	Yield Limit State
Displacement (in.)	+	2.75	2.46
	-	3.81	3.27
	Average	3.28	2.87
Shear Force (lb)	+	15763	13298
	-	17185	14607
	Average	16474	13953
Shear Modulus (lbf/in.)	+	5742	5407
	-	4506	4461
	Average	5124	4934
Ductility	+	1.31	
	-	1.14	
	Average	1.22	
Shear Strength (lbf/ft)	+	1970	
	-	2148	
	Average	2059	
Elastic Stiffness (lbf/in.)	+	5112	
	-	3632	
	Average	4372	
Seismic Compatibility		No	

Specimen A4-2C has very similar results as Specimen A4-1C. All of the values are within 10% of each other except for ductility which is within 16%. According to ASTM E 2126-08 values within 10% can be averaged together without performing a third test.

According to the results of the calculations presented, Specimen A4-2C does not meet the seismic specifications set forth by ICC-ES AC130 (2007) and described in Section 5.1. As a result, alternate means must be used to determine the response modification coefficient, system overstrength factor, and the deflection amplification factor.

5.3.4 Specimen A4-3C

Specimen A4-3C was a replicate of Specimens A4-1C and A4-2C and was tested and analyzed in the same manner in order to validate the results of the previously screwed walls. ASTM E 2126-08 was followed to determine the parameters found in Table 5.8. Refer to Appendix A for an example of the calculations used.

Table 5.8: Specimen A4-3C Results

		Strength Limit State	Yield Limit State
Displacement (in.)	+	3.09	2.67
	-	3.94	3.21
	Average	3.51	2.94
Shear Force (lb)	+	17241	14655
	-	16034	13629
	Average	16638	14142
Shear Modulus (lbf/in.)	+	5588	5492
	-	4072	4243
	Average	4830	4868
Ductility	+	1.21	
	-	1.51	
	Average	1.36	
Shear Strength (lbf/ft)	+	2155	
	-	2004	
	Average	2080	
Elastic Stiffness (lbf/in.)	+	5176	
	-	3514	
	Average	4345	
Seismic Compatibility		No	

The results found for Specimen A4-3C are all within 10% of both Specimen A4-1C and Specimen A4-2C.

Similar to Specimen A4-2C, Specimen A4-3C does not meet the seismic specifications set forth by ICC-ES AC130 (2007). As a result, alternate means must be used to determine the response modification coefficient, system overstrength factor, and the deflection amplification factor.

5.4 Specimens A1

Specimens A1 had a 7/16 in. x 3 in. x 8 ft OSB spline which was connected to the SIP facing with 8d common nails at 6 in. o.c. The framing lumber was also attached to

the SIP facing with 8d common nails at 6 in. o.c. As explained in Chapter 4, the A1 specimens were stronger than anticipated so a series of polynomial trend lines and failure points estimated by failure behavior of Specimens A3 and A4 were used to determine the 80% drop in peak load, or the failure of the specimen. The following tables will include minimum and maximum parameter values which provide a range of where the specimen would have failed.

5.4.1 Specimen A1-1M

Specimen A1-1M was tested under monotonic loading in correspondence with ASTM E 564-06. The facility was able to bring the specimen to a maximum displacement of 4.57 in. and a maximum load of 17584 lb. The range of values obtained by analyzing the trend lines according to ASTM E 2126-08 are shown in Table 5.9**.**

Table 5.9: Specimen A1-1M Results

	Strength Limit State		Yield Limit State	
	Minimum	Maximum	Minimum	Maximum
Displacement (in.)	4.50	5.00	2.89	2.69
Shear Force (lb)	17565	17631	17494	16244
Shear Modulus (lbf/in.)	3903	3526	6054	6044
Ductility	1.74	2.57		
Shear Strength (lbf/ft)	2196	2204		
Elastic Stiffness (lbf/in.)	6054	6044		

5.4.2 Specimen A1-1C

Specimen A1-1C was tested under cyclic loading and with a target displacement of 6 in. for the CUREE protocol. The calculations used to determine the parameters found in Table 5.10 are similar to those for Specimens A3 and A4 except each step was repeated for each trend line. For instance, the calculations in Sections 9.1.1 through 9.1.4 of ASTM E 2126-08 and Sections 5.1.3.1 and 5.2 of ICC-ES AC130 were followed to determine the performance parameters of Specimen A1-1C in terms of the third power polynomial trend line. Next, the fourth power polynomial trend line was anayzed in the same manner. This was repeated until all of the trend lines were analyzed. By determining the performance values according to each trend line, a range of values was determined for the specimen.

Table 5.10: Specimen A1-1C Results

		Strength Limit State		Yield Limit State	
		Minimum	Maximum	Minimum	Maximum
Displacement (in.)	+	4.96	5.46	3.70	3.82
	-	4.88	5.38	4.43	4.51
	Average	4.92	5.42	4.06	4.17
Shear Force (lb)	+	17605	17783	16193	16714
	-	17856	18384	17273	17701
	Average	17730	18083	16733	17207
Shear Modulus (lbf/in.)	+	3255	3547	4374	4375
	-	3417	3659	3902	3921
	Average	3336	3603	4138	4148
Ductility	+	1.45	1.84		
	-	1.26	1.57		
	Average	1.36	1.70		
Shear Strength (lbf/ft)	+	2201	2223		
	-	2298	2232		
	Average	2216	2260		
Elastic Stiffness (lbf/in.)	+	4374	4375		
	-	3902	3921		
	Average	4138	4148		
Seismic Compatibility		Yes			

According to the results presented in Table 5.10, Specimen A1-1C meets the requirements stated in ICC-ES AC130 (2007). Accordingly, the specimen can be considered qualified within a seismic-force resisting system with the following values of seismic response parameters:

Response Modification Coefficient: $R = 6.5$

System Overstrength Factor: $\Omega_0 = 3$

Deflection Amplification Factor: $Cd = 4$

However, Specimen A1-1C did not meet the specifications in Section 5.2.4 of ICC-ES AC130. Therefore, in order to be considered compliant, the evaluation report for the

panel must include "a requirement that collectors and their connections, bearing and anchorage of the panel, and the lateral load path to the panel are designed in accordance with the special load combinations of Section 12.4.3 of ASCE 7, using E_m where E_m is calculated using the test panel overstrength" (ICC-ES AC130, 2007).

5.4.2.1 Specimen A1-1C Fatigue 1

Specimen A1-1C did not reach an 80% drop in peak load under the initial set of cyclic loading. This provided the opportunity to test the specimen under additional cyclic loading in order to determine the wall's reaction under fatigue loading. In order to estimate the failure point of Specimen A1-1C, Fatigue 1 polynomial trend lines were fitted to the existing data and an estimated failure point based on the failure behavior of Specimens A3 and A4. The polynomial trend lines did not match up close enough with the existing data properly. Analyzing the polynomial trend lines would have produced inaccurate results. Therefore, the parameters in Table 5.11 for Specimen A1-1C Fatigue 1 were determined using the estimated failure point based on Specimens A3 and A4.

The displacement and ductility of Specimen A1-1C Fatigue 1 are within 10% of Specimen A1-1C. The fatigue loading caused a significant drop in shear force by 30%, shear modulus by 25%, shear strength by 30%, and the elastic stiffness by 60%.

Tables 5.11, 5.12 and 5.13 show that the fatigue tests of Specimen A1-1C were seismically compatible. However, just like the original Specimen A1-1C, the fatigue test specimens did not meet the specifications in Section 5.2.4 of ICC-ES AC130. Therefore, the previously stated requirements in Section 5.4.2 of this report must be addressed.

Table 5.11: Specimen A1-1C Fatigue 1 Results

		Strength Limit State	Yield Limit State
Displacement (in.)	+	4.93	4.53
	-	5.01	4.61
	Average	4.97	4.57
Shear Force (lb)	+	11076	9415
	-	13607	11566
	Average	12342	10490
Shear Modulus (lbf/in.)	+	2246	2078
	-	2715	2510
	Average	2481	2294
Ductility	+	1.37	
	-	1.24	
	Average	1.31	
Shear Strength (lbf/ft)	+	1385	
	-	1701	
	Average	1543	
Elastic Stiffness (lbf/in.)	+	1497	
	-	1805	
	Average	1651	
Seismic Compatibility		Yes	

5.4.2.2 Specimen A1-1C Fatigue 2

Specimen A1-1C was sent through a third set of cyclic loading and the data was titled Specimen A1-1C Fatigue 2. The Fatigue 2 test was analyzed in the same manner as Specimen A1-1C Fatigue 1 test. Table 5.12 shows the range of values obtained by analyzing the trend lines according to ASTM E 2126-08.

The parameters for Specimen A1-1C Fatigue 2 were all within 5% of those found for Specimen A1-1C Fatigue 1.

Table 5.12: Specimen A1-1C Fatigue 2 Results

		Strength Limit State	Yield Limit State
Displacement (in.)	+	4.71	4.26
	-	4.83	4.45
	Average	4.77	4.35
Shear Force (lb)	+	12752	10839
	-	11256	9567
	Average	12004	10203
Shear Modulus (lbf/in.)	+	2707	2546
	-	2332	2149
	Average	2519	2347
Ductility	+	1.39	
	-	1.24	
	Average	1.32	
Shear Strength (lbf/ft)	+	1594	
	-	1407	
	Average	1500	
Elastic Stiffness (lbf/in.)	+	1880	
	-	1533	
	Average	1707	
Seismic Compatibility		Yes	

5.4.2.3 Specimen A1-1C Fatigue 3

The fourth set of cyclic loading placed on Specimen A1-1C was considered Fatigue 3. Specimen A1-1C Fatigue 3 was analyzed in the same way as Fatigues 1 and 2. Table 5.13 shows the parameters found for Specimen A1-1C Fatigue 3 based on ASTM E 2126-08. The displacement and shear strength of Fatigue 3 was very similar to those for Fatigue 2. There was a drop in shear force, shear modulus, elastic stiffness, and ductility by about 16% in Fatigue 3 in comparison to Fatigue 2.

Table 5.13: Specimen A1-1C Fatigue 3 Results

		Strength Limit State	Yield Limit State
Displacement (in.)	+	4.60	4.15
	-	4.94	4.54
	Average	4.77	4.35
Shear Force (lb)	+	10706	9100
	-	9394	7985
	Average	10050	8543
Shear Modulus (lbf/in.)	+	2327	2192
	-	1901	1757
	Average	2114	1974
Ductility	+	1.40	
	-	1.24	
	Average	1.32	
Shear Strength (lbf/ft)	+	1338	
	-	1174	
	Average	1256	
Elastic Stiffness (lbf/in.)	+	1688	
	-	1234	
	Average	1461	
Seismic Compatibility		Yes	

5.4.3 Specimen A1-2C

Specimen A1-2C is a replicate of Specimen A1-1C and was tested and analyzed in the same manner in order to validate the results of Specimen A1-1C. The calculations used to determine the parameters found in Table 5.14 are similar to those for Specimens A3 and A4 except each step was repeated for each trend line as described in Section 5.4.2. In the strength limit state column of the table, all of the parameters except for ductility have a single value because these values were determined by examining the envelope curve developed from the actual data obtained during cyclic loading. However, the values in the yield limit state column were found by analyzing the trend lines which,

resulted in a range of possible values. The shear modulus in the yield limit state only has one value because the trend lines were so similar that they all produced the same results.

Table 5.14: Specimen A1-2C Results

		Strength Limit State		Yield Limit State	
		Minimum	Maximum	Minimum	Maximum
Displacement (in.)	+	5.32		4.80	4.92
	-	5.02		4.12	4.23
	Average	5.17		4.5	4.58
Shear Force (lb)	+	17781		16837	17301
	-	18750		17815	17646
	Average	18265		17182	17472
Shear Modulus (lbf/in.)	+	3339		3508	
	-	3732		4172	
	Average	3536		3840	
Ductility	+	1.31	1.40		
	-	1.37	2.22		
	Average	1.38	1.77		
Shear Strength (lbf/ft)	+	2223			
	-	2344			
	Average	2283			
Elastic Stiffness (lbf/in.)	+	3508			
	-	4172			
	Average	3840			
Seismic Compatibility		Yes			

The values obtained for Specimen A1-2C are all within 10% of those for Specimen A1-1C. Similar to Specimen A1-1C, Specimen A1-2C meets the requirements stated in ICC-ES AC130 (2007). Accordingly, the specimen can be considered qualified within a seismic-force resisting system with the following values of seismic response parameters:

Response Modification Coefficient: $R = 6.5$

System Overstrength Factor: $\Omega_0 = 3$

Deflection Amplification Factor: Cd = 4

However, Specimen A1-2C did not meet the specifications in Section 5.2.4 of ICC-ES AC130. Therefore, in order to be considered compliant, the evaluation report for the panel must include "a requirement that collectors and their connections, bearing and anchorage of the panel, and the lateral load path to the panel are designed in accordance with the special load combinations of Section 12.4.3 of ASCE 7, using E_m where E_m is calculated using the test panel overstrength" (ICC-ES AC130, 2007).

5.4.3.1 Specimen A1-2C Fatigue 1

Specimen A1-2C was placed under another thirty-seven cycles of the CUREE loading protocol in order to determine the effects fatigue loading has on the specimen. The data obtained was analyzed in the same way as the previous A1 specimens. The ranges of the performance parameters obtained are shown in Table 5.15**.**

The minimum edge of the displacement range of Specimen A1-2C Fatigue 1 was about 6% greater than the displacement of Specimen A1-2C for the strength limit state while it was about 12% greater for the yield limit state. The shear modulus and ductility of Specimen A1-2C Fatigue 1 were about 21% less than Specimen A1-2C. The shear force and shear strength of Fatigue 1 in the strength limit state were both about 4% less than those in Specimen A1-2C. The greatest change occurred in the elastic shear stiffness where the values dropped by about 46% after Fatigue 1 of Specimen A1-2C.

Tables 5.15, 5.16 and 5.17 show that the fatigue tests of Specimen A1-2C were seismically compatible. However, just like the original Specimen A1-2C, the fatigue test

specimens did not meet the specifications in Section 5.2.4 of ICC-ES AC130. Therefore, the previously stated requirements in Section 5.4.3 of this report must be addressed.

Table 5.15: Specimen A1-2C Fatigue 1 Results

		Strength Limit State		Yield Limit State	
		Minimum	Maximum	Minimum	Maximum
Displacement (in.)	+	5.68	6.68	5.13	5.53
	-	5.27	5.77	4.76	5.00
	Average	5.48	6.23	4.95	5.26
Shear Force (lb)	+	16738	18918	14227	16080
	-	14963	16176	12719	13750
	Average	15851	17547	13473	14915
Shear Modulus (lbf/in.)	+	2949	2834	2772	2906
	-	2837	2801	2672	2752
	Average	2893	2817	2722	2829
Ductility	+	1.39	1.40		
	-	1.27	1.39		
	Average	1.33	1.39		
Shear Strength (lbf/ft)	+	2092	2365		
	-	1870	2022		
	Average	1981	2193		
Elastic Stiffness (lbf/in.)	+	2043	2149		
	-	1908	1985		
	Average	1976	2067		
Seismic Compatibility		Yes			

5.4.3.2 Specimen A1-2C Fatigue 2

Specimen A1-2C was sent through a third set of cyclic loading and the data was titled Specimen A1-2C Fatigue 2. Fatigue 2 was analyzed in the same manner as Specimen A1-2C and A1-2C Fatigue 1. In order to estimate the failure point of Specimen A1-2C Fatigue 2 polynomial trend lines were fitted to the existing data and an estimated failure point based on the failure behavior of Specimens A3 and A4. The

polynomial trend lines did not match up closely with the existing data properly, so the parameters in Table 5.16 for Specimen A1-2C Fatigue 2 were determined from using the estimated failure point based on Specimens A3 and A4.

The displacement of Fatigue 2 fell within the range of Specimen A1-2C Fatigue 2. The shear force, shear modulus, and ductility of Specimen A1-2C Fatigue 2 were all within 10% of the minimum end of the range of Specimen A1-2C Fatigue 1. The elastic shear stiffness was 14% less than the minimum end of the range of Fatigue 1.

Table 5.16: Specimen A1-2C Fatigue 2 Results

		Strength Limit State	Yield Limit State
Displacement (in.)	+	5.90	5.41
	-	5.30	4.87
	Average	5.60	5.14
Shear Force (lb)	+	15653	13305
	-	13812	11740
	Average	14732	12522
Shear Modulus (lbf/in.)	+	2651	2458
	-	2605	2410
	Average	2628	2434
Ductility	+	1.37	
	-	1.25	
	Average	1.31	
Shear Strength (lbf/ft)	+	1957	
	-	1726	
	Average	1842	
Elastic Stiffness (lbf/in.)	+	1738	
	-	1671	
	Average	1705	
Seismic Compatibility		Yes	

5.4.3.3 Specimen A1-2C Fatigue 3

The fourth set of cyclic loading placed on Specimen A1-2C was considered Fatigue 3. Specimen A1-2C Fatigue 3 was analyzed in the same way as Fatigue 2. Table 5.17 shows the parameters found for Specimen A1-2C Fatigue 3 based on ASTM E 2126-08. The parameters for Specimen A1-2C Fatigue 3 were all within 10% of those found for Specimen A1-2C Fatigue 2.

Table 5.17: Specimen A1-2C Fatigue 3 Results

		Strength Limit State	Yield Limit State
Displacement (in.)	+	6.02	5.51
	-	5.43	4.99
	Average	5.72	5.25
Shear Force (lb)	+	14558	12374
	-	12701	10796
	Average	13629	11585
Shear Modulus (lbf/in.)	+	2419	2244
	-	2341	2163
	Average	2380	2204
Ductility	+	1.38	
	-	1.24	
	Average	1.31	
Shear Strength (lbf/ft)	+	1820	
	-	1588	
	Average	1704	
Elastic Stiffness (lbf/in.)	+	1583	
	-	1492	
	Average	1537	
Seismic Compatibility		Yes	

5.4.4 Specimen A1Bearing-3C

Specimen A1Bearing-3C was different than Specimens A1-1C and A1-2C because the sheathing of the SIP was bearing directly on the loading elements. The calculations used to determine the parameters found in Table 5.18 are similar to those for Specimens A3 and A4 except each step was repeated for each trend line. The parameters in the strength limit state column, except for ductility, were determined by examining the actual envelope curve based on the cyclic loading of the specimen so there is only one value as opposed to a range of values. The parameters in the yield limit state column were determined by anayzling the trend lines which resulted in a range of values. The trend lines were so similar that they all produced the same shear modulus values.

Table 5.18: Specimen A1Bearing-3C

		Strength Limit State		Yield Limit State	
		Minimum	Maximum	Minimum	Maximum
Displacement (in.)	+	4.14		2.92	2.95
	-	4.25		3.96	4.16
	Average	4.20		3.46	3.55
Shear Force (lb)	+	19996		18377	18588
	-	19414		19363	20342
	Average	19705		18972	19441
Shear Modulus (lbf/in.)	+	4827		6292	
	-	4564		4889	
	Average	4695		5590	
Ductility	+	1.59	1.79		
	-	1.12	1.37		
	Average	1.36	1.56		
Shear Strength (lbf/ft)	+	2500			
	-	2427			
	Average	2463			
Elastic Stiffness (lbf/in.)	+	6292			
	-	4889			
	Average	5590			
Seismic Compatibility		Yes			

The sheathing bearing in Specimen A1Bearing-3C had an effect on the wall performance. In comparison to Specimens A1-1C and A1-2C, Specimen A1Bearing-3C had about a 17% decrease in displacement, about an 8% increase in shear force, about a 24% increase in shear modulus, about an 8% increase in shear strength and a significant 29% increase in elastic stiffness. This demonstrates the significance sheathing bearing has on a wall specimen.

Similar to Specimens A1-1C and A1-2C, Specimen A1Bearing-3C meets the requirements stated in ICC-ES AC130 (2007). Accordingly, the specimen can be

considered qualified within a seismic-force resisting system with the following values of seismic response parameters:

Response Modification Coefficient: R = 6.5

System Overstrength Factor: $\Omega_0 = 3$

Deflection Amplification Factor: Cd = 4

However, Specimen A1Bearing-3C did not meet the specifications in Section 5.2.4 of ICC-ES AC130. Therefore, in order to be considered compliant, the evaluation report for the panel must include "a requirement that collectors and their connections, bearing and anchorage of the panel, and the lateral load path to the panel are designed in accordance with the special load combinations of Section 12.4.3 of ASCE 7, using E_m where E_m is calculated using the test panel overstrength" (ICC-ES AC130, 2007).

5.4.4.1 Specimen A1Bearing-3C Fatigue 1

Due to the 20,000 lb load capacity of the facility Specimen A1Bearing-3C did not achieve an 80% drop in peak load capacity under the first run of cyclic testing. This provided the opportunity to test the specimen under fatigue loading by running the same cyclic loading a second time. Table 5.19 shows the characteristic values of Specimen A1Bearing-3C after Fatigue 1. Fatigue 1 was analyzed in the same way as Specimen A1Bearing-3C and the previous A1 specimens.

The displacement after Fatigue 1 increased between 1% and 10% in comparison to Specimen A1Bearing-3C. The shear force, shear modulus and shear strength decreased by about 30% while the ductility decreased by about 9%. The greatest

decrease occurred in the elastic shear stiffness which dropped by about 61% in comparison to the Specimen A1Bearing-3C.

Table 5.19 shows that the fatigue test of Specimen A1Bearing-3C was seismically compatible. However, just like the original Specimen A1Bearing-3C, the fatigue test specimen did not meet the specifications in Section 5.2.4 of ICC-ES AC130. Therefore, the previously stated requirements in Section 5.4.4 of this report must be addressed.

Table 5.19: Specimen A1Bearing-3C Fatigue 1 Results

		Strength Limit State		Yield Limit State	
		Minimum	Maximum	Minimum	Maximum
Displacement (in.)	+	4.00	4.50	3.54	3.60
	-	4.44	4.94	4.03	4.29
	Average	4.22	4.72	3.78	3.95
Shear Force (lb)	+	12645	12963	10748	11018
	-	15086	16806	12823	14285
	Average	13866	14885	11786	12652
Shear Modulus (lbf/in.)	+	3164	2881	3040	3060
	-	3400	3402	3184	3328
	Average	3282	3141	3112	3194
Ductility	+	1.38	1.42		
	-	1.26	1.39		
	Average	1.34	1.39		
Shear Strength (lbf/ft)	+	1581	1620		
	-	1886	2101		
	Average	1733	1861		
Elastic Stiffness (lbf/in.)	+	2057	2088		
	-	2223	2356		
	Average	2140	2222		
Seismic Compatibility		Yes			

5.4.5 Specimen A1Internal-4C

The only difference between Specimen A1Internal-4C and Specimens A1-1C and A1-2C is the location of the USP PHD 6 hold-down. The USP PHD 6 hold-downs were placed on the interior of the double studded end posts instead of the exterior. The calculations used to determine the parameters found in Table 5.20 are similar to those for Specimens A3 and A4 except each step was repeated for each trend line. For some parameters either all of the trend lines produced the same value or the parameter was determined by examining the actual envelope curve created by cyclically loading the specimen. This is represented by a single value in the cell of the table instead of a maximum and minimum value.

Table 5.20: Specimen A1Internal-4C

		Strength Limit State		Yield Limit State	
		Minimum	Maximum	Minimum	Maximum
Displacement (in.)	+	4.91		2.68	2.74
	-	5.31		4.72	4.85
	Average	5.11		3.72	3.77
Shear Force (lb)	+	17577		15719	16031
	-	15629		15448	15879
	Average	16603		15638	15808
Shear Modulus (lbf/in.)	+	3583		5857.91	
	-	2942		3273	
	Average	3262		4566	
Ductility	+	2.04	2.51		
	-	1.22	1.48		
	Average	1.63	1.99		
Shear Strength (lbf/ft)	+	2197			
	-	1954			
	Average	2075			
Elastic Stiffness (lbf/in.)	+	5858			
	-	3273			
	Average	4566			
Seismic Compatibility		Yes			

Specimen A1Internal-4C performed similarly to Specimens A1-1C and A1-2C. The displacement, shear force, shear modulus, and shear strength values are all within 10% of each other. A1Internal-4C has a 15% increase in ductility and a 13% increase in elastic stiffness

Similar to Specimens A1-1C and A1-2C, Specimen A1Internal-4C meets the requirements stated in ICC-ES AC130 (2007). Accordingly, the specimen can be considered qualified within a seismic-force resisting system with the following values of seismic response parameters:

Response Modification Coefficient: R = 6.5

System Overstrength Factor: $\Omega_0 = 3$

Deflection Amplification Factor: Cd = 4

However, Specimen A1Internal-4C did not meet the specifications in Section 5.2.4 of ICC-ES AC130. Therefore, in order to be considered compliant, the evaluation report for the panel must include "a requirement that collectors and their connections, bearing and anchorage of the panel, and the lateral load path to the panel are designed in accordance with the special load combinations of Section 12.4.3 of ASCE 7, using E_m where E_m is calculated using the test panel overstrength" (ICC-ES AC130, 2007).

5.4.5.1 Specimen A1Internal-4C Fatigue 1

Similar to Specimens A1, A2 and A1Bearing, Specimen A1Internal-4C did not reach an 80% drop in load capacity under the first run of cyclic testing due to facility restricitons. This provided the opportunity to test the specimen under fatigue loading by running the same cyclic loading a second time. Table 5.21 shows the characteristic values of Specimen A1Internal-4C after Fatigue 1. Fatigue 1 was analyzed in the same way as Specimen A1Internal-4C and the previously stated A1 specimens. All of estimated failure values were analyzed according to ASTM E 2126-08 and the range of values obtained are in Table 5.21.

After Fatigue 1, the displacement increased by 5% for the strength limit state and about 37% for the yield limit state. The shear strength and shear force of Specimen A1Internal-4C were within the range of the values obtained after Fatigue 1. The shear modulus dropped by about 19% after Fatigue 1 and the ductility dropped by about 23%.

Similar to previous fatigues, the greatest change occurred in the elastic shear stiffness which decreased by about 56% after Fatigue 1.

Tables 5.21, 5.22 and 5.23 show that the fatigue tests of Specimen A1Internal-4C were seismically compatible. However, the fatigue test specimens did not meet the specifications in Section 5.2.4 of ICC-ES AC130. Therefore, the previously stated requirements in Section 5.4.5 of this report must be addressed.

Table 5.21: Specimen A1Internal-4C Fatigue 1 Results

		Strength Limit State		Yield Limit State	
		Minimum	Maximum	Minimum	Maximum
Displacement (in.)	+	5.41	6.91	4.88	5.57
	-	5.28	6.78	4.77	5.38
	Average	5.35	6.85	4.83	5.47
Shear Force (lb)	+	15869	19328	13489	16429
	-	12627	15200	10733	12920
	Average	14248	17264	12111	14674
Shear Modulus (lbf/in.)	+	2796	2932	2765	2952
	-	2241	2390	2248	2401
	Average	2518	2661	2507	2677
Ductility	+	1.40	1.43		
	-	1.27	1.43		
	Average	1.33	1.43		
Shear Strength (lbf/ft)	+	1984	2416		
	-	1578	1900		
	Average	1781	2158		
Elastic Stiffness (lbf/in.)	+	2064	2234		
	-	1645	1780		
	Average	1855	2007		
Seismic Compatibility		Yes			

5.4.5.2 Specimen A1Internal-4C Fatigue 2

Specimen A1Internal-4C was sent through a third set of cyclic loading and the data was titled Specimen A1Internal-4C Fatigue 2. Fatigue 2 was analyzed in the same manner as Specimen A1Internal-4C and A1Internal-4C Fatigue 1. Table 5.22 shows the range of performance parameters obtained.

The displacement of Fatigue 2 fell within the range of Specimen A1Internal-4C Fatigue 1. The shear force, shear modulus, shear strength, and ductility of Specimen A1Internal-4C Fatigue 2 were all within 10% of the minimum end of the range of Specimen A1Internal-4C Fatigue 1. The elastic shear stiffness was 18% less than the minimum end of the range of Fatigue 1.

Table 5.22: Specimen A1Internal-4C Fatigue 2 Results

		Strength Limit State	Yield Limit State
Displacement (in.)	+	5.63	5.15
	-	5.52	5.02
	Average	5.57	5.09
Shear Force (lb)	+	13801	11730
	-	11727	9968
	Average	12764	10849
Shear Modulus (lbf/in.)	+	2453	2278
	-	2126	1984
	Average	2289	2131
Ductility	+	1.38	
	-	1.26	
	Average	1.32	
Shear Strength (lbf/ft)	+	1725	
	-	1466	
	Average	1595	
Elastic Stiffness (lbf/in.)	+	1620	
	-	1437	
	Average	1529	
Seismic Compatibility		Yes	

5.4.5.3 Specimen A1Internal-4C Fatigue 3

Specimen A1Internal-4C was tested under a fourth set of cyclic loading and the data obtained was titled Specimen A1Internal-4C Fatigue 3. Fatigue 3 was analyzed in the same manner as Specimen A1Internal-4C, A1Internal-4C Fatigue 1, and A1Internal-4C Fatigue 2. Table 5.23 shows the range of values obtained, according to ASTM E 2126-08.

The displacement of A1Internal-4C Fatigue 3 increased by about 4% in comparison to A1Internal-4C Fatigue 2 while the shear modulus decreased by about 10%. The shear force, shear strength, elastic shear stiffness, and ductility of Fatigue 3

were all within range of Fatigue 2. This shows that there was minimal difference between Fatigue 2 and Fatigue 3 of Specimen A1Internal-4C.

Table 5.23: Specimen A1Internal-4C Fatigue 3 Results

		Strength Limit State		Yield Limit State	
		Minimum	Maximum	Minimum	Maximum
Displacement (in.)	+	5.90	7.40	5.35	6.20
	-	5.70	9.20	5.19	7.64
	Average	5.80	8.30	5.27	6.92
Shear Force (lb)	+	11792	14843	10023	12617
	-	10232	19520	8697	16592
	Average	11012	17182	9360	14605
Shear Modulus (lbf/in.)	+	1998	2005	1872	2035
	-	1795	2122	1676	2173
	Average	1897	2064	1774	2104
Ductility	+	1.39	1.43		
	-	1.26	1.44		
	Average	1.32	1.43		
Shear Strength (lbf/ft)	+	1474	1855		
	-	1279	2440		
	Average	1377	2148		
Elastic Stiffness (lbf/in.)	+	1367	1495		
	-	1206	1596		
	Average	1286	1546		
Seismic Compatibility		Yes			

5.5 Specimens B

Specimens B had a (2) 2x4 spline in which the 2x4's were connected with (2) 16d common nails spaced at 4 in. from each end of the 7 ft 9 in. spline and 24 in. o.c. The spline and the framing lumber were attached to the OSB sheathing of the SIP with 8d common nails spaced at 6 in. o.c. The USP PHD6 hold-downs were placed at the exterior of the 8 ft x 8 ft wall.

All except for one of the Specimen B walls were stronger than anticipated and due to the limitations of the test facility they could not be tested to an 80% drop in load. In order to determine the failure of these specimens trend lines were added to the envelope curve, as demonstrated in Chapter 4. Each trend line was analyzed according to ASTM E 2126-08 and ICC-ES AC130 and the range of values found are presented in the following tables. If a parameter only has one value, not a minimum and maximum, then the trend lines all produced the same value.

5.5.1 Specimen B-1M

Specimen B-1M was tested under monotonic loading in correspondence with ASTM E 564-06. The facility was able to bring the specimen to a maximum displacement of 5.30 in. and a maximum load of 17191 lb. The load began to decrease as the displacement increased but the displacement limitations of the facility did not allow the specimen to reach an 80% drop in peak load. The maximum and minimum trend lines fit to the existing data were analyzed and the range of values obtained according to ASTM E 2126-08 is shown in Table 5.24.

Table 5.24: Specimen B-1M Results

	Strength Limit State		Yield Limit State	
	Minimum	Maximum	Minimum	Maximum
Displacement (in.)	5.15		3.82	4.71
Shear Force (lb)	17191		14613	18008
Shear Modulus (lbf/in.)	3340		3823	
Ductility	1.28	1.45		
Shear Strength (lbf/ft)	2149			
Elastic Stiffness (lbf/in.)	3823			

5.5.2 Specimen B-1C

Specimen B-1C was tested under cyclic loading using a target displacement of 6 in. for the CUREE protocol. Refer to Table 5.25 for the specimen parameters.

Table 5.25: Specimen B-1C Results

		Strength Limit State		Yield Limit State	
		Minimum	Maximum	Minimum	Maximum
Displacement (in.)	+	5.17		4.59	4.77
	-	5.12	6.12	4.59	5.82
	Average	5.15	5.65	4.59	5.27
Shear Force (lb)	+	17709		17020	17672
	-	17112	18186	14545	18667
	Average	17410	17947	15782	18067
Shear Modulus (lbf/in.)	+	3424		3707	
	-	2973	3344	3170	3207
	Average	3198	3384	3438	3457
Ductility	+	1.26	1.42		
	-	1.26	1.34		
	Average	1.26	1.35		
Shear Strength (lbf/ft)	+	2214			
	-	2139	2273		
	Average	2176	2243		
Elastic Stiffness (lbf/in.)	+	3707			
	-	3170	3207		
	Average	3438	3457		
Seismic Compatibility		Yes			

According to the results presented, Specimen B-1C meets the requirements stated in ICC-ES AC130 (2007). Accordingly, the specimen can be considered qualified within a seismic-force resisting system with the following values of seismic response parameters:

Response Modification Coefficient: $R = 6.5$

System Overstrength Factor: $\Omega_0 = 3$

Deflection Amplification Factor: $Cd = 4$

However, Specimen B-1C did not meet the specifications in Section 5.2.4 of ICC-ES AC130, and in order to be considered compliant, the evaluation report for the panel must

include “a requirement that collectors and their connections, bearing and anchorage of the panel, and the lateral load path to the panel are designed in accordance with the special load combinations of Section 12.4.3 of ASCE 7, using E_m where E_m is calculated using the test panel overstrength” (ICC-ES AC130, 2007).

5.5.2.1 Specimen B-1C Fatigue 1

Specimen B-1C was tested under a second run of cyclic loading in order to determine the specimen’s characteristics under fatigue loading. Specimen B-1C failed during a trailing cycle of Fatigue 1 but due to the displacement limitations of the facility the next primary cycle could not be run so the drop in the envelope curve was not plotted. The trend lines and estimated failure points were analyzed according to ASTM E 2126-08 and the range of values obtained is shown in Table 5.26**.**

In comparison to Specimen B-1C, the displacement of Specimen B-1C Fatigue 1 increased by about 18%. There was also a 5% increase in ductility of Fatigue 1. The decrease in shear force, shear modulus, and shear strength ranged from about 14% to 25%. Similar to previous specimens placed under fatigue, the elastic shear stiffness of Specimen B-1C Fatigue 1 decreased by about 47% in comparison to Specimen B-1C.

Table 5.26 shows that Fatigue 1 of Specimen B-1C was seismically compatible to the specifications of ICC-ES AC130. However, the Fatigue 1 test did not meet all of the conditions of Section 5.2.4 of ICC-ES AC130. Therefore, the previously stated requirements in Section 5.5.2 of this report must be addressed.

Table 5.26: Specimen B-1C Fatigue 1 Results

		Strength Limit State		Yield Limit State	
		Minimum	Maximum	Minimum	Maximum
Displacement (in.)	+	5.60	6.10	5.07	5.29
	-	5.29	6.29	4.78	5.28
	Average	5.45	6.20	4.93	5.28
Shear Force (lb)	+	14716	15789	12059	13421
	-	13689	16052	11636	13644
	Average	14203	15920	12072	13532
Shear Modulus (lbf/in.)	+	2588	2627	2467	2537
	-	2553	2589	2433	2585
	Average	2570	2608	2450	2561
Ductility	+	1.38	1.39		
	-	1.27	1.41		
	Average	1.33	1.39		
Shear Strength (lbf/ft)	+	1839	1974		
	-	1711	2006		
	Average	1775	1990		
Elastic Stiffness (lbf/in.)	+	1742	2060		
	-	1799	1819		
	Average	1770	1939		
Seismic Compatibility		Yes			

5.5.3 Specimen B-2C

Specimen B-2C is a replicate of Specimen B-1C and was tested and analyzed in the same manner in order to validate the results of Specimen B-1C. Refer to Table 5.27 for the specimen parameters.

Table 5.27: Specimen B-2C Results

		Strength Limit State		Yield Limit State	
		Minimum	Maximum	Minimum	Maximum
Displacement (in.)	+	4.85		4.30	4.48
	-	5.13	5.63	4.46	5.76
	Average	4.99	5.24	4.38	5.09
Shear Force (lb)	+	19992		19148	19977
	-	19412	20005	16500	21291
	Average	19702	19998	17824	20503
Shear Modulus (lbf/in.)	+	4120		4458	
	-	3554	3785	3697	3718
	Average	3837	3952	4077	4088
Ductility	+	1.23	1.46		
	-	1.08	1.35		
	Average	1.20	1.40		
Shear Strength (lbf/ft)	+	2499			
	-	2426	2501		
	Average	2463	2500		
Elastic Stiffness (lbf/in.)	+	4458			
	-	3697	3718		
	Average	4077	4088		
Seismic Compatibility		Yes			

The parameters found for Specimen B-2C are similar to those of Specimen B-1C. The displacement, ductility, and shear strength are all within about 10% of each other. The shear forces between the two specimens are within about 12% and the shear modulus and elastic stiffness are within 15% of the specimens.

Similar to Specimen B-1C, Specimen B-2C meets the requirements stated in ICC-ES AC130 (2007). Accordingly, the specimen can be considered qualified within a seismic-force resisting system with the following values of seismic response parameters:

Response Modification Coefficient: $R = 6.5$

System Overstrength Factor: $\Omega_0 = 3$

Deflection Amplification Factor: Cd = 4

However, Specimen B-2C did not meet the specifications in Section 5.2.4 of ICC-ES AC130, and in order to be considered compliant, the evaluation report for the panel must include "a requirement that collectors and their connections, bearing and anchorage of the panel, and the lateral load path to the panel are designed in accordance with the special load combinations of Section 12.4.3 of ASCE 7, using E_m where E_m is calculated using the test panel overstrength" (ICC-ES AC130, 2007).

5.5.3.1 Specimen B-2C Fatigue 1

Similar to Specimen B-1C, Specimen B-2C was tested under fatigue loading by running the same cyclic loading a second time. All of the estimated failure values from the trend lines and estimated failure points were analyzed according to ASTM E 2126-08 and the range of values obtained are in Table 5.28.

Fatigue 1 of Specimen B-2C resulted in about an 11% increase in displacement and a 10% to 15% decrease in shear force, shear modulus, and shear strength in comparison to Specimen B-2C. There was a minimal change in ductility between the two tests but the elastic shear stiffness dropped by about 45% in Specimen B-2C Fatigue 1.

Tables 5.28 and 5.29 show that the fatigue tests of Specimen B-2C were seismically compatible. However, just like the original Specimen B-2C, the fatigue test specimens did not meet the specifications in Section 5.2.4 of ICC-ES AC130. Therefore, the previously stated requirements in Section 5.5.3 of this report must be addressed.

Table 5.28: Specimen B-2C Fatigue 1 Results

		Strength Limit State		Yield Limit State	
		Minimum	Maximum	Minimum	Maximum
Displacement (in.)	+	5.48	5.98	4.96	5.17
	-	5.10	6.10	4.65	5.18
	Average	5.29	6.04	4.80	5.17
Shear Force (lb)	+	18657	19979	15858	16982
	-	16611	19963	14120	16969
	Average	17634	19971	14989	16976
Shear Modulus (lbf/in.)	+	3340	3403	3200	3287
	-	3260	3275	3040	3277
	Average	3307	3331	3120	3282
Ductility	+	1.37	1.39		
	-	1.26	1.38		
	Average	1.32	1.38		
Shear Strength (lbf/ft)	+	2332	2497		
	-	2076	2495		
	Average	2204	2496		
Elastic Stiffness (lbf/in.)	+	2296	2375		
	-	2124	2325		
	Average	2210	2350		
Seismic Compatibility		Yes			

5.5.3.2 Specimen B-2C Fatigue 2

Specimen B-2C was placed under a third set of cyclic loading and the data was titled Specimen B-2C Fatigue 2. Fatigue 2 was analyzed in the same manner as Specimen B-2C and B-2C Fatigue 1. The polynomial trend lines and the estimated failure points were analyzed according to ASTM E 2126-08 and the range of values obtained are shown in Table 5.29**.**

There were minimal differences between Fatigue 1 and Fatigue 2 of Specimen B-2C. The shear force, shear modulus, shear strength, shear elastic stiffness, and ductility

decreased by 10% or less while the displacement only increased by about 4% in Fatigue 2.

Table 5.29: Specimen B-2C Fatigue 2 Results

		Strength Limit State		Yield Limit State	
		Minimum	Maximum	Minimum	Maximum
Displacement (in.)	+	5.78		5.29	
	-	5.19	6.69	4.75	5.65
	Average	5.49	6.24	5.02	5.47
Shear Force (lb)	+	17413		14801	
	-	15980	21533	13583	18303
	Average	16697	19473	14192	16552
Shear Modulus (lbf/in.)	+	3010		2800	
	-	3077	3217	2860	3239
	Average	3044	3114	2830	3020
Ductility	+	1.38			
	-	1.25	1.39		
	Average	1.32	1.38		
Shear Strength (lbf/ft)	+	2177			
	-	1998	2692		
	Average	2087	2434		
Elastic Stiffness (lbf/in.)	+	1948			
	-	2003	2284		
	Average	1976	2116		
Seismic Compatibility		Yes			

5.5.4 Specimen B-3C

Specimen B-3C is a replicate of Specimens B-1C and B-2C and was tested and analyzed in the same manner in order to validate the results of Specimen B-1C. Refer to Table 5.30 for the specimen parameters.

Table 5.30: Specimen B-3C Results

		Strength Limit State		Yield Limit State	
		Minimum	Maximum	Minimum	Maximum
Displacement (in.)	+	5.01		3.67	3.75
	-	5.77	6.27	5.32	6.95
	Average	5.39	5.64	4.50	5.35
Shear Force (lb)	+	17121		16273	16597
	-	18315	18511	15568	20406
	Average	17718	17816	15920	18501
Shear Modulus (lbf/in.)	+	3418		4429	
	-	2951	3173	2925	2935
	Average	3184	3295	3677	3682
Ductility	+	1.53			
	-	1.10	1.32		
	Average	1.32	1.48		
Shear Strength (lbf/ft)	+	2140			
	-	2289	2314		
	Average	2215	2227		
Elastic Stiffness (lbf/in.)	+	4429			
	-	2925	2934		
	Average	3677	3682		
Seismic Compatibility		Yes			

The parameters of Specimen B-3C are very similar to those of Specimens B-1C and B-2C. All of the parameters for Specimen B-3C are within 10% of Specimen B-1C and all except for the shear modulus of Specimen B-2C are within 10% as well. The shear modulus of Specimen B-3C is about 17% less than that of Specimen B-2C.

Similar to Specimens B-1C and B-2C, Specimen B-3C meets the requirements stated in ICC-ES AC130 (2007). Accordingly, the specimen can be considered qualified within a seismic-force resisting system with the following values of seismic response parameters:

Response Modification Coefficient: R = 6.5

System Overstrength Factor: $\Omega_0 = 3$

Deflection Amplification Factor: Cd = 4

However, Specimen B-3C did not meet the specifications in Section 5.2.4 of ICC-ES AC130, so in order to be considered compliant the evaluation report for the panel must include "a requirement that collectors and their connections, bearing and anchorage of the panel, and the lateral load path to the panel are designed in accordance with the special load combinations of Section 12.4.3 of ASCE 7, using E_m where E_m is calculated using the test panel overstrength" (ICC-ES AC130, 2007).

5.6 Specimens C

Specimens C were conventional wood-frame walls. Both sides of the wall were sheathed with 7/16 in. x 4 ft x 8 ft sheets of OSB oriented vertically with the OSB running parallel to the studs. The studs were 2x4 SPF No. 2 or better spaced at 16 in. o.c. nailed according to the IBC. The sheathing was attached to the wall with 8d common nails spaced at 6 in. o.c. along the outer perimeter and spline and 12 in. o.c. along the studs. There was a double top plate and a single base plate.

Similar to Specimens A1 and B, trend lines and failure points from previous tests were used to estimate the failure points of the specimen. Unlike Specimens A1 and B, the hysteresis loops for Specimen C-1C did not begin to level off towards the end of the test. As a result, trend lines were drawn from the actual peak point of the eighth primary cycle of the test and they were drawn from a point extended to a 15% increase in load. The maximum trend line and the minimum trend line were then analyzed to determine the

maximum and minimum values. Refer to Chapter 4 for the envelope curves and trend lines used to develop the values in the following tables.

5.6.1 Specimen C-1M

Specimen C-1M was tested under monotonic loading according to ASTM E 564-08. The specimen was taken to a maximum load of about 19000 lb and a maximum displacement just under 6 in. Due to displacement limitations of the test facility the specimen was not pushed to a point where the displacement increased as the load decreased. In order to analyze the wall various power polynomial trend lines were fitted to the existing data. The trend lines were analyzed according to ASTM E 2126-08 and the range of values obtained is shown in Table 5.31.

Table 5.31: Specimen C-1M Results

	Strength Limit State		Yield Limit State	
	Minimum	Maximum	Minimum	Maximum
Displacement (in.)	7.00	9.50	7.30	7.68
Shear Force (lb)	20354	25366	22545	24372
Shear Modulus (lbf/in.)	2908	2670	3089	3172
Ductility	1.07	1.61		
Shear Strength (lbf/ft)	2544	3171		
Elastic Stiffness (lbf/in.)	3089	3172		

5.6.2 Specimen C-1C

Specimen C-1C was tested under cyclic loading using a target displacement of 6 in. for the CUREE protocol. Refer to Table 5.32 for the specimen parameters.

Table 5.32: Specimen C-1C Results

		Strength Limit State		Yield Limit State	
		Minimum	Maximum	Minimum	Maximum
Displacement (in.)	+	4.99	6.20	4.24	5.34
	-	4.23	5.38	4.14	4.32
	Average	4.61	5.79	4.19	4.83
Shear Force (lb)	+	20003	23003	17002	22256
	-	19957	22951	20626	21767
	Average	19980	22977	18814	22011
Shear Modulus (lbf/in.)	+	3710	4010	4011	4170
	-	4264	4722	4691	5041
	Average	3987	4366	4351	4606
Ductility	+	1.27	1.50		
	-	1.33	1.66		
	Average	1.30	1.58		
Shear Strength (lbf/ft)	+	2500	2875		
	-	2495	2869		
	Average	2497	2872		
Elastic Stiffness (lbf/in.)	+	4011	4170		
	-	4977	5041		
	Average	4494	4605		
Seismic Compatibility		Yes			

According to the results presented, Specimen C-1C meets the requirements stated in ICC-ES AC130 (2007). Accordingly, the specimen can be considered qualified within a seismic-force resisting system with the following values of seismic response parameters:

Response Modification Coefficient: $R = 6.5$

System Overstrength Factor: $\Omega_0 = 3$

Deflection Amplification Factor: $Cd = 4$

Of course, it should be noted that these seismic response parameters have been developed for wood-frame walls in the first place. Therefore it should not be surprising to see that

Specimen C-1C meets the ICC-ES AC130 requirements. However, Specimen C-1C did not meet the specifications in Section 5.2.4 of ICC-ES AC130, so in order to be considered compliant the evaluation report for the panel must include "a requirement that collectors and their connections, bearing and anchorage of the panel, and the lateral load path to the panel are designed in accordance with the special load combinations of Section 12.4.3 of ASCE 7, using E_m where E_m is calculated using the test panel overstrength" (ICC-ES AC130, 2007).

5.6.2.1 Specimen C-1C Fatigue 1

Specimen C-1C did not achieve an 80% drop in peak load under the first run of cyclic testing due to facility restricitons. This provided the opportunity to test the specimen under fatigue loading by running the same cyclic loading a second time. The estimated failure values were analyzed according to ASTM E 2126-08 and the range of values obtained is in Table 5.33.

In comparison to Specimen C-1C, the displacement of Fatigue 1 increased by about 19%. The shear modulus decreased by about 21% while the shear force, shear strength, and ductility were all within the range of Specimen C-1C. The greatest difference occurred in the elastic shear stiffness which dropped by about 48% for Fatigue 1.

Tables 5.33 and 5.34 show that the fatigue tests of Specimen C-1C were seismically compatible in terms of ICC-ES AC130. However, the fatigue test specimens

did not meet all of the conditions of Section 5.2.4 in ICC-ES AC130. Therefore, the previously stated requirements in Section 5.6.2 of this report must be addressed.

Table 5.33: Specimen C-1C Fatigue 1 Results

		Strength Limit State		Yield Limit State	
		Minimum	Maximum	Minimum	Maximum
Displacement (in.)	+	5.37	7.80	4.95	6.41
	-	5.07	6.58	4.57	5.31
	Average	5.22	7.19	4.76	5.86
Shear Force (lb)	+	19544	31188	16613	26510
	-	14291	17972	12147	15276
	Average	16918	24580	14380	20893
Shear Modulus (lbf/in.)	+	3637	3998	3359	4138
	-	2817	2731	2660	2879
	Average	3227	3365	3009	3509
Ductility	+	1.24	1.38		
	-	1.40	1.41		
	Average	1.32	1.40		
Shear Strength (lbf/ft)	+	2443	3898		
	-	1786	2247		
	Average	2115	3072		
Elastic Stiffness (lbf/in.)	+	2447	2872		
	-	1964	2169		
	Average	2205	2520		
Seismic Compatibility		Yes			

5.6.2.2 Specimen C-1C Fatigue 2

Specimen C-1C was placed under a third set of cyclic loading. Specimen C-1C Fatigue 2 was analyzed in the same manner as Specimens C-1C and C-1C Fatigue 1. Table 5.34 shows the range of values which were obtained from analyzing Fatigue 2 according to ASTM E 2126-08.

The change in displacement and ductility of Fatigue 2 were both less than 5% in comparison to Fatigue 1. The shear force, shear modulus, and shear strength decreased by about 12% while the elastic shear stiffness decreased by about 18%.

Table 5.34: Specimen C-1C Fatigue 2 Results

		Strength Limit State		Yield Limit State	
		Minimum	Maximum	Minimum	Maximum
Displacement (in.)	+	5.55	8.00	5.11	6.62
	-	5.34	5.76	4.93	5.28
	Average	5.45	6.88	5.02	5.95
Shear Force (lb)	+	17325	27600	14726	23460
	-	12946	14887	11004	12654
	Average	15135	21244	12865	18057
Shear Modulus (lbf/in.)	+	3119	3451	2881	3544
	-	2422	2586	2232	2396
	Average	2771	3018	2556	2970
Ductility	+	1.24	1.38		
	-	1.37	1.37		
	Average	1.30	1.38		
Shear Strength (lbf/ft)	+	2166	3450		
	-	1618	1861		
	Average	1892	2655		
Elastic Stiffness (lbf/in.)	+	2075	2463		
	-	1585	1662		
	Average	1830	2063		
Seismic Compatibility		Yes			

5.6.3 Specimen C-2C

Specimen C-2C was a replicate of Specimen C-1C and was tested and analyzed in the same manner in order to validate the results of Specimen C-1C. Refer to Table 5.35 for the specimen parameters.

Table 5.35: Specimen C-2C Results

		Strength Limit State		Yield Limit State	
		Minimum	Maximum	Minimum	Maximum
Displacement (in.)	+	4.11	5.97	4.09	4.16
	-	4.31	6.31	3.61	6.27
	Average	4.21	6.14	3.85	5.22
Shear Force (lb)	+	19993	22992	20827	21421
	-	19924	25333	16935	26017
	Average	19958	24163	18881	23719
Shear Modulus (lbf/in.)	+	3849	4870	5090	5149
	-	4015	4623	4149	4689
	Average	3932	4747	4649	4890
Ductility	+	1.15	1.81		
	-	1.25	1.37		
	Average	1.26	1.53		
Shear Strength (lbf/ft)	+	2499	2874		
	-	2490	3167		
	Average	2495	3020		
Elastic Stiffness (lbf/in.)	+	5090	5149		
	-	3798	4149		
	Average	4444	4649		
Seismic Compatibility		Yes			

All of the parameters for Specimen C-2C are within 10% of those for Specimen C-1C. This demonstrates accuracy in the testing procedure and analysis. Just like Specimen C-1C, Specimen C-2C meets the requirements stated in ICC-ES AC130 (2007). Accordingly, the specimen can be considered qualified within a seismic-force resisting system with the following values of seismic response parameters:

Response Modification Coefficient: R = 6.5

System Overstrength Factor: $\Omega_0 = 3$

Deflection Amplification Factor: Cd = 4

However, Specimen C-2C did not meet the specifications in Section 5.2.4 of ICC-ES AC130, so in order to be considered compliant, the evaluation report for the panel must include "a requirement that collectors and their connections, bearing and anchorage of the panel, and the lateral load path to the panel are designed in accordance with the special load combinations of Section 12.4.3 of ASCE 7, using E_m where E_m is calculated using the test panel overstrength" (ICC-ES AC130, 2007).

5.6.3.1 Specimen C-2C Fatigue 1

Specimen C-2C was placed under fatigue loading by running the same cyclic loading a second time. The estimated failure values from the trend lines and estimated failure points fit to the existing data were analyzed according to ASTM E 2126-08 and Table 5.36 shows the range of values obtained.

In comparison to Specimen C-2C, the displacement for Fatigue 1 increased by about 12%. The shear force, shear strength, shear modulus and ductility of Fatigue 1 and Specimen C-2C were all within range of each other. There was a decrease of about 39% in the elastic shear stiffness of Fatigue 1.

Tables 5.36 and 5.37 show that the fatigue tests of Specimen C-2C were seismically compatible in terms of ICC-ES AC130. However, the fatigue test specimens did not meet all of the conditions of Section 5.2.4 in ICC-ES AC130. Therefore, the previously stated requirements in Section 5.6.3 of this report must be addressed.

Table 5.36: Specimen C-2C Fatigue 1 Results

		Strength Limit State		Yield Limit State	
		Minimum	Maximum	Minimum	Maximum
Displacement (in.)	+	4.94	6.39	4.49	5.13
	-	4.90	6.33	4.47	5.36
	Average	4.92	6.36	4.48	5.24
Shear Force (lb)	+	19990	25006	16992	21255
	-	19811	27038	16839	22983
	Average	19901	26022	16916	22119
Shear Modulus (lbf/in.)	+	3916	4049	3786	4146
	-	4044	4274	3767	4285
	Average	4047	4095	3776	4216
Ductility	+	1.26	1.39		
	-	1.38	1.40		
	Average	1.32	1.40		
Shear Strength (lbf/ft)	+	2499	3126		
	-	2476	3380		
	Average	2488	3253		
Elastic Stiffness (lbf/in.)	+	2579	2931		
	-	2640	3052		
	Average	2610	2991		
Seismic Compatibility		Yes			

5.6.3.2 Specimen C-2C Fatigue 2

Specimen C-2C was placed under a third set of cyclic loading. Specimen C-2C Fatigue 2 was analyzed in the same way as Specimen C-2C and Fatigue 1. The ranges of values obtained from the analysis are shown in Table 5.37**.**

Specimen C-2C Fatigue 2 is very similar to Fatigue 1. The displacement, shear modulus, shear strength, shear force and ductility of Fatigue 2 are all within range or within 10% of Fatigue 1. The elastic shear stiffness of Fatigue 2 decreased by about 14%, in comparison to Fatigue 1.

Table 5.37: Specimen C-2C Fatigue 2

		Strength Limit State		Yield Limit State	
		Minimum	Maximum	Minimum	Maximum
Displacement (in.)	+	5.54	7.02	5.07	5.89
	-	5.02	5.40	4.64	4.96
	Average	5.28	6.21	4.86	5.42
Shear Force (lb)	+	20198	26343	17169	22392
	-	18062	20771	15352	17655
	Average	19130	23557	16260	20024
Shear Modulus (lbf/in.)	+	3643	3754	3385	3804
	-	3598	3846	3310	3558
	Average	3621	3800	3347	3681
Ductility	+	1.25	1.38		
	-	1.36	1.37		
	Average	1.31	1.38		
Shear Strength (lbf/ft)	+	2525	3293		
	-	2258	2596		
	Average	2391	2945		
Elastic Stiffness (lbf/in.)	+	2336	2676		
	-	2255	2405		
	Average	2295	2540		
Seismic Compatibility		Yes			

5.6.4 Specimen C-3C

Specimen C-3C was a replicate of Specimens C-1C and C-2C and was tested and analyzed in the same manner in order to validate the results of Specimen C-1C. Refer to Table 5.38 for the specimen parameters.

Table 5.38: Specimen C-3C Results

		Strength Limit State		Yield Limit State	
		Minimum	Maximum	Minimum	Maximum
Displacement (in.)	+	4.72	6.07	3.61	5.72
	-	4.03	5.43	3.14	4.54
	Average	4.38	5.75	3.37	5.13
Shear Force (lb)	+	20000	23000	17000	22594
	-	19990	23222	16992	22459
	Average	19995	23111	16995	22527
Shear Modulus (lbf/in.)	+	4239	3787	4711	3947
	-	4958	4274	5417	4951
	Average	4598	4031	5064	4449
Ductility	+	1.49	1.34		
	-	1.48	1.54		
	Average	1.48	1.44		
Shear Strength (lbf/ft)	+	2500	2875		
	-	2499	2903		
	Average	2499	2889		
Elastic Stiffness (lbf/in.)	+	3768	3947		
	-	4657	4951		
	Average	4212	4449		
Seismic Compatibility		Yes			

The results found for Specimen C-3C are very similar to the results found for Specimens C-1C and C-2C. All of the parameters for Specimen C-3C are within 12% of those for Specimen C-2C. All of the Specimen C-3C parameters except for the yield limit state displacement are within 10% of Specimen C-1C. The yield limit state displacements are within 20% of each other. All values for Specimens C-1C, C-2C, and C-3C are within 15% of the average of the three specimens, which allows the average value to be used in describing Specimens C. (ICC-ES AC130, 2007)

Just like Specimens C-1C and C-2C, Specimen C-3C meets the requirements stated in ICC-ES AC130 (2007). Accordingly, the specimen can be considered qualified within a seismic-force resisting system with the following values of seismic response parameters:

Response Modification Coefficient: R = 6.5

System Overstrength Factor: $\Omega_0 = 3$

Deflection Amplification Factor: Cd = 4

However, Specimen C-3C did not meet the specifications in Section 5.2.4 of ICC-ES AC130, so in order to be considered compliant, the evaluation report for the panel must include "a requirement that collectors and their connections, bearing and anchorage of the panel, and the lateral load path to the panel are designed in accordance with the special load combinations of Section 12.4.3 of ASCE 7, using E_m where E_m is calculated using the test panel overstrength" (ICC-ES AC130, 2007).

5.6.4.1 Specimen C-3C Fatigue 1

Specimen C-3C did not reach an 80% drop in peak load under the first run of cyclic testing due to facility restricitons. This provided the opportunity to test the specimen under fatigue loading by running the same cyclic loading a second time. Table 5.39 shows the range of characteristic values of Specimen C-3C Fatigue 1.

The displacement of Specimen C-3C Fatigue 1 increased by about 9% in comparison to Specimen C-3C. The shear force, shear modulus, and shear strength in the strength limit state of Fatigue 1 are all within the range of values found for Specimen C-

3C. In the yield limit state, the shear force decreased by about 3% and the shear modulus decreased by about 16%. The greatest change occurred in the elastic shear stiffness of Fatigue 1 because it decreased by about 34% percent in comparison to Specimen C-3C.

Tables 5.39 and 5.40 show that the fatigue tests of Specimen C-3C were seismically compatible in terms of ICC-ES AC130. However, the fatigue test specimens did not meet all of the conditions of Section 5.2.4 in ICC-ES AC130. Therefore, the previously stated requirements in Section 5.6.4 of this report must be addressed.

Table 5.39: Specimen C-3C Fatigue 1 Results

		Strength Limit State		Yield Limit State	
		Minimum	Maximum	Minimum	Maximum
Displacement (in.)	+	4.97	5.49	4.45	4.89
	-	4.76	6.67	4.35	5.37
	Average	4.87	6.08	4.40	5.13
Shear Force (lb)	+	19990	22989	16992	19540
	-	19593	27898	16654	23714
	Average	19792	25444	16823	21627
Shear Modulus (lbf/in.)	+	4020	4186	3816	3992
	-	4114	4181	3827	4418
	Average	4067	4183	3822	4205
Ductility	+	1.41	1.41		
	-	1.25	1.40		
	Average	1.33	1.41		
Shear Strength (lbf/ft)	+	2499	2874		
	-	2449	3487		
	Average	2474	3180		
Elastic Stiffness (lbf/in.)	+	2663	2881		
	-	2700	3137		
	Average	2681	3009		
Seismic Compatibility		Yes			

5.6.4.2 Specimen C-3C Fatigue 2

Specimen C-3C Fatigue 2 is Specimen C-3C placed under a third set of cyclic loading. The specimen was analyzed in the same way as Specimen C-3C and C-3C Fatigue 1. The ranges of values obtained by following ASTM E 2126-08 are shown in Table 5.40**.**

Specimen C-3C Fatigue 2 is very similar to Fatigue 1. The displacement, shear force, shear modulus, shear strength, and ductility of Fatigue 2 are all within 10% of Fatigue 1. The elastic shear stiffness of Fatigue 2 decreased by about 12%.

Table 5.40: Specimen C-3C Fatigue 2 Results

		Strength Limit State		Yield Limit State	
		Minimum	Maximum	Minimum	Maximum
Displacement (in.)	+	5.35	6.82	4.88	5.65
	-	4.84	5.20	4.48	4.78
	Average	5.09	6.01	4.68	5.22
Shear Force (lb)	+	19982	25779	16985	21912
	-	17975	20671	15278	17570
	Average	18979	23225	16132	19741
Shear Modulus (lbf/in.)	+	3736	3779	3482	3876
	-	3717	3979	3414	3675
	Average	3726	3879	3448	3775
Ductility	+	1.38	1.39		
	-	1.24	1.24		
	Average	1.31	1.32		
Shear Strength (lbf/ft)	+	2498	3222		
	-	2247	2584		
	Average	2372	2903		
Elastic Stiffness (lbf/in.)	+	2459	2783		
	-	2331	2471		
	Average	2395	2627		
Seismic Compatibility		Yes			

5.7 Summary

This chapter has shown the application of the methodology described in ICC-ES AC130 and ASTM E2126 to determine seismic response parameters and the possible equivalency of the SIP system to conventional wood-frame system. The results presented are based on preliminary testing and follow-up testing is necessary to develop such parameters for design purposes. The preceding sections demonstrate the potential effect of hardware and spline design on the engineering values of a specimen. Specimens A3 and A4 were able to withstand the least amount of displacement and shear force before they failed. According to ICC-ES AC130, Specimens A3 and A4 failed to meet the requirements necessary to make them seismically compatible. The peak displacement of Specimen A1 was slightly less than Specimen B which can be attributed to the difference in spline designs. The double 2x4 spline in Specimen B slightly reduced the shear modulus, shear strength, and elastic shear stiffness in comparison to the OSB spline in Specimen A1. Specimen C had the highest shear force, shear modulus, shear strength, and elastic shear stiffness. These values are based on a timber wall with sheathing on both sides which is not consistent with actual construction methods. Table 5.41 is a compilation of the previous tables presented in this chapter. Table 5.41 compares the average characteristic values obtained by analyzing data from the cyclic tests performed on each specimen. Specimens A3-2C(2), A1Bearing-3C, and A1Internal-4C were not included in their appropriate specimen averages because they were not an identical replica of the original walls tested.

Similar to Specimens A1, B and C the fatigue tests of these specimens were deemed seismically compatible but did not meet the full criteria of Section in 5.2.4 in ICC-ES AC130. Under fatigue loading the Specimens C had the least amount of loss in shear force, shear modulus, shear strength, elastic shear stiffness, and ductility. The following chapter will further review the fatigue data.

Table 5.41: Average Characteristic Values of Each Specimen

	Specimens A3	Specimens A4	Specimens A1		Specimens B		Specimens C	
			Min	Max	Min	Max	Min	Max
Δ_{max} (in.)	3.13	3.48	5.05	5.30	5.18	5.51	4.40	5.89
Δ_{yield} (in.)	2.73	3.02	4.28	4.37	4.49	5.24	3.80	5.06
F_{max} (lb)	11413	16689	17998	18174	18277	18587	19978	23417
F_{yield} (lb)	10844	14381	16958	17340	16509	19024	18230	22752
G' (lbf/in.)	3791	4893	3436	3569	3407	3544	3983	4570
G'_{yield}	4041	4834	3989	3994	3731	3742	4483	4853
Ductility	1.36	1.34	1.36	1.73	1.26	1.41	1.33	1.53
V_{peak} (lbf/ft)	1427	2086	2250	2272	2285	2323	2497	2927
K_e (lbf/in.)	4041	4369	3989	3994	3731	3742	4383	4568
Seismic Compatibility	No	No	Yes		Yes		Yes	

Chapter 6

Parametric Analysis of Specimens

6.1 Introduction

The preceding chapters demonstrate the failure modes, load-displacement graphs and characteristic values of four SIP specimen designs and one wood-frame wall design tested. This chapter presents a direct comparison between each specimen in terms of characteristic values, allowable drift, energy dissipation, loss of strength during fatigue testing, and the structural insulated panel's compatibility with a traditional wood-frame wall.

6.2 Characteristic Values Based on ASTM E 2126-08

Parameters such as elastic stiffness, strength, and ductility are some of the factors which govern the response a shear wall has under seismic loading. These deformational characteristics are based on the wall's load-displacement relationship under cyclic loading. Figure 6.1 shows an example of the envelope curve and the values used to determine the performance parameters of each specimen. The following section compares the characteristic values of each specimen in order to determine the effects hardware and design have on the seismic response of a structure.

This section contains charts comparing the average values of the parameters obtained by analyzing the data from the cyclic tests performed on each specimen. For

instance the average value of Specimens A4 is based on the results of testing Specimens A4-1C, A4-2C, and A4-3C. Specimens A3-2C(2), A1Bearing-3C, and A1Internal-4C were not included in their appropriate specimen averages because they were not an identical replica of the original walls tested. Refer to Appendix B for charts containing parameter values for every single specimen tested, not simply the average of the specimens tested under cyclic loading.

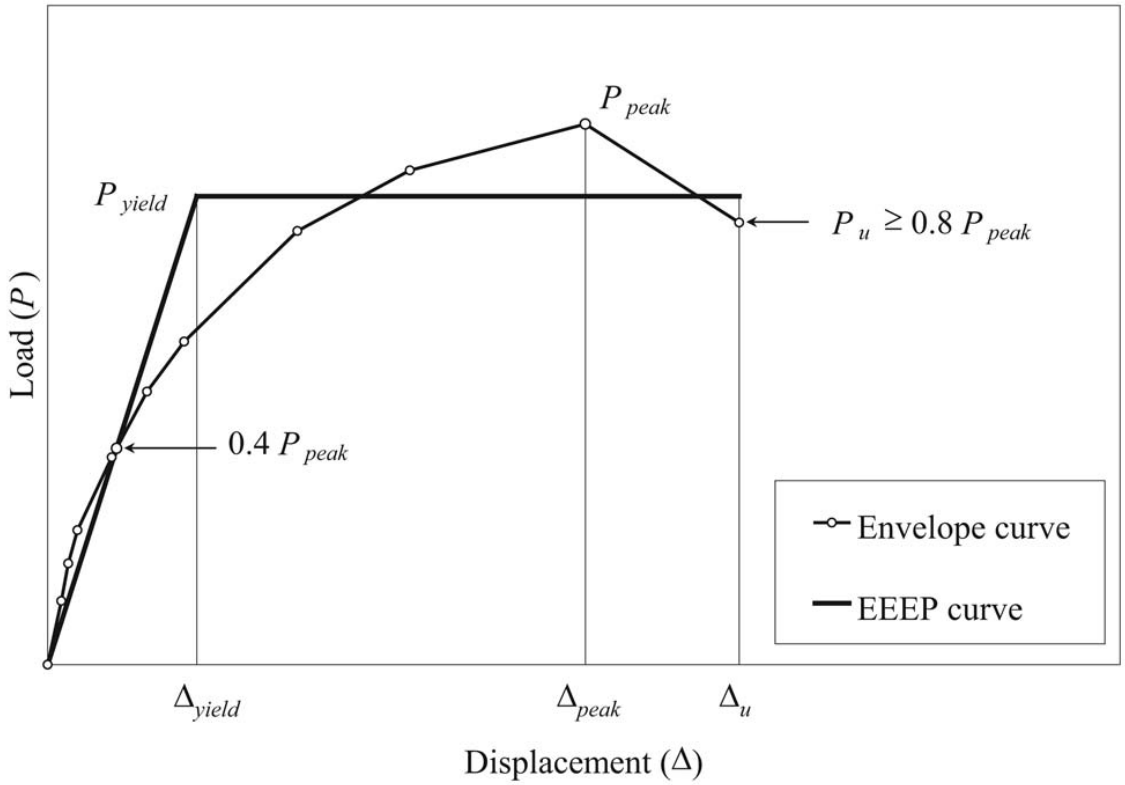

Figure 6.1: Performance parameters of specimen (ASTM E 2126-08, 2008)

6.2.1 Peak Load and Displacement

Specimen C was able to withstand the greatest force and displacement before the capacity of the wall began to decline. A larger peak load results in a larger load at the yield limit strength. As a result, Specimen C performed elastically under a higher load and displacement compared to other SIP specimens tested. Figures 6.2 and 6.3 show the average peak load and displacement values for the specimens at the strength limit state. The graphs show that Specimens A1 and B performed similarly. This shows that the adjustment in spline design did not have a large effect on the load-displacement relationship of the specimen.

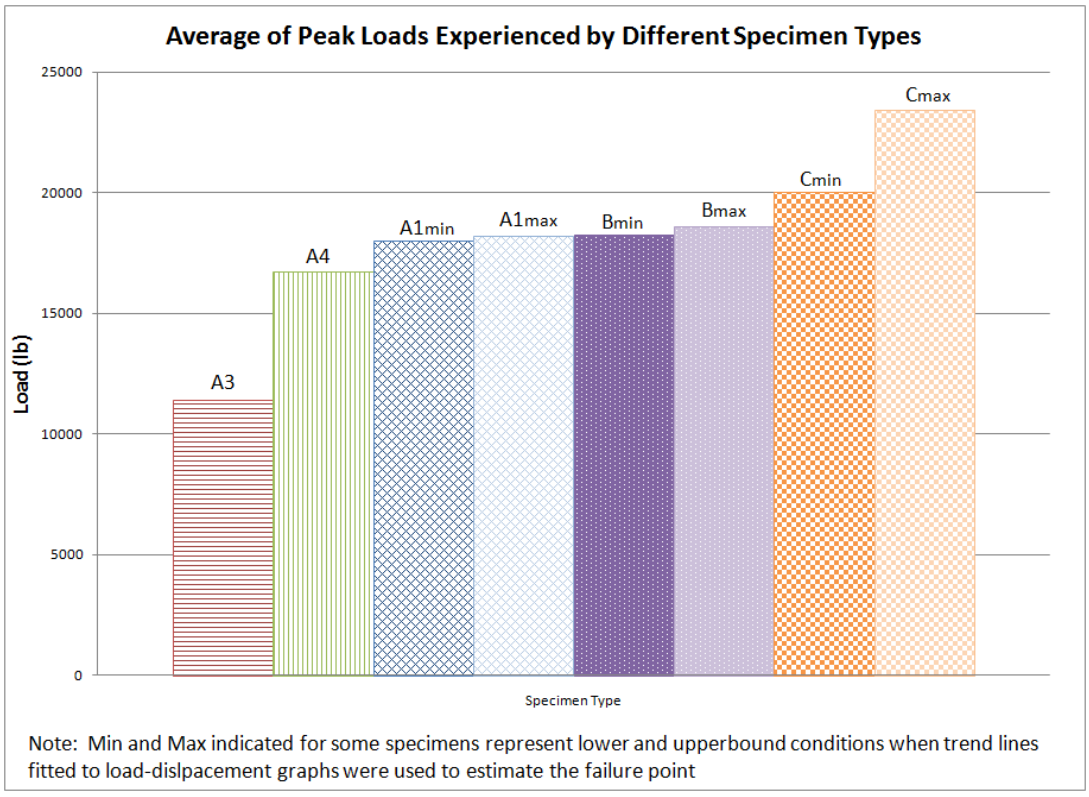

Figure 6.2: Average of peak loads experienced by different specimen types

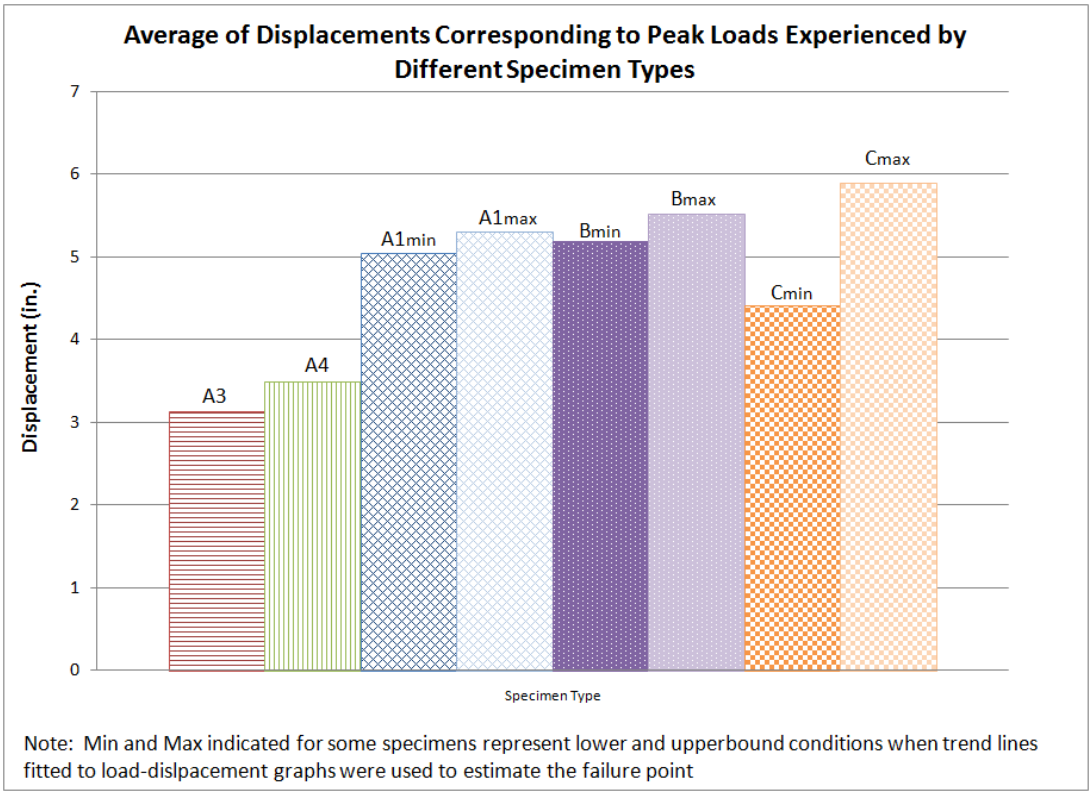

Figure 6.3: Average of displacements corresponding to peak loads experienced by different specimen types

6.2.2 Shear Modulus

According to the definition given by ASTM E 2126 (ASTM, 2008), the shear modulus of a specimen is the secant shear stiffness at the peak load of a specimen multiplied by the aspect ratio. In equation form, G'=(P/Δ)*(H/L). Figure 6.4 shows a chart comparing the average shear modulus of each specimen. Specimen A4 had the greatest shear modulus, it was about 13% greater than Specimen C and 23% greater than Specimen A3. Specimens A1 and B had the lowest shear modulus values.

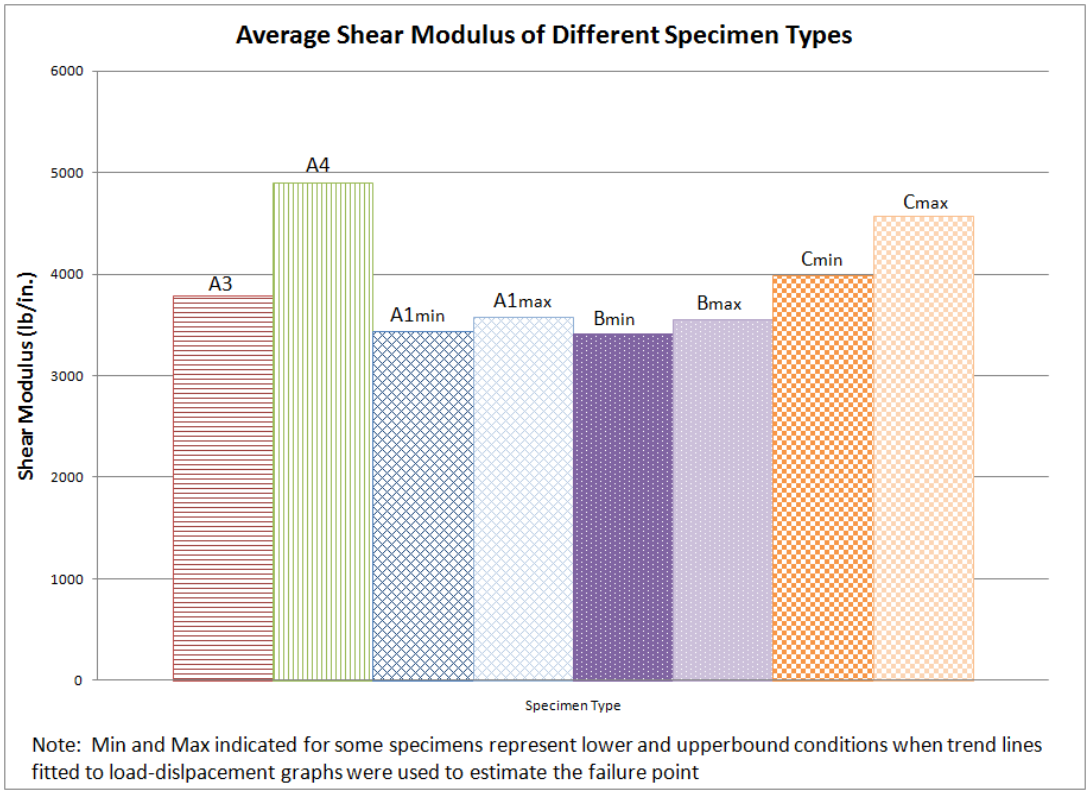

Figure 6.4: Average shear modulus of different specimen types

6.2.3 Ductility

Ductility is determined by dividing the ultimate displacement which is found at the failure limit state, by the displacement found at the yield limit state, which is defined as the point in the load-displacement relationship where there is a 5% or more drop in elastic shear stiffness (ASTM, 2008). Refer to Figure 6.1. The value serves as a measure of the performance of a specimen between its yield and failure points. A specimen with a large ductility has the ability to yield and deform inelastically without experiencing a significant loss of load resistance. However, the ductility property should be examined in

conjunction with other characteristic values because a high ductility factor does not directly mean that the specimen will perform well under seismic loading. Figure 6.5 shows a chart comparing the average ductility values of specimens tested under cyclic loading.

Specimen A1 had the highest ductility. This ductile behavior was evident during the testing and subsequent failure of Specimen A1. The failure occurred when nails along the spline, top plate and base plate pulled out. Rarely did the nails shear which would have resulted in a brittle failure. As can be seen in the chart, Specimen C had the next highest ductility followed by Specimen B that had slightly higher ductility values compared to Specimens A3 and A4. This is due to the ductile nature of the nailed fasteners which were used. Specimen A3 with staples and Specimen A4 with screws had similar ductility values. The failure of Specimen A4 was sudden and brittle, which is reflected in the ductility factor.

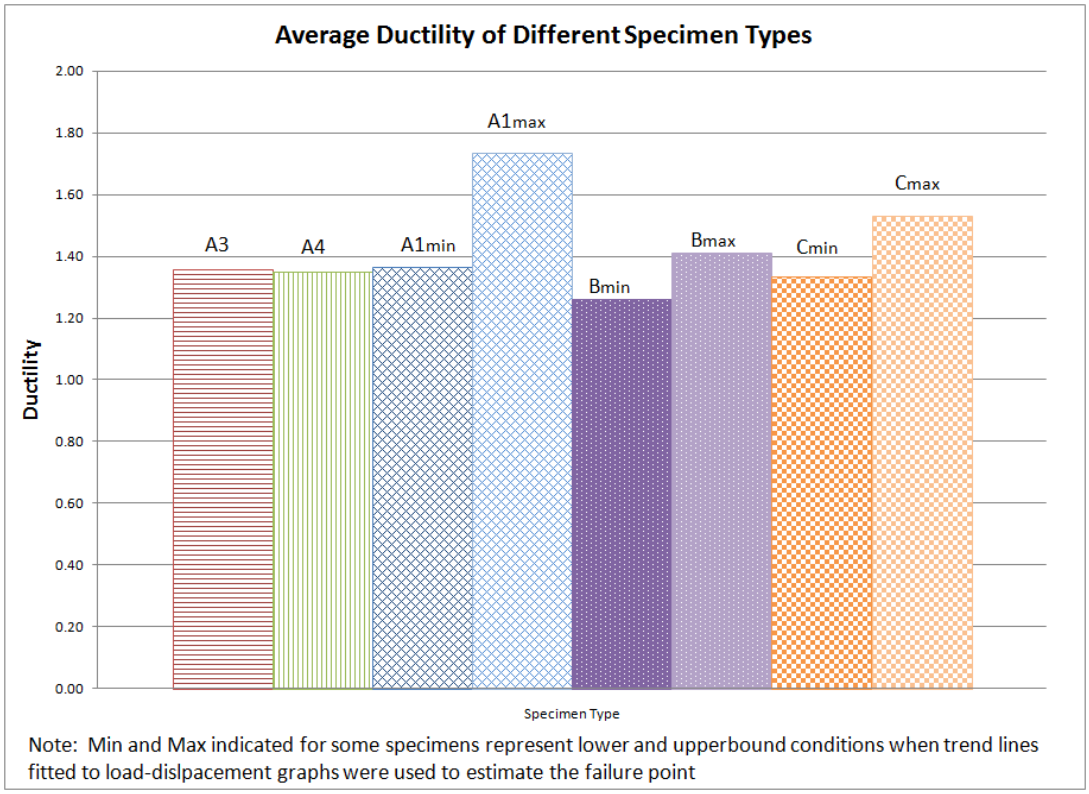

Figure 6.5: Average ductility of different specimen types

6.2.4 Shear Strength

The shear strength of a specimen is found by dividing the average of the absolute values of the peak loads by the length of the wall. The shear strength value is the load capacity of the wall per unit length. Figure 6.6 shows a chart comparing the average shear strength of each specimen. Specimen C had the highest shear strength while Specimen A3 had the lowest shear strength. Specimen A4 was slightly lower than Specimens A1 and B, which had very similar shear strength values.

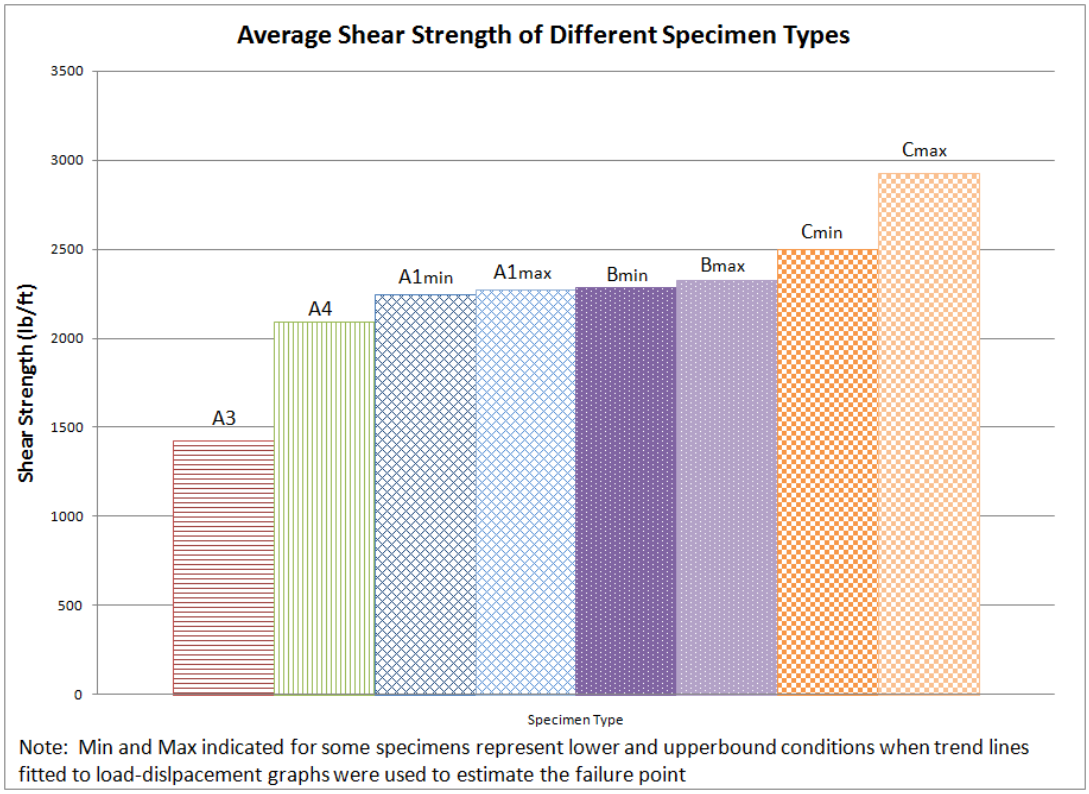

Figure 6.6: Average shear strength of different specimen types

6.2.5 Elastic Stiffness

Elastic stiffness is defined as follows in ASTM E 2126 (ASTM, 2008): $K_e=0.4P_{peak}/\Delta_e$. Δ_e is the displacement of the top edge of the wall at the corresponding $0.4P_{peak}$, as shown in Figure 6.1. K_e is found for the negative and positive sides of the envelope curve and the average of the absolute values of both sides are the final elastic stiffness value. A chart comparing the average of each specimen's elastic stiffness can be found in Figure 6.7.

Specimens C and A4 had very similar elastic stiffness values which was unexpected. Screws were used to connect framing members to the SIPs for Specimen A4 which led to brittle and severe failures between 15,000 lb and 16,000 lb. Wood-frame walls used for Specimen C had very gradual and ductile failures between loads of 20,000 lb and 23,400 lb. The similar elastic stiffness values found for Specimens A4 and C signify that both specimens will have reduced lateral drift during seismic loading which would reduce nonstructural damage (Johnston et al., 2006).

Specimens A3 and A1 had very similar elastic stiffness values which demonstrates that the staples and nails perform similarly in terms of elastic stiffness. Specimen B had the lowest elastic stiffness value.

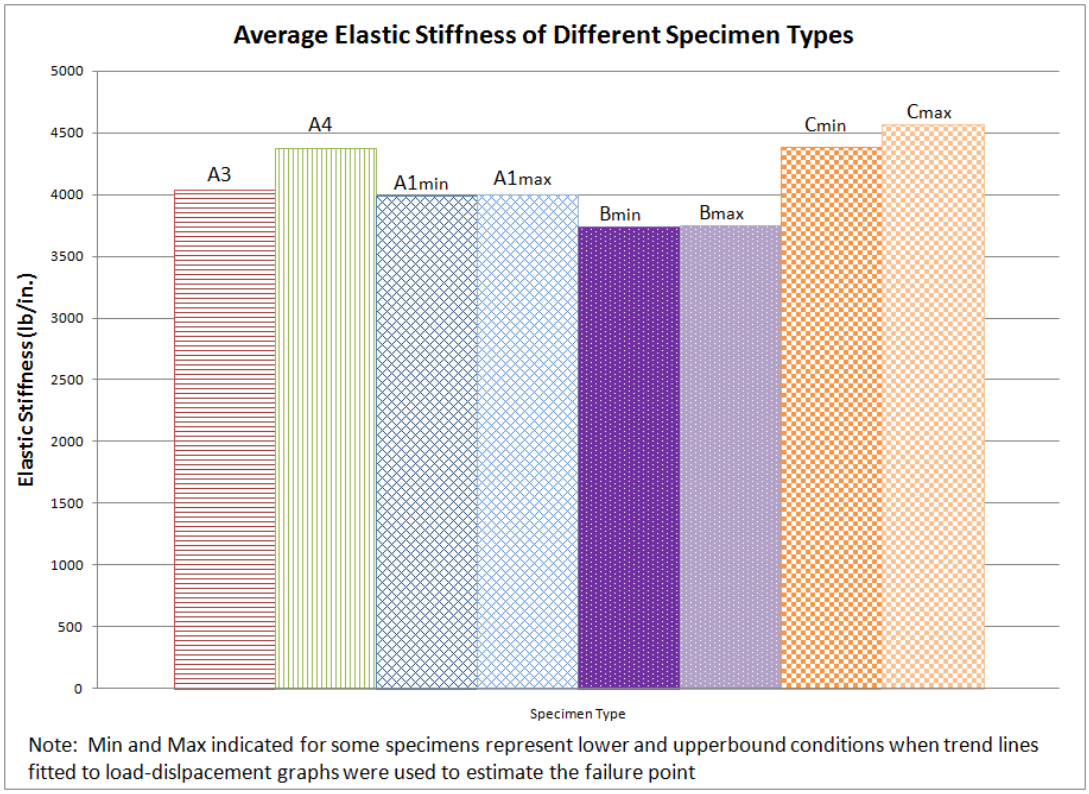

Figure 6.7: Average elastic stiffness of different specimen types

6.3 Allowable Drift Capacity

The allowable drift for service wind loading is found by using H/400. In this case, H/400 = 8 ft/400 = 0.02 ft*12 in./ft = 0.24 in. The allowable seismic drift is 2.5% of the height of the specimen, or 0.025*H = 0.025*8 ft = 0.20 ft*12 in./ft = 2.4 in. (ICC-ES AC04, 2005). Table 6.1 shows the load capacity of each specimen at the allowable drift for service wind loading and the allowable seismic drift. It also lists the peak load capacity and its corresponding drift.

The SIP specimens tested under monotonic loading had higher load capacities at both the allowable wind and seismic drifts than the specimens tested under cyclic loading. For Specimens A3, A4, A1 and B the load capacity at the allowable drift for service wind loading ranged from 35% to 50% greater under monotonic loading than cyclic loading. For example, in Table 6.1 the load capacity of Specimen A3-1M (monotonic test) is 2632 lb at a deflection of 0.24 in. while the load capacity of Specimen A3-1C (cyclic test) is only 1464 lb at the same deflection. At the allowable seismic drift the load capacity under monotonic loading ranged from 9% to 34% greater than the SIP specimens under cyclic loading. Once again, the load capacity of Specimen A3-1M at 2.4 in. is 10314 lb while the load capacity of Specimen A3-1C is 9357 lb. Specimen C, the wood-frame shear wall, had larger load capacities at the allowable drifts under cyclic loading than monotonic loading.

In terms of cyclic loading, the largest amount of load was needed to force Specimen A1Internal-4C to a drift of 0.24 in. than any other specimen. Specimen A1Bearing-3C was high as well, within 10% of Specimen A1Internal-4C. Specimens A3, A4, and C had load capacities ranging from about 1675 lb to 1575 lb, which were 27% to 31% less than Specimen A1Internal-4C. The largest amount of force was needed to push Specimen A1Bearing-3C to the allowable seismic drift of 2.4 in. out of all the specimens. Specimen C and A4 needed about 20% less force than A1Bearing-3C.

Table 6.1: Allowable Drift Capacity

Specimen	Capacity (lb) at 0.24 in. Drift	Capacity (lb) at 2.40 in. Drift	Peak (Load (lb), Drift (in.))
A3-1M	2632	10314	(12522, 3.64)
A3-1C	1464	9357	(11577, 3.15)
A3-2C	1886	9421	(11249, 3.11)
A3-2C(2)	1306	7060	(7921, 2.70)
A4-1M	2723	16680	(18613, 3.10)
A4-1C	1705	10715	(16956, 3.65)
A4-2C	1266	11190	(16474, 3.28)
A4-3C	1951	11363	(16638, 3.51)
A1-1M	2667	12932	(17565 to 17631, 4.50 to 5.00)
A1-1C	1998	10058	(17730 to 18083, 4.92 to 5.42)
A1-2C	648	9856	(18265, 5.17)
A1Bearing-3C	2060	13856	(19705, 4.20)
A1Internal-4C	2295	10196	(16604, 5.11)
B-1M	1756	10300	(17191, 5.15)
B-1C	1203	8579	(17410 to 17947, 5.15 to 5.65)
B-2C	1588	10200	(19702 to 19998, 4.99 to 5.24)
B-3C	641	9174	(17718 to 17816, 5.39 to 5.64)
C-1M	854	7310	(20354 to 25366, 7.00 to 9.50)
C-1C	2021	11431	(19980 to 22977, 4.61 to 5.79)
C-2C	1291	11332	(19958 to 2416, 4.21 to 6.14)
C-3C	1415	11073	(19995 to 23111, 4.38 to 5.75)

6.4 Energy Dissipation

The energy dissipation of a specimen is determined by finding the area enclosed by the hysteresis loops obtained from the load vs. displacement graph of a specimen under cyclic loading. In this report, the trapezoid rule was used to determine the area within the hysteresis loops. To perform well during an earthquake a structure must be able to dissipate large amounts of energy. When a shear wall is within its elastic limit it

will not dissipate any hysteretic energy. This is evident in Figures 6.8 through 6.12. The energy dissipated in the early cycles is minimal compared to the large spikes found in the later primary cycles. When a shear wall is pushed past its elastic limit, the energy is dissipated through inelastic behavior or fracture of fasteners and other materials making up the sheathing-to-framing connections. A minimal amount of energy is also dissipated through the friction forces created by panel sheathing rubbing up against an adjacent panel or framing members (Bredel, 2003). Figures 6.8**,** 6.9**,** 6.10**,** 6.11 and 6.12 show the average energy dissipated per cycle and the average total (cumulative) energy dissipated up to the current cycle of the specimens tested under cyclic loading. Similar to the average values presented in the bar charts in Section 6.2, Specimens A3-2C(2), A1Bearing-3C, and A1Internal-4C were not included in their appropriate specimen averages because they were not an identical replica of the original walls tested.

Specimens A1 and C had the ability to dissipate the largest amount of energy within 37 cycles while Specimens A4 dissipated the least amount of energy within the same number of cycles. This is consistent with the strength and displacement capacities of the specimens. Specimen A4 was able to withstand three more cycles of the CUREE loading protocol than Specimen A3 and at the forty-first cycle Specimen A4 dissipated 24% more cumulative energy than Specimen A3.

Table 6.2 shows the cumulative energy dissipated at the allowable wind drift, Δ=0.24 in., and the allowable seismic drift, Δ=2.4 in. The ratio between the cumulative energy dissipated by the SIP specimen and the average cumulative energy dissipated of Specimens C-1C, C-2C, and C-3C are also in Table 6.2. The ratio between the cumulative energy dissipated at the allowable drift in relation to the total cumulative

energy dissipated by the specimen at the completion of the cyclic loading is also shown in the table. These values demonstrate the comparison between the wood-frame wall and the structural insulated panel specimens at the allowable drifts. For instance, Specimens A4-3C, A1-1C, and A1Internal dissipate greater amounts of energy at the allowable wind drift than Specimens C. The ratio of energy dissipated at allowable wind drift and allowable seismic drift to the total cumulative energy dissipated show that the shear walls only dissipate a fraction of the total cumulative energy dissipated at the allowable drift limits.

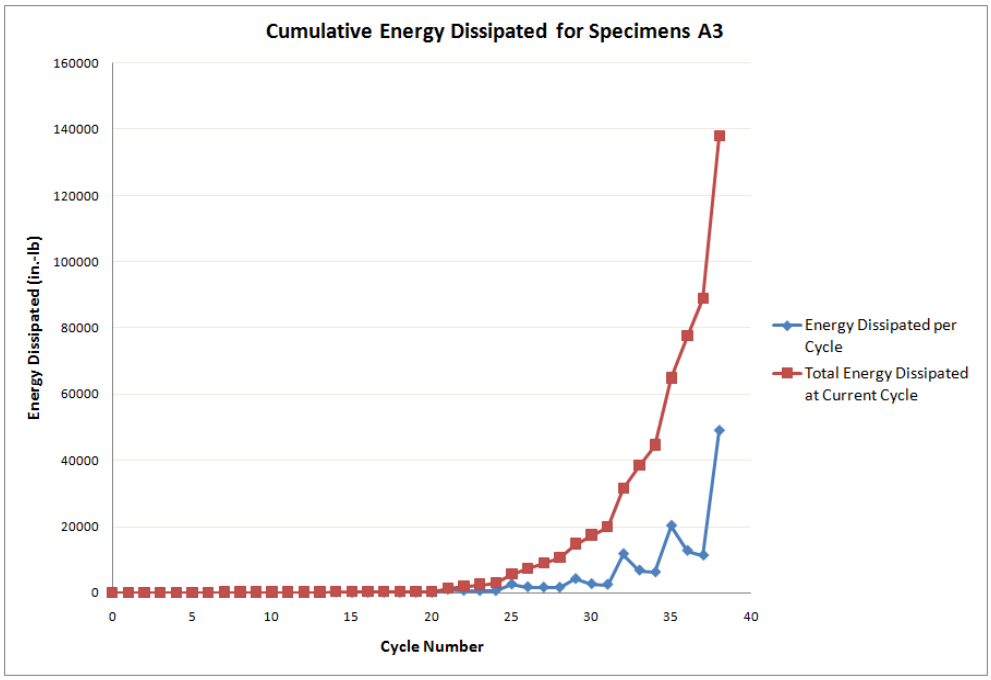

Figure 6.8: Cumulative energy dissipated for Specimens A3

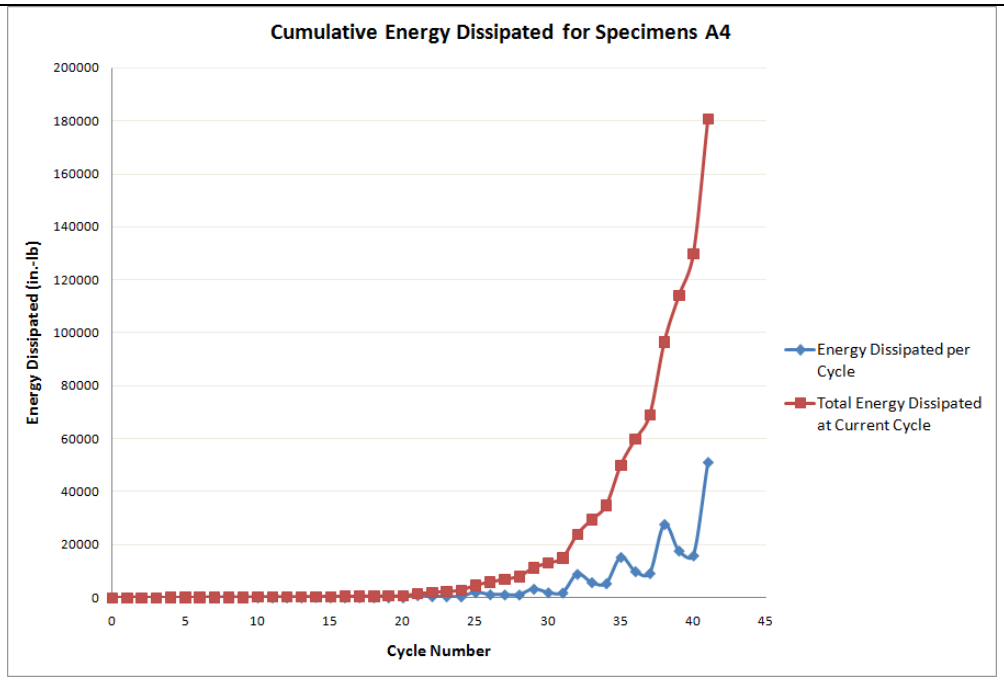

Figure 6.9: Cumulative energy dissipated for Specimens A4

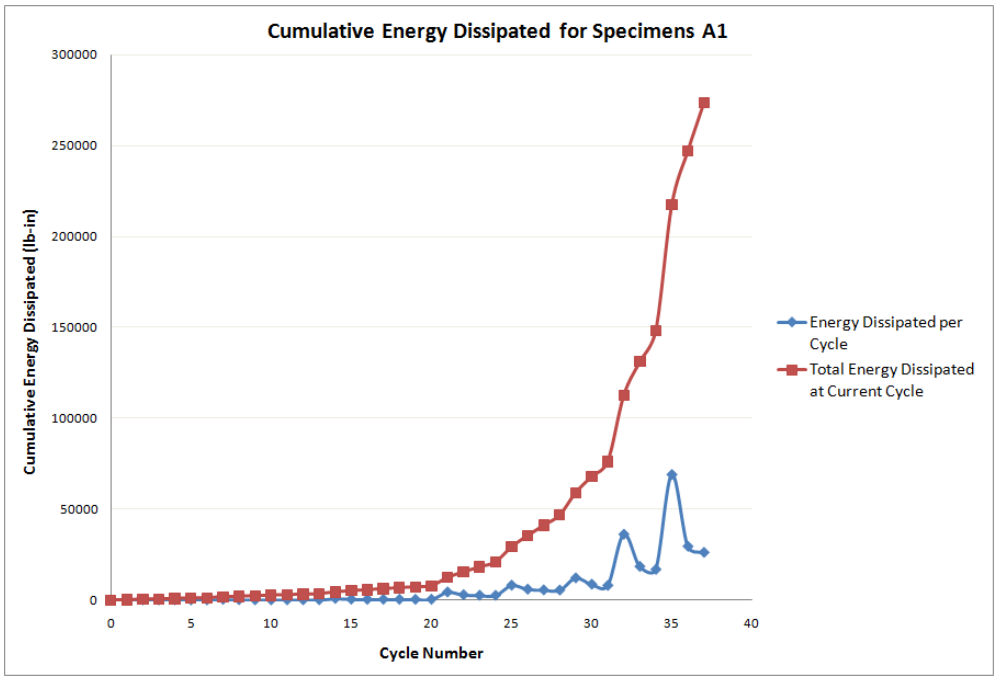

Figure 6.10: Cumulative energy dissipated for Specimens A1

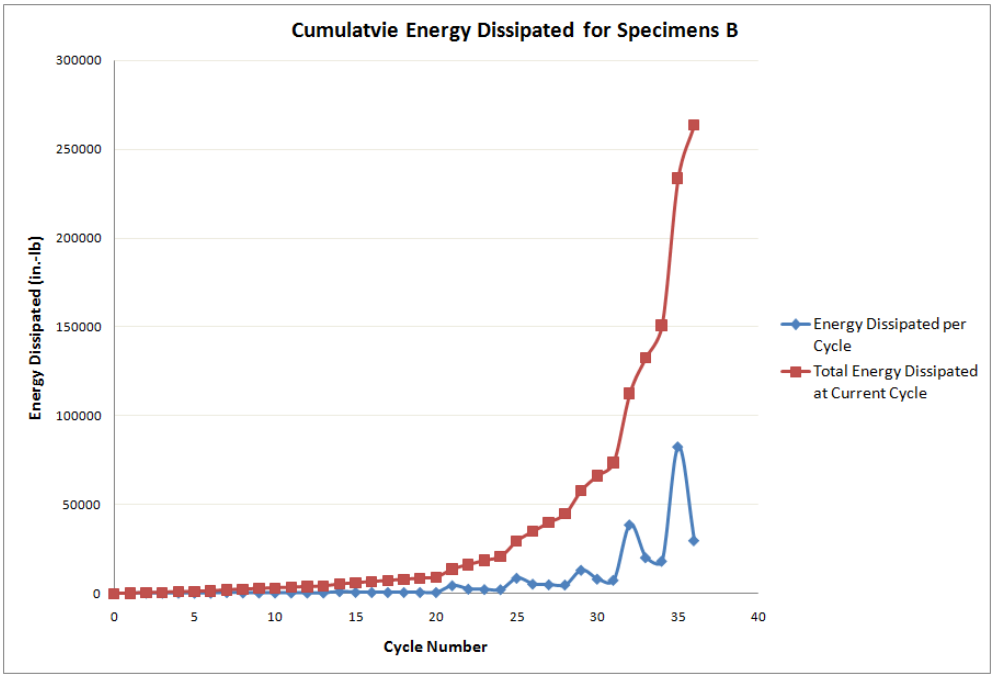

Figure 6.11: Cumulative energy dissipated for Specimens B

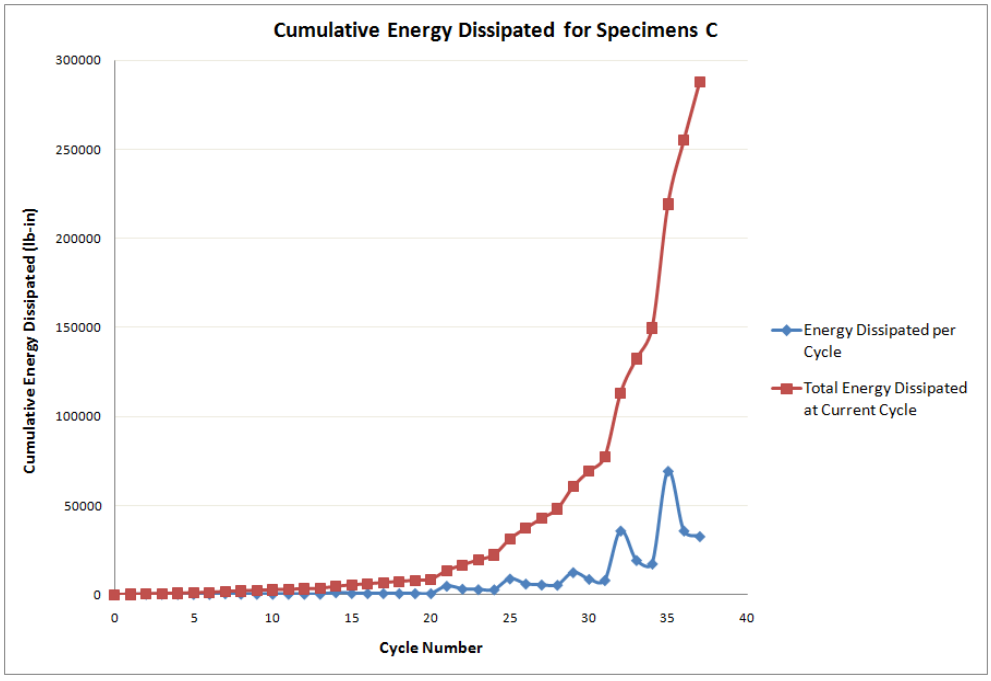

Figure 6.12: Cumulative energy dissipated for Specimens C

Table 6.2: Cumulative Energy Dissipated at Allowable Wind and Seismic Drift

	Δ=0.24			Δ=2.4		
Specimen	**Cum. Energy @ Drift**	**SIP/Wood-frame**	**Drift/Ult.**	**Cu□. Energy @ Drift**	**SIP/Wood-frame**	**Drift/Ult.**
A3-1C	1091	0.33	0.00	63008	0.59	0.28
A3-2C	874	0.26	0.01	65897	0.62	0.46
A3-2C(2)	1175	0.35	0.01	64588	0.60	0.53
A4-1C	979	0.29	0.00	76760	0.72	0.35
A4-2C	1077	0.32	0.01	91412	0.86	0.49
A4-3C	3844	1.15	0.02	97999	0.92	0.48
A1-1C	3705	1.11	0.01	103826	0.97	0.39
A1-2C	315	0.09	0.00	97487	0.91	0.35
A1Bearing	2352	0.71	0.01	79068	0.74	0.36
A1Internal	6944	2.08	0.03	99344	0.93	0.37
B-1C	2165	0.65	0.01	90495	0.85	0.34
B-2C	1580	0.47	0.01	102510	0.96	0.35
B-3C	202	0.06	0.00	93618	0.88	0.33
C-1C	2571	-	0.01	114145	-	0.37
C-2C	2266	-	0.01	103057	-	0.38
C-3C	5165	-	0.02	103466	-	0.42

Note: The SIP/Wood-frame column is the ratio of the cumulative energy at the drift of the SIP specimen to that of the average cumulative energy of Specimens C-1C, C-2C and C-3C at the same drift. The Drift/Ult. column is the ratio of the cumulative energy of the specimen at the allowable drift specified to the total cumulative energy dissipated at the completion of the cyclic testing.

6.5 Structural Insulated Panels' Compatibility with a Wood-frame Shear Wall

The 2005 edition of ICC-ES AC04 contains an Appendix A, which provides a list of criteria a structural insulated panel must meet in order to be used in Seismic Design Categories D, E, and F of the 2003 International Building Code (IBC). If the SIP specimens meet all of the criteria they are deemed equivalent to a light-framed wood-based shear wall under cyclic loading. The appendix does not determine any seismic

characteristics such as the response modification coefficient or the deflection amplification factor though.

In this research, Specimen C is considered the benchmark, or the traditional wood-frame wall to which the SIP specimens are compared. In order for a SIP specimen to be deemed equivalent to Specimen C, the backbone curve and cumulative energy dissipated must meet the requirements stated in Section A.3.0 of Appendix A. First, the peak load strength of the SIP specimen cannot be less than 90% of that of the benchmark. Next, the stiffness of the SIP specimen cannot be less than 85% of the benchmark. Stiffness is the slope of the backbone curve between the point of origin and the point where the load is one-third the peak strength load. The load capacity of the SIP specimen at the allowable story drift under seismic loading (Δ_{all}=2.4 in.) cannot be less than 85% of that for the wood-frame wall. Table 6.3 shows that Specimens A1 and A1Bearing-3C are the only designs that met all of the backbone curve requirements. In accordance with Section A.3.2 of Appendix A, the cumulative energy dissipated of Specimens A1 and A1Bearing-3C were then compared to Specimens C. Figure 6.13 shows the cumulative energy dissipated by Specimens C, A1, and A1Bearing-3C within 37 cycles. The figure shows that the cumulative energy dissipated by Specimen A1Bearing-3C is less than 85% of the cumulative energy dissipated by Specimens C. Specimens A1, on the other hand, were within 85% of Specimens C. Therefore, according to Appendix A of ICC-ES AC04 (2005), Specimens A1 should be permitted to be used as shear walls in buildings located in Seismic Design Categories A through F.

Table 6.3: Backbone Curve Comparison Between SIP Specimens and Specimens C

Performance Requirement	Section	Specimens						
		A3	A3-2C(2)	A4	A1	A1Bearing -3C	A1Internal -4C	B
Peak strength load within 90%	A.3.1.1	X	X	X	√	√	X	√
Stiffness within 85%	A.3.1.2	√	X	√	√	√	√	√
Load at Δall=2.4 in. within 85%	A.3.1.3	X	X	√	√	√	√	X

Note: The cells with the dark colored filling and the √ mean the specimen met the criteria while the light colored filling and X mean the specimen did not meet the criteria

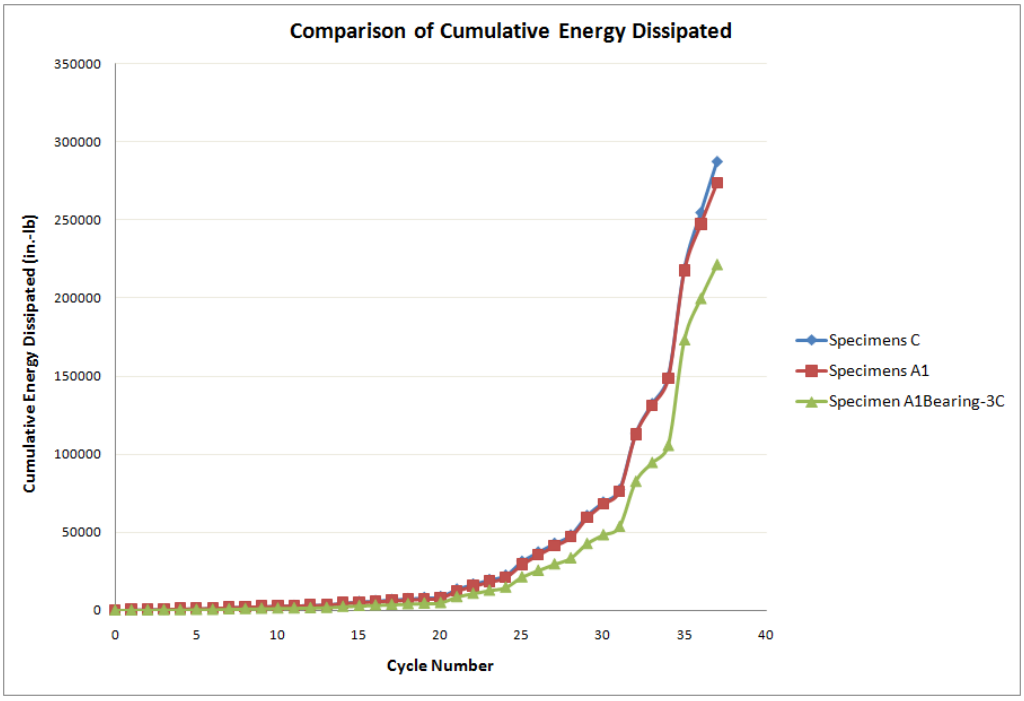

Figure 6.13: Comparison of cumulative energy dissipated

6.6 Loss of Strength in Fatigue Testing

Specimens A1, B and C were placed under fatigue testing in order to determine their ability to withstand repeated cyclic loading. In this research the word "fatigue" refers to loading the specimens under the first thirty-seven cycles of the CUREE loading protocol after it has already been loaded to the facility capacity. The specimens were not repaired in any way in between each fatigue test. Table 6.4 shows the percentage change in the specimens in the strength limit state, defined as the maximum absolute load and corresponding maximum absolute displacement point on the envelope curve. The specimens were fatigued up to three times. Table 6.5 shows the percentage change of the specimens at the yield limit state, defined as the point where there is a 5% or more drop in elastic shear stiffness in the load-displacement relationship. Each column, Fatigue 1, Fatigue 2, and Fatigue 3 of Tables 6.4 and 6.5, represents the percentage change in characteristic values of the specimen at the current (given fatigue) loading in comparison to the previous (original or fatigue) loading. For instance, the values found after Fatigue 1 were compared to those found after the original cyclic loading. The values in the Fatigue 2 column are a comparison between Fatigue 2 and Fatigue 1, and the values in the Fatigue 3 column are a comparison between Fatigue 3 and Fatigue 2. Specimens A1 were the only walls fatigued a total of three times.

On average, Specimen C had the least amount of loss or change after the first fatigue loading. The shear strength did not change at all and the shear modulus and ductility had less than a 10% decrease in value. If Specimen C experienced a seismic event there is a good chance that without repair it would be able to withstand a second

seismic event with the same amount of strength and ductility as the first time. The Fatigue 2 test did not have as much of an impact on the specimens as the Fatigue 1 test. Specimen A1 had the least amount of change after Fatigue 2 in comparison to Specimens C and B. Unlike Specimen B, which completely failed after the second fatigue, Specimen A1 was able to withstand a third fatigue test. Specimen C would have been able to withstand a third fatigue test but because there was such minimal change between the first two fatigues and the original cyclic loading it was assumed that third fatigue would produce similar results.

Table 6.4: Average Percentage Loss (-) or Gain (+) in Characteristic Values at Strength Limit State After Fatigue Tests of Specimens

	Fatigue 1			Fatigue 2			Fatigue 3
Specimens	C	A1	B	C	A1	B*	A1
Displacement	+13	+3	+10	0	-2	+3	+1
Shear Force	0	-18	-12	-9	-5	-4	-12
Shear Modulus	-7	-23	-19	-10	-4	-8	-13
Shear Strength	0	-17	-13	-9	-3	-4	-4
Elastic Shear Stiffness	-40	-53	-46	-15	-9	-10	-13
Ductility	-2	-8	-3	-2	+1	0	-7

*Specimen B-2C failed before a second fatigue test so the values in this column are not an average, they are the loss or gain experienced only by Specimen B-3C after Fatigue 2 test

Table 6.5: Average Percentage Loss (-) or Gain (+) in Characteristic Values at Yield Limit State After Fatigue Tests of Specimens

	Fatigue 1			Fatigue 2			Fatigue 3
Specimens	C	A1	B	C	A1	B*	A1
Displacement	+9	+11	+3	+5	-3	+5	+1
Shear Force	-9	-28	-21	-9	-5	-4	-12
Shear Modulus	-20	-36	-24	-12	-5	-9	-13

*Specimen B-2C failed before a second fatigue test so the values in this column are not an average, they are the loss or gain experienced only by Specimen B-3C after Fatigue 2 test

6.7 Comparison of Results with Previous Studies

Similar to studies performed by Carradine et. al (2004), Jamison (1997), Kermani and Hairstans (2006), Lebeda et al. (2005), Toothman (2003), and Bredel (2003) the performance of the SIP and wood-frame specimens was controlled by the fastener-slip behavior of the sheathing-to-framing connection. As previously stated in Chapter 2, a technical bulletin created by R-Control, SIP No. 2067 (2008) and Jamison's research (1997) were the only published research available which tested SIP specimens under cyclic loading. In SIP No. 2067, an 8 ft x 8 ft x 4.5 in. SIP wall with 8d cooler nails spaced at 2 in. o.c. was cyclically loaded according to the SPD protocol. The specimen had a peak load capacity of about 25600 lb and a corresponding displacement of 1.6 in. Compared to the average peak load of Specimens A1 (SIP with OSB surface spline and 8d common nails) in this study, 17998 lb to 18174 lb and the average displacement of 5.05 in. to 5.30 in., the R-Control specimen had a larger load and smaller displacement at the strength limit state. The difference in load capacity is due to the reduced spacing of the fasteners and the SPD loading protocol which was used when testing the R-Control specimen. According to Gatto and Uang (2003), the SPD loading protocol reduces the ultimate strength by 25% and the deformation capacity by 47% in comparison to the CUREE loading protocol.

In Jamison's research, an 8 ft x 8 ft x 4.5 in. SIP wall attached with drywall screws spaced at 6 in. o.c. and adhesive was tested using the SPD cyclic loading protocol. At the initial loading, Jamison's specimen had a peak load capacity of 6650 lb at a drift of 0.52 in. Specimen A4 (SIP with OSB surface spline and 1.25 in. long screws) in this

study had a peak load of 16689 lb at a drift of 3.48 in. The load and displacement are larger than Jamison's specimen which can be due to the fastener hardware used, loading protocol (Gatto and Uang, 2003), and the use of adhesives (Filiatrault and Foschi, 1991).

Table 6.6 shows previous studies performed on wood-frame walls under cyclic loading in comparison to Specimen C (wood-frame wall with 8d common nails) from this study. In Bredel's (2003) research an 8 ft x 8 ft wood-frame wall with 8d nails spaced at 6 in. o.c. along the edge and 12 in. o.c. along the studs was tested under the CUREE loading protocol. The peak load capacity was reached at 2500 lb and a displacement of 1.2 in. Gatto and Uang's (2003) research involved an 8 ft x 8 ft wood wall with 8d box nails spaced at 4 in. o.c. along the edge and 12 in. o.c. along the interior. The CUREE loading protocol was also used to cyclically load the specimen to a peak load capacity of 8900 lb at a drift of 4.88 in. An 8 ft x 8 ft wood-frame wall attached with 16 gauge staples at 2 in. o.c. was loaded according to the SPD loading protocol in Talbot et al.'s (2009) paper. The specimen reached a peak load of 10200 lb at a displacement of 1.5 in. As a means for comparison, Table 6.6 provides the load experienced by Specimen C at the peak load displacement of the previous published studies. The differences in load can be attributed to the differences in shear wall design and loading protocol used among the various specimens. For instance, the SPD loading protocol used on Talbot et al.'s specimen has a 25% reduction in ultimate strength and a 47% reduction in deformation capacity in comparison to the CUREE loading protocol (Gatto and Uang, 2003). Bredel's specimen did not have hold-down anchors which have the ability to increase the ultimate load and corresponding displacement of a shear wall by 50% (Bredel, 2003; Johnston et al., 2006). According to SEAOC (2000), the box nails used in Gatto and

Uang's study can reduce the allowable load of a shear wall by 22% in comparison to common nails. Box nails also allow shear walls to drift more than common nails. Unlike Specimen C, all of the studies reported in Table 6.6 only had OSB sheathing on one side of their specimen. A wood-frame wall sheathed on both sides has a 50% higher load failure than those sheathed on one side only (Patton-Mallory et al., 1984).

Table 6.6: Comparison Between Specimen C and Previous Studies

Research		Bredel, 2003	Gatto and Uang, 2003	Talbot et al., 2009	Specimen C
Loading Protocol		CUREE	CUREE	SPD	CUREE
Fastener Type		SENCO 8d nail	8d box nail	16 gauge, 1 ½ in. long staple	8d common nail
Fastener Spacing		6"edge/12" int.	4" edge/12" int.	2" o.c.	6" edge/12" int.
Hold-down		No	Yes	Yes	Yes
Sheathing		Single-sided	Single-sided	Single-sided	Double-sided
Research Values	**F_{max} (lb)**	2500	8900	10200	19978 to 23417
	Δ_{max} (in.)	1.2	4.88	1.5	4.40 to 5.89
Specimen C capacity at Δ_{max} obtained by other tests	**F_{max} (lb)**	4843	21353	6090	
	Δ_{max} (in.)	1.2	4.88	1.5	

6.8 Industry Requirements

In terms of seismic performance the specimens tested in this study have been analyzed according to ICC-ES AC130 (2007), ICC-ES AC04 (2005), and ASTM E 2126-08 (2008). The "General Overview of NTA Structural Insulated Panel Qualification and Quality Assessment Procedures" supplied by NTA, Inc. defines the seismic factors of a

SIP panel as: Response Modification Factor, R=2.0; System Overstrength Factor Ω_o=2.5; Deflection Amplification Factor, Cd=2.0. The requirements stated in NTA IM 14 TSK 10.0 (2009) must be met in order for a SIP specimen to have higher seismic factors.

NTA IM 14 TSK 10.0 (2009) is similar to Appendix A of ICC-ES AC04 (2005) in that the performance of a SIP specimen under cyclic loading is compared to the performance of a conventional wood-frame wall. If a SIP panel meets the performance requirements stated in NTA IM 14 TSK 10.0 it should be deemed equivalent to System A13 in ASCE 7 Table 12.2-1. In other words, R=6.5, Ω_o=3, and Cd=4. These are the same seismic factors applied in ICC-ES AC130 (2007). The difference between ICC-ES AC130 and NTA AM I4 TIP 10.0 is that the Allowable Stress Design (ASD) load used in the equivalency analysis is based on IBC Table 2306.4.1 or a code research report instead of Section 5.1.3 of ICC-ES AC130.

To meet the first performance requirement of Section 7 in the NTA IM 14 TIP 10.0, the peak strength load of the SIP panel cannot be less than 90% of that of the wood-frame shear wall (Specimen C). Next, the displacement at the ASD design load, P=2240 lb (ICC, 2006), for the SIP panel cannot be less than 85% of that of the benchmark (Specimen C). The ultimate displacement (Δ_U) shall not be less than 85% of the benchmark specimen. The ratio of the ultimate displacement to the ASD design load displacement shall not be less than 85% of that of the benchmark specimen. The load at the maximum allowable story drift (Δ_{all}=2.4) cannot be less than 85% of that of Specimen C. The final requirement states that the cumulative energy dissipated by the SIP specimen cannot be less than 85% of that for Specimen C.

Table 6.7 shows the values which were compared between the SIP specimen and the benchmark wood-frame specimen. The P_{peak} values for both wall types were peak loads obtained before the cyclic testing was stopped due to the displacement or load capacity of the testing facility. In order to be conservative, the Δ_U values were the minimum ultimate displacements obtained by examining the trend lines used to predict the failure of the specimens. By examining Table 6.7 it is evident that the peak strength of Specimen A1 is exactly 90% of the peak strength of Specimen C. The P_{peak}/P_{ASD} of Specimen C is greater than the ratio of Specimen A1. The displacement of the ASD design load of Specimen A1 is 30% greater than that of Specimen C, while the ultimate displacement of Specimen A1 is 16% greater than that of Specimen C. The ratio of the ultimate displacement to the ASD displacement of the SIP specimen is within 94% of that of the wood-frame specimen. As stated in Section 6.5 of this report, the load at the allowable story drift of 2.4 in. and the cumulative energy dissipated for Specimen A1 are not less than 85% of those of Specimen C.

According to NTA IM 14 TIP 10.0, Specimen A1 is deemed equivalent to a wood-frame wall under cyclic loading. As a result, the SIP specimen should have the following seismic factors: Response Modification Factor, R=6.5; System Overstrength Factor Ω_o=3.0; Deflection Amplification Factor, Cd=4.0.

Table 6.7: Data to Meet Performance Requirements of NTA, Inc.

Specimen	P_{peak}	P_{peak}/P_{ASD}	Δ_U	Δ_{ASD}	Δ_U/Δ_{ASD}
C-1C	19980	8.92	5.09	0.28	18.18
C-2C	19959	8.91	4.83	0.53	9.11
C-3C	19995	8.93	5.0	0.40	12.5
Average C	19978	8.92	4.97	0.40	13.26
A1-1C	17730	7.92	5.54	0.32	17.31
A1-2C	18265	8.15	6.23	0.82	7.60
Average A1	17998	8.03	5.89	0.57	12.46

6.9 Summary

A total of twenty-one walls were tested under monotonic and cyclic loading. Characteristic values such as shear modulus and shear strength were found for each wall, as well as the allowable drift capacity, the amount of energy dissipated during cyclic loading, the SIP panel walls' equivalency to the wood-frame wall, and the behavior of the specimens under fatigue loading. This chapter presented the information for each specimen in a manner which allows the information to be compared easily. From the figures and charts located in this chapter, the following summary statements can be drawn:

- The spline design, whether the SIP specimens were connected with OSB surface splines or (2) 2x4 splines, did not have a significant effect on the load-displacement relationship of the specimen.
- Fastener hardware had a significant effect on the specimen's load-displacement relationship.

- Specimen A4, the SIP wall that used screws to connect the sheathing to the framing members, had the highest shear modulus out of all the specimens tested.
- The specimens tested under monotonic loading showed a higher load capacity corresponding to both the allowable seismic and wind drift compared to the specimens tested under cyclic loading.
- Under cyclic loading, Specimen A1Internal-4C showed the largest force capacity corresponding to the allowable wind drift load of 0.24 in. Specimen A1Bearing-3C showed the largest load capacity corresponding to the allowable seismic drift of 2.4 in. The required load capacity for Specimens C and A4 were only about 20% less than Specimen A1Bearing-3C.
- Specimens C and A1 had the ability to dissipate the largest amount of energy.
- According to ICC-ES AC04 Appendix A (2005), the SIP Specimen A1 was deemed equivalent to the wood-frame Specimen C. This should allow Specimen A1 to be used in Seismic Design Categories A through F.
- According to NTA IM 14 TIP 10.0 (2009), the SIP Specimen A1 was deemed equivalent to the wood-frame Specimen C. Specimen A1 should have the following seismic factors: Response Modification Factor, R=6.5; System Overstrength Factor Ω_o=3.0; Deflection Amplification Factor, Cd=4.0.
- Specimen C was able to retain the largest strength after Fatigue 1 test in comparison to Specimens A1 and B. Specimen A1 had the smallest decrease in strength after Fatigue 2 test.

- During fatigue loading of Specimens C, A1 and B the largest drop occurred in the elastic shear stiffness. The specimens had an average loss of 40% to 53% after Fatigue 1 test and a 9% to 15% loss after Fatigue 2 test.

Chapter 7

Summary, Conclusions, and Limitations

7.1 Summary

A total of twenty-one 8 ft x 8 ft shear walls were tested in this study. The structural insulated panels tested were 8 ft x 8 ft x 4.5 in. and provided by Timberline Panel Company LLC. Parameters such as spline design, fastener hardware, hold-down anchor location, and sheathing bearing were varied in order to determine their effect on shear wall performance. A traditional wood-frame shear wall was built out of Spruce Pine Fir, No. 2 or better grade and 4 ft x 8 ft x 7/16 in. OSB sheathing arranged vertically on both sides of the wall. The specimens were loaded monotonically in accordance with ASTM E 564-06 and cyclically following the CUREE protocol and ASTM E 2126-08. Performance characteristics such as elastic shear stiffness, energy dissipation, allowable drift load capacity and seismic compatibility were compared.

7.2 Conclusions

The information presented in this report provides much needed information about the effect parameters and loading have on a structural insulated panel's performance. The comparison between the SIP specimens and wood-frame specimens will aid the SIP industry in receiving code approval for SIPs in high seismic locations. The information

comparing fastener hardware will be helpful to small SIP manufacturers with limited resources for extensive testing.

The following conclusions can be drawn from this research:

- The fastener hardware was the mode of failure for all of the walls. Specimens A3, A4, A1, and C experienced fastener to sheathing failure. The staples in Specimen A3 withdrew and sheared, the screws in Specimen A4 sheared, and the nails used in Specimens A1 and C withdrew. The nailed specimens also experienced sheathing tear-out.
- Specimen B failed when the (2) 2x4 spline separated allowing the SIP panels to rotate independently of each other. This is not a typical failure method of SIP specimens. Additional 16d common nails at a reduced spacing would allow Specimen B to fail at its peak capacity.
- The top plate was consistently a point of failure for the SIP specimens. Strengthening the connection between the top plate and sheathing or top plate and end posts with additional fasteners at reduced spacing would increase the capacity of the specimens.
- The SIP and wood specimens in this test had significantly higher load and displacement capacities than reported by previous published research. This may be due to the strength of the USP PHD 6 hold-down anchors used, the structural grade OSB sheathing which Timberline Panel Company LLC uses on their SIPs, or the test facility.
- Specimens built with the common nails were able to withstand a larger load and displacement capacity than those built with staples and screws. The nailed walls

had an average peak load range of 17998 to 18174 which is about 37% higher than the stapled walls. At the peak load, the average displacement of the nailed walls ranged from 5.05 in. to 5.30 in. which is about 31% higher than the screwed walls and 38% higher than the stapled walls.

- Specimen A4, the walls with screw fasteners, had sudden and brittle failures.
- The spline type did not have a significant effect on the performance of the SIP specimens. The load, displacement and ductility of Specimen A1 (OSB surface spline) and Specimen B (double 2x4 spline) were within 10% of each other.
- Sheathing bearing of Specimen A1Bearing-3C had a moderate effect on the peak load and peak displacement of the specimen. The peak load was 8% higher than the average peak load of Specimens A1-1C and A1-2C, and the corresponding displacement was 17% less than the average of Specimens A1. The greatest difference occurred in the elastic shear stiffness, Specimen A1Bearing-3C was 29% higher than the average of Specimens A1-1C and A1-2C. The sheathing bearing also caused more extensive damage to the panels during cyclic loading than Specimens A1-1C, A1-2C, and A1Internal-4C.
- Ductility and elastic shear stiffness increased by about 13% when the hold-down anchors were placed on the interior of the SIP specimen.
- Monotonic loading produced non-conservative results in comparison to cyclic loading. The allowable peak load capacities at a drift of 0.24 in. corresponding to the allowable drift limit under wind loading (IBC 2007) for the specimens were an average 35% to 50% larger under static loading than cyclic loading.

- Out of all the specimens, Specimen A1Internal-4C required the greatest amount of force, 2295 lb, to push the wall to an allowable wind drift of 0.24 in. (IBC 2007). Specimen A1Bearing-3C required a force about 10% less while Specimens A3, A4, and C needed forces 27% to 31% less than Specimen A1Internal-4C. The internal placement of the hold-down anchors had an effect on the drift because the load required to deflect Specimen A1 to the same allowable wind drift was about 42% less.
- Sheathing bearing caused Specimen A1Bearing-3C to require the most amount of load to displace the specimen an allowable seismic drift of 2.4 in. Specimens C and A4 were within 20% while Specimens A1 and A3 were about 30% less.
- As long as the framing members are not damaged, a SIP specimen can be repaired (re-nailing, etc) after experiencing seismic loading and expect to have a minimal loss in strength.
- The ductile nature of 8d common nails allowed Specimens C and A1 to dissipate the greatest amount of energy in comparison to the screwed and stapled specimens.
- According to ICC-ES AC130 (2007), Specimens A1, A1Bearing-3C, A1Internal - 4C, B, and C can be used within a seismic force resisting system and be characterized with the following seismic values:
    - Response Modification Coefficient: R=6.5
    - System Overstrength Factor: Ω_o=3
    - Deflection Amplification Factor: C_d=4

- According to ICC-ES AC04 Appendix A (2005), the SIP Specimen A1 is deemed equivalent to the wood-frame shear wall Specimen C and should be allowed to be used in Seismic Design Categories A through F.
- According to NTA IM 14 TIP 10.0 (2009), the SIP Specimen A1 was deemed equivalent to the wood-frame Specimen C. Specimen A1 should have the following seismic factors: Response Modification Factor, R=6.5; System Overstrength Factor Ω_o=3.0; Deflection Amplification Factor, Cd=4.0. Specimen A1 was composed of two 4.5 in. thick 4 ft x 8 ft SIPs arranged vertically and connected along the 8 ft side with two 7/16 in. thick 3 in. x 7 ft 9 in. sheets of OSB. The end posts consisted of (2)2x4 Spruce Pine Fir No. 2 grade or better, the top and base plate were single 2x4 SPF No. 2 or better. The wood-frame and OSB surface spline were attached to the sheathing of the SIP with Grip Rite 8d common nails spaced at 6 in. o.c.
- Specimen C was able to retain the greatest amount of strength after Fatigue 1 test in comparison to Specimens A1 and B. Specimen A1 had the smallest decrease in strength after Fatigue 2 test.
- During fatigue loading of Specimens C, A1 and B the largest drop occurred in the elastic shear stiffness. The specimens had an average loss of 40% to 53% after Fatigue 1 test and a 9% to 15% loss after Fatigue 2 test.
- Out of the various SIP designs, Specimen A1 the wall with the OSB surface spline and nails, proved to be the most effective design in terms of load capacity, ductility, resistance under fatigue loading and seismic compatibility.

7.3 Limitations

This research should be seen as preliminary testing which can be used to provide a better understanding of the performance of structural insulated panels with varying parameters under monotonic and cyclic loading. Each specimen was tested once under monotonic loading and the minimal amount of cyclic tests according to the ASTM standards. To provide a more thorough investigation additional monotonic and cyclic testing should be performed. The specimens in this study were much stronger than previously published research. A testing facility with a load capacity of preferably 30,000 lb and a drift capacity of 10 in. should be able to bring the specimens to their ultimate failure in future testing.

ASTM 2126-08 which was followed in this study, limits the amount of axial loading applied to the specimens under lateral loading. Future testing should place the SIPs under biaxial loading in order to mimic actual field conditions. If the gravity loading does not have an effect on the performance of a SIP or the SIP performs similarly to a wood-frame wall under biaxial loading the SIP industry will be another step closer to adjusting ICC-ES AC04 (2007).

References

American Society of Civil Engineers, (2005). *Minimum Design Loads for Buildings and Other Structures*, ASCE Standard – ASCE/SEI 7-05, Reston, Virginia.

American Society for Testing and Materials, (2005). "Standard Test Methods of Conducting Strength Tests of Panels for Building Construction," ASTM E72-05, *ASTM Annual Book of Standards*. Vol. 04.11. West Conshohocken, Pennsylvania.

American Society for Testing and Materials, (2006). "Standard Practice for Static Load Test for Shear Resistance of Framed Walls for Buildings," ASTM E564-06, *ASTM Annual Book of Standards*. Vol. 04.11. West Conshohocken, Pennsylvania.

American Society for Testing and Materials, (2007). "Standard Test Methods for Cyclic (Reversed) Load Test for Shear Resistance of Vertical Elements of the Lateral Force Resisting Systems for Buildings," ASTM E2126-07a, *ASTM Annual Book of Standards*. Vol. 04.12. West Conshohocken, Pennsylvania.

APA – The Engineered Wood Association, (1990). *Design and Fabrication of Plywood Sandwich Panels,* APA – The Engineered Wood Association Supplement 4.

Applied Technology Council, (1995). *ATC-19 Structural Response Modification Factors*, Applied Technology Council (ATC). Redwood City, California.

Architectural Testing, (2005). *Performance Test Report Rendered to: Agriboard Industries Report No. 57743.01-122-18*, Architectural Testing. York, Pennsylvania.

Bredel, D. H., (2003). *Performance Capabilities of Light-Frame Shear Walls Sheathed with Long OSB Panels,* Thesis submitted in partial fulfillment of the Master of Science Degree at the Virginia Polytechnic Institute and State University, Blacksburg, Virginia.

Carradine, D. M., Woeste, F.E., and Dolan, J.D. (2004). "Timber Frame and Structural Insulated Panel Building Design Concepts," *Proceedings of the 8th World Conference on Timber Engineering*, Finland, 14-17 June 2004, pp. 1-4.

Carradine, D. M., (2002). *Methodology for the Design of Timber Frame Structures Utilizing Diaphragm Action*, Thesis submitted in partial fulfillment of the Doctor of Philosophy Degree at the Virginia Polytechnic Institute and State University, Blacksburg, Virginia.

Cathart, (1998). "SIPs, Not Studs," *Architecture*, pp. 148-153.

Conbere, S., (2007). "Code Change Lowers Hurdles for SIPs, Green Building," *Professional Builder*, 11 Nov. 2007, http://www.housingzone.com/probuilder/article/CA6471995.html.

Cushman, T., (2008). "Defeating the Wind - Structural Panels Gain an Edge in Meeting the Wind Codes," *Coastal Contractor Online*, 6 June 2008, www.coastalcontractor.net/cgi-bin/article.pl?id=61

Filiatrault, A., (2001). "Wood-frame Project Testing And Analysis Literature Reviews," *CUREE-Caltech Wood-frame Project Rep. No. W-03*, Stanford University, Stanford, California.

Filiatrault, A. and Folz, B., (2002). "Performance-Based Seismic Design of Wood-framed Buildings," *J. Structural Engineering*, Vol. 128, No. 1, pp. 39-47.

Filiatrault, A. and Foschi, R.O., (2001). "Static and Dynamic Tests of Timber Shear Walls Fastened with Nails and Wood Adhesive," *Canadian Journal of Civil Engineering*, Vol. 18, No. 5, pp. 749-755.

Folz, B. and Filiatrault, A., (2001). "Cyclic Analysis of Wood Shear Walls," *J. Structural Engineering*, Vol. 127, No. 4, pp. 433-441.

Gatto, K., and Uang, C., (2003). "Effects of Loading Protocol on the Cyclic Response of Wood-frame Shearwalls," *J. Structural Engineering,* Vol. 129, No. 10, pp. 1384-1393.

Gnip, I. J., Veyelis, S. A., and Kersulis, V. I., (2007). "Deformability and Strength of Expanded Polystyrene (EPS) Under Short-Term Shear Loading." *Mechanics of Composite Materials*, Vol. 43, pp. 85-94.

ICBO Evaluation Service, Inc., (2002). *ES Report for Precision Panel Structures, Inc.*, PFC-6054, Whittier, California.

ICC Evaluation Service, Inc., (2003). *ICC ES Legacy Report for Intermountain Building Panels L.L.C.*, PFC-5361, Whittier, California.

ICC Evaluation Service, Inc., (2004). *ICC ES Legacy Report for INSULSPAN Structural Insulated Panels*, NER-520, Whittier, California.

INSULSPAN, (2007). *Technical Bulletin – Racking Shear Strength Test Results*, INSULSPAN Structural Insulating Panel System, Bulletin No. 111, Blissfield, Michigan.

INSULSPAN, (2008). *Insulspan Homes are More Energy Efficient*, 28 October 2008, www.insulspan.com/homeowners/why_use_sip/energy_efficient.html

International Code Council (ICC), (2006). *2006 International Building Code*, Country Club Hills, Illinois.

International Code Council (ICC), (2007). "AC 130 - Acceptance Criteria for Prefabricated Wood Shear Panel," *ICC Evaluation Service, Inc.,* Whittier, California.

International Code Council (ICC), (2007). "AC 322 – Acceptance Criteria for Prefabricated Cold-Formed, Steel Lateral-Force-Resisting Vertical Assemblies," *IIC Evaluation Service, Inc.,* Whittier, California.

International Code Council (ICC), (2007). "AC 04 – Acceptance Criteria for Sandwich Panels," *IIC Evaluation Service, Inc.,* Whittier, California.

International Code Council (ICC), (2005). "AC 04 – Acceptance Criteria for Sandwich Panels," *IIC Evaluation Service, Inc.,* Whittier, California.

International Code Council (ICC), (2007). "Section R614 Structural Insulated Panel Wall Construction," *International Residential Code*, Whittier, California.

International Code Council (ICC), (2006). *International Residential Code*, Whittier, California.

International Code Council (ICC), (2006). *International Building Code*, Whittier, California.

ICC Evaluation Service, Inc., (2006). *Report to Address the Application of a One-Third Stress Increase When Designing Pre-Fabricated Shear Panels Using the 1997 UBC and the 2000 IBC Allowable Stress Design Provisions*, 28 March 2008, www.icc-es.org.

Jamison, J. B., (1997). *Monotonic and Cyclic Performance of Structurally Insulated Panel Shear Walls,* Thesis submitted in partial fulfillment of the Master of Science Degree at the Virginia Polytechnic Institute and State University, Blacksburg, Virginia.

Johnston, A. R., Dean, P. K., and Shenton III, H.W., (2006). "Effects of Vertical Load and Hold-Down Anchors on the Cyclic Response of Wood-framed Shear Walls," *J. Structural En*gineering, Vol. 132, No. 9, pp. 1426-1434.

Keith, E. L., (2006). *APA Report T2006P-33, Standardization Testing of Structural Insulated Panels (SIPs) for The Structural Insulated Panel Association, Gig Harbor, Washington,* APA The Engineered Wood Association, Tacoma, Washington.

Kermani, A. and Hairstans, R., (2006). "Racking Performance of Structural Insulated Panels," *J. Structural Engineering*, pp. 1806-1812.

Kermani, A., (2006). "Performance of Structural Insulated Panels." *Journal of Buildings & Structures,* Vol. 159, Issue SB1, pp. 13-19.

Krawinkler, H., Parisi, F., Ibarra, L., Ayoub, A., and Medina, R., (2001). *Development of a Testing Protocol for Wood-frame Structures*, CUREE-Caltech Wood-frame Project Rep. No. W-02, Stanford University, Stanford, California.

Lebeda, D. J., Gupta, R., Rosowsky, D. V., and Dolan, J. D., (2005). "Effect of Hold-Down Misplacement on Strength and Stiffness of Wood Shear Walls," *Practice Periodical on Structural Design and Construction*, Vol. 10, No. 2, pp. 79-87.

Mandbeck, H. B. and Taylor, S. B., (1991). "Structural Evaluation of the Murus Stress-Skin Urethane Sandwich Panel," *Paper prepared for H.R.C. Research Series by NAHB/NRC Designated Housing Research Center at Penn State*. Report No. 15, State College, Pennsylvania.

Maxwell, S., (2007). *Personal communication with Scott Maxwell about code acceptance of SIPs*. Insulspan, Blissfield, Michigan.

McMullin, K. M. and Merrick, D. S., (2007). "Seismic Damage Thresholds for Gypsum Wallboard Partition Walls," *Journal of Architectural Engineering*, Vol. 13, No. 1, pp. 22-29.

Morley, M., (2000). *Building with Structural Insulated Panels (SIPs)*. The Taunton Press, Inc., Connecticut.

Morley, M., (2007). "Building with Structural Insulated Panels (SIPS) – Strength and Energy Efficiency Through Structural Panel Construction," *Design Basics Home Plans,* 12 April 2007. http://www.designbasics.com/Home/planbooks-sipbook-02.asp

Morse-Fortier, L. J., (1995). "Structural Implications of Increased Panel Use in Wood-Frame Buildings," *J. Structural Engineering*, Vol. 121, No. 6, pp. 995-1003.

Mullens, M. A., and Arif, M., (2006). "Structural Insulated Panels: Impact on the Residential Construction Process," *J. Construction Eng. And Management.*, Vol. 132, No. 7, pp. 786-794.

NAHB Research Center, Inc., (1995). *Innovative Structural Systems for Home Construction: Wood Structural Insulated Panels and Insulating Concrete Forms*, U.S. Department of Housing and Urban Development, Upper Marlboro, Maryland.

NTA, Inc., (2009). *General Overview of NTA Structural Insulated Panel Qualification and Quality Assessment Procedures*, NTA IM 14.1, Nappanee, Indiana.

NTA, Inc., (2009). *Qualification of Wood Structural Panel Faced SIPs for Use in Seismic Zone D, E and F*, NTA IM 14 TIP 10.0, Nappanee, Indiana.

Palms, J., and Sherwood, G. E., (1979). "Structural Sandwich Performance After 31 Years of Service," *Forest Service Research Paper*, Madison, Wisconsin.

Patton-Mallory, M., Gutkowski, R. M., Soltis, L. A., (1984). "Racking Performance of Light-Frame Walls Sheathed on Two Sides," *Forest Service Research Paper FPL 448*, Forest Products Laboratory, Madison, Wisconsin.

Pugh, G., (2006). "Building with Structural Insulated Panels," *Journal of Light Construction*, Vol. 24, No. 2, pp 1-10.

R-Control Building Systems, (2008). *Tech Bulletin – SIP No. 2067, Seismic Performance*, 29 April 2008, www.r-control.com/downloads/techbulletin/rcontrol2067.pdf

R-Control Building Systems, (2008). *Load Design Charts*, 5 June 2008, www.r-control.com\

Structural Engineers Association of California, (2000). *Seismic Design Manual*, Structural Engineers Association of California (SEAOC), Sacramento, California.

Structural Engineers Association of Southern California, (1996). *Standard Method of Cyclic (Reversed) Load Test for Shear Resistance of Framed Walls for Buildings,* Structural Engineers Association of Southern California (SEAOSC), Whittier, California.

Talbot, K. C., Reaveley, L. D., Pantelides, C. P., (2009). "Structural Performance of Stapled Wood Shear Walls Under Dynamic Cyclic Loads," Earthquake Spectra, Vol. 25, No. 1, pp. 161-183.

Toothman, A. D., (2003). *Monotonic and Cyclic Performance of Light-Frame Shear Walls with Various Sheathing Materials*, Thesis submitted in partial fulfillment of the Master of Science Degree at the Virginia Polytechnic Institute and State University, Blacksburg, Virginia.

Tracy, J. M., (2000). "SIPs Overcoming the Elements," *Forest Products Journal*, Vol. 50, pp. 12-18.

Tuomi, R. L. and McCutcheon, W. J., (1978). "Racking Strength of Light-Frame Nailed Walls," *Journal of the Structural Division*, Vol. 104, pp. 1131-1140.

Wilcoski, J., Fischer, C., Allison, T., and Malach, K. J., (2002). *Alternative Shear Panel Configurations for Light Wood Construction*, U.S. Army Construction Engineering Research Laboratory (CERL), Champaign, Illinois.

Appendix A

ASTM E 2126-08 and ICC-ES AC130 Calculations

A.1 Calculations for Specimen A3-2C

ASTM E 2126-08

9.1.1 Shear Strength

(+)	Vpeak	= 10259 lb/8 ft	=	1282 lb/ft
(-)		= 12238 lb/8 ft	=	1530 lb/ft

9.1.2 Secant Shear Modulus

(+)	G' at Ppeak	= 10259 lb/2.47 in.	=	4154 lb/in.
(-)		= 12238 lb/3.75 in.	=	3262 lb/in.
(average)			=	3708 lb/in.
(+)	G' at 0.4Ppeak	= 4104 lb/0.94 in.	=	4377 lb/in.
(-)		= 4895 lb/1.27 in.	=	3846 lb/in.
(average)			=	4112 lb/in.

9.1.3 Cyclic Ductility Ratio and EEEP Curve

(+)	D	=	3.60 in./2.25 in.	=	1.60
(-)		=	3.94 in./2.94 in.	=	1.34

G' at Ppeak < G' at 0.4Ppeak ⟶ Generate EEEP Curve

9.1.4 Generating an EEEP Curve and determining yield limit state

(+)	Pu	=	0.8*10259 lb	=	8207 lb

(-) = 0.8*12238 lb = 9791 lb

(+) Δu = 3.60 in. (from graph)

(-) = 3.94 in. (from graph)

(+) Ke = 4104 lb/ 0.94 in. = 4377 lb/in.

(-) = 4895 lb/1.27 in. = 3846 lb/in.

(+) Area Under Backbone Curve = 24367 lb*in.

(-) = 27984 lb*in.

(+) $\Delta u^2 = 3.60^2 = 12.94$ in^2 > $2A/Ke = 2(24367)/4377 = 11.13$ in^2

⟶ Pyield = (3.60 – sqrt(12.94 – 11.13)*4377 = 9862 lb

⟶ Δyield = 9862 lb/ 4377 lb/in. = 2.25 in.

(-) $\Delta u^2 = 3.94^2 = 15.56$ in^2 > $2A/Ke = 2(27984)/3846 = 14.55$ in^2

⟶ Pyield = (3.94 – sqrt(15.56 – 14.55)*3846 = 11312 lb

⟶ Δyield = 11312 lb/ 3846 lb/in. = 2.94 in.

ICC ES AC130

5.1.3.1 Allowable Stress Design

5.1.3.1.1 Drift Limit (Seismic)

a) бx = min(Δa = 2.40 in. or Δpeak = 3.11 in.)⟶ бx = 2.40 in.

b) бxe = (бx*I)/Cd = 2.40 in.*(1.0)/4 = 0.60 in.

c) P at бxe = 3000 lb (average of positive and negative P values from graph)

d) P_{ASD} = 0.7*(3000 lb) = 2100 lb

e) Δ_{ASD} = 0.29 in. (average of positive and negative delta values from graph)

5.1.3.1.2 Drift Limit (Wind)

Δ = 8 ft/180 = 0.53 in.

0.53 in. > 0.29 in. ⟶ No need to continue with calculations

5.1.3.1.3 Strength Limit (Wind and Seismic)

(+) Δ at Pu/2.5 = 8207 lb/2.5 = 3283 lb

(-) = 9791 lb/2.5 = 3916 lb

P at Strength Limit > P at Drift Limit ⟶ No need to continue with calculations

Allowable Stress Design

P_{ASD} = 2100 lb

Δ_{ASD} = 0.29 in.

5.2 Seismic Design Compatibility

5.2.2

$\Delta u/\Delta_{ASD}$ = 3.77 in./0.29 in. = 12.99 > 11 ⟶ Good!

5.2.3

Δu = 3.77 in. > 0.028*(8 ft *12) = 2.688 in. ⟶ Good!

5.2.4

P_{peak}/P_{ASD} = 11249 lb/2100 lb = 5.36 >2.5 ⟶ Good!

>5 ⟶ No Good!

⟶ Meets Seismic Specifications*

*In order to be considered compliant the evaluation report for the panel must include "a requirement that collectors and their connections, bearing and anchorage of the panel, and the lateral load path to the panel are designed in accordance with the special load

combinations of Section 12.4.3 of ASCE 7, using Em where Em is calculated using the test panel overstrength." (ICC-ES AC130, 2007)

A.2 Calculations for Specimen A3-2C(2)

ASTM E 2126-08

9.1.1 Shear Strength

(+)	Vpeak	= 7777 lb/8 ft	=	972 lb/ft
(-)		= 8065 lb/8 ft	=	1008 lb/ft

9.1.2 Secant Shear Modulus

(+)	G' at Ppeak	= 7777 lb/2.75 in.	=	2824 lb/in.
(-)		= 8065 lb/2.65 in.	=	3040 lb/in.
(average)			=	2932 lb/in.
(+)	G' at 0.4Ppeak	= 3111 lb/0.85 in.	=	3669 lb/in.
(-)		= 3226 lb/.98 in.	=	3276 lb/in.
(average)			=	3473 lb/in.

9.1.3 Cyclic Ductility Ratio and EEEP Curve

(+)	D	=	3.75 in./1.86 in.	=	2.01
(-)		=	3.01 in./2.16 in.	=	1.39

G' at Ppeak < G' at 0.4Ppeak ⟶ Generate EEEP Curve

9.1.4 Generating an EEEP Curve and determining yield limit state

(+)	Pu	=	0.8*7777 lb	=	6222 lb

(-) = 0.8*8065 lb = 6452 lb

(+) Δu = 3.75 in. (from graph)

(-) = 3.01 in. (from graph)

(+) Ke = 3111 lb/0.85 in.. = 3669 lb/in.

(-) = 3226 lb/.98 in. = 3276 lb/in.

(+) Area Under Backbone Curve = 19241 lb*in.

(-) = 13639 lb*in.

(+) $\Delta u^2 = 3.75^2 = 14.03$ in^2 > $2A/Ke = 2(19241)/3669 = 10.49$ in^2

⟶ Pyield = (3.75 – sqrt(14.03 – 10.49)*3669 = 6836 lb

⟶ Δyield = 6836 lb/ 3669 lb/in. = 1.86 in.

(-) $\Delta u^2 = 3.01^2 = 9.05$ in^2 > $2A/Ke = 2(13639)/3276 = 8.33$ in^2

⟶ Pyield = (3.01 – sqrt(9.05 – 8.33)*3276 = 7075 lb

⟶ Δyield = 7075 lb/ 3276 lb/in. = 2.16 in.

ICC ES AC130

5.1.3.1 Allowable Stress Design

5.1.3.1.1 Drift Limit (Seismic)

a) бx = min(Δa = 2.40 in. or Δpeak = 2.70 in.)⟶ бx = 2.40 in.

b) бxe = (бx*I)/Cd = 2.40 in.*(1.0)/4 = 0.60 in.

c) P at бxe = 2162 lb (average of positive and negative P values from graph)

d) P_{ASD} = 0.7*(2162 lb) = 1513 lb

e) Δ_{ASD} = 0.37 in. (average of positive and negative delta values from graph)

5.1.3.1.2 Drift Limit (Wind)

Δ = 8 ft/180 = 0.53 in.

0.53 in. > 0.29 in. ⟶ No need to continue with calculations

5.1.3.1.3 Strength Limit (Wind and Seismic)

(+) Δ at Pu/2.5 = 6222 lb/2.5 = 2489 lb

(-) = 6452 lb/2.5 = 2581 lb

P at Strength Limit > P at Drift Limit ⟶ No need to continue with calculations

Allowable Stress Design

P_{ASD} = 1513 lb

Δ_{ASD} = 0.37 in.

5.2 Seismic Design Compatibility

5.2.2

$\Delta u/\Delta_{ASD}$ = 3.38 in./0.37 in. = 9.19 < 11 ⟶ No Good!

5.2.3

Δu = 3.38 in. > 0.028*(8 ft *12) = 2.688 in. ⟶ Good!

5.2.4

P_{peak}/P_{ASD} = 7921 lb/1513 lb = 5.23 >2.5 ⟶ Good!

>5 ⟶ No Good!

⟶ Does Not Meet Seismic Specifications

Appendix B

Parametric Analysis of Specimens

In Chapter 6 the average characteristic values of the specimen types according to ASTM E 2126-08 were presented. The following bar charts include the values for every single specimen tested under both monotonic and cyclic testing. These charts also include Specimens A3-2C(2), A1Bearing-3C, and A1Internal-4C which were not included in the averages of the specimens presented in Chapter 6. Figures 2.1 through 2.6 also show the effect cyclic versus monotonic loading have on a specimen.

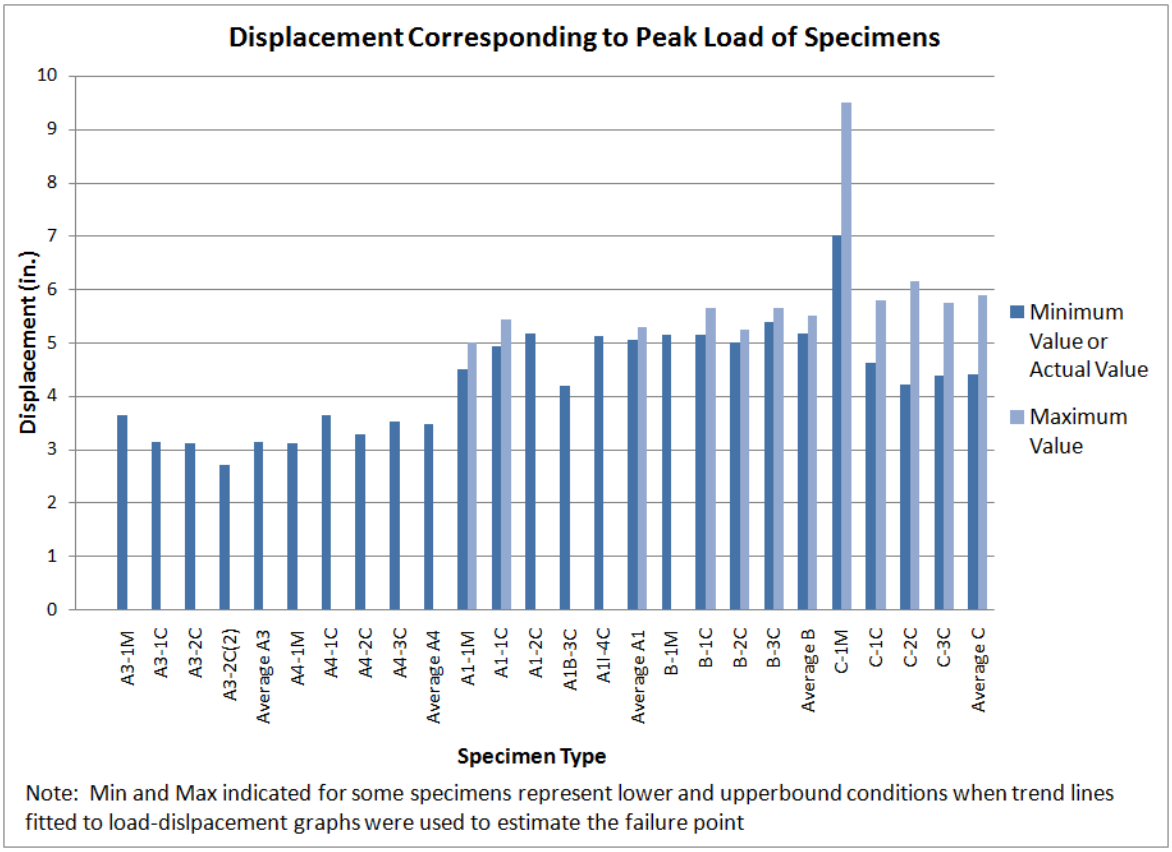

Figure B.1: Displacement corresponding to peak load of specimens

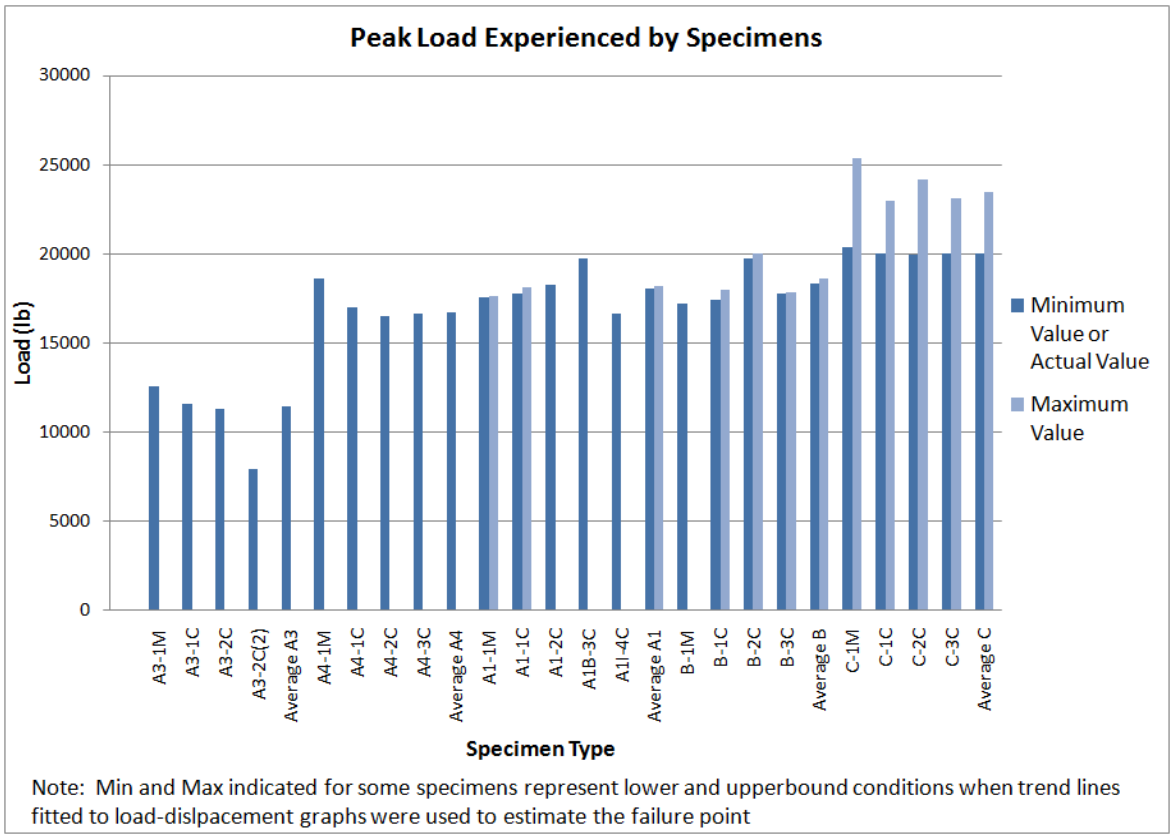

Figure B.2: Peak load experienced by specimens

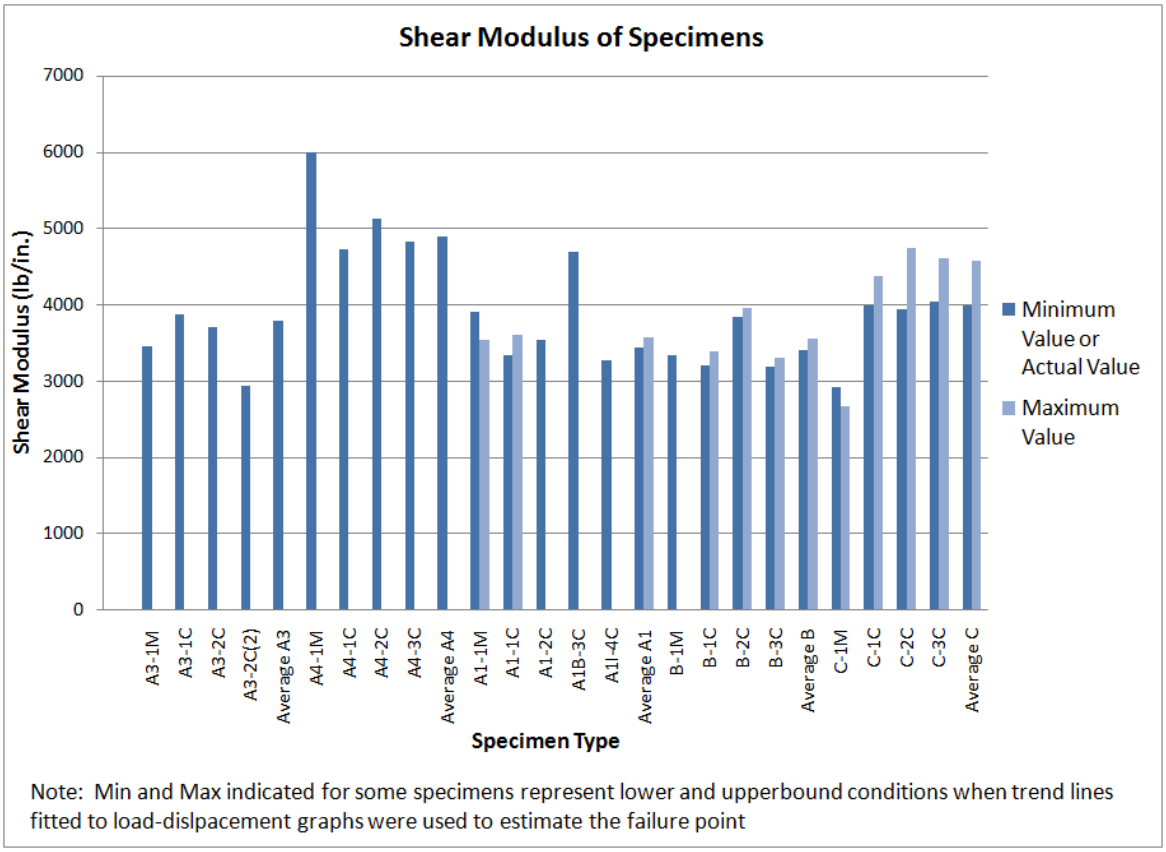

Figure B.3: Shear modulus of specimens

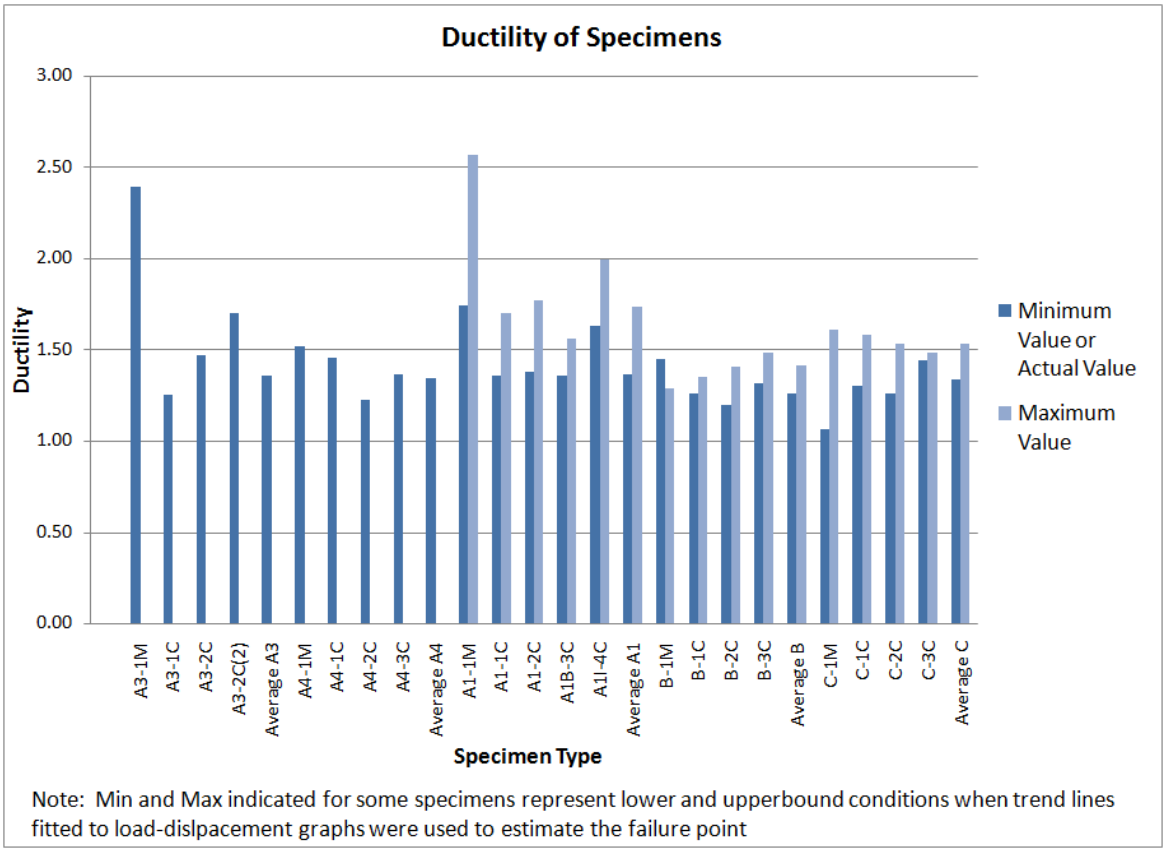

Figure B.4: Ductility of specimens

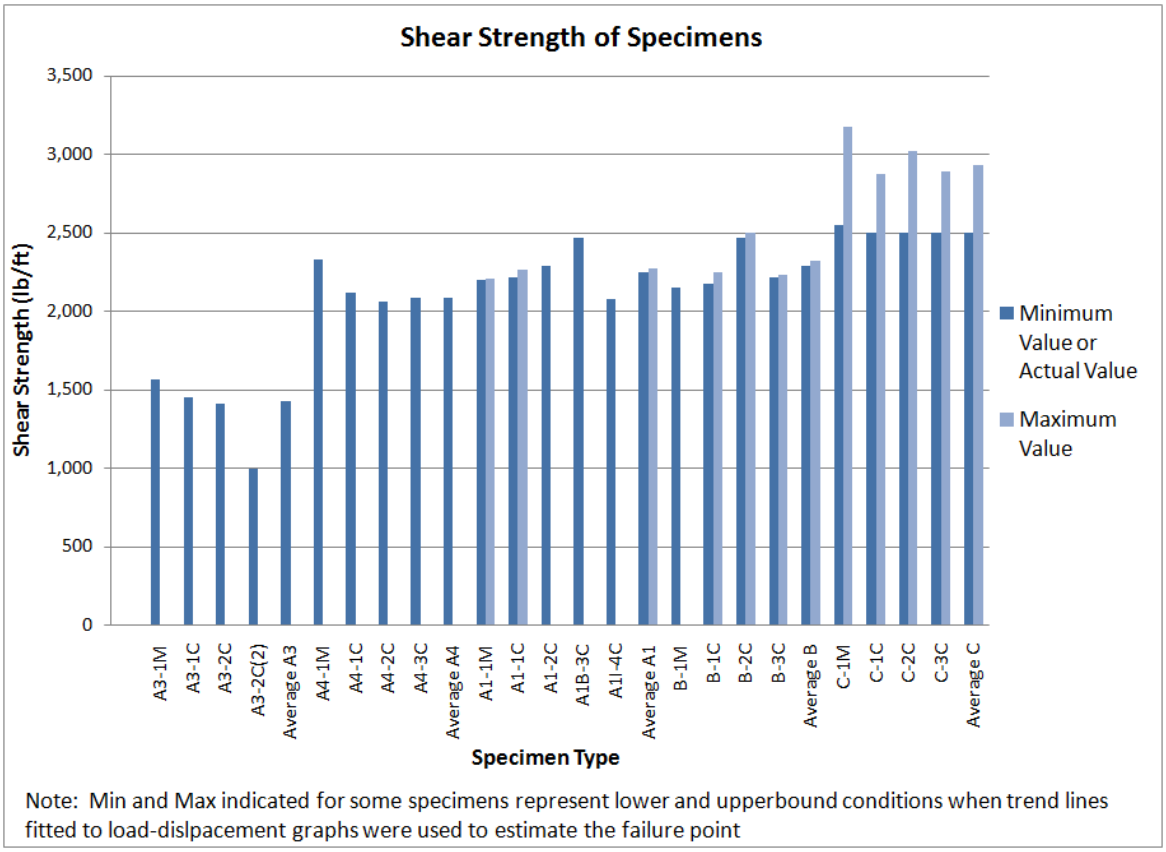

Figure B.5: Shear strength of specimens

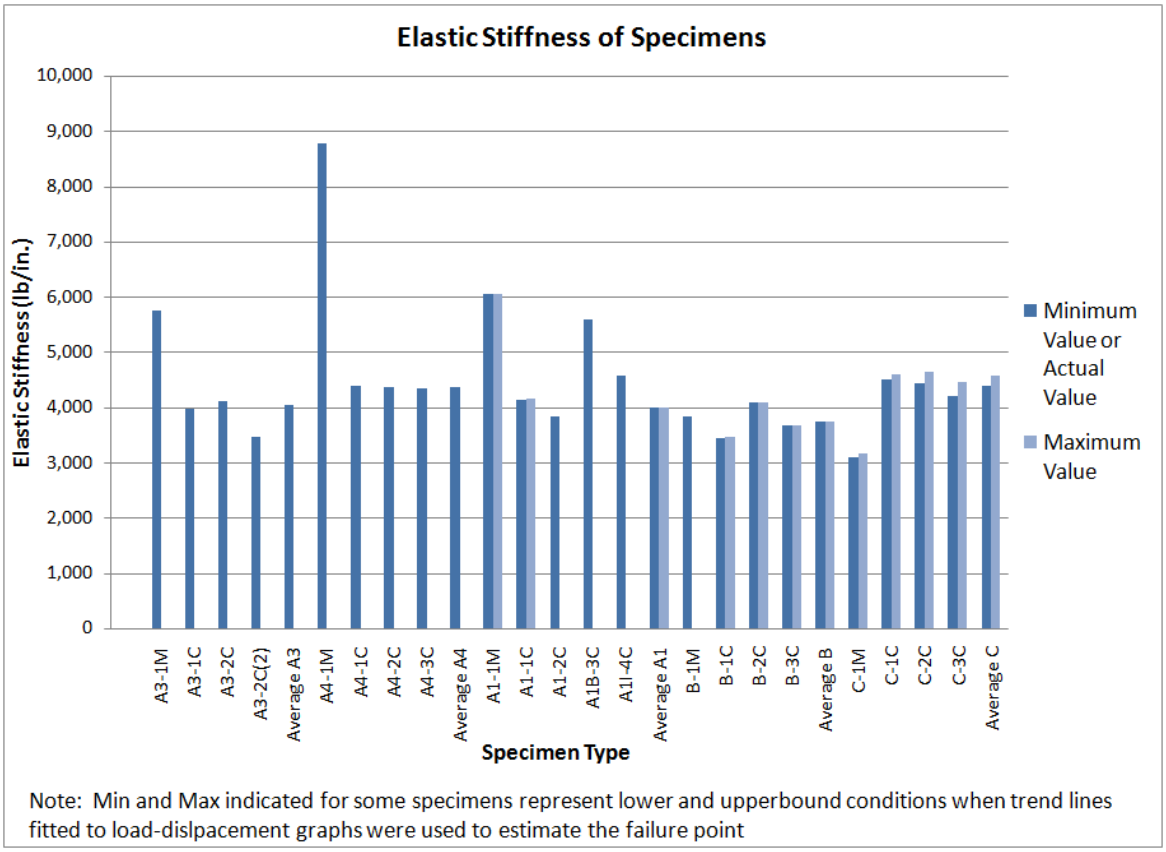

Figure B.6: Elastic stiffness of specimens